



National Library  
of Canada

Acquisitions and  
Bibliographic Services Branch

395 Wellington Street  
Ottawa, Ontario  
K1A 0N4

Bibliothèque nationale  
du Canada

Direction des acquisitions et  
des services bibliographiques

395, rue Wellington  
Ottawa (Ontario)  
K1A 0N4

*Your file* *Votre référence*

*Our file* *Notre référence*

## NOTICE

The quality of this microform is heavily dependent upon the quality of the original thesis submitted for microfilming. Every effort has been made to ensure the highest quality of reproduction possible.

If pages are missing, contact the university which granted the degree.

Some pages may have indistinct print especially if the original pages were typed with a poor typewriter ribbon or if the university sent us an inferior photocopy.

Reproduction in full or in part of this microform is governed by the Canadian Copyright Act, R.S.C. 1970, c. C-30, and subsequent amendments.

## AVIS

La qualité de cette microforme dépend grandement de la qualité de la thèse soumise au microfilmage. Nous avons tout fait pour assurer une qualité supérieure de reproduction.

S'il manque des pages, veuillez communiquer avec l'université qui a conféré le grade.

La qualité d'impression de certaines pages peut laisser à désirer, surtout si les pages originales ont été dactylographiées à l'aide d'un ruban usé ou si l'université nous a fait parvenir une photocopie de qualité inférieure.

La reproduction, même partielle, de cette microforme est soumise à la Loi canadienne sur le droit d'auteur, SRC 1970, c. C-30, et ses amendements subséquents.

UNIVERSITY OF ALBERTA

SOLVENT EFFECTS ON THE REACTIVITIES OF SOLVATED ELECTRONS  
WITH IONIC SOLUTES IN *t*-BUTANOL/WATER, AND ORGANIC SOLUTES IN  
1-BUTYLAMINE/WATER MIXED SOLVENTS

by

YIXING ZHAO



A thesis submitted to the Faculty of Graduate Studies and Research in partial fulfillment  
of the requirements for the degree of DOCTOR OF PHILOSOPHY

DEPARTMENT OF CHEMISTRY

Edmonton, Alberta

FALL 1995



National Library  
of Canada

Acquisitions and  
Bibliographic Services Branch

395 Wellington Street  
Ottawa, Ontario  
K1A 0N4

Bibliothèque nationale  
du Canada

Direction des acquisitions et  
des services bibliographiques

395, rue Wellington  
Ottawa (Ontario)  
K1A 0N4

*Your file* *Votre référence*

*Our file* *Notre référence*

THE AUTHOR HAS GRANTED AN IRREVOCABLE NON-EXCLUSIVE LICENCE ALLOWING THE NATIONAL LIBRARY OF CANADA TO REPRODUCE, LOAN, DISTRIBUTE OR SELL COPIES OF HIS/HER THESIS BY ANY MEANS AND IN ANY FORM OR FORMAT, MAKING THIS THESIS AVAILABLE TO INTERESTED PERSONS.

L'AUTEUR A ACCORDE UNE LICENCE IRREVOCABLE ET NON EXCLUSIVE PERMETTANT A LA BIBLIOTHEQUE NATIONALE DU CANADA DE REPRODUIRE, PRETER, DISTRIBUER OU VENDRE DES COPIES DE SA THESE DE QUELQUE MANIERE ET SOUS QUELQUE FORME QUE CE SOIT POUR METTRE DES EXEMPLAIRES DE CETTE THESE A LA DISPOSITION DES PERSONNE INTERESSEES.

THE AUTHOR RETAINS OWNERSHIP OF THE COPYRIGHT IN HIS/HER THESIS. NEITHER THE THESIS NOR SUBSTANTIAL EXTRACTS FROM IT MAY BE PRINTED OR OTHERWISE REPRODUCED WITHOUT HIS/HER PERMISSION.

L'AUTEUR CONSERVE LA PROPRIETE DU DROIT D'AUTEUR QUI PROTEGE SA THESE. NI LA THESE NI DES EXTRAITS SUBSTANTIELS DE CELLE-CI NE DOIVENT ETRE IMPRIMES OU AUTREMENT REPRODUITS SANS SON AUTORISATION.

ISBN 0-612-06316-X

Canada

UNIVERSITY OF ALBERTA

RELEASE FORM

NAME OF AUTHOR: YIXING ZHAO

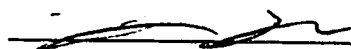
TITLE OF THESIS: SOLVENT EFFECTS ON THE REACTIVITIES OF SOLVATED  
ELECTRONS WITH IONIC SOLUTES IN *t*-BUTANOL/WATER, AND ORGANIC  
SOLUTES IN 1-BUTYLAMINE/WATER MIXED SOLVENTS

DEGREE: DOCTOR OF PHILOSOPHY

YEAR THIS DEGREE GRANTED: 1995

Permission is hereby granted to the University of Alberta Library to reproduce single copies of this thesis and to lend or sell such copies for private, scholarly or scientific research purposes only.

The author reserves all other publication and other rights in association with the copyright in the thesis, and except as hereinbefore provided neither the thesis nor any substantial portion thereof may be printed or otherwise reproduced in any material form whatever without the author's prior written permission.



(Signed)

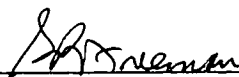
PERMANENT ADDRESS: Apt. 203, 10556-84 Avenue  
Edmonton, Alberta  
Canada T6E 2H4

Date: *Aug. 30*....., 1995

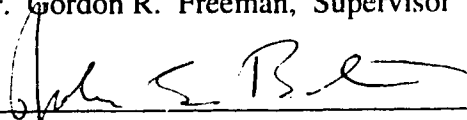
UNIVERSITY OF ALBERTA

FACULTY OF GRADUATE STUDIES AND RESEARCH

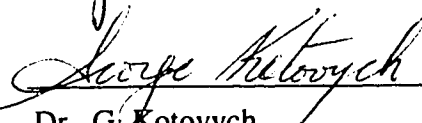
The undersigned certify that they have read, and recommend to the Faculty of Graduate Studies and Research for acceptance, a thesis entitled SOLVENT EFFECTS ON THE REACTIVITIES OF SOLVATED ELECTRONS WITH IONIC SOLUTES IN *t*-BUTANOL/WATER, AND ORGANIC SOLUTES IN 1-BUTYL AMINE/WATER MIXED SOLVENTS submitted by YIXING ZHAO in partial fulfillment of the requirements for the degree of DOCTOR OF PHILOSOPHY



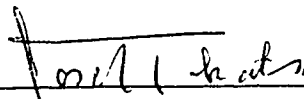
Dr. Gordon R. Freeman, Supervisor



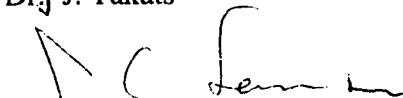
Dr. J. E. Bertie, Chairman



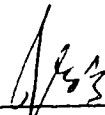
Dr. G. Kotovych



Dr. J. Takats



Dr. J. C. Samson



Dr. R. A. Holroyd, External Examiner

DATE: 21 August....., 1995

**献给我敬爱的父母**

**献给我亲爱的妻子凤卫**

**To My Dear Parents**

**To My Lovely Wife Wei**

## Abstract

The most fundamental electron transfer reagent is solvated electrons,  $e_s^-$ . Reaction rates of  $e_s^-$  can be greatly influenced by changing the solvent. Kinetic behavior of  $e_s^-$  has been measured in *t*-butanol/water and 1-butylamine/water mixed solvents because of the substantially different physical properties of these solvents.

The relative reactivities of  $NH_{4,s}^+$  and  $NO_{3,s}^-$  with  $e_s^-$  reverse on going from pure *t*-butanol solvent, in which  $NH_{4,s}^+$  is the more reactive, to pure water solvent. The reversal is attributed to changes in the structure and reactivity of the solvent around the reaction site. The rate constants of  $e_s^-$  with  $H_s^+$  are the highest of those of the ions studied, in the whole region of *t*-butanol/water mixtures, because  $H_s^+$  has the highest diffusion coefficient. The calculated effective reaction radius ( $\kappa R_r$ ) of each ionic solute decreases on going from pure *t*-butanol to pure water. The activation energies ( $E_2$ ) for all reactions have the highest values in pure *t*-butanol. The high  $\kappa R_r$  and  $E_2$  in pure *t*-butanol are attributed to a high mobility and activation energy of diffusion of  $e_s^-$  in the alcohol.

The measured optical absorption spectra of  $e_s^-$  and the reactivities of  $e_s^-$  with organic solutes in 1-butylamine/water mixed solvents show different behavior of  $e_s^-$  from that obtained in alcohol/water mixed solvents, and it opens a new research area. The energy at maximum absorbance,  $E_{Amax}$ , increases smoothly on going from pure 1-butylamine to pure water, indicating that the electron is less selectively solvated by water molecules than anticipated, and the amine/water mixtures are more randomly structured than are alcohol/water mixed solvents. However, the temperature coefficient ( $-dE_{Amax}/dT$ ) has a minimum at 50 mol% water, which indicates that the solvent structure in the amine-rich region may be different from that in the water-rich region.

The rate constants of the efficient reactions of  $e_s^-$  with nitrobenzene and acetone are high ( $k_2 > 10^6 \text{ m}^3/\text{mol}\cdot\text{s}$ ) and inversely proportional to the viscosity of the 1-butylamine/water mixed solvents. The rate constants of the inefficient reactions of  $e_s^-$  with toluene and phenol ( $k_2 < 10^5 \text{ m}^3/\text{mol}\cdot\text{s}$ ) have a maximum at 50 mol% water. The solvent molecules protonate the transient anions of toluene and phenol. In the water-rich solvents,  $e_s^-$  is preferentially solvated by water and toluene or phenol is preferentially solvated by amine; this tends to keep the reactants apart, and decreases the value of  $k_2$ .



## **Acknowledgements**

The sincerest thanks are due to Professor Gordon R. Freeman for the direction I received in the course of the thesis work. I could not finish this Ph.D. project without his wisdom, intelligence, strict training and patience.

I would like to thank the staff of the Radiation Research Center at the University of Alberta, Mr. L. Coulson and Mr. R. J. Gardner, for aid with electronics and maintenance of the pulse radiolysis equipment. It is also a pleasure to express my gratitude to Dr. Ruzhong Chen for his valuable help, discussions and cooperation. I am very grateful for the help I received from Dr. Norman Gee during my graduate study and in the teaching assistant work. I also want to thank Ms Erica Schamedatus for typing the manuscripts of the papers.

Appreciation is extended to the Natural Sciences and Engineering Research Council of Canada for financial assistance to the research project and Department of Chemistry, University of Alberta for teaching and research assistantship.

## Table of Contents

<b>Chapter One:</b> .....	1
<b>Introduction</b>	
1.Solvation of Electrons .....	1
2. Properties of Solvated Electrons .....	3
2.1. Mobility of Solvated Electrons .....	3
2.2. Optical Absorption Spectrum .....	3
2.2.1. Energy and Shape of the Optical Absorption Band of Solvated Electrons .....	4
2.2.2. Transitions .....	5
2.2.3. Optical Absorption in Hydroxylic Solvents and Mixed Solvents .....	5
2.3. Models of Solvated Electrons .....	7
3. Structure and Properties of Water, Alcohols, and Amines .....	9
3.1. Structure and Properties of Water .....	9
3.2. Structure and Properties of Alcohols .....	10
3.3. Structure and Properties of Alcohol/Water Mixed Solvents .....	10
3.4. Structure and Properties of Amine/Water Mixed Solvents .....	13
4. Reactivity of Solvated Electrons .....	15
5. Present Work .....	19
References .....	20

**Chapter Two:** .....33  
**Solvent Effects on the Reactivity of Solvated Electrons with  
Ions in *tert*-Butanol/Water Mixtures**

1. Introduction .....33  
2. Experimental .....33  
3. Results and Discussion .....34  
References .....60

**Chapter Three:** .....63  
**Solvated Electron Mobility in Liquid *t*-Butanol**

1. Introduction .....63  
2. Experimental and Results .....64  
3. Discussion .....65  
References

**Chapter Four** .....73  
**Solvent Effects on the Reactivity of Solvated Electrons with  
Nitrate Ions in C<sub>1</sub> to C<sub>4</sub> Alcohols**

1. Introduction .....73  
2. Data .....74  
3. Discussion .....74  
References .....86

**Chapter Five .....88**

**Unusual Behavior of the Conductivity of LiNO<sub>3</sub> in *t*-Butanol:  
Ion Clustering or Ion-Pair Aggregation**

1. Introduction .....	88
2. Experimental .....	89
3. Results and Discussion .....	89
References .....	102

**Chapter Six .....104**

**Optical Absorption Spectra of Solvated Electrons in  
1-Butylamine/Water Mixed Solvents**

1. Introduction .....	104
2. Experimental .....	105
3. Results and Discussion .....	106
References .....	118

**Chapter Seven .....120**

**Solvent Effects on the Reactivity of Solvated Electrons with  
Organic Solutes in 1-Butylamine/Water Mixtures**

1. Introduction .....	120
2. Experimental .....	121
3. Results and Discussion .....	121
References .....	140

<b>Chapter Eight</b>	142
<b>Conclusions and Future Work</b>	
1. Conclusions	142
2. Suggestions of Future Work	143
<b>Appendix One</b>	145
<b>Experimental Methods</b>	145
1. Apparatus for Optical Measurement	145
2. Apparatus for Electrical Conductivity Measurement	150
3. Experimental Techniques	152
<b>Appendix Two</b>	169
<b>Experimental Results</b>	
1. Results of the Rate Constant Measurements in <i>t</i> -Butanol/Water Mixtures	169
2. Results of the Rate Constant Measurements in 1-Butylamine/Water Mixtures	188
3. Results of the Electrical Conductance Measurements in <i>t</i> -Butanol/Water Mixtures	208
4. Results of Optical Absorption Spectrum Measurement in 1-Butylamine/Water Mixtures	229

## List of Tables

Table	Page
2-1. Symbols in Figures 2-1 to 2-4.....	45
2-2. Reaction Rate Parameters in <i>t</i> -BuOH/Water Solvents at 298 K.....	46
2-3. Estimated Values of $R_f$ (nm) in <i>t</i> -BuOH/Water Mixtures.....	49
3-1. Estimation of mobility of $e_s^-$ in <i>t</i> -butanol.....	67
3-2. Measured conductivities of HClO <sub>4</sub> and NH <sub>4</sub> ClO <sub>4</sub> ; estimated ionic conductivity of H <sub>g</sub> <sup>+</sup> in <i>t</i> -butanol.....	68
3-3: Comparison of mobilities of ions and solvated electrons with parameters in alcohols and water at 298 K.....	69
4-1. Reaction Rates and Parameters for $e_s^- + NO_{3,s}^-$ in C <sub>1</sub> to C <sub>4</sub> Alcohols at 298 K. ....	80
5-1. Arrhenius activation energies of viscosities and conductances of salts in some solvents at 298 K.....	94
5-2. Physical properties of salts at 298 K.....	95
5-3. $\Lambda_0$ of salts in <i>t</i> -butanol at different temperatures.....	96
6-1: Parameters of solvated electron spectra in 1-butylamine/water at 298 K.....	110
6-2. Half life of solvated electron in 1-butylamine/water mixtures at 298 K.....	111
7-1: Symbols for Figures 7-1 to 7-4.....	129
7-2: Reaction Rate Parameters in 1-Butyl amine/Water Mixed Solvents at 298 K.....	130

A-2-1. The values of $k_{\text{obs}}$ of the reactions of solvated electrons with ammonium nitrate in <i>t</i> -butanol/water mixed solvent.....	170
A-2-2. Temperature and composition dependences of $k_2$ for the reaction of $e_s^-$ with ammonium nitrate in <i>t</i> -butanol/water mixed solvents.....	173
A-2-3. The values of $k_{\text{obs}}$ of the reactions of solvated electrons with lithium nitrate in <i>t</i> -butanol/water mixed solvent.....	174
A-2-4. Temperature and composition dependences of $k_2$ for the reaction of $e_s^-$ with lithium nitrate in <i>t</i> -butanol/water mixed solvents.....	177
A-2-5. The values of $k_{\text{obs}}$ of the reactions of solvated electrons with perchloric acid in <i>t</i> -butanol/water mixed solvent.....	178
A-2-6. Temperature and composition dependences of $k_2$ for the reaction of $e_s^-$ with perchloric acid in <i>t</i> -butanol/water mixed solvents.....	181
A-2-7. The values of $k_{\text{obs}}$ of the reactions of solvated electrons with ammonium perchlorate in <i>t</i> -butanol/water mixed solvent.....	182
A-2-8. Temperature and composition dependences of $k_2$ for the reaction of $e_s^-$ with ammonium perchlorate in <i>t</i> -butanol/water mixed solvents .....	186
A-2-9. The values of $k_{\text{obs}}$ of the reactions of solvated electrons with lithium perchlorate in <i>t</i> -butanol/water mixed solvent.....	187
A-2-10. Temperature and composition dependences of $k_2$ for the reaction of $e_s^-$ with ammonium nitrate in <i>t</i> -butanol/water mixed solvents.. .....	187
A-2-11. The values of $k_{\text{obs}}$ of the reactions of solvated electrons with nitrobenzene in 1-butyl amine/water mixed solvent.. .....	188
A-2-12. Temperature and composition dependences of $k_2$ for the reaction of $e_s^-$ with nitrobenzene in 1-butyl amine/water mixed solvents .....	192

A-2-13. The values of $k_{\text{obs}}$ of the reactions of solvated electrons with acetone in 1-butyl amine/water mixed solvent.....	193
A-2-14. Temperature and composition dependences of $k_2$ for the reaction of $e_s^-$ with acetone in 1-butyl amine/water mixed solvents.....	196
A-2-15. The values of $k_{\text{obs}}$ of the reactions of solvated electrons with phenol in 1-butyl amine/water mixed solvent.. ..	197
A-2-16. Temperature and composition dependences of $k_2$ for the reaction of $e_s^-$ with phenol in 1-butyl amine/water mixed solvents.....	201
A-2-17. The values of $k_{\text{obs}}$ of the reactions of solvated electrons with toluene in 1-butyl amine/water mixed solvent.....	203
A-2-18. Temperature and composition dependences of $k_2$ for the reaction of $e_s^-$ with toluene in 1-butyl amine/water mixed solvents.....	206
A-2-19. The values of specific conductance ( $\kappa$ ) of perchloric acid in <i>t</i> -butanol/water mixed solvent.....	208
A-2-20. Temperature and composition dependences of molar conductivity ( $\Lambda_0$ ) of perchloric acid in <i>t</i> -butanol/water mixed solvents.. ..	211
A-2-21. The values of specific conductance ( $\kappa$ ) of lithium nitrate in <i>t</i> -butanol/water mixed solvent.....	212
A-2-22. Temperature and composition dependences of molar conductivity ( $\Lambda_0$ ) of lithium nitrate in <i>t</i> -butanol/water mixed solvents... ..	216
A-2-23. The values of specific conductance ( $\kappa$ ) of ammonium nitrate in <i>t</i> -butanol/water mixed solvent.....	217
A-2-24. Temperature and composition dependences of molar conductivity ( $\Lambda_0$ ) of ammonium nitrate in <i>t</i> -butanol/water mixed solvents... ..	220



A-2-25. The values of specific conductance ( $\kappa$ ) of ammonium perchlorate in <i>t</i> -butanol/water mixed solvent. ....	221
A-2-26. Temperature and composition dependences of molar conductivity ( $\Lambda_0$ ) of ammonium perchlorate in <i>t</i> -butanol/water mixed solvents.....	224
A-2-27. The values of specific conductance ( $\kappa$ ) of lithium perchlorate in <i>t</i> -butanol/water mixed solvent.....	225
A-2-28. Temperature and composition dependences of molar conductivity ( $\Lambda_0$ ) of lithium perchlorate in <i>t</i> -butanol/water mixed solvents.....	228
A-2-29 Parameters of Solvated Electron Spectra in 1-Butyl Amine/Water Mixed Solvents at Different Temperatures.....	229

## List of Figures

Figure	Page
2-1. Arrhenius plots of $k_2$ for the reaction of $e_s^-$ with $Li_s^+ + NO_{3,s}^-$ in <i>n</i> -butanol/water mixed solvents. ....	50
2-2. Arrhenius plots of $k_2$ for the reaction of $e_s^-$ with $NH_{4,s}^+ + NO_{3,s}^-$ in <i>t</i> -butanol/water. ....	51
2-3. Arrhenius plots of $k_2$ for the reaction of $e_s^-$ with $NH_{4,s}^+ + ClO_{4,s}^-$ in <i>t</i> -butanol/water. ....	52
2-4. Arrhenius plots of $k_2$ for the reaction of $e_s^-$ with $H_s^+ + ClO_{4,s}^-$ in <i>t</i> -butanol/water. ....	53
2-5. Solvent composition dependence of $k_2$ in <i>t</i> -butanol/water mixtures at 298 K. ....	54
2-6. Dependence of Debye $f$ on $\epsilon R_T$ for $Li_s^+ + NO_{3,s}^-$ and $NH_{4,s}^+ + ClO_{4,s}^-$ in <i>t</i> -butanol/water mixtures at 298 K. ....	55
2-7. $k_2/f$ in <i>t</i> -butanol/water mixtures at 298 K. ....	56
2-8. Composition dependence of $\Lambda_0$ in <i>t</i> -butanol/water at 298 K. ....	57
2-9. Solvent composition dependence of $r_d$ of <i>t</i> -butanol/water mixtures at 298 K. ....	58
2-10. Solvent composition dependence of apparent values of $\kappa R_T$ in <i>n</i> -butanol/water mixtures at 298 K. ....	59
2-11. Solvent composition dependence of $E_2$ and $E_{\Lambda_0}$ in <i>t</i> -BuOH/water mixtures. .	60
3-1. Arrhenius plots of $k_2$ ( $e_s^- + H_s^+$ ), Debye $f$ , $\mu_{H^+}$ , and $\mu_e$ in pure <i>t</i> -butanol solvent. ....	71
4-1. Correlations of $k_2$ with $\eta(A)$ and $E_T(B)$ in $C_1$ to $C_4$ alcohols and water at 298 K. ....	81

4-2.	Correlation of viscosity $\eta$ and dielectric relaxation time $\tau$ of C <sub>1</sub> to C <sub>4</sub> alcohols and water at 298 K, 323 K and 343 K.....	82
4-3.	Correlation of apparent $\kappa R_T$ values and $E_T/\tau$ in C <sub>1</sub> to C <sub>4</sub> alcohols and water at 298 K, 323 K and 343 K. ....	83
4-4.	Correlation of $C_\tau$ with $\tau$ (298 K) of C <sub>1</sub> to C <sub>4</sub> alcohols and water. ....	84
4-5.	Correlation of $p_\tau$ and $E_2-E_{\Lambda 0}$ with $k_2(e_s^- + NO_3^-_s)$ in C <sub>1</sub> to C <sub>4</sub> alcohols and water at 298 K.....	85
5-1.	Dependence of specific conductance of LiNO <sub>3</sub> on concentration in water/ <i>t</i> -butanol mixtures (100 to 70 mol % water) at different temperatures. ....	97
5-2.	Dependence of specific conductance of LiNO <sub>3</sub> on concentration in water/ <i>t</i> -butanol mixtures (50 to 0 mol % water) at different temperatures. ....	98
5-3.	Dependence of specific conductance of NH <sub>4</sub> ClO <sub>4</sub> , LiClO <sub>4</sub> , NH <sub>4</sub> NO <sub>3</sub> and LiNO <sub>3</sub> on concentration in pure <i>t</i> -butanol at different temperatures. ....	99
5-4.	Arrhenius plots of $\Lambda_0$ or initial slopes of salts in <i>t</i> -butanol, and of fluidity ( $1/\eta$ ) of <i>t</i> -butanol.....	100
5-5:	Temperature dependence of $\epsilon T$ of some solvents, normalized to the values at 298 K. ....	101
6-1.	Optical spectra of solvated electrons in 1-butylamine/water mixed solvents at 298 K. ....	112
6-2.	Composition dependence of $E_{Amax}$ and other parameters for mixed solvents at 298 K.....	113
6-3.	Composition dependence of $E_b$ , $E_T$ , $G\epsilon_{max} \times 30$ , $W_{1/2}$ , and $W_b/W_T \times 50$ in 1-butylamine/water mixtures at 298 K.....	114
6-4.	The temperature effect on $e_s^-$ optical spectra in pure 1-butylamine and the amine-rich mixtures with water. ....	115
6-5.	Temperature dependence of $E_{Amax}$ in 1-butylamine/water mixtures. ....	116

6-6.	Temperature coefficient ( $-dE_{Amax}/dT$ ) and viscosity in 1-butylamine/water mixtures. ....	117
7-1.	Arrhenius plots of $k_2(e_s^- + \text{nitrobenzene})$ in 1-butyl amine/water mixed solvents. ....	132
7-2.	Arrhenius plots of $k_2(e_s^- + \text{acetone})$ in 1-butyl amine/water mixed solvents. ....	133
7-3.	Arrhenius plots of $k_2(e_s^- + \text{phenol})$ in 1-butyl amine/water mixed solvents. ....	134
7-4.	Arrhenius plots of $k_2(e_s^- + \text{toluene})$ in 1-butyl amine/water mixed solvents. ....	135
7-5.	Solvent composition dependence of $k_2$ in 1-butyl amine/water mixed solvents at 298 K. ....	136
7-6.	Solvent composition dependence of $\eta k_2$ in 1-butyl amine/water mixtures at 298 K. ....	137
7-7.	Correlations of $k_2$ (phenol and toluene) with $-dE_{Amax}/dT$ in 1-butyl amine/water mixtures at 298 K. ....	138
7-8.	Solvent composition dependence of $E_2$ . ....	139
A-1-1.	The secondary emission monitor .....	162
A-1-2.	Path of analyzing light .....	163
A-1-3.	The temperature control of the water bath .....	164
A-1-4.	The temperature regulation system .....	165
A-1-5.	The bubbling system .....	166
A-1-6.	The sealing technique .....	167
A-1-7.	The typical solvated electron optical absorption trace .....	168

## Chapter One

### Introduction

Electron transfer is a basic process in many chemical reactions. The most fundamental electron transfer reagent is solvated electrons,  $e_s^-$ . Study of the behavior and properties of electrons is essential in chemistry.

A solvated electron ( $e_s^-$ ) is an excess electron in a liquid; the electron is in a localized state and in thermal equilibrium with the solvent molecules. Distinctive properties of solvated electrons in different liquids include the optical absorption spectrum (1), mobility (2), and reactivity with other substances (3). To seek understanding of the behavior and properties of electrons we study how these properties change when the solvent is changed.

In the present work, solvent effects on the reactivity of solvated electrons in strongly hydrogen-bonded mixed solvents, *t*-butanol/water, and less strongly hydrogen-bonded mixed solvents, 1-butyl amine/water, have been studied. In this introduction, I briefly summarize the properties of solvated electrons, the relevant properties of solvents, and chemical reactions of solvated electrons in different solvents.

#### 1. Solvation of Electrons

Blue solutions of sodium metal in liquid ammonia were made in 1864 by Weyl (4). These solutions were used as reducing agents. The reactive agent in the solutions was later identified by electrical conductivity to be the solvated electron (5). Later, solvated electrons were also found in other solvents such as amines (6), hydrocarbons (7), water (1) and alcohols (8). In most cases,  $e_s^-$  is produced by irradiating a material (usually a liquid) with ionizing radiation such as X- or  $\gamma$ -rays or high energy electrons.

Pulse radiolysis (3), combined with sensitive electrical conductance (9), or optical absorption (10) measurement instruments, is widely used in the study of the properties and behavior of  $e_s^-$ . In pulse radiolysis, a short pulse (ns -  $\mu$ s) of high energy electrons or X rays ( $\sim 0.1$  to 20 MeV) is used to irradiate a solvent, then the subsequent evolution of the electrical conductance or optical absorption of the system is observed. When high energy radiation penetrates a liquid, molecules are ionized, thereby producing energetic secondary electrons in local microzones (11) of ionized, excited and dissociated molecules. The reactive intermediates in these microzones dissipate in a few nanoseconds by reacting together or diffusing into the bulk of the liquid. The secondary electrons also lose their excess energy by ionization and excitation of the molecules in the medium. Once the energy of the electron is sufficiently lowered it can form a localized state in most liquids.

The electron localization process depends on whether the electron affinity of the liquid is positive or negative. If the molecules have positive electron affinity the electron gets localized on a solvent molecule and forms a negative ion (12, 13). If it is negative, localization is affected by the polarity of the molecules: (i) an electron in a polar solvent gets trapped in a coulombic potential well created by several molecular dipoles; (ii) in a nonpolar solvent, electron localization occurs due to nonspherical shape and anisotropic polarization of the molecules. If the molecules are isotropically polarizable, the electron remains delocalized and is very mobile (14).

An electron polarizes electronically the adjacent medium in about  $10^{-15}$  s. When an energetic delocalized electron becomes localized, it immediately finds itself in an electronically polarized potential well (trap) (15). The electric field of the electron then causes the molecular dipoles to reorient. The trap becomes deeper. The time for this process is related to the dielectric relaxation time of the medium (16). It takes about a picosecond for the trapped electron to relax into the solvated state in water (15, 17-19).

## 2. Properties of Solvated Electrons

Solvent structure (solvent molecular structure and molecular packing) and polarity of the solvent molecules affect the physical and chemical properties of  $e_s^-$ . The properties of  $e_s^-$  can be studied by 1) mobility, 2) optical absorption, and 3) reactivity.

### 2.1. Mobility of Solvated Electrons

Pulse radiolysis-conductivity studies provide data on the mobility of  $e_s^-$  in hydrocarbons (20-23), water (24), and others (25-30). The mobility of  $e_s^-$  is strongly dependent on the structure and properties of solvents (30). In water the mobility of  $e_s^-$  is  $19 \times 10^{-8} \text{ m}^2/\text{V}\cdot\text{s}$  (24), which is close to that of hydroxide ions and smaller than that of protons (24, 25). However, the activation energy of diffusion of  $e_s^-$  in water is 20 kJ/mol, which is larger than the 15 kJ/mol for diffusion of hydroxide ions in water (24). This indicates that the diffusion mechanism of  $e_s^-$  is not quite the same as that of hydroxide ions. In methanol and ethanol, the mobility of  $e_s^-$  is close to that of alkoxide ions ( $\text{RO}^-$ ) (26-28). From ethanol to butanol, the mobility seems to increase (29). In nonpolar liquids the mobilities depend strongly on the structure of the solvent molecules, and are usually several orders of magnitude greater than those of ordinary ions (20, 30).

### 2.2. Optical Absorption Spectrum

Optical absorption spectra of  $e_s^-$  in various solvents have been extensively studied during the last thirty years. Solvated electrons can absorb light at wave lengths ranging from visible to infrared and, depending on the nature of the solvent, the lifetime of  $e_s^-$  can be very long, as is the case in liquid ammonia, or very short as is the case in amines.

### 2.2.1. Energy and Shape of the Optical Absorption band of $e_s^-$

The first optical absorption spectrum of  $e_s^-$  in water was obtained by pulse radiolysis in 1962 (1). It has a peak at 715 nm at 25°C with  $G\epsilon_{Amax} = 8.3 \times 10^{-21} \text{ m}^2/16 \text{ aJ}$  (that is,  $5.0 \times 10^4 e_s^- \cdot L/100 \text{ eV} \cdot \text{mol} \cdot \text{cm}$ ) (31, 32), where  $e_s^-$  yield  $G(e_s^-/16 \text{ aJ}$  or  $e_s^-/100 \text{ eV}$  in old unit) is the number of  $e_s^-$  produced for each 16 aJ or 100 eV of dose absorbed in a solvent and  $\epsilon_{Amax}$  ( $\text{M}^{-1}\text{cm}^{-1}$ ) is the molar extinction coefficient at the wavelength of maximum absorbance. The absorption band lacks fine structure, has a long tail extending to higher energies. The energy at the absorption maximum,  $E_{Amax}$ , and the width of the band depend on the polarity and the structure of the solvent (33-35).

The value of  $E_{Amax}$  is the most characteristic feature. It represents the extent of a solvated electron being trapped in a potential well. In general, the higher the value of  $E_{Amax}$ , the deeper the potential well, therefore, the stronger the interaction between the electron and the dipoles of the solvent molecules. The  $E_{Amax}$  value of  $e_s^-$  in a solvent depend on many factors such as the Kirkwood structure factor,  $g_k$  value (33, 36) which is calculated from the dielectric constant, dipole moment and density to measure the short range interaction of solvent molecules (37), the types and number of functional groups, and the number of alkyl groups attached to the functional group (35, 38). In polar solvents such as water, alcohols (39), ammonia (35, 40), and amines (35, 41), the energy of maximum absorption  $E_{Amax}$  lies in the visible to near-infrared regions. Some optical spectra of  $e_s^-$  have also been measured in aliphatic amine glasses from 4 to 77 K(42) and  $E_{Amax}$  is in the near-infrared regions. In nonpolar hydrocarbons the measurements of some optical spectra of  $e_s^-$  have been carried out in glasses (43-45) because the  $E_{Amax}$  is very low at room temperature.

Values of  $E_{Amax}$  are dependent on the temperature and density of the medium. Thermal agitation of the solvent molecules makes the traps shallower. Therefore, values of  $E_{Amax}$  decrease with increasing temperature (39).



The  $e_s^-$  absorption band has a similar form in a wide range of solvents: it is always broad and asymmetric, skewed to higher energies. The absorption band of  $e_s^-$  in pure water is relatively symmetrical with some skewing towards the high energy range (32), but in alcohols (39, 46) it becomes more and more asymmetrical on going from methanol to butanols. The asymmetry and breadth of the absorption band, and the lack of fine structure, are due to both homogeneous (41, 47) and heterogeneous broadening (48, 49) effects. Since both factors play a role, we say that the band is nonhomogeneously broadened.

### 2.2.2. *Transitions*

There are many studies (50-54) on the transitions involved when photons are absorbed by the ground state  $e_s^-$ . It has been suggested that they are (i) bound to bound transitions (50), (ii) bound to continuum transitions (51), (iii) bound to bound and bound to continuum transitions (52-54), and (iv) trap to trap transitions (52, 53).

The broad, asymmetrical absorption band of  $e_s^-$ , with skewing tail into the high energy region, indicates that the optical absorption is not due to any single transition. The absorption band results from a distribution of various transitions. By estimating the threshold energy  $E_{th}$  for photo conductivity and comparing it with the characteristics of the optical absorption spectrum as a whole, an idea of the extent of bound to continuum transitions in the absorption spectrum can be obtained (54-58). Both bound to bound and bound to continuum transitions contribute to the spectrum. In a glassy solid of water it has been found that  $E_{th}$  (1.38 eV) is less than  $E_{Amax}$  (1.86 eV) of solvated electron(55). In general we can say that the absorption in the energy range higher than  $E_{Amax}$  is mainly due to bound to continuum transitions, and in the energy range lower than  $E_{Amax}$  is mainly due to bound to bound (often assumed to be similar to 1s to 2p) transition(59).

### 2.2.3. *Optical Absorption in Hydroxylic Solvents and Mixed solvents*

Many studies of the optical spectra of  $e_s^-$  have been done in water (1, 32), alcohols (38, 46, 60), amines (35, 61, 62), ethers (36, 63) and other solvents (34, 63), as well as mixed solvents (39, 47, 64, 65). The values of  $E_{Amax}$  in water, alcohol and their mixtures are greater than those in other polar solvents such as ammonia, amines and ethers, because of the electron interaction with the larger dipole moment of the O-H bond (33).

The  $E_{Amax}$  values of  $e_s^-$  in alcohols are in the order: primary > secondary > tertiary (39, 66). The  $E_{Amax}$  values are almost independent of the chain length for primary alcohols (67), because the alkyl group beyond the  $\alpha$ -carbon has not much effect on the interaction between the electron and the solvent (33, 67, 68). A weaker orientational alignment of solvent dipoles in secondary and tertiary alcohols around the electron is probably the reason for the lower  $E_{Amax}$  values (steric hindrance).

The widths of  $e_s^-$  absorption band at half height ( $W_{1/2}$ ) in alcohols are about twice that in water (63). The  $W_{1/2}$  values in amines are also about twice that in ammonia (35) which has a little higher value of  $W_{1/2}$  than that in water (35). In alcohols (63), bound to continuum transitions have been considered as the major contributor to the absorption spectra of  $e_s^-$ . The extent of bound to bound transition depends on the type of alcohol (56, 63).

In a binary solvent mixture system, the absorption band shapes, the values of  $E_{Amax}$  and band width are strongly dependent on the solvent structure (39, 47, 65) and usually lie between the two extreme values of pure solvents. In alcohol/water mixtures (39) the solvent composition dependence shows that electrons are selectively solvated by water molecules from water up to 10 mol% water. The minimum of  $E_{Amax}$  and  $W_{1/2}$  in primary alcohol/water mixtures such as 1-propanol/water indicates that a special structure is formed in the mixed solvent resulting in minimum interaction between electron and solvent O-H groups (39). The shape of the absorption bands in some amine mixed

solvents can be explained by a two-absorber model (47, 65, 69) based on a solvated solvent-anion (12, 13, 70).

### 2.3. Models of $e_s^-$

Appropriate models and calculations for  $e_s^-$  require computations with a supercomputer. Therefore, the models of  $e_s^-$  that emerged before 1980s are now inadequate.

Historically, the earliest model assumed that a solvated electron was confined in a spherical cavity with infinite potential walls(71). Jortner's continuum model (72) of electrons in ammonia considers the effect of medium polarization produced by the electrons. The solvent is viewed as a dielectric continuum around a cavity that contains the electron (72). Calculations of  $E_{Amax}$  can be adjusted to the observed values for ammonia (72) by using adjustable parameters. Semi-continuum models (73) assume that the electron is at the center of a spherical cavity surrounded by a solvation shell of a fixed number of solvent molecules, and that the solvent beyond the solvation shell is a dielectric continuum. Calculated values of  $E_{Amax}$  can be adjusted to the observed values in liquid ammonia and water (73). However, the line shape calculated from these models is more narrow and symmetrical than observed.

In the last ten years, with the development of supercomputation and new algorithm techniques, some progress has been made in simulation calculations of molecular dynamics around an electron in liquid. Chandler's model (74-77) considers an electron dissolved in a fluid of simple atomic particles, and assumes that the electrons inside each solvent particle satisfy a closed shell structure. The free thermal electron is repelled from the neighborhood of each atom by the exclusion principle, but there are also attractive polarization interactions. Based on this model, the reference interaction site method (RISM) polaron theory has been applied to the prediction of the optical absorption spectrum (76) and diffusion behavior (77).

M. J. Klein's group simulated the optical absorption spectrum and diffusion of  $e_s^-$  in ammonia (78-83). The path integral Monte Carlo calculations were used to monitor the energy and certain other distribution functions which characterize the local structure around the solvated electron. Combined with the staging algorithm to sample the quantum paths of the electron, the charge distribution of the electron in liquid ammonia was calculated (78, 79). However, compared to the measured absorption spectrum of  $e_s^-$  in ammonia (84), the calculated spectrum was in a higher energy range (78, 81). They also studied the adiabatic dynamics of an electron in liquid ammonia by means of a molecular dynamics technique for the coupled electron-solvent system (81, 82). The calculated diffusion coefficient for  $e_s^-$  in ammonia was about 1/3 of the measured one (82). The difference between the calculations and the experiment is likely due to the contribution of nonadiabatic effects in the transport of the electron and some of the less realistic features in the models used for both the solvent and the electron solvent interactions.

P.J. Rossky's group's first study of electron trapping in pure water only explored the existence of "trapping sites," probing the sites with a "test charge" to evaluate the capacity of the traps to host an electron (85). But they could only simulate electronically adiabatic relaxation of the ground state in a water bath. The results did not match experimental observations (86). Later on, Rossky's group developed a new algorithm for the quantum dynamical simulation of a mixed classical-quantum system that rigorously includes nonadiabatic quantum transitions and applied the new method to the problem of the solvation dynamics of an initially energetic excess electron in liquid water (87-89). Computed results revealed that there were two possible routes for the solvation of an initially energetic (2eV) quasifree excess electron (86). The simulation results based on these two routes are generally consistent with experimental optical absorption observations in water (88). Murphrey and Rossky also combined the classic flexible water model (90, 91) in the nonadiabatic molecular dynamics simulation of the optical

absorption spectrum of  $e_s^-$  in pure water and the results are generally consistent with experimental observations (92).

### **3. Structure and Properties of Water, Alcohol, Amines, and Mixed Solvents**

#### **3.1. Structure and Properties of Water**

The structure of liquid water has been extensively studied by X-ray, neutron, and electron diffraction measurements and modern spectroscopic techniques (93). Based on experimental results, statistical mechanical calculations (94) and computer simulation (95) have been carried out to build models for the structure of liquid water.

According to the earliest model based on radial distribution functions, liquid water was considered to have a "broken down" ice structure (96). In the solid state, each water molecule is hydrogen bonded tetrahedrally to four other molecules. The distribution functions of water (97, 98) indicate slightly more than four nearest neighbors. Since this early model, numerous models have been proposed for the structure of water. These models fall into two broad categories: (i). uniformist models (99-102); and (ii). mixture models (103-106).

According to the uniformist models, water consists of a single type of three-dimensional random hydrogen bond network. There is no significant amount of monomer water. Water is treated as a simple chemical equilibrium between free and hydrogen-bonded hydroxyl groups. The structure is visualized as a network of cavities and the structural order as only short range with local structure being approximately tetrahedral.

The mixture models assume that water consists of a mixture of two or more species. These are water molecules with no hydrogen bonds or with up to four hydrogen

bonds. The hydrogen bonded water molecules form an open network full of cavities or clusters of water molecules. These exist in equilibrium with monomer water and clusters, which make the medium denser than ice.

Recent efforts have focused on exploring the feasibility of long-lived clusters of water molecules to account for the observed large heat capacity of liquid water and a simple two-structure model for liquid water has been proposed (107). In this model, the structure of water is considered as primarily a mixture of tetramers and octamers.

However, no single model has yet explained all the properties of water.

### **3.2. Structure and Properties of Alcohols**

The liquid structures of alcohols are simpler than those of water because there is only one hydroxyl group per molecule. The hydroxyl groups in alcohols can hydrogen bond with each other. Alcohols have the ability to form up to three hydrogen bonds per molecule. Water, on the other hand, can form up to four hydrogen bonds. Various spectroscopic studies have shown that monomers, dimers, and polymers all exist (108-110).

Alcohols form chain or ring structures with approximately two hydrogen bonds per molecule. Alcohols with larger alkyl groups tend to exist mainly as monomers and ring-like polymers because of the steric hindrance (111). Lower alcohols can make a third hydrogen bond which leads to a three-dimensional linkage of polymer chains (112, 113).

### **3.3. Structure and Properties of Alcohol/Water Mixtures**

Since an alcohol contains both a hydrophilic hydroxyl group and a hydrophobic alkyl group, it shows strong composition-dependent physical properties in alcohol/water mixtures. The amount of hydrogen bonding between the alcohol hydroxyl group and water molecules depends on the sizes of the hydrophobic alkyl groups and the number of

hydrophilic hydroxyl groups in the alcohols. Alcohols that contain less than four carbon atoms are completely miscible with water. As the hydrophobic alkyl group becomes larger the solubility decreases (114). The sphere-like molecules of *t*-butanol are completely miscible with water, but the other isomers 1-, 2-, and *iso*-butanol are miscible only in the approximately ranges up to ~50 mol% water in butanol and up to ~2 mol% butanol in water (115).

### 3.3.1. Kirkwood structure factor, $g_k$

Information about the short range interactions in a liquid can be obtained from the Kirkwood structure factor,  $g_k$  which is calculated from the dielectric constant, dipole moment and density (37). In water and primary alcohols the  $g_k$  values are greater than unity (33, 35, 116, 117). The value of  $g_k$  increases with increasing chain length for primary alcohols because the alcohols with longer chains are better aligned. Small alcohols can form a third hydrogen bond cross-linking the polymer chains. This must be the reason for its lower  $g_k$  value, because of the difficulty of alignment. The  $g_k$  values increase slightly when water is added to methanol or tertiary alcohols (117, 118). Water can make hydrogen bonds with those alcohol molecules resulting in a better linear arrangement of dipoles. Thus water has a structure-building effect in these cases. On the other hand, the  $g_k$  values decrease when water is added to other alcohols (117), and water acts as a structure breaker in these alcohols.

### 3.3.2. Thermodynamic Properties and Hydrogen Bonds

The thermodynamic functions of mixing of alcohols and water gives useful information in the study of the structure of alcohol/water mixtures (119-121). The extent of change depends on the alkyl group. By mixing water and alcohols, if hydrogen bonds are formed, a negative enthalpy of mixing is obtained; a positive enthalpy of mixing indicates the rupture of hydrogen bonds in the mixture.

When a small amount of a small alcohol is dissolved in water a decrease in enthalpy and entropy results. The interpretation is that: (i) the alcohol molecule promotes water-water hydrogen bonding (122, 123); or (ii) water molecules order around the alcohol molecule and form clathrate-like structures (124). Therefore, the structure of water is strengthened by adding of small amount of alcohol molecules in this case (121, 123). The enthalpy of mixing of higher alcohols with water is positive (endothermic), water acts as a structure breaker (119, 120).

### 3.3.3. *Viscosity*

The viscosity of a single liquid component is related to the rate of diffusion in the liquid. The viscosity is higher in alcohols with longer and/or branched alkyl groups. The bulkiness of the alkyl group makes it difficult to flow.

Viscosities are strongly composition dependent in mixtures of alcohol and water. The following are the important qualitative features of viscosity of completely miscible alcohol/water mixtures (106, 125-127): (i) A maximum in viscosity occurs at a composition around 75 mol% water; (ii) a sharp increase in viscosity occurs when a few mole percent of alcohol is added to water; (iii) only small changes in viscosity occur in the alcohol-rich region.

The increase of viscosity when a little alcohol is added to water is perhaps due to clathrate-like structure formation (124).

When a little water is added to the small alcohols, water acts as a structure maker, indicated by an increase in viscosity. Viscosity decreases when water is added to larger alcohols, which can be explained by the formation of water-nucleated alcohol complexes (39, 120); or by the breakdown of alcohol structure by water (128).



#### 3.3.4. Dielectric Relaxation Times

Dielectric relaxation time is related to the reorientation of molecular dipoles along the applied field direction in a liquid. Water has a single dielectric relaxation process, with a dielectric relaxation time ( $\tau$ ) equal to  $10^{-11}$  s at normal temperature and pressure. There are three relaxation times in alcohols(129): (i)  $\tau_1$ , the time required for the breaking of intermolecular hydrogen bonds and reorientation of the molecule; (ii)  $\tau_2$ , the reorientation time of a free monomer; and (iii)  $\tau_3$ , the reorientation time of free -OH dipoles.

The process that relates to the liquid structure is associated with  $\tau_1$ . This is called the primary relaxation process. The reorientation of larger alcohol molecules depends on the steric hindrance of the alkyl group and the hydrogen bonds (130). Reorientation of these molecules needs the cooperation of the other molecules. Small alcohol molecules display relatively small steric effects, hence reorientation depends mostly on hydrogen bond breaking; relaxation times in these alcohols are shorter.

When a small amount of water is added to an alcohol at room temperature, the dielectric relaxation time varies as follows: (i) In a small alcohol such as methanol, it increases slightly (131); (ii) in other lower alcohols it decreases (132).

Dielectric relaxation times decrease and viscous flow become easier when temperature increases. This is because of the increasing thermal agitation of the molecules. In a liquid under constant pressure the increase agitation energy also increases the amount of free space between molecules, so the liquid density decreases with increasing temperature and the amount of steric hindrance decreases.

### 3.4. Structure and Properties of Amine/Water Mixtures

Similar to an alcohol, an amine consists of an alkyl group and a polar group in this case -NH<sub>2</sub>. Amines are weak bases ( $pK_a = 10.6$  for 1-butyl amine in water at 298 K (133)), and can also form hydrogen bonds within themselves and with water molecules.

However, the hydrogen bonding is weaker than that in alcohols and water because nitrogen is less electronegative than oxygen and the N-H bond is less polar (134, 135). This is supported by the lower solvation enthalpy of amines in water than that of alcohols (136), and by the smaller  $g_k$  factors (33, 35, 137) than alcohols. The primary C<sub>1</sub> - C<sub>5</sub> amines are completely miscible with water (138). Dielectric constants of amines (137, 139) are lower than those of the corresponding alcohols (at 298 K, for 1-butyl amine  $\epsilon = 4.6 - 4.8$  (137, 140), whereas for 1-butyl alcohol  $\epsilon = 17.1$ (141)). The relaxation times ( $\tau$ ) of amines (137, 139) are also lower than those of the corresponding alcohols and even lower than that of water. For example, at 298 K  $\tau_1$  for 1-butyl amine is about 4 ps (137) whereas for water it is 8.3 ps and for 1-butanol 479 ps (142). At 293 K the relaxation time of amine increases from propylamine (3.05 ps) to the maximum of heptylamine (9.07 ps), and then it decreases with increasing number of carbon atoms in the amine(137). This behavior is independent of temperature. This indicates that the rotation of -NH<sub>2</sub> group is the main contribution to the relaxation time. For alcohols, the relaxation time  $\tau_3$  which is considered as the reorientation time of free -OH dipoles (129) increases continuously from 2.12 ps (n-propanol) to 2.35 ps (1-butanol) to 3.87 ps (1-dodecyl alcohol) (129). The low relaxation times of amines indicate that because of the weaker hydrogen bonds the hindrance to the free rotation of -NH<sub>2</sub> group is lower than that in alcohols, and the intramolecular rotation is the predominant mechanism (137) . It has been suggested (137, 143) that when there are more than three carbon atoms in the aliphatic chain of primary amines a molecular spiral conformation is formed by a hydrogen bond between the N atom and an H-atom on the fourth carbon of the amine. This spiral conformation is called a Newman coil. However, this structure is unlikely predominant in amines because of the weak hydrogen bonding.

Though various physicochemical properties of aqueous solutions of alcohols and amines show similarity, there are some differences. For example, alcohols produce a rise in the temperature of maximum density of water, while amines lower it (144, 145).

Further, solid clathrate hydrates have been isolated from some amines (146, 147), but not for alcohols. The study of the limiting excess volumes of alcohols and amines in aqueous solution shows that water-structure-compatible O-H group reinforces water structure, while NH<sub>2</sub> group disrupts it due to its inability to participate in cooperative hydrogen bonding with water. Therefore, the amine group acts as a structure breaker (148).

The study of compressions and densities of C<sub>1</sub>-C<sub>4</sub> amine/water mixed solvents (149) found that the compressibility has a minimum in the region from 98.3 (1-butyl amine) to 88 mol% water (methyl amine), and partial molar volumes also have a minimum in the region from 99.1 (1-butyl amine) to 88 mol% water (methyl amine).

The viscosities of amine/water solutions follow a different pattern from that of alcohol/water solutions. The viscosity of 1-butyl amine/water mixed solvent at 298 K increases from water (0.89 mPa·s) to the maximum at 20 mol% water (2.4 mPa·s) and then decreases to 0.47 mPa·s in pure 1-butyl amine (150, 151). For *t*-butyl alcohol/water mixed solvent at 298 K, the viscosity increases from water (0.89 mPa·s) to the maximum at 30 mol% water (4.98 mPa·s), which is about double of the maximum in 1-butyl amine solution, and then decreases a little to 4.2 mPa·s at 10 mol% water and increases back to 4.5 mPa·s in pure *t*-butyl alcohol (152). The viscosity in *t*-butyl alcohol is almost 10 times of that in 1-butyl amine. This indicates that liquid 1-butyl amine is much less hydrogen-bonded than the alcohol.

#### 4. Reactivity of Solvated Electrons

Besides the optical absorption spectra and mobility of solvated electrons, the study of the reactivity of e<sub>s</sub><sup>-</sup> with solutes in various solvents is another way to learn the properties of e<sub>s</sub><sup>-</sup>. The reactivity of e<sub>s</sub><sup>-</sup> depends on the nature of the coreactant (153-157)

and the nature of the solvent (158-160). Some reactions are fast and near diffusion-controlled, and some are slow.

The reactions of  $e_s^-$  with various solutes in water have been extensively studied (156, 157, 161-165). Depending on the coreactants (161-163), some are diffusion-controlled, such as the reaction of  $e_s^-$  with nitrobenzene (164), and some are slower, such as the reaction of  $e_s^-$  with  $S_2O_3^{2-}$  (164). Some reactions of  $e_s^-$  with solutes such as  $N_2O$ , or  $NO_2^-$  can change from non-diffusion-controlled to diffusion-controlled reactions as the temperature increases (157).

The kinetics of  $e_s^-$  reactions have been also studied in nonpolar solvents (166-173). The electron mobility and reaction rates are influenced by the solvent molecular structure. Electron mobility is larger in liquids of sphere-like molecules than in those of nonspherical molecules (20, 21). The probability of reaction per encounter of  $e_s^-$  with  $N_2O$  is much smaller in liquids of spherical molecules such as xenon or methane than in those of nonspherical molecules such as cyclohexane (167). When  $N_2O$  captures an electron, the molecular shape changes from linear to bent. The change of shape requires time, say a ps, so the probability of electron capture increases with the duration of the encounter up to several ps. Allen and Holroyd studied electron reactions in nonpolar solvents by conductance measurement. They found that usually the rate constant increases with mobility, but the reverse occurs when the encounter efficiency decreases more than the mobility increases (168, 174).

Holroyd's group studied the pressure effect on the electron reactions with solutes such as  $CO_2$  and 1,3-butadiene in toluene (175). The rates of the reactions of  $e_s^-$  with solutes in toluene are much faster than that expected for diffusion-controlled reactions of the ordinary ions, and the reaction rates are pressure-independent. The results confirmed that toluene attaches an electron to form an anion, and the high reactivity and high mobility of electrons in toluene are due to a hopping mechanism (175-

178). When toluene is in dilute solute in n-pentane, toluene reversibly attaches an electron, and the anion is more stable at high pressures, above 100 MPa (176).

Solvent effects are also shown in the reactions of  $e_s^-$  in alcohols (153, 154, 179-182). In  $C_1 - C_{10}$  normal alcohols, reactions of  $e_s^-$  with  $H_s^+$ ,  $Ag_s^+$  (180, 182), and phenanthrene (181, 183) have the relation  $k_2 \propto \eta^{-1}$  ( $\eta$  is viscosity of solvent). These reactions are diffusion-controlled and follow the Smoluchowski-Debye-Stokes model (184, 185). However, for the reaction of  $e_s^-$  with nitrate ion in  $C_1 - C_{10}$  normal alcohols (160, 182)  $k_2$  increases as  $\eta^{+1}$  indicating the participation of solvent molecules in the reaction (158, 160, 182).

The reaction rates of  $e_s^-$  are also affected by branching the alkyl groups of alcohols. For example, on going from  $CH_3OH$  to  $C_2H_5OH$  to  $2-C_3H_7OH$  to  $t-C_4H_9OH$  (154),  $k_2$  for inefficient scavengers increases and for efficient scavengers decreases in that order. The former is due to the decrease of electron trap depth ( $E_{Amax}$ ), and the latter is due to the increase of solvent viscosity (diffusion coefficients).

The reactions of  $e_s^-$  have been studied in methanol or ethanol/water (27, 153, 186-188), isomeric propanol/water (189-191), and isomeric butanol/water mixed solvents (159, 160, 192-195). The reaction is strongly dependent on the solvent structure (both molecular structure and molecular packing). For example, in the reaction of  $e_s^-$  with nitrate ion, the solvent molecules participate in the reaction, and the molecular structure of solvent affects the rate constant; the more branched and the bigger the solvent molecule, the higher is the rate constant (158, 160, 182). Solvent structure and solvation of both the electron and solutes such as  $NH_{4,s}^+$  (159, 160) differ in different regions of the mixed solvent, and this has a strong influence on the reaction rates. The reaction rate of  $e_s^-$  with  $NH_{4,s}^+$  in the water-rich region is much lower than that in the alcohol-rich region (159, 160). This is attributed to  $NH_{4,s}^+$  being symmetrically solvated in water, and difficult to access by  $e_s^-$ , but unsymmetrically solvated in alcohol, which apparently facilitates the attachment of  $e_s^-$  (159).

Two types of models have been applied to the kinetics of the reactions of  $e_s^-$  in hydroxylic solvents.

i) Smoluchowski-Debye model (184, 196) and its modifications (159, 191, 193, 197). This model connects the rate constant with bulk physical properties of the solvent, the relative permittivity  $\epsilon$  and viscosity  $\eta$ . If a reaction of  $e_s^-$  is diffusion-controlled, it follows the Smoluchowski-Debye equation:

$$[1] \quad k_2 = 4\pi N_A (D_e + D_s)(R_e + R_s)f = 4\pi N_A (D_e + D_s)R_r f,$$

where  $k_2$  is the rate constant,  $N_A$  is Avogadro's constant,  $D_e$  and  $D_s$  are the diffusion coefficients for  $e_s^-$  and reactive solute,  $R_e$  and  $R_s$  are the reaction radii,  $R_r$  is the average center-to-center reactant separation when reaction occurs, and  $f$  is the Debye factor which is given by:

$$[2] \quad f = \frac{x}{(e^x - 1)},$$

$$[3] \quad x = -\frac{Z\xi}{4\pi\epsilon_0\epsilon R_r k_B T},$$

where  $x$  is the ratio of the coulombic energy of the reactants at  $R_r$  to thermal agitation energy  $k_B T$ , and  $\epsilon$  is the relative permittivity of the medium between the reactants at separation  $R_r$ , and  $Z$  is the charge on a charged solute or the dipole moment of a neutral solute.

In the most cases the diffusion coefficient of  $e_s^-$  is unknown, so a modified model is used. The Stokes-Einstein relation (197) for the diffusion coefficient  $D$  of a spherical particle of radius  $r$  at temperature  $T$  is

$$[4] \quad D = \frac{k_B T}{6\pi\eta r} \quad .$$

We insert eq. [4] into eq. [1] and introduce factor  $\kappa$ , the probability that reaction occurs during one encounter (159, 191, 194) for reactions slower than diffusion-controlled, and obtain

$$[5] \quad k_2 = \frac{N_A k_B T}{1.5\eta} \left( \frac{1}{r_e} + \frac{1}{R_s} \right) (R_e + R_s) \kappa f = \frac{N_A k_B T}{1.5\eta} \cdot \frac{1}{r_d} \cdot f \kappa R_r \quad .$$

Here  $r_d$  is the effective hydrodynamic radius for mutual diffusion of  $e_s^-$  and solute, and  $\kappa R_r$  is considered as an effective reaction radius (159, 191, 194) . This is the Smoluchowski-Debye-Stokes-Einstein model(127, 190, 193). From equation 5 we can see that if a reaction is diffusion-controlled,  $\kappa \approx 1$  and  $k_2 \propto \eta^{-1}$ , as in the case of the reactions of  $e_s^-$  with nitrobenzene in alcohol/water mixtures (127, 187, 189, 192, 193), and with some ions in a series alcohols (180-183, 195).

For the reactions of  $e_s^-$  with ions eq. 5 can be simplified by using the measured electrical conductivity of the electrolyte. The Einstein-Nernst equation is(198):

$$[6] \quad \lambda_i = \frac{z_i^2 D_i F^2}{RT} \quad ,$$

where  $\lambda_i$  is the molar conductivity of ion  $i$  or electron  $e$ ,  $z_i$  is the number of charges of the ion,  $F = N_A \xi$  is the Faraday constant, and  $R = N_A k_B$  is the gas constant. Combining eqs.[1] and [6], we get the Smoluchowski-Debye-Nernst-Einstein model (160, 182, 194):

$$[7] \quad k_2 = \frac{4\pi k_B T}{\xi^2} (\lambda_e + \lambda_i/z_i^2) \kappa R_r f \quad ,$$

which can be rearranged to

$$[8] \quad \kappa R_r = 1.48 \times 10^{-16} k_2 / f(\lambda_e + \lambda_i/z_i^2) T \quad .$$

By measuring  $k_2$  and molar conductivity of  $e_s^-$  and ions we can determine  $\kappa R_r$ . In most solvents the value of  $\lambda_e$  is not known and is approximated (160, 182, 195).

ii) For inefficient reactions, with  $\kappa \ll 1$ , an electron trap-depth model is sometimes used to interpret the reaction rates (154, 155, 192, 193). This model considers the solvation energy of the electron. The optical absorption energy of  $e_s^-$  is a measure of the electron solvation energy (solvent trap depth) (199). The  $k_2$  values are correlated with the shallower traps in the depth distribution. As a measure of smaller trap depths, we use the energy  $E_r$  on the low energy (red) side of the absorption band at half the maximum absorbance. In some reactions of  $e_s^-$ , the rate constant increases as  $E_r$  decreases.

Most reactions of  $e_s^-$  follow the Arrhenius relation (157):

$$[9] \quad k_2 = A_2 e^{-E_2/RT} \quad ,$$

where  $A_2$  is the frequency factor and  $E_2$  the activation energy for the reaction. Information about the activation energy is useful to help understand the reaction mechanism. If the reaction is diffusion-controlled, the activation energy  $E_2$  is usually similar to the activation energy  $E_\eta$  of solvent viscosity. If the value of  $E_2$  is very different from that of  $E_\eta$ , the reaction is far from diffusion-controlled, or the activation energy for  $e_s^-$  diffusion is high.



## 5. Present Work

In this work we study the reactions of  $e_s^-$  with some ions of widely differing reactivity ( $\text{NO}_{3,s}^-$ ,  $\text{NH}_{4,s}^+$ , and  $\text{H}_s^+$ ) in the whole region of *t*-butanol/water mixtures, to further understand the solvent effects. The reaction rates were measured as functions of temperature. Electrical conductivity of the corresponding electrolytes were also measured in *t*-butanol/water mixed solvents to obtain information about the ion diffusion coefficients. This, combined with the  $e_s^-$  rate constants, led us to estimate a relatively large mobility of  $e_s^-$  in pure *t*-butanol.

The unusual changes of rate constant of  $e_s^-$  with  $\text{NO}_{3,s}^-$  in C<sub>1</sub> - C<sub>4</sub> alcohols, which *increase* with increasing liquid viscosity, was examined.

To obtain information about the properties of  $e_s^-$  in solvents, that are less hydrogen-bonded than are alcohol/water solvents, amine/water mixed solvents were studied: the optical absorption spectrum of  $e_s^-$  and the reactivity of  $e_s^-$  with organic solutes (nitrobenzene, acetone, phenol and toluene) in 1-butyl amine/water mixed solvents. The behavior of  $e_s^-$  in amine/water solvents was found to be quite different from that in alcohol/water solvents. A new area of fruitful investigation has been opened.

## References

- 1 E. J. Hart and J. W. Boag. *J. Am. Chem. Soc.* **84**, 4090 (1962).
- 2 K. H. Schmidt and W. L. Buck. *Science*. **151**, 70 (1966).
- 3 L. M. Dorfman and M. S. Matheson. *In Progress in Reaction Kinetics*. Vol. 3. Edited by G. Porter. Pergamon Press, London. 1965.
- 4 W. Weyl. *Ann. Phys.* **121**, 601 (1864).
- 5 C. A. Kraus. *The Properties of Electrically Conducting System*. Chemical Catalogue Co., New York. 1922. p. 375.
- 6 G. W. A. Fowles, W. R. McGregor, and M. C. R. Symons. *J. Chem. Soc.* 3329 (1957).
- 7 G. R. Freeman. *J. Chem. Phys.* **38**, 1022 (1963).
- 8 J. E. Bennet, B. Mile, and A. Thomas. *J. Chem. Soc. (A)*. 1393 (1967).
- 9 P. G. Fuoichi and G. R. Freeman. *J. Chem. Phys.* **56**, 2333 (1972).
- 10 J. P. Keene. *J. Sci. Instrum.* **41**, 493 (1964).
- 11 G. R. Freeman. *In Kinetics of Nonhomogeneous Processes*. Edited by G. R. Freeman. John Wiley & Sons Inc., New York. 1987. chap.6.
- 12 S. Golden and J. Tuttle T.R. *J. Phys. Chem.* **82**, 944 (1978).
- 13 S. Ray. *Chem. Phys. Lett.* **11**, 573 (1971).
- 14 P. H. Tewari and G. R. Freeman. *J. Chem. Phys.* **49**, 4394 (1968).
- 15 G. R. Freeman. *In Radiation Research*. Edited by G. Silini. North Holland, Amsterdam. 1967. p. 113.
- 16 Y. Wang, M. K. Cravford, M. J. McAuliffe, and K. B. Eisenthal. *Chem. Phys. Lett.* **74**, 160 (1980).
- 17 G. A. Kenney-Wallace and D. C. Walker. *J. Chem. Phys.* **55**, 447 (1971).

- 18 P. M. Rentzepis, R. P. Jones, and J. Jortner. *J. Chem. Phys.* **59**, 766 (1973).
- 19 W. J. Chase and J. W. Hunt. *J. Chem. Phys.* **79**, 2835 (1975).
- 20 P. H. Tewari and G. R. Freeman. *J. Chem. Phys.* **51**, 1276 (1969).
- 21 W. F. Schmidt and A. O. Allen. *J. Chem. Phys.* **52**, 4788 (1970).
- 22 R. A. Holroyd, S. Ehrenson, and J. M. Press. *J. Phys. Chem.* **89**, 4244 (1985).
- 23 R. C. Munoz, R. A. Holroyd, and K. Itoh. *J. Phys. Chem.* **91**, 6439 (1987).
- 24 K. H. Schmidt, P. Han, and D. M. Bartels. *J. Phys. Chem.* **96**, 199 (1992).
- 25 G. C. Barker, P. Fowles, D. C. Sammon, and B. Stringer. *Trans. Faraday Soc.* **66**, 1498 (1970).
- 26 P. Fowles. *Trans. Faraday Soc.* **67**, 428 (1971).
- 27 O. I. Micic and B. Cercek. *J. Phys. Chem.* **81**, 833 (1977).
- 28 Y. Maham and G. R. Freeman. *J. Phys. Chem.* **92**, 1506 (1988).
- 29 A. V. Vannikov, E. I. Mal'tzev, V. I. Zolotarevsky, and A. V. Rudnev. *Int. J. Radiat. Phys. Chem.* **4**, 135 (1972).
- 30 G. R. Freeman. *In Kinetics of Nonhomogeneous Processes. Edited by G. R. Freeman.* John Wiley & Sons Inc., New York. 1987. chap.2.
- 31 B. D. Michael, E. J. Hart, and K. H. Schmidt. *J. Phys. Chem.* **75**, 2798 (1971).
- 32 F. Y. Jou and G. R. Freeman. *J. Phys. Chem.* **83**, 2383 (1979).
- 33 G. R. Freeman. *J. Phys. Chem.* **77**, 7 (1973).
- 34 J. Jay-Gerin and C. Ferradini. *In Excess Electrons in Dielectric Media. Edited by C. Ferradini and J. Jay-Gerin.* CRC Press, London. 1991. chapter 8.
- 35 F. Y. Jou and G. R. Freeman. *Can. J. Chem.* **60**, 1809 (1982).
- 36 J.-P. Jay-Gerin and C. Ferradini. *Radiat. Phys. Chem.* **36**, 317 (1990).
- 37 J. G. J. Kirkwood. *J. Chem. Phys.* **7**, 911 (1939).
- 38 F. Y. Jou and G. R. Freeman. *J. Phys. Chem.* **83**, 261 (1979).

- 39 A. D. Leu, K. N. Jha, and G. R. Freeman. *Can. J. Chem.* **60**, 2342 (1982).
- 40 J. C. Thompson. *Electrons in Liquid Ammonia*. Clarendon press, Oxford. 1976. p. 297.
- 41 D. Huppert, P. Avouris, and P. A. Rentzepis. *J. Phys. Chem.* **82**, 2282 (1978).
- 42 T. Ito, K. Fueki, A. Namiki, and H. Hase. *J. Phys. Chem.* **77**, 1803 (1973).
- 43 J. Paraszczak and J. E. Willard. *J. Chem. Phys.* **70**, 5823 (1979).
- 44 N. V. Klassen and G. G. Teather. *J. Phys. Chem.* **83**, 326 (1979).
- 45 N. V. Klassen and G. G. Teather. *J. Phys. Chem.* **89**, 2048 (1985).
- 46 K. N. Jha, G. L. Bolton, and G. R. Freeman. *J. Phys. Chem.* **76**, 3876 (1972).
- 47 T. R. J. Tuttle, S. Golden, S. Lwenje, and C. M. Stupak. *J. Phys. Chem.* **88**, 3811 (1984).
- 48 D. C. Walker. *Can. J. Chem.* **55**, 1987 (1977).
- 49 N. Okabe, T. Kimura, and K. Fueki. *Can. J. Chem.* **61**, 2199 (1983).
- 50 J. Jortner and N. R. Kestner. *J. Phys. Chem.* **77**, 1040 (1973).
- 51 A. Kajiwara, K. Funabashi, and C. Naleway. *Phys. Rev.* **A6**, 808 (1972).
- 52 G. L. Hug and I. Carmichael. *J. Phys. Chem.* **86**, 3410 (1982).
- 53 K. Funabashi, I. Carmichael, and W. H. Hamill. *J. Chem. Phys.* **69**, 2652 (1978).
- 54 J. K. Baird and C. H. Morales. *J. Phys. Chem.* **89**, 774 (1985).
- 55 J. K. Baird, L. K. Lee, and E. J. Meehan Jr. *J. Chem. Phys.* **83**, 3710 (1985).
- 56 T. Kimura, K. Hirao, N. Okabe, and K. Fueki. *Can. J. Chem.* **62**, 64 (1984).
- 57 K. F. Baverstock and P. J. Dyne. *Can. J. Chem.* **48**, 2182 (1970).
- 58 N. Kato, S. Takagi, and K. Fueki. *J. Phys. Chem.* **85**, 2684 (1981).
- 59 T. Shida, S. Iwata, and T. Watanabe. *J. Phys. Chem.* **76**, 3683 (1972).
- 60 F. Y. Jou and G. R. Freeman. *J. Phys. Chem.* **88**, 3900 (1984).

- 61 W. A. Seddon, J. W. Fletcher, and F. C. Sopchyshyn. *Can. J. Chem.* **56**, 839 (1978).
- 62 T. R. J. Tuttle, S. Golden, S. Lwenje, and C. M. Stupak. *J. Phys. Chem.* **89**, 2436 (1984).
- 63 F. Y. Jou and G. R. Freeman. *Can. J. Chem.* **57**, 591 (1979).
- 64 V. V. Shornikov, G. I. Khaikin, and V. A. Zhigunov. *High Energy Chem.* **15**, 226 (1981).
- 65 C. M. Stupak, T. R. J. Tuttle, and S. Golden. *J. Phys. Chem.* **88**, 3804 (1984).
- 66 A. D. Leu, K. N. Jha, and G. R. Freeman. *Can. J. Chem.* **61**, 1115 (1983).
- 67 R. R. Hentz and G. A. Kenney-Wallace. *J. Phys. Chem.* **78**, 514 (1974).
- 68 G. E. Hall and G. A. Kenney. *Chem. Phys.* **32**, 313 (1978).
- 69 T. R. Tuttle Jr., and S. Golden. *J. Phys. Chem.* **95**, 5725 (1991).
- 70 S. Golden and T. R. J. Tuttle. *J. Phys. Chem.* **95**, 4109 (1991).
- 71 R. A. Ogg. *Phys. Rev.* **69**, 243 (1946).
- 72 J. Jortner. *J. Chem. Phys.* **30**, 839 (1959).
- 73 D. A. Copeland, N. R. Kestner, and J. Jortner. *J. Chem. Phys.* **53**, 1189 (1970).
- 74 D. Chandler, Y. Singh, and D. M. Richardson. *J. Chem. Phys.* **81**, 1975 (1984).
- 75 A. L. Nichols III and D. Chandler. *J. Chem. Phys.* **84**, 398 (1986).
- 76 A. L. Nichols III and D. Chandler. *J. Chem. Phys.* **87**, 6671 (1987).
- 77 K. Leung and D. Chandler. *Phys. Rev. E, Stat. Phys.* **49**, 2851 (1994).
- 78 M. Sprik, R. W. Impey, and M. L. Klein. *J. Chem. Phys.* **83**, 5802 (1985).
- 79 M. Sprik, R. W. Impey, and M. L. Klein. *Phys. Rev. Lett.* **56**, 2326 (1986).
- 80 M. Sprik and M. L. Klein. *J. Chem. Phys.* **87**, 5987 (1987).
- 81 M. Sprik and M. L. Klein. *J. Chem. Phys.* **89**, 1592 (1988).

- 82 M. Sprik and M. L. Klein. *J. Chem. Phys.* **91**, 5665 (1989).
- 83 Z. Deng, G. J. Martyna, and M. L. Klein. *J. Chem. Phys.* **100**, 7590 (1994).
- 84 F.-Y. Jou and G. R. Freeman. *J. Phys. Chem.* **85**, 629 (1981).
- 85 J. Schnitker, P. J. Rossky, and G. A. Kenney-Wallace. *J. Chem. Phys.* **85**, 2986 (1986).
- 86 E. Keszei, S. Nagy, T. H. Murphrey, and P. J. Rossky. *J. Chem. Phys.* **99**, 2004 (1993).
- 87 J. C. Tully. *J. Chem. Phys.* **93**, 1061 (1990).
- 88 F. A. Webster, J. Schnitker, M. S. Friedrichs, and P. J. Rossky. *Phys. Rev. Lett.* **66**, 3172 (1991).
- 89 F. A. Webster, P. J. Rossky, and R. A. Friesner. *Comput. Phys. Commun.* **93**, 494 (1991).
- 90 C. Romero and C. D. Jonah. *J. Chem. Phys.* **90**, 1877 (1989).
- 91 R. B. Barnett and U. Landman. *J. Chem. Phys.* **90**, 4413 (1989).
- 92 T. H. Murphrey and P. J. Rossky. *J. Chem. Phys.* **99**, 515 (1993).
- 93 F. Franks (ed.). *Water; A Comprehensive Treatise*, Plenum, New York, 1975.
- 94 J. P. Hansen and I. R. McDonald. *Theory of Simple Liquids*. Academic Press, New York. 1976.
- 95 M. P. Allen and D. J. Tildesley. *Computer Simulation of Liquids*. Clarendon Press, Oxford, UK. 1987.
- 96 J. D. Bernal and P. H. Fowler. *J. Chem. Phys.* **1**, 515 (1933).
- 97 A. H. Narten and H. A. Levy. *J. Chem. Phys.* **55**, 2263 (1971).
- 98 A. H. Narten. *J. Chem. Phys.* **56**, 5681 (1972).
- 99 S. A. Rice and M. G. Sceats. *J. Phys. Chem.* **85**, 1107 (1981).
- 100 S. A. Rice and M. G. Sceats. *In Water: A Comprehensive Treatise*. Vol. 7. Edited by F. Franks. Plenum, New York. 1982.

- 101 F. H. Stillinger and A. Rahman. *J. Chem. Phys.* **60**, 1545 (1974).
- 102 H. E. Stanley and J. Teixeira. *J. Chem. Phys.* **73**, 3404 (1980).
- 103 H. S. Frank and Y. W. Wen. *Discuss Faraday Soc.* **24**, 133 (1957).
- 104 G. J. Safford, P. S. Leung, A. W. Naumann, and P. C. Schaffer. *J. Chem. Phys.* **50**, 4444 (1969).
- 105 G. Nemethy and H. A. Scheraga. *J. Chem. Phys.* **36**, 3382 (1962).
- 106 M. S. Jhon, J. Grosh, T. Ree, and H. Eyring. *J. Chem. Phys.* **44**, 1465 (1966).
- 107 S. W. Benson and E. D. Siebert. *J. Am. Chem. Soc.* **114**, 4269 (1992).
- 108 P. Huyskens. *J. Mol. Struct.* **100**, 403 (1983).
- 109 P. Schuster, G. Zundel, and C. Sandorfy (ed.). *The Hydrogen Bond*. 3.ed. North Holland Publing, Amstadem, 1976.
- 110 M. C. R. Symons and V. K. Thomas. *J. Chem. Soc. Faraday Trans. I.* **77**, 1883 (1981).
- 111 H. H. Eysel and J. E. Bertie. *J. Mol. Struct.* **142**, 227 (1986).
- 112 B. M. Petit and P. J. Rossky. *J. Chem. Phys.* **78**, 7296 (1983).
- 113 W. L. Jorgensen. *J. Phys. Chem.* **90**, 1276 (1986).
- 114 J. Timmermans (ed.). *Physico-chemical Constants of Binary Mixtures*. 4.ed. Wiley-Interscience, New York, 1960.
- 115 J. M. Sorensen and W. Arlt. *Liquid-Liquid Equilibrium Data Collection*, DECHEMA Chem. Data Series. Frankfurt. 1979. p. 237.
- 116 J. Liszi, L. Meszaros, and I. Ruff. *Acta Chimica Academiae Scientiarum Hungaricae.* **104**, 273 (1980).
- 117 J. B. Hasted. *In Aqueous Dielectrics. Edited by Chapman and Hall, London.* 1973. p. 176.
- 118 A. D'Aprano, I. D. Donato, G. D'Arrigo, D. Bertolini, M. Cassettari, and G. Salvetti. *Molecular Physics.* **55**, 475 (1985).

- 119 B. Marongiu, I. Perino, R. Monaci, and R. Monaci. *J. Molecular Liq.* **28**, 229 (1984).
- 120 A. C. Brown and D. J. G. Ives. *J. Chem. Soc. II.* 1608 (1962).
- 121 Y. I. Naberukhin and V. A. Rogov. *Russ. Chem. Rev.* **40**, 207 (1971).
- 122 H. Tanaka, K. Nakanishi, and H. Touhara. *J. Chem. Phys.* **81**, 4065 (1984).
- 123 T. M. Bender and R. Pecora. *J. Phys. Chem.* **90**, 1700 (1986).
- 124 W. L. Jorgensen, J. Gao, and C. Ravimohan. *J. Phys. Chem.* **89**, 3470 (1985).
- 125 A. H. Hafez and H. Sadek. *Acta Chim. Acad. Sci. Hung.* **89**, 257 (1976).
- 126 P. C. Senanayake, N. Gee, and G. R. Freeman. *Can. J. Chem.* **65**, 2441 (1987).
- 127 Y. Maham and G. R. Freeman. *J. Phys. Chem.* **91**, 1561 (1987).
- 128 A. D'Aprano, D. Donato, E. Caponetti, and V. Agrigento. *J. Sol. Chem.* **8**, 793 (1979).
- 129 S. K. Garg and C. P. Smyth. *J. Phys. Chem.* **69**, 1294 (1965).
- 130 W. Dannhauser and A. F. Flueckinger. *Phys. Chem. Liq.* **2**, 37 (1970).
- 131 D. Bertolini, M. Cassettari, and G. Salvetti. *J. Chem. Phys.* **78**, 365 (1983).
- 132 D. Bertolini, M. Cassettari, and G. Salvetti. *J. Chem. Phys.* **76**, 3285 (1982).
- 133 L. A. Errede. *J. Org. Chem.* **43**, 1880 (1978).
- 134 R. J. Fessenden and J. S. Fessenden. *Organic Chemistry*. Willard Grant Press, Boston. 1979. p. 705.
- 135 C. D. Gutsche and D. J. Pasto. *Fundamental of Organic Chemistry*. Prentice-Hall, Englewood Cliffs. 1975. p. 132.
- 136 J. Konicek and I. Wadsoe. *Acta Chem. Scandinavica.* **25**, 1541 (1971).
- 137 F. J. Arcega Solsona and J. M. Fornies-Marquina. *J. Phys. D: Appl. Phys.* **15**, 1783 (1982).



- 138 H. F. Mark (ed.). Kirk-Othmer Encyclopedia of Chemical Technology., 2. ed. Vol.2. Interscience, New York, 1963. p. 103.
- 139 S. K. Garg and P. K. Kadaba. J. Phys. Chem. **68**, 737 (1964).
- 140 Y. Y. Akhadov. Dielectric Properties of Binary Solutions. Pergamon Press, Oxford, New York, Toronto. 1980. p. 144.
- 141 A. A. Maryott and E. R. Smith. Table of Dielectric Constants of Pure Liquids, NBS Circular 514. Washington D. C. 1951.
- 142 R. C. Weast (ed.). Handbook of Chemistry and Physics., 70th edn. CRC Press, Boca Raton, 1979. F.41-44.
- 143 L. A. Errede and G. V. D. Tiers. J. Org. Chem. **43**, 1887 (1978).
- 144 G. Wada and S. Umeda. Bull. Chem. Soc. Jpn. **35**, 646 (1962).
- 145 G. Wada and S. Umeda. Bull. Chem. Soc. Jpn. **35**, 1797 (1962).
- 146 T. H. Jordan and R. K. Mullan. Science. **155**, 689 (1967).
- 147 F. Franks. Water, A comprehensive Treatise.2. Plenum, New York. 1973. p. 35.
- 148 M. V. Kaulgud, V. S. Bhagde, and A. Shrivastava. J. Chem. Soc., Faraday Trans. I. **78**, 313 (1982).
- 149 T. Moriyoshi, T. Tsubota, and K. Hamaguchi. J. Chem. Thermodynamics. **23**, 155 (1991).
- 150 M.-J. Lee, S.-M. Hwang, and Y.-C. Kuo. J. Chem. & Eng. Data. **38**, 577 (1993).
- 151 K. Y. Liew, C. E. Seng, and C. G. Lee. J. Sol. Chem. **23**, 1293 (1994).
- 152 T. L. Broadwater and R. L. Kay. J. Phys. Chem. **74**, 3802 (1970).
- 153 H. A. Schwarz and P. S. Gill. J. Phys. Chem. **81**, 22 (1977).
- 154 A. M. Afanassiev, K. Okazaki, and G. R. Freeman. J. Phys. Chem. **83**, 1244 (1979).

- 155 A. M. Afanassiev, K. Okazaki, and G. R. Freeman. *Can. J. Chem.* **57**, 839 (1979).
- 156 G. V. Buxton, C. L. Greenstock, W. P. Helman, and A. B. Ross. *J. Phys. Chem. Ref. Data.* **17**, 513 (1988).
- 157 G. V. Buxton and S. R. Mackenzie. *J. Chem. Soc. Faraday Trans.* **88**, 2833 (1992).
- 158 T. B. Kang and G. R. Freeman. *Can. J. Chem.* **71**, 1297 (1993).
- 159 R. Chen and G. R. Freeman. *Can. J. Chem.* **71**, 1303 (1993).
- 160 R. Chen, Y. Avotins, and G. R. Freeman. *Can. J. Chem.* **72**, (1994).
- 161 M. Anbar and E. J. Hart. *J. Phys. Chem.* **69**, 973 (1965).
- 162 M. Anbar, M. Bambenek, and A. B. Ross. "Selected Specific Rates of Reactions of Transients from Water in Aqueous Solution. 1. Hydrated Electron." NSRDS-NBS 43, Washington, D.C., 1973.
- 163 M. Anbar, Farhataziz, and A. B. Ross. "Selected Specific Rates of Reactions of Transients from Water in Aqueous Solution. II. Hydrated Atoms." NSRDS-NBS 51, Washington, D.C. 1975.
- 164 A. J. Elliot. *Radiat. Phys. Chem.* **34**, 753 (1989).
- 165 A. J. Elliot and G. V. Buxton. *J. Chem. Soc. Faraday Trans.* **88**, 2465 (1992).
- 166 K. Horacek and G. R. Freeman. *J. Chem. Phys.* **53**, 4486 (1970).
- 167 M. G. Robinson and G. R. Freeman. *Can. J. Chem.* **51**, 650 (1973).
- 168 A. O. Allen and R. A. Holroyd. *J. Phys. Chem.* **78**, 796 (1974).
- 169 K. Ito and Y. Hatano. *J. Phys. Chem.* **78**, 853 (1974).
- 170 J. H. Baxendale, P. J. Keene, and E. J. Rasburn. *J. Chem. Soc. Faraday Trans. I.* **70**, 718 (1974).
- 171 K. Funabashi and J. L. Magee. *J. Chem. Phys.* **62**, 4428 (1975).
- 172 R. A. Holroyd, R. D. MaCreary, and G. Bakale. *J. Phys. Chem.* **83**, 1979 (1979).

- 173 W. H. Hamill. *J. Phys. Chem.* **85**, 3588 (1981).
- 174 A. O. Allen and R. A. Holroyd. *J. Phys. Chem.* **79**, 25 (1975).
- 175 R. A. Holroyd, E. Stradowska, and K. Itoh. *J. Phys. Chem.* **98**, 13524 (1994).
- 176 K. Ito and R. A. Holroyd. *J. Phys. Chem.* **94**, 8854 (1990).
- 177 K. Ito and R. A. Holroyd. *J. Phys. Chem.* **94**, 8850 (1990).
- 178 K. Ito, M. Nishikawa, and R. A. Holroyd. *J. Phys. Chem.* **97**, 503 (1993).
- 179 G. L. Bolton and G. R. Freeman. *J. Am. Chem. Soc.* **98**, 6825 (1976).
- 180 M. S. Tunuli and Farhataziz. *J. Phys. Chem.* **90**, 6587 (1986).
- 181 Farhataziz, S. Kalachandra, and M. S. Tunuli. *J. Phys. Chem.* **88**, 3837 (1984).
- 182 R. Chen and G. R. Freeman. *J. Phys. Chem.* in press (1995).
- 183 Farhataziz and S. Kalachandra. *Radiation Effects Letters.* **68**, 139 (1983).
- 184 P. Debye. *Trans. Electrochem. Soc.* **82**, 265 (1942).
- 185 R. H. Stokes and R. Mills. *Viscosity of Electrolytes and Related Properties.* Pergamon Press, Oxford. 1965. p. 151.
- 186 B. H. Milosavljevic and O. I. Micic. *J. Phys. Chem.* **82**, 1359 (1978).
- 187 C. C. Lai and G. R. Freeman. *J. Phys. Chem.* **94**, 302 (1990).
- 188 C. C. Lai and G. R. Freeman. *J. Phys. Chem.* **94**, 4891 (1990).
- 189 Y. Maham and G. R. Freeman. *J. Phys. Chem.* **89**, 4347 (1985).
- 190 Y. Maham and G. R. Freeman. *Can. J. Chem.* **66**, 1706 (1988).
- 191 S. A. Peiris and G. R. Freeman. *Can. J. Phys.* **68**, 940 (1990).
- 192 P. C. Senanayake and G. R. Freeman. *J. Phys. Chem.* **91**, 2123 (1987).
- 193 P. C. Senanayake and G. R. Freeman. *J. Chem. Phys.* **87**, 7007 (1987).
- 194 S. A. Peiris and G. R. Freeman. *Can. J. Chem.* **69**, 884 (1991).
- 195 S. A. Peiris and G. R. Freeman. *Can. J. Chem.* **69**, 157 (1991).
- 196 M. V. Smoluchowski. *Z. Phys. Chem.* **92**, 129 (1917).

- 197 A. Einstein. *Investigations on the Theory of Brownian Movement*. Dover Publications, New York. 1956.
- 198 P. W. Atkins. *Physical Chemistry*. 4 ed. Freeman, New York. 1990. p. 765.
- 199 J. Jortner and R. M. Noyes. *J. Phys. Chem.* **70**, 770 (1966).

## Chapter Two <sup>a</sup>

### Solvent Effects on the Reactivity of Solvated Electrons with Ions in *t*-Butanol/Water Mixtures.

#### 1. Introduction

The reactivity of solvated electrons  $e_s^-$  depends mainly on the natures of the coreactant and solvent (1-5). The study of rates of reaction of  $e_s^-$  with solutes in different solvents provides useful information about solvent effects, which helps us understand the behavior of electrons and the nature of solvents. The reaction rates in single component and mixed solvents are related to transport properties, as in Smoluchowski-type models for diffusion-controlled reactions (1,3,4,6-8), and relative energy levels of the reactants, as in the electron trap-depth model (2,7,8a). Electron reaction rates with inefficient capturers are larger when the electron solvation energy, represented by the optical absorption energy  $E_T$  (2), is smaller.

The physical properties of *t*-butanol/water mixed solvents vary markedly with composition (9,10). The present paper reports a continuation of the study of  $e_s^-$  reaction rates in this solvent system (11).

#### 2. Experimental

The *t*-butanol was obtained from BDH (Assured grade, 98%), and later from Fluka (>99.7%). The purification method was similar to that in ref. 11a. *t*-Butanol was

---

<sup>a</sup> A version of this chapter has been published. Y. Zhao and G. R. Freeman. Canadian Journal of Chemistry. 73, 392(1995).

dried at 304 K for at least one week on Davison 3Å Molecular Sieves, then bubbled with UHP argon (99.999%, Liquid Carbonic Canada) and treated with sodium borohydride (2 g/L) under argon at 323 K for 24 hrs. Then the alcohol was fractionally distilled under argon through an 80 x 2.3 cm column packed with glass beads (6 mm). The first 20-25% of the distillate was discarded; distillate was collected after there was no further reduction in optical absorption between 260 and 280 nm, which is due to carbonyl compounds (12). The middle 50% portion was collected and stored in a flask under argon positive pressure. The water content, measured by Karl-Fisher titration, was 0.05 mol %. The solvated electron half-life after a 100 ns pulse of 340 fJ (2.1 MeV) electrons (4J/kg) at 300 K was over 10  $\mu$ s.

Perchloric acid (70 wt % in water, reagent) was obtained from Fisher Scientific. LiNO<sub>3</sub> (99.999% Gold label), NH<sub>4</sub>NO<sub>3</sub> (99.999%), LiClO<sub>4</sub> (reagent grade) and NH<sub>4</sub>ClO<sub>4</sub> (99.8%) were from Aldrich.

Techniques of sample solution preparation, irradiation and optical measurements were the same as described in ref. 13 and Appendix One of this thesis. Conductance measurement was as in ref. 14 and Appendix One of this thesis.

*t*-Butanol is completely miscible with water. The following mol % of water in *t*-butanol were used for rate constant measurements of all solutes: 0, 5, 10, 30, 50, 70, 90, 97, 100. Measurements of electrical conductance were done in the same solvents, except 5 mol %.

### 3. Results and Discussion

#### *Rate constants*

The reactions are:





The observed first-order decay rate constant  $k_{\text{obs}}$  ( $= k_1 + k_2 [S]$ ) in a given solvent was measured for the pure solvent and six concentrations of solute S. The value of  $k_1$  might include a contribution from trace impurities in the solvent:  $k_1 = k_1' + k_i[I]$ . The value of the second-order rate constant  $k_2$  was obtained from the slope of a plot of  $k_{\text{obs}}$  against solute concentration. The precision of the  $k_2$  values determined by repeating the measurements on freshly prepared solutions, is 3%. The values of  $k_2$  for each solvent were measured at temperatures from 273 K to 343 K, except in pure *t*-butanol whose mp is 298.7 K.

Arrhenius plots of  $k_2$  for the four solutes ( $\text{Li}_s^+ + \text{NO}_{3,s}^-$ ), ( $\text{NH}_{4,s}^+ + \text{NO}_{3,s}^-$ ), ( $\text{NH}_{4,s}^+ + \text{ClO}_{4,s}^-$ ) and ( $\text{H}_s^+ + \text{ClO}_{4,s}^-$ ) are given in Figs. 1–4. Table 1 contains the symbols for these Figures. The reaction parameters are listed in Table 2.

The value of  $k_2$  for the reaction of  $e_s^- + (\text{Li}_s^+ + \text{ClO}_{4,s}^-)$  is very small, being  $110 \text{ m}^3/\text{mol}\cdot\text{s}$  in water and  $660 \text{ m}^3/\text{mol}\cdot\text{s}$  in *t*-butanol at 298 K (Table 2). Thus the large value of  $k_2$  of ( $\text{Li}_s^+ + \text{NO}_{3,s}^-$ ) is due to  $\text{NO}_{3,s}^-$ , of ( $\text{H}_s^+ + \text{ClO}_{4,s}^-$ ) is due to  $\text{H}_s^+$  and of ( $\text{NH}_{4,s}^+ + \text{ClO}_{4,s}^-$ ) is due to  $\text{NH}_{4,s}^+$  (Table 2).

The solvent composition dependence of  $k_2$  at 298 K is shown in Fig. 5. Values of the optical absorption energy  $E_r$  (15), relative permittivity (16) and viscosity (10) are shown for comparison.

The value of  $k_2$  of ( $\text{NH}_{4,s}^+ + \text{NO}_{3,s}^-$ ) in the water-rich region is due to  $\text{NO}_{3,s}^-$ , and in the alcohol-rich region is due to  $\text{NH}_{4,s}^+$ . This conclusion agrees with earlier work (14). In the alcohol-rich solvents the rate constants for  $\text{NH}_{4,s}^+$  are about 10 times higher than those for  $\text{NO}_{3,s}^-$  (Fig. 5). The coulombic attraction of the opposite charges ( $\text{NH}_{4,s}^+ + e_s^-$ ) and repulsion of the like charges ( $e_s^- + \text{NO}_{3,s}^-$ ) is the main cause of this difference (see f in Table 2).

The value of  $k_2 (e_s^- + H_s^+)$  stays  $\geq 2 \times 10^7 \text{ m}^3/\text{mol}\cdot\text{s}$  at all solvent compositions. It is higher than those of the other three reactions. In the region of 30–100 mol % water, the variation of the  $k_2$  of  $H_s^+$  is very different from those of the reactions with  $\text{NO}_{3,s}^-$  and  $\text{NH}_{4,s}^+$  (Fig. 5).

Addition of 5–10 mol % of water to *t*-butanol decreases the rate constant of each reaction by a factor of 0.5 to 0.3 (Fig. 5). We attribute this to a decrease in mobility of  $e_s^-$ , which is unusually high in pure *t*-butanol (17).

The variation of  $k_2$  with solvent composition between 50 and 100 mol % of water is different for each of the four solutes (Fig. 5). The variation of  $k_2(\text{NO}_{3,s}^-)$  varies in the expected way with viscosity  $\eta$  and relative permittivity  $\epsilon$ , but not with  $e_s^-$  trap depth  $E_T$  (2). In the water-rich region (100–70 mol %), values of  $k_2$  for  $\text{NO}_{3,s}^-$  and  $(\text{NH}_{4,s}^+ + \text{NO}_{3,s}^-)$ , mainly due to  $\text{NO}_{3,s}^-$ , increase as diffusion rates increase (viscosity decreases). In the alcohol-rich region (0–50 mol % water),  $k_2$  for  $\text{NO}_{3,s}^-$  increases as the viscosity increases, indicating a change of reaction mechanism.

#### *Reaction radius and Debye factor $f$*

For a diffusion-controlled reaction of  $e_s^-$  with a solute of charge  $z\xi$  the Smoluchowski-Debye equation (18) is:

$$[3] \quad k_2 = 4\pi N_A (D_e + D_s) R_r f \quad ,$$

where  $N_A$  is Avogadro's constant,  $D_i$  is the diffusion coefficient of  $i$ , and  $R_r$  is the average center-to-center reactant separation when reaction occurs. The Debye factor  $f$  is given by:

$$[4] \quad f = \frac{x}{(e^x - 1)} \quad ,$$

$$[5] \quad x = - \frac{z\xi^2}{4\pi\epsilon_0\epsilon R_r k_B T} \quad ,$$



where  $x$  is the ratio of the coulombic energy of the reactants at  $R_r$  to the thermal agitation energy  $k_B T$ , and  $\epsilon$  is the relative permittivity of the medium between the reactants at separation  $R_r$ . The factor  $f$  reflects the effect of the coulombic interaction between the two reactants on the probability that they will approach each other to within the distance  $R_r$  at which reaction can occur.

Values of  $R_r$  are not well defined and can be quite different for different solutes and solvents; the estimated value also depends on the method of estimation. Sometimes  $R_r$  estimated from the Smoluchowski-Debye equation [3] is called the effective reaction radius ( $R_{eff}$ ) to distinguish it from the real reaction radius  $R_r$ . Milosavljevic and Micic (6) estimated  $R_{eff}$  for reactions of  $e_s^-$  with several solutes in methanol or ethanol mixed with water, using the Smoluchowski equation and estimated values of diffusion coefficients. For nitrobenzene in methanol/water solvents they obtained  $R_{eff} = 0.8$  nm in pure water solvent, 0.9 nm in 20 mol % methanol and 1.2 nm in pure methanol. For nitrobenzene in ethanol/water solvents they obtained  $R_{eff} = 0.9$  nm in water, 0.7 nm in 20% mol ethanol and 1.3 nm in pure ethanol. However, Lai and Freeman (8a) used  $R_r = 0.8$  nm for nitrobenzene over the whole range of water mixtures with methanol or ethanol.

Tunuli (19) applied equation [3] to the reaction of  $e_s^-$  with  $Ag_s^+$  in  $C_{1-10}$  alcohols. He used different methods to estimate  $R_r$  and obtained  $R_r = 1.22-1.28$  nm for methanol, 1.42-1.48 nm for ethanol, 1.52-1.74 nm for 1-propanol, and 1.54-2.0 nm for 1-butanol.

Schwarz and Gill (1) calculated effective reaction radii  $r_r$  in the study of the diffusion-controlled reactions of  $e_s^-$  with  $NH_4^+$ ,  $Ag_s^+$  and other solutes in ethanol. For charged solutes, they used eqs. [6] and [7] to calculate  $r_r$ :

$$[6] \quad r_r = r_0 / [1 - \exp(-r_0/r_0)] ,$$

$$[7] \quad r_c = -\frac{z\xi^2}{4\pi\epsilon_0\epsilon k_B T} \quad ,$$

where  $r_c$  is the distance at which the coulombic interaction between the ions equals the thermal agitation energy  $k_B T$ , and  $r_0$  is the center-to-center separation of the solvated reactant ions in contact. Schwarz used  $r_0 = 1.1$  nm and the static value of  $\epsilon$  of the bulk solvent in eqs. [6] and [7]. The reactants (electron and ion) are solvated, which means each reactant is surrounded by a layer of ethanol molecules oriented by the charge-dipole interaction. The average diameter of an ethanol molecule is about 0.4 nm, which with the radii of the electron cavity and the solute ion gives  $r_0 \approx 1.1$  nm. Since there are only two solvent molecules between the two charged reactants and they can not reorient freely, the relative permittivity  $\epsilon$  of these two molecules is less than the static value of bulk ethanol. The static value of  $\epsilon$  probably requires at least one more solvent molecule between those that solvate the reactant ions, or a minimum of  $r \approx 1.5$  nm. The value of  $r_c$  in ethanol is 2.3 nm at 298 K, for  $z = 1$  and  $\epsilon = 24.3$ . The use of the simple ratio  $r_c/r_0$  in eq. [6] requires that the same value of  $\epsilon$  be applicable for both  $r_0$  and  $r_c$ . This is improbable for  $r_0 = 1.1$  nm in ethanol. If we release the "contact" restriction and replace  $r_0$  in eq. [6] by  $R_r$  of eq. [3] then  $r_r$  in eq. [6] equals  $R_r f$  in eq. [3].

For neutral solutes, eq. [8] was used (1).

$$[8] \quad k_1' r_r = r_0 + \left(\frac{2}{b}\right)(\ln Z_0 + 0.57)$$

where  $Z_0 = 2v^{1/2}/b(D_e + D_s)^{1/2}$ ,  $v$  and  $b$  are from the fitted reaction probability  $\beta(r)$  based on electron transfer through overlapping wave functions ("tunneling", 1,20):

$$[9] \quad \beta(r) = v e^{-b(r-r_0)} \quad ,$$

where  $\nu = 10^{15}$  cy/s is the orbital oscillation frequency of the solvated electron, and  $b^{-1} \approx 10^{-10}$  m is the separation distance ( $r - r_0$ ) where the reaction probability is decreased by a factor of 1/3 from the value  $\nu$  at contact ( $r - r_0 = 0$ ).

For mixed solvents the values of the diffusion coefficient of  $e_s^-$  are not known, so it is difficult to estimate the reaction radius. Therefore, for the reactions of  $e_s^-$  with  $\text{NO}_{3,s}^-$  and  $\text{H}_s^+$  in propanols (21) and butanols (13,14,21b), fixed values of  $R_r$  were used for  $f$  factor calculation in eqs. [4] and [5], namely,  $R_r(e_s^- + \text{NO}_{3,s}^-) = 1.5$  nm,  $R_r(e_s^- + \text{H}_s^+) = R_r(e_s^- + \text{NH}_{4,s}^+) = 1.0$  nm. Then  $\kappa$ , the probability that reaction occurs during one encounter, was inserted into [3] (21):

$$[10] \quad k_2 = 4\pi N_A (D_e + D_s) f \kappa R_r \quad ,$$

where  $\kappa R_r$  can be considered as an effective reaction radius.

One might expect  $R_r$  to be larger when the solvating molecules are larger, hence larger for alcohol solvation than for water solvation. In most *t*-butanol/water mixtures, from 30–100 mol % of water,  $e_s^-$  is preferentially solvated by water (15), so  $R_r(e_s^- + \text{NO}_{3,s}^-) = 1.5$  nm and  $R_r(e_s^- + \text{NH}_{4,s}^+) = 1.0$  nm are still used. This implies that there are, including the solvating molecules, about four water molecules between  $e^-$  and  $\text{NO}_3^-$ , and about three between  $e^-$  and  $\text{NH}_4^+$  when reaction occurs. In pure *t*-butanol, there could be about three and a half *t*-butanol molecules between  $e^-$  and  $\text{NO}_3^-$ , and three between  $e^-$  and  $\text{NH}_4^+$  to attain the bulk, static value of  $\epsilon$  between the charges. The diameter of *t*-butanol is about 0.5 nm, which gives a center-to-center  $R_r(e_s^- + \text{NO}_{3,s}^-) = 2.1$  nm and  $R_r(e_s^- + \text{NH}_{4,s}^+) = 1.6$  nm by the replacement of water molecules whose van der Waals diameter is 0.29 nm (22). In the solvent region 0–30 mol % of water, the relative numbers of *t*-butanol and water molecules between the reactants gradually change and the values of  $R_r$  gradually decrease. The values of  $R_r$  are listed in Table 3, and are assumed to be relatively insensitive to temperature. The corresponding values of  $f$  are in Table 2; the values of  $f$  for  $\text{H}_s^+$  are the same as for  $\text{NH}_{4,s}^+$ .

The value of  $k_2$  is dependent on both  $R_r$  and the factor  $f$  (eq. [10]), while  $f$  is dependent on  $R_r$ , the charge of the reactant ion, and the  $\epsilon$  of the solvent between the electron and ion (eqs. [4] and [5]). Fig. 6 shows the solvent composition dependence of  $\epsilon R_r$  and hence  $f$  for the reactions  $e_s^- + \text{NO}_{3,s}^-$  and  $e_s^- + \text{NH}_{4,s}^+$  (or  $\text{H}_s^+$ ). As  $\epsilon R_r$  increases the coulombic interaction becomes weaker;  $f$  decreases towards unity for  $e_s^-$  reaction with a cation, and increases toward unity for reaction with an anion.

#### *Normalized Rate constants $k_2/f$*

Eq. [10] can be rearranged to [11]:

$$[11] \quad k_2/f = 4\pi N_A (D_e + D_s) \kappa R_r$$

where  $k_2/f$  normalizes the rate constant for the coulombic effect. Fig. 7 shows the changes of  $k_2/f$  with solvent composition for different solutes in *t*-butanol/water mixtures at 298 K. The method described in ref. 13 was used to calculate  $k_2/f$  for  $e_s^- + (\text{NH}_{4,s}^+ + \text{NO}_{3,s}^-)$ . The  $k_2/f$  curves for different solutes are closer together than are the  $k_2$  curves in Fig. 5.

#### *Molar conductivity of solutes*

The solvent composition dependences of molar conductivities of all four solutes at 298 K are shown in Fig. 8 and listed in Table 2. The concentration ranges used in conductance measurements were close to those used to determine rate constants. The measured value of  $\Lambda$  for  $\text{LiNO}_3$  in *t*-butanol is about  $0.46 \times 10^{-4} \text{ S}\cdot\text{m}^2/\text{mol}$ , compared to  $3.86 \times 10^{-4} \text{ S}\cdot\text{m}^2/\text{mol}$  for  $\text{LiClO}_4$ . This indicates that  $(\text{Li}_s^+ \text{NO}_{3,s}^-)$  ion pairs form in *t*-butanol. The value of  $\Lambda_0 = \sim 5 \times 10^{-4} \text{ S}\cdot\text{m}^2/\text{mol}$  for  $\text{Li}_s^+ + \text{NO}_{3,s}^-$  in *t*-butanol is estimated from the values of the other three solutes  $\text{Li}_s^+ + \text{ClO}_{4,s}^-$ ,  $\text{NH}_{4,s}^+ + \text{ClO}_{4,s}^-$  and  $\text{NH}_{4,s}^+ + \text{NO}_{3,s}^-$  (Table 2, Fig. 8). The ion pairing will be discussed later in chapter 5.

The values of  $\Lambda_o$  are proportional to the mobilities  $\mu_i$  of the ions (23):

$$[12] \quad \Lambda = \nu_+ \lambda_+ + \nu_- \lambda_- \quad ,$$

where  $\nu_+$  is the number of cations and  $\nu_-$  is the number of anions in a formula of the electrolyte, and

$$[13] \quad \lambda_i = z_i \mu_i F = \frac{z_i^2 D_i F^2}{RT} \quad ,$$

where  $\lambda_i$  is the molar conductivity of ion  $i$ ,  $z_i$  is the number of charges of the ion,  $F$  is the Faraday constant, and  $R$  is the gas constant. Substitution of  $D_i$  by the Stokes-Einstein relation (23),

$$[14] \quad D_i = \frac{k_B T}{6\pi\eta r_{di}} \quad ,$$

where  $r_{di}$  is the effective hydrodynamic radius of the solvated ion, gives

$$[15] \quad \lambda_i = \frac{z_i^2 F^2}{N_A 6\pi\eta r_{di}} \quad .$$

For the 1:1 electrolytes ( $z = 1$ ) in the present study, the effective radius  $r_d$  for mutual diffusion of the positive and negative ions is

$$[16] \quad r_d = \frac{F^2}{N_A 6\pi\eta \Lambda_o} = 8.2 \times 10^{-16} / \eta \Lambda_o \quad ,$$

where  $r_d^{-1} = (r_{d+}^{-1} + r_{d-}^{-1})$  (21c).

The values of  $r_d$  decrease as the water content of the solvent increases up to 90-97 mol %, pass through a minimum and increase somewhat toward pure water solvent (Fig. 9). The decrease of  $D_i$  on going from water to *t*-butanol is due to the increasing

viscosity of the solvent and the larger size of the molecules that solvate the ions. The reason for the apparent decrease of  $r_d$  upon addition of a few percent of alcohol to water is that the viscosity of the bulk solvent increases considerably, due to a more ordered structure of the mixed solvent (24), while the ions are selectively solvated by the water and presumably remain in lower viscosity microzones (21c). Use of the bulk viscosity in eq. [16] makes  $r_d$  appear to decrease.

### *Smoluchowski-Debye-Nernst-Einstein Model*

Diffusion coefficients from eq. [13] can be substituted in eq. [11]:

$$[17] \quad k_2/f = \frac{4\pi k_B T}{\xi^2} (\lambda_e + \lambda_i/z_i^2) \kappa R_f \quad ,$$

which can be rearranged to

$$[18] \quad \kappa R_f = 1.48 \times 10^{-16} k_2 / (\lambda_e + \lambda_i/z_i^2) f T \quad ,$$

where  $\lambda_e$  is the molar conductivity of  $e_s^-$ . For the solutes studied in this work,  $z_i = \pm 1$ . In water, the diffusion of  $e_s^-$  dominates the relative motion of each pair except that with  $H_s^+$  (21b). The values of the individual ionic conductivities in the mixed solvents are unknown, so an approximation is made in order to estimate  $\kappa R_f$  from measured molar conductivities of the electrolytes. In water:

$$[\lambda_e + \lambda(H_s^+)]/\Lambda_0(H_s^+, ClO_{4,s}^-) = 1.3 \quad (21b),$$

$$\text{so} \quad \kappa R_f = 1.1 \times 10^{-16} k_2 / \Lambda_0(H_s^+, ClO_{4,s}^-) f T;$$

$$[\lambda_e + \lambda(NO_{3,s}^-)]/\Lambda_0(Li_s^+, NO_{3,s}^-) = 2.3 \quad (21b),$$

$$\text{so} \quad \kappa R_f = 0.6 \times 10^{-16} k_2 / \Lambda_0(Li_s^+, NO_{3,s}^-) f T;$$

$$[\lambda_e + \lambda(NH_{4,s}^+)]/\Lambda_0(NH_{4,s}^+, ClO_{4,s}^-) = 1.6 \quad (14),$$

$$\text{so} \quad \kappa R_f = 0.9 \times 10^{-16} k_2 / \Lambda_0(NH_{4,s}^+, ClO_{4,s}^-) f T.$$

For the lack of anything better, these equations were used for all solvent compositions to estimate  $\kappa R_r$ .

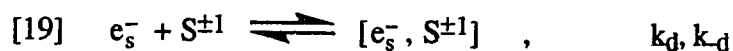
The estimated values of  $\kappa R_r$  are plotted in Fig. 10. The curves are again different from those in Figs. 5 and 7. The value of  $\kappa R_r$  for each solute increases continuously with increasing *t*-butanol content. This indicates that the reactivity of  $e_s^-$  with all solutes gradually increases on going from water to *t*-butanol solvent.

For all solutes in pure *t*-butanol solvent the apparent values of  $\kappa$  are much larger than unity, in spite of the large values of  $R_r$  chosen, 2.1 nm for  $\text{NO}_{3,s}^-$  and 1.6 nm for  $\text{NH}_{4,s}^+$  and  $\text{H}_s^+$ . The true value of  $\kappa$  can not be greater than unity. The apparent values of  $\kappa$  for the reaction  $e_s^- + \text{H}_s^+$  in 10–70 mol % water are larger than 1.0 (Table 4), but they are within the uncertainty of the approximations. By arbitrarily reducing  $\kappa$  to 1.0 for  $k_2(e_s^- + \text{H}_s^+)$  in *t*-butanol, the mobility of  $e_s^-$  in this solvent is estimated to be  $\mu(e_s^-) \approx 4 \times 10^{-8} \text{ m}^2/\text{V}\cdot\text{s}$  at 298 K, and  $E_{\mu e} \approx 41 \text{ kJ/mol}$  (17); refer to Chapter 3 of this thesis.

### *E<sub>2</sub> and E<sub>Λ0</sub>*

The solvent dependences of the Arrhenius activation energies  $E_2$  of reaction and  $E_{\Lambda 0}$  of mobility for all four solutes are plotted in Fig. 11. The values of  $E_2$  increase from water to alcohol, whereas  $E_{\Lambda 0}$  for the salts have a maximum at 50 mol % water.

For reaction [2] to occur, the reactants  $e_s^-$  and  $\text{S}^{\pm 1}$ , must diffuse together



then react



From the steady-state approximation one obtains

$$[21] \quad k_2 = \frac{k_d k_{20}}{k_{-d} + k_{20}} \quad .$$

If  $k_{20} \gg k_{-d}$ , then  $k_2 \approx k_d$  and  $E_2$  should be close to  $E_{\Lambda 0}$ . For the reactions  $e_s^- + \text{NO}_{3,s}^-$  and  $e_s^- + \text{H}_s^+$  in the water-rich region of 100–70 mol % of water, the reactions are not far

from diffusion-controlled and  $E_2$  and  $E_{\Lambda 0}$  are similar (Table 2). For  $\text{NH}_4^+$  in 100–70 mol % of water the rate constants are low, and the values of  $E_2$  are much higher than  $E_{\Lambda c}$ .

In the alcohol-rich region from 50 to 10 mol % water, the values of  $E_2$  do not change much, while  $E_{\Lambda 0}$  decreases somewhat. In the solvents 10 to 0% water  $E_2$  increases greatly, while  $E_{\Lambda 0}$  for the salts decrease and that for  $\text{HClO}_4$  remains constant. The increase of  $E_2$  is attributed to a large temperature coefficient of diffusion of  $e_s^-$ , which reaches 41 kJ/mol in pure *t*-butanol (17).



**Table 2-1. Symbols in Figures 2-1 to 2-4.**

	mol % Water		mol % Water
■	0	△	70
X	5	▲	90
◆	10	+	97
□	30	○	100
◇	50		

Table 2-2. Reaction Rate Parameters in *t*-BuOH/Water Solvents at 298 K.

$E_r(zJ)^a$	$\eta^b$ (mPa·s)	$\epsilon^c$	H <sub>2</sub> O mol %	$f^d$	$k_2$ ( $10^6 \text{ m}^3/\text{mol}\cdot\text{s}$ )	$k_2/f$	$E_2$ (kJ/mol)	$\Lambda_o^e$	$E_{\Lambda_o}^e$
<b>NO<sub>3</sub><sup>-</sup> (1.5 – 42 x 10<sup>-2</sup> mol/m<sup>3</sup> for k<sub>2</sub>)</b>									
104	4.45	12.4	0	0.283	3.2	11	53	~4 <sup>f</sup>	15
	4.33	12.0	5	0.229	1.7	7.3	34		
171	4.20	11.5	10	0.195	1.2	6.2	32	4.6	18
	4.41	12.0		0.193	0.96	5.0	31	8.2	24
215	4.76	17.		0.288	0.76	2.6	29	14.0	26
	4.98	27.2		0.465	1.3	2.7	26	19.6	25
	3.23	53.2		0.69	3.3	4.8	22	38.0	23
223	1.60	70.0	97	0.76	6.2	8.2	18	80	20
219	0.89	78.4	100	0.78	9.8	13	14	113	13
<b>NH<sub>4</sub><sup>+</sup> (0.3 – 900 x 10<sup>-2</sup> mol/m<sup>3</sup> for k<sub>2</sub>)</b>									
			0	3.00	13	4.3	43	4.9	17
			5	3.47	9.2	2.7	34		
			10	3.83	9.2	2.4	29	6.0	21
			30	4.02	14	3.4	29	8.9	24
			50	3.33	6.0	1.8	30	15.2	26
			70	2.36	0.32	0.14	30	22.5	25
			90	1.62	0.028 <sup>g</sup>	0.012	30	48.5	22
			97	1.45	0.0048 <sup>g</sup>	0.0031	31	90	18
			100	1.40	0.0028 <sup>g</sup>	0.0014	30	140	14

Table 2-2. Continued

$E_r(zJ)^a$	$\eta^b$ (mPa·s)	$\epsilon^c$	H <sub>2</sub> O mol %	$f^d$	$k_2$ (10 <sup>6</sup> m <sup>3</sup> /mol·s)	$k_2/f$	$E_2$ (kJ/mol)	$\Lambda_0^e$	$E_{\Lambda_0^e}$
<b>NH<sub>4,s</sub><sup>+</sup> + NO<sub>3,s</sub><sup>-</sup> (0.25 – 12.0 x 10<sup>-2</sup> mol/m<sup>3</sup> for <math>k_2</math>)</b>									
			0	3.00	11	3.8	43	~5 $f$	19
			5	3.47	6.5	1.9	27		
			10	3.83	6.2	1.6	28	4.6	21
			30	4.02	11	2.7	29	8.3	25
			50	3.33	7.1	2.1	30	16.6	26
			70	0.465	1.6	3.4	28	25.0	26
			90	0.690	3.5	5.1	24	56	23
			97	0.757	6.1	8.1	17	118	18
			100	0.779	10	13	15	150	17
<b>H<sub>g</sub><sup>+</sup> (0.1 – 3.0 x 10<sup>-2</sup> mol/m<sup>3</sup> for <math>k_2</math>)</b>									
			0	3.00	42	14	50	10.6	27
			5	3.47	23	6.6	36		
			10	3.83	20	5.3	33	12.7	25
			30	4.02	28	7.0	30	17.0	25
			50	3.33	38	11	28	30.0	25
			70	2.36	44	18	24	66	24
			90	1.62	39	24	19	170	22
			97	1.45	35	24	15	345	14
			100	1.40	29	20	11	400	12

Table 2-2. Continued

$E_T(zJ)^a$	$\eta^b$ (mPa·s)	$\epsilon^c$	H <sub>2</sub> O mol %	$f^d$	$k_2$ (10 <sup>6</sup> m <sup>3</sup> /mol·s)	$k_2/f$	$E_2$ (kJ/mol)	$\Lambda_0^e$	$E_{\Lambda_0}^e$
<b>Li<sup>+</sup> + ClO<sub>4,s</sub> (100 – 6000 mol/m<sup>3</sup> for k<sub>2</sub>)</b>									
			0		6.6x10 <sup>-4</sup>			3.9	14
			10					6.6	19
			30					9.0	23
			50					12.4	25
			70					18.3	25
			90					37.0	21
			97					74	18
			100		1.1x10 <sup>-4</sup>			105	15

*a*: Ref. 16, except *t*-butanol is from the authors' unpublished work.

*b*: Ref. 10.

*c*: Ref. 16.

*d*: Debye factor, see text.

*e*: Molar conductivity, 10<sup>-4</sup> S·m<sup>2</sup>/mol; activation energy, kJ/mol.

*f*: Estimated value, to be discussed in a later paper.

*g*: Corrected for NH<sub>4,s</sub><sup>+</sup>  $\rightleftharpoons$  NH<sub>3,s</sub> + , as in ref. 14.

**Table 2-3. Estimated Values of  $R_f$ (nm) in *t*-BuOH/Water Mixtures <sup>a</sup>**

Water % (mol)	0	5	10	30	50-100
$R_f(e_s^- + NO_{3,s}^-)$ nm	2.1	1.9	1.8	1.6	1.5
$R_f(e_s^- + NH_{4,s}^+)$ nm	1.6	1.4	1.3	1.1	1.0

<sup>a</sup> Assumed to be relatively insensitive to temperature.

**Table 2-4. Apparent  $\kappa$  Values in *t*-Butanol/Water Mixtures at 298 K.**

Water % (mol)	100	97	90	70	50	30	10	0
$\kappa(NO_{3,s}^-)$	0.16	0.15	0.19	0.20	0.27	0.82	1.4	3.0
$\kappa(NH_{4,s}^+)$	$3.1 \times 10^{-5}$	$1.1 \times 10^{-4}$	$7.9 \times 10^{-3}$	0.019	0.37	0.88	0.95	1.7
$\kappa(H_s^+)$	0.20	0.27	0.53	1.07	1.45	1.42	1.24	3.3

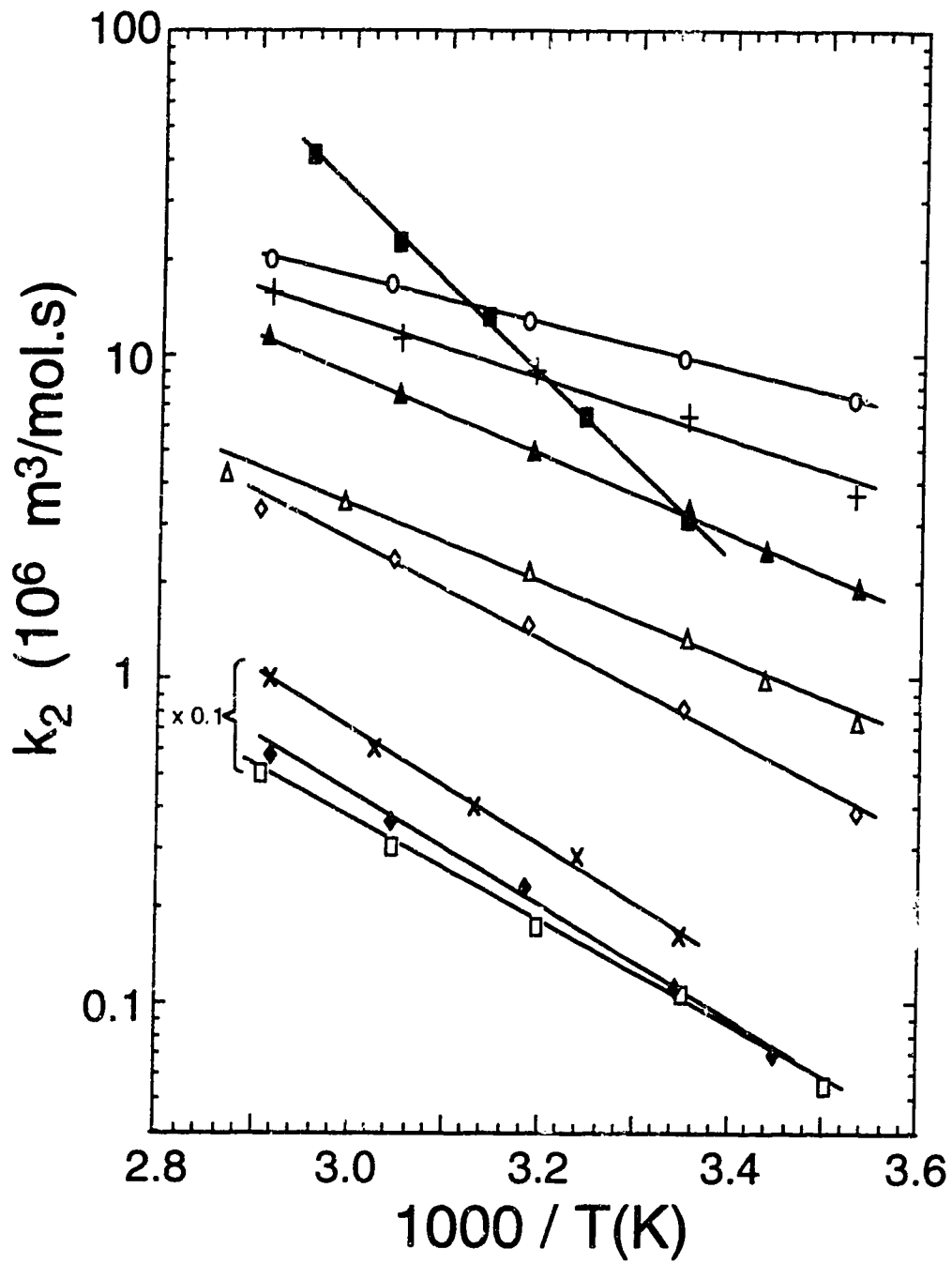


Fig. 2-1. Arrhenius plots of  $k_2$  for the reaction of  $e_s^-$  with  $\text{Li}_s^+ + \text{NO}_3_s^-$  in *t*-butanol/water mixed solvents. Refer to Table 1 for symbols.

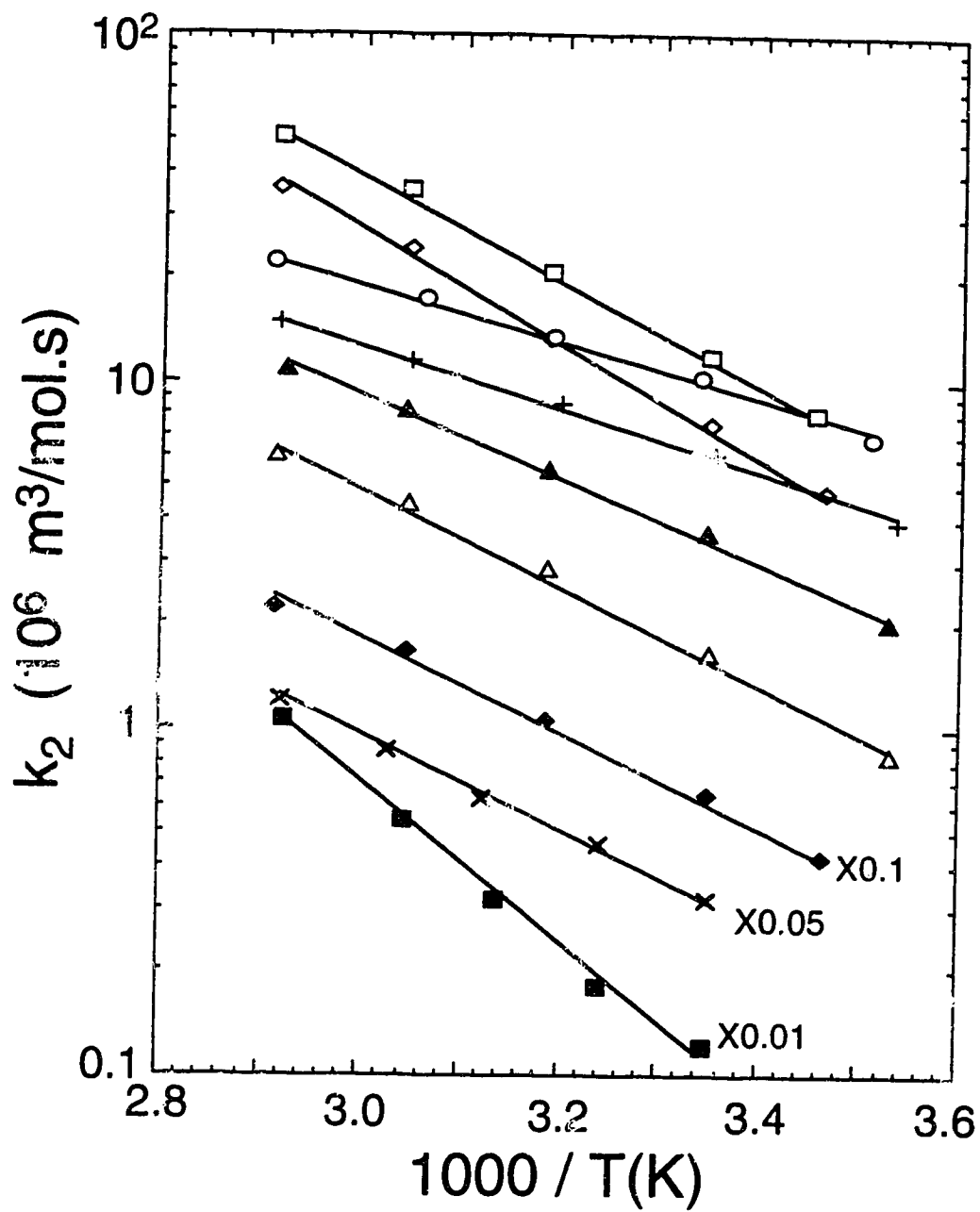


Fig. 2-2. Arrhenius plots of  $k_2$  for the reaction of  $e_s^-$  with  $\text{NH}_{4,s}^+ + \text{NO}_{3,s}^-$  in *t*-butanol/water. Refer to Table 1 for symbols.

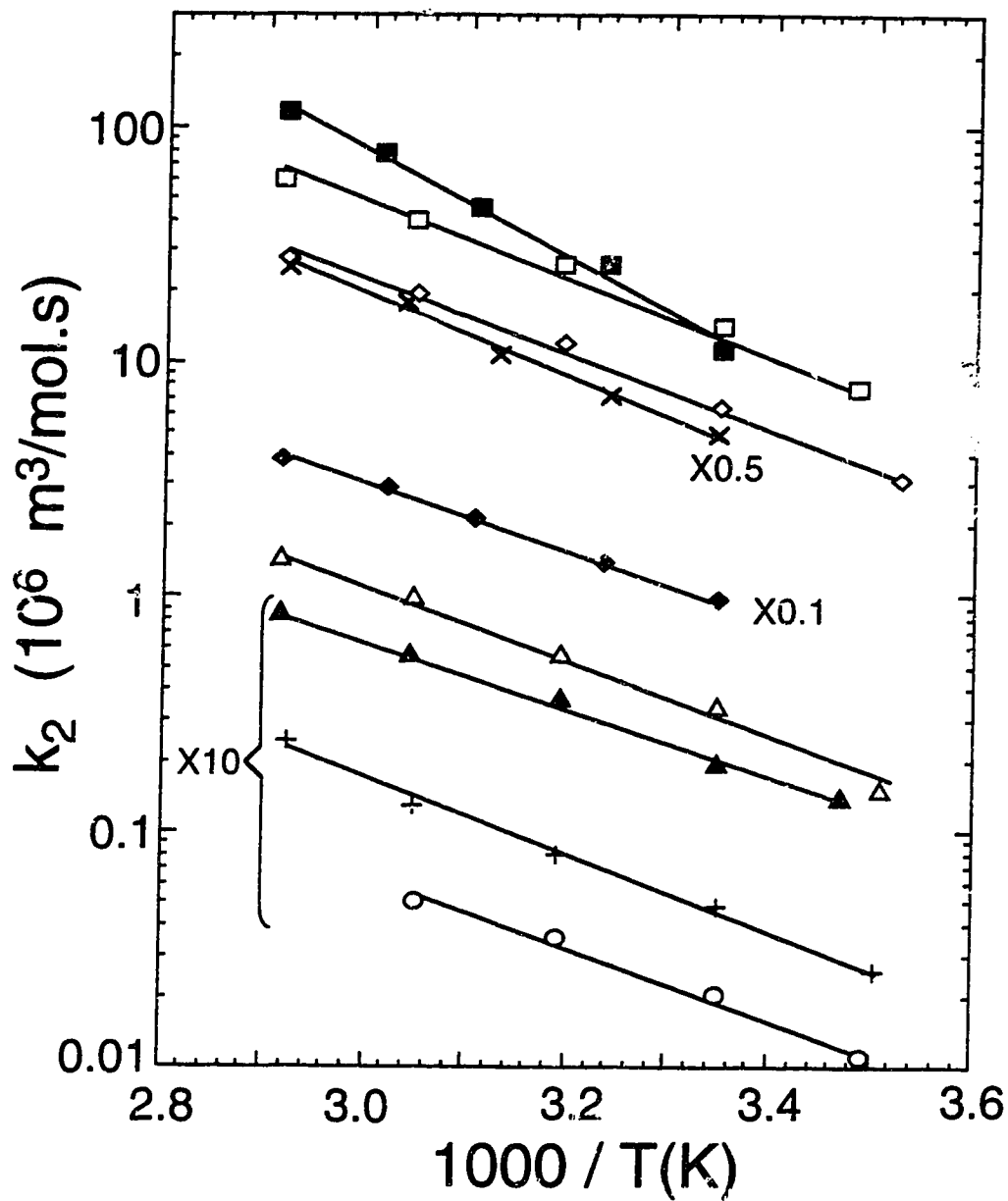


Fig. 2-3. Arrhenius plots of  $k_2$  for the reaction of  $e_s^-$  with  $NH_{4,s}^+ + ClO_{4,s}^-$  in *t*-butanol/water. Refer to Table 1 for symbols. The data for 100, 97 and 90 mol % of water have been corrected for the contribution of the reaction of  $e_s^-$  with  $H_s^+$ . Refer to Ref. 14 for the correction method.



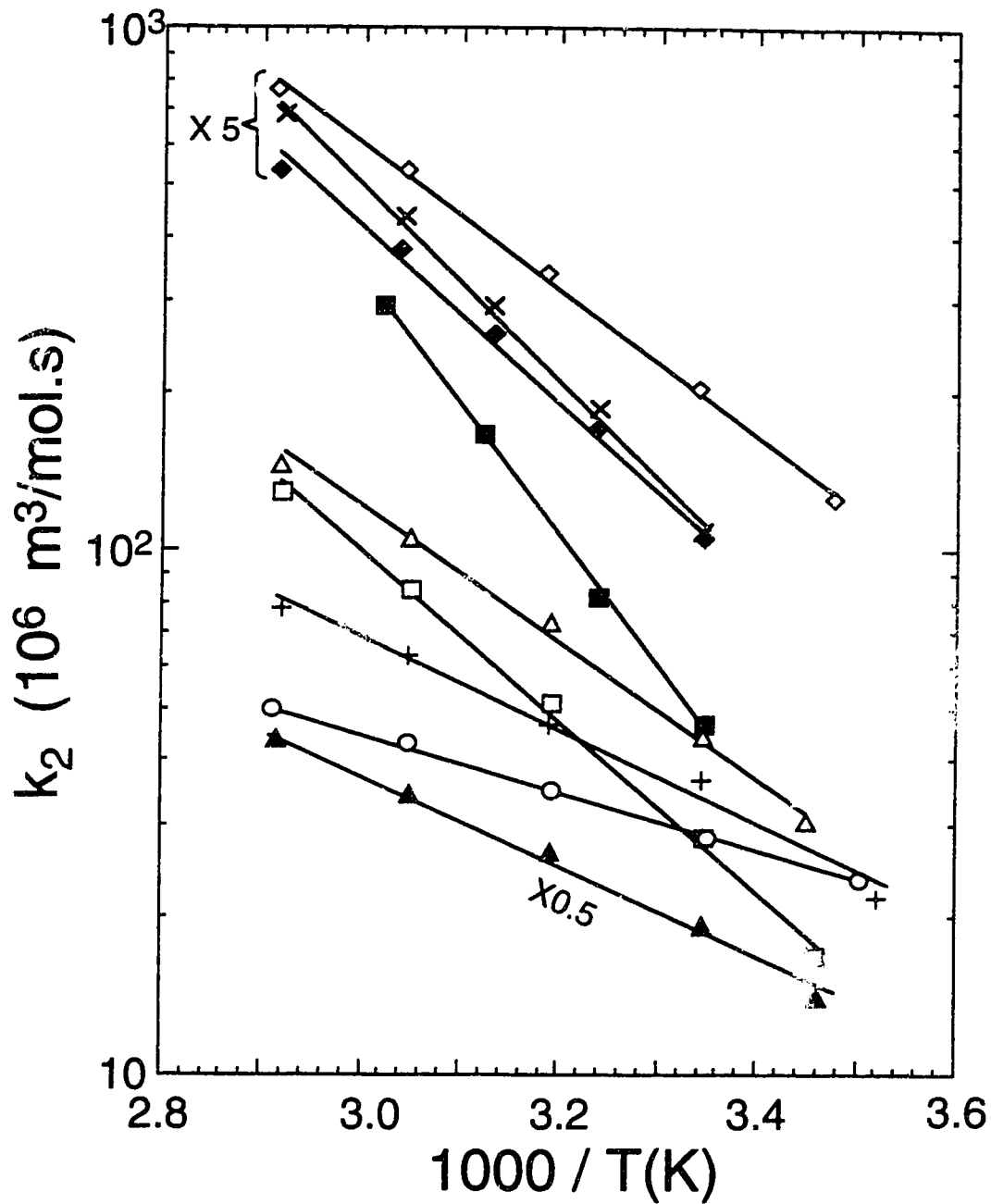


Fig. 2-4. Arrhenius plots of  $k_2$  for the reaction of  $e_s^-$  with  $H_s^+ + ClO_{4,s}^-$  in *t*-butanol/water. Refer to Table 1 for symbols.

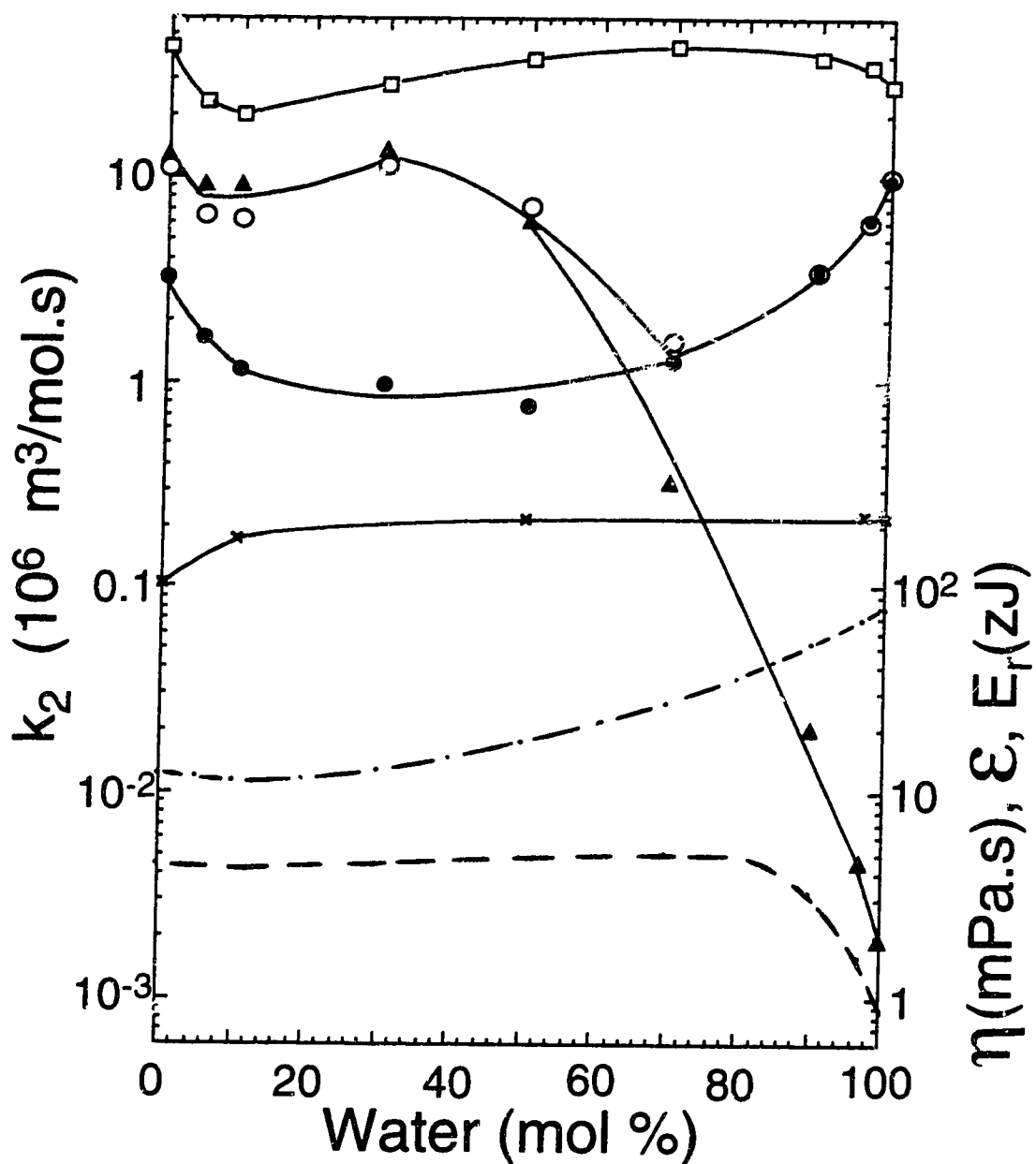


Fig. 2-5. Solvent composition dependence of  $k_2$  in *t*-butanol/water mixtures at 298 K. The solutes are:  $\bullet$ ,  $\text{Li}_s^+ + \text{NO}_{3,s}^-$ ;  $\circ$ ,  $\text{NH}_{4,s}^+ + \text{NO}_{3,s}^-$ ;  $\blacktriangle$ ,  $\text{NH}_{4,s}^+ + \text{ClO}_{4,s}^-$ ;  $\square$ ,  $\text{H}_s^+ + \text{ClO}_{4,s}^-$ . Physical parameter reference lines are:  $\times$ ,  $E_r$  (15);  $- \cdot -$  relative permittivity  $\epsilon$  (16);  $- - -$  viscosity,  $\eta$  (10).

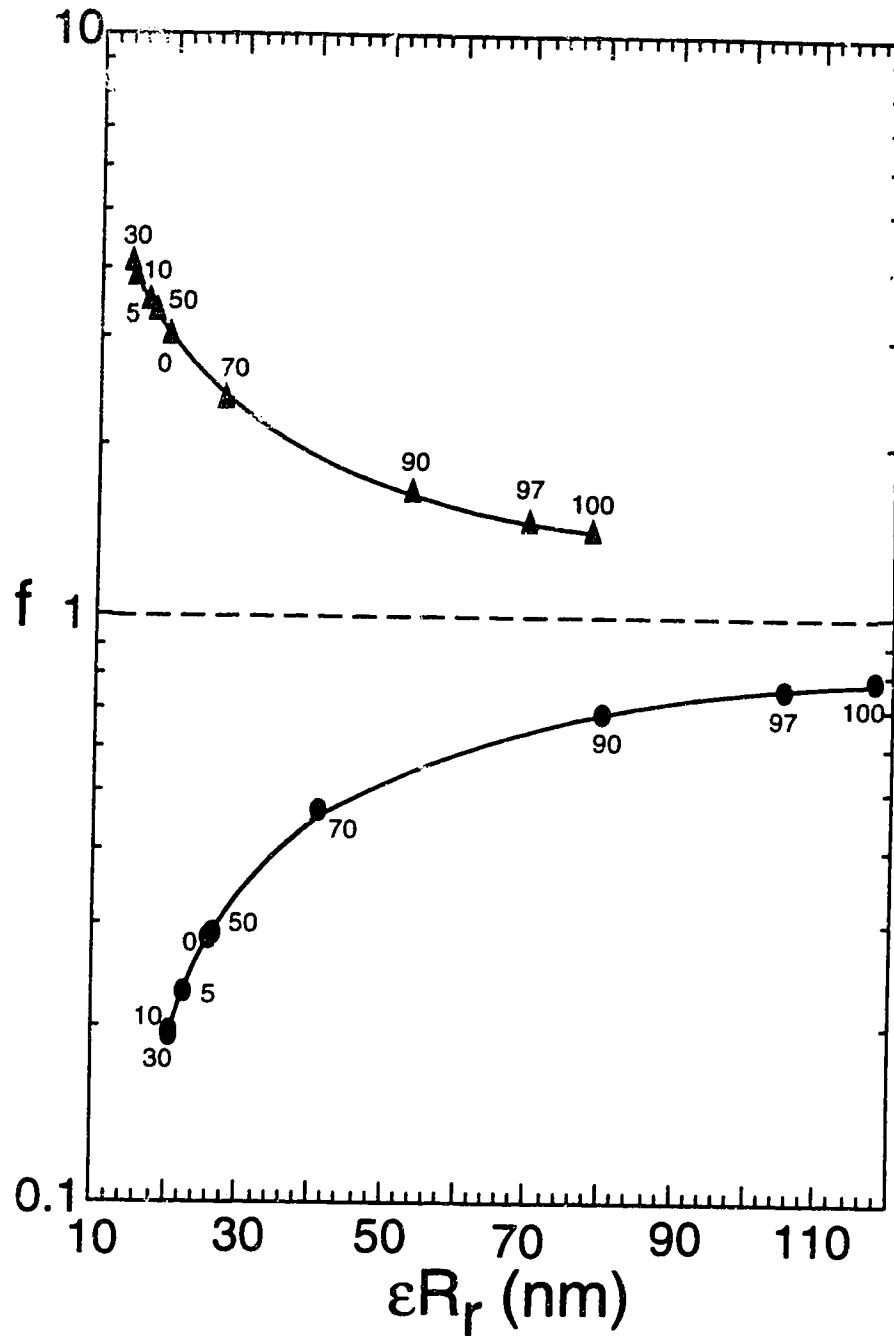


Fig. 2-6. Dependence of Debye  $f$  on  $\epsilon R_f$  for  $\text{Li}_5^+ + \text{NO}_{3,s}^-$  (●) and  $\text{NH}_{4,s}^+ + \text{ClO}_{4,s}^-$  (▲) in *t*-butanol/water mixtures at 298 K. The numbers on the curves are mol % of water.

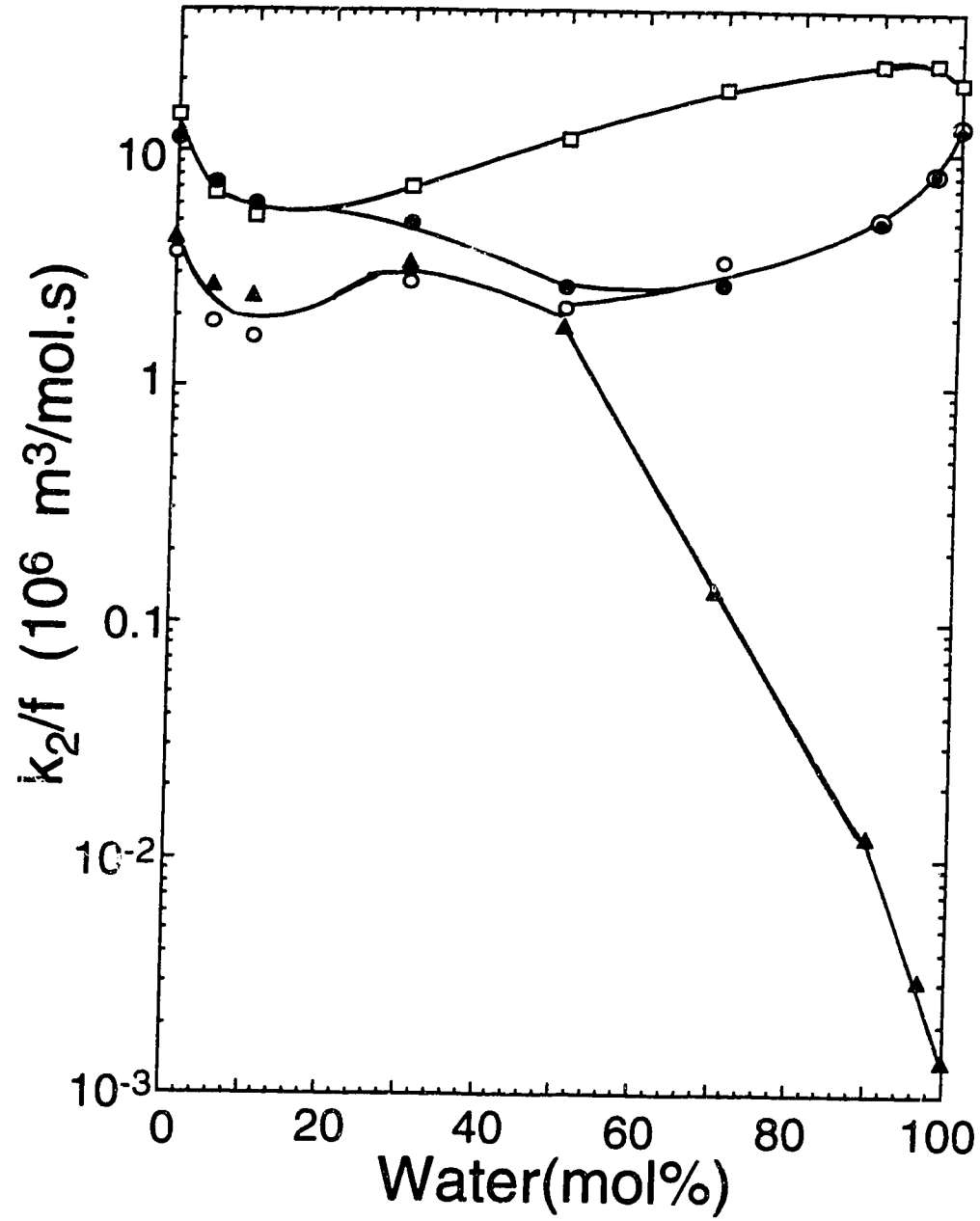


Fig. 2-7.  $k_2/f$  in *t*-butanol/water mixtures at 298 K. Symbols are as in Fig. 2-5.

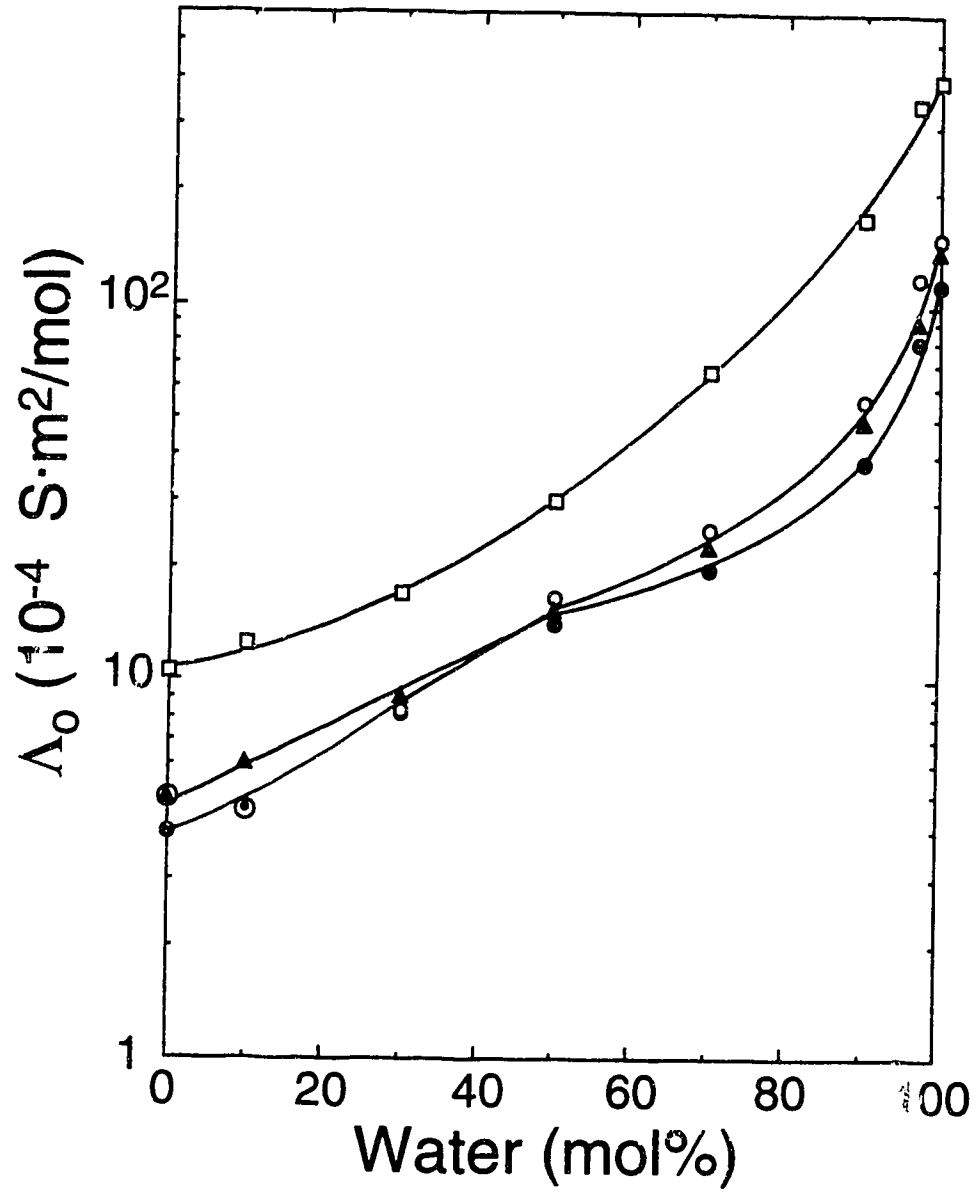


Fig. 2-8. Composition dependence of  $\Lambda_0$  in *t*-butanol/water at 298 K. Symbols are as in Fig. 2-5.

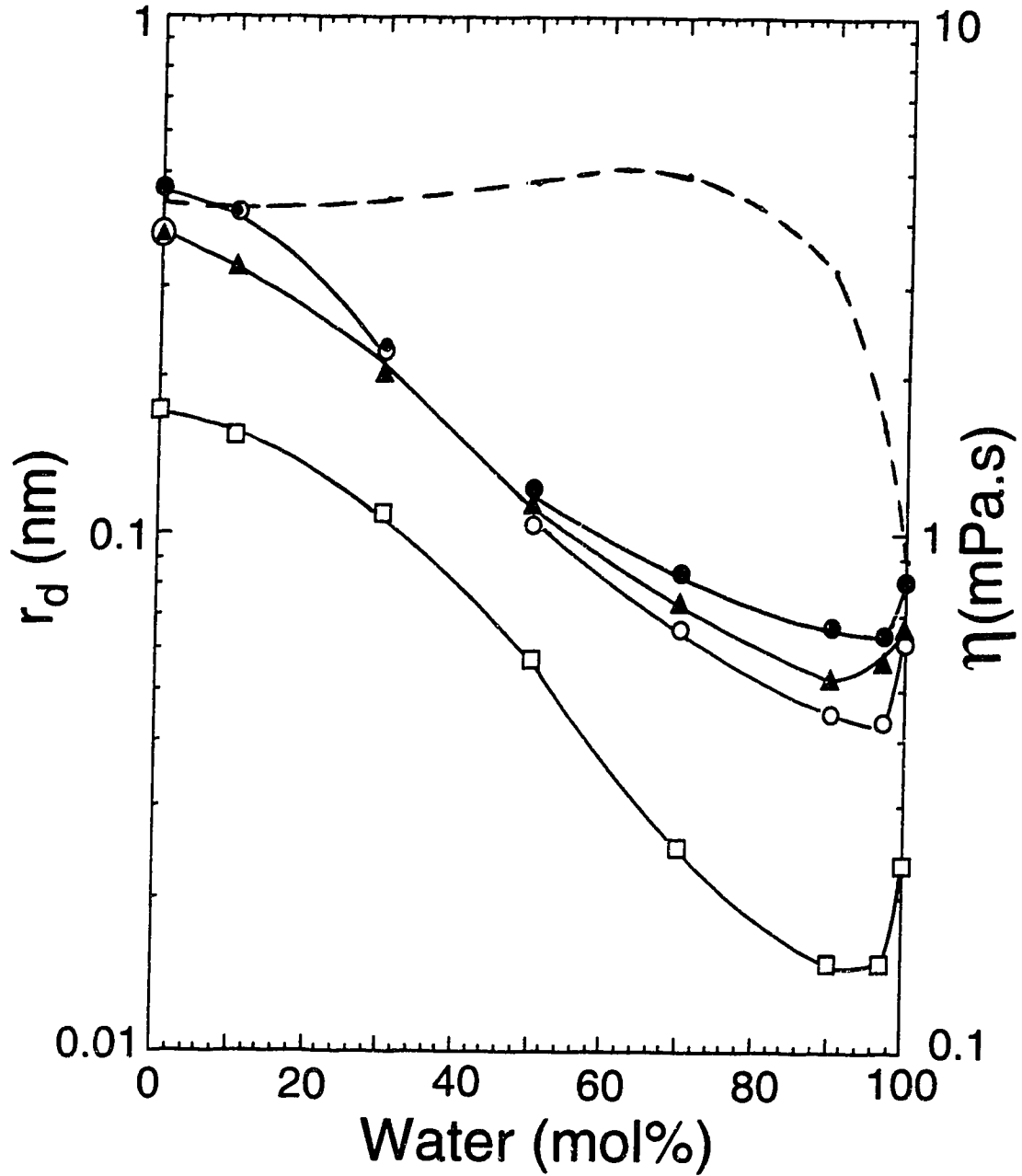


Fig. 2-9. Solvent composition dependence of  $r_d$  of *t*-butanol/water mixtures at 298 K. Symbols are as in Fig. 2-5 — — — represents  $\eta$  (10).

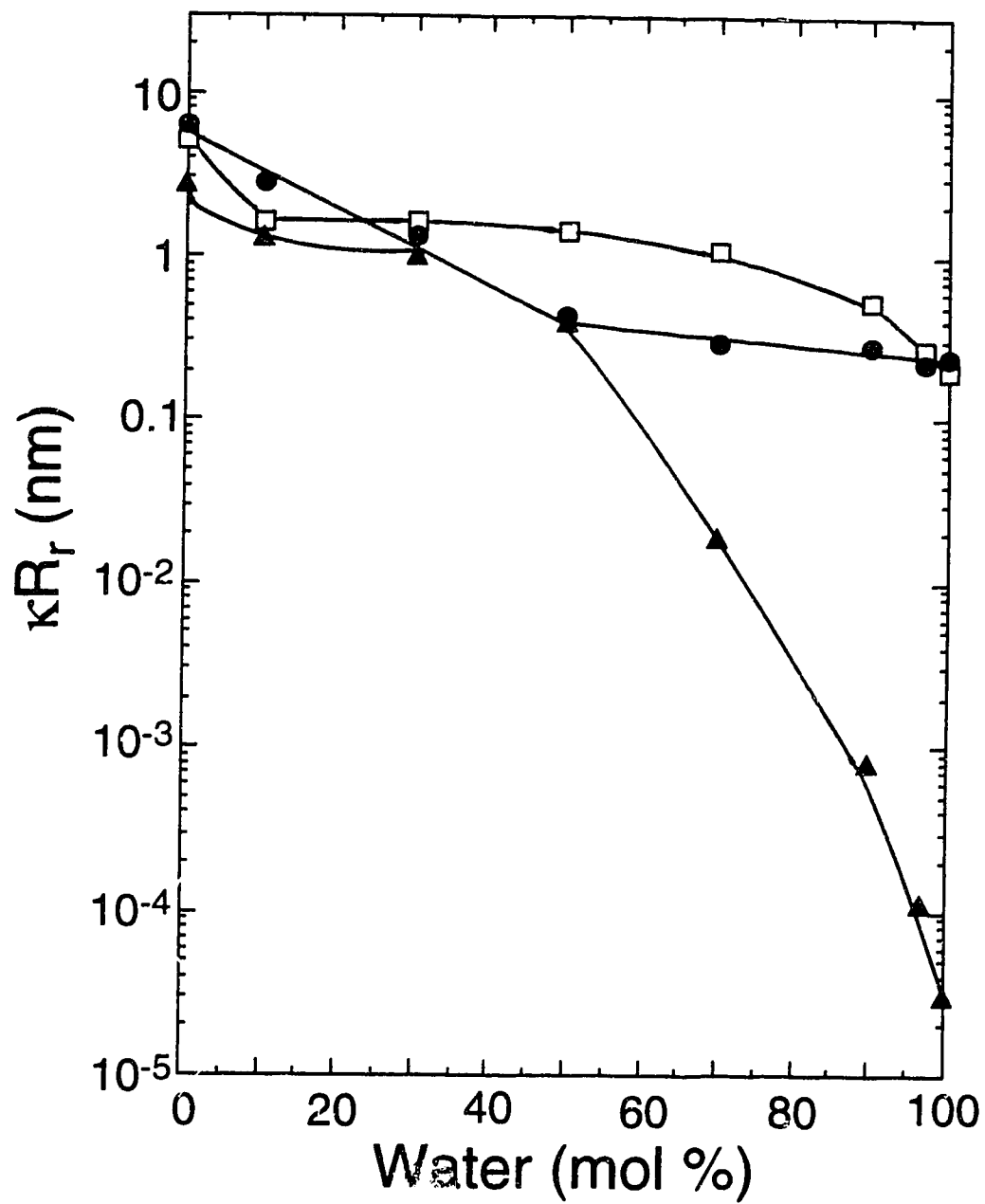


Fig. 2-10. Solvent composition dependence of apparent values of  $\kappa R_r$  in *t*-butanol/water mixtures at 298 K. Symbols are as in Fig. 2-5.

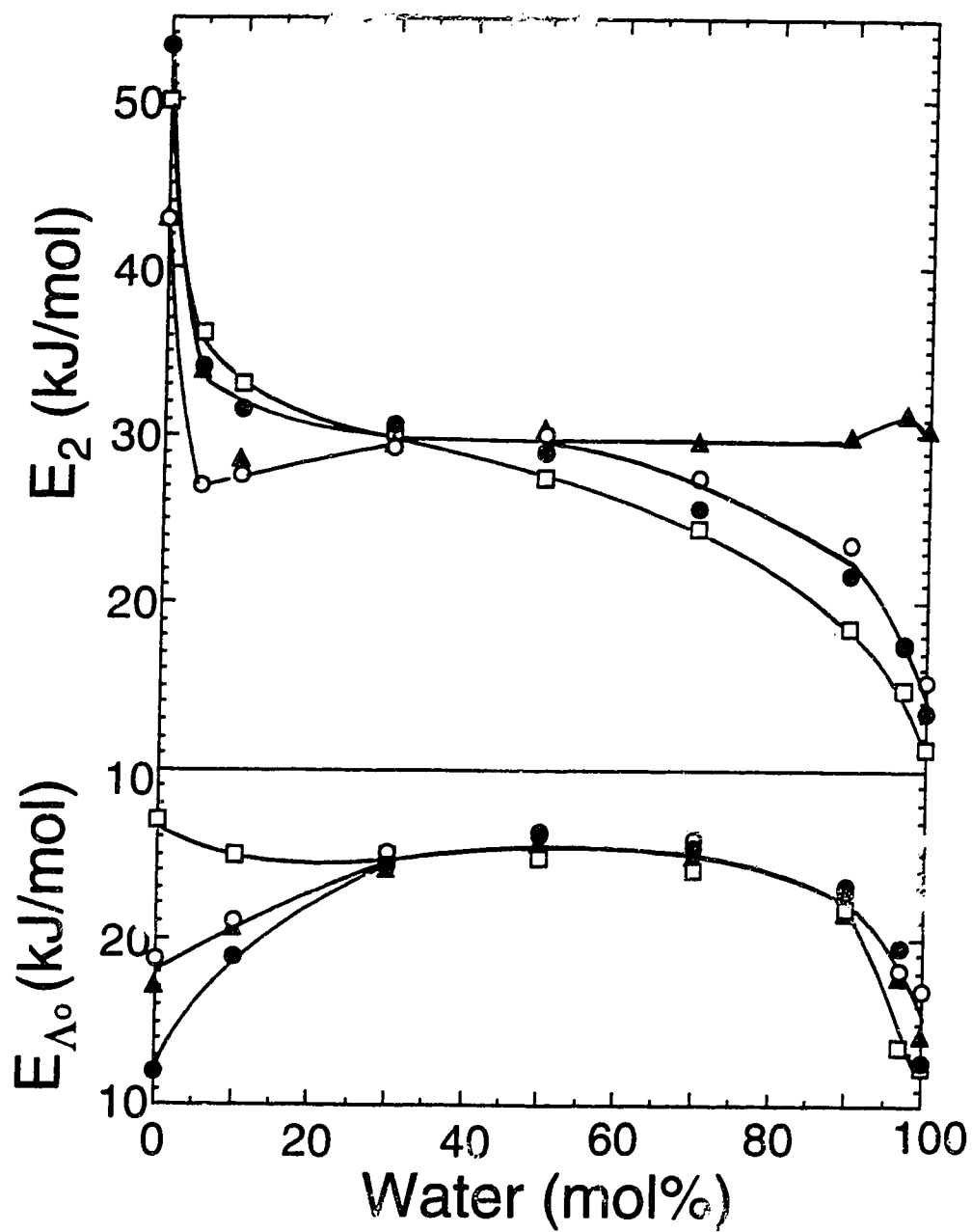


Fig. 2-11. Solvent composition dependence of  $E_2$  and  $E_{\Lambda_0}$  in *t*-BuOH/water mixtures. Symbols are as in Fig. 2-5.



## References

1. H.A. Schwarz and P.S. Gill. *J. Chem. Phys.* **81**, 22 (1977).
2. A.M. Afanassiev, K. Okazaki, and G.R. Freeman. *J. Phys. Chem.* **83**, 1244 (1979).
3. Farhataziz, S. Kalachandra and M.S. Tunuli. *J. Phys. Chem.* **88**, 3837 (1984).
4. A.J. Elliot, D.R. McCracken, G.V. Buxton and N.D. Wood. *J. Chem. Soc. Faraday Trans.* **86**, 1539 (1990).
5. G.V. Buxton and S.R. Mackenzie. *J. Chem. Soc. Faraday Trans.* **88**, 2833 (1992).
6. B.H. Milosavljević and O.I. Mičić. *J. Phys. Chem.* **82**, 1359 (1978).
7. P.C. Senanayake and G.R. Freeman. *J. Chem. Phys.* **87**, 7007 (1987).
8. C.C. Lai and G.R. Freeman. *J. Phys. Chem.* (a) **94**, 302 (1990); (b) **94**, 4891 (1990).
9. A.K. Covington and P. Jones (Ed). *Hydrogen-Bonded Solvent Systems*. Taylor & Francis, London, 1986. (a) D.N. Gloew, H.D. Mak and N.S. Rath, p. 195; (b) M.C.R. Symons and M.J. Blandamer, p. 211.
10. P.C. Senanayake, N. Gee and G.R. Freeman. *Can. J. Chem.* **65**, 2441 (1987).
11. P.C. Senanayake and G.R. Freeman. *J. Phys. Chem.* (a) **91**, 2123 (1987); (b) **92**, 5142 (1988).
12. R.M. Silverstein, G.C. Bassler and T.C. Morrill. *Spectrometric Identification of Organic Compounds* (4th Ed). Wiley, New York. 1981, p. 315.
13. R. Chen. Y. Avotins, and G.R. Freeman. *Can. J. Chem.* **72**, 1083 (1994).
14. R. Chen and G.R. Freeman. *Can. J. Chem.* **71**, 1303 (1993).
15. A.D. Leu, K.N. Jha, and G.R. Freeman. *Can. J. Chem.* **60**, 2342 (1982).

16. Y.Y. Akhadov. *Dielectric Properties of Binary Solutions*. Pergamon Press, New York. 1980, p. 475.
17. Y. Zhao and G.R. Freeman. *Can. J. Chem.* **73**, 389 (1995).
18. P. Debye. *Trans. Electrochem. Soc.* **82**, 265 (1942).
19. M.S. Tunuli and Farhatziz. *J. Phys. Chem.* **90**, 6587 (1986).
20. J.R. Miller. *J. Phys. Chem.* **79**, 1070 (1975).
21. S.A. Peiris and G.R. Freeman. (a) *Can. J. Phys.* **68**, 940 (1990); (b) *Can. J. Chem.* **69**, 884 (1991); (c) *Can. J. Chem.* **69**, 157 (1991).
22. R.C. Weast (ed). *Handbook of Chemistry and Physics*. 70th edn. CRC Press, Boca Raton, FL. 1989, p. D-190.  $r_{vdW} = \left( \frac{3}{4\pi N_A} \cdot \frac{b}{4} \right)^{1/3} = 4.63 \times 10^{-9} b^{1/3}$ .
23. W.P. Atkins. *Physical Chemistry*. 4th ed. Freeman, New York. 1990, Chapter 25.
24. F. Franks and D.J.G. Ives. *Quart. Rev. (London)*, **20**, 1 (1966).

## Chapter Three <sup>a</sup>

### Solvated Electron Mobility in Liquid *t*-Butanol

#### 1. Introduction

The mobilities of electrons in alcohols are difficult to measure directly, for two reasons: (i) proton transfer reactions (acid-base autodissociation) of alcohols produce a relatively high intrinsic conductivity, which means that relatively high concentrations of  $e_s^-$  must be used to obtain a sufficiently high  $e_s^-$  conductance signal above the background conductance; (ii) the large radiation pulse dose needed to produce the high, uniform  $e_s^-$  concentration in the sample requires equipment that is available at only two or three labs in the world (1-5).

The accurate interpretation of measured rates of reactions of  $e_s^-$  requires knowledge of the values of their diffusion coefficients  $D_e$  (or the mobilities  $\mu_e$ ) and activation energies  $E_\mu$ . Values of  $\mu_e$  and  $E_\mu$  in water are well established (5). Values of  $\mu_e$  in alcohols are less certain, and the  $E_\mu$  have not been measured (1-3,6).

Values of  $\mu_e$  in water, methanol, and ethanol are similar to those of the hydroxide (5) and respective alkoxide (1) ions. In mixed methanol/water and ethanol/water solvents this similarity appears to persist, judging from the solvent composition dependences of rate constants of diffusion-controlled reactions (7-9).

---

<sup>a</sup> A version of this chapter has been published. Y. Zhao and G. R. Freeman. Canadian Journal of Chemistry. 73, 389 (1995).

However, in *iso*-propanol (3) and larger alcohols (2,3)  $\mu_e$  appears to be larger than the mobility of a normal anion or alkoxide ion. These measurements have not been repeated, and must therefore be viewed with caution. In support of them, our study of  $e_s^-$  reactivity in *t*-butanol (10) provides evidence that  $\mu_e$  in *t*-butanol is about 10 times higher than the mobility of a normal anion in this alcohol. The relevant data are presented below.

## 2. Experimental and Results

The purified alcohol contained  $5 \times 10^{-4}$  mol fraction of water (10). Up to  $1 \times 10^{-5}$  mol fraction more water was added with the  $\text{HClO}_4$  to measure the rate constant  $k_2$  and molar conductance.

The experimental techniques are described in reference 10 and Appendix One.

The sum of the mobilities of  $e_s^-$  and  $\text{H}_s^+$ , ( $\mu_e + \mu_{\text{H}^+}$ ), in *t*-butanol was estimated from the measured rate constant  $k_2$  of the diffusion controlled reaction  $e_s^- + \text{H}_s^+ \rightarrow \text{H}_s$  (10). A rearranged version of the Smoluchowski-Debye-Nernst-Einstein equation was used (11):

$$[1] \quad \mu_e + \mu_{\text{H}^+} = 1.48 \times 10^{-16} k_2 / f F \kappa R_f \quad ,$$

where  $f$  is the Debye coulombic interaction factor,  $T$  is the temperature,  $F$  is the Faraday,  $\kappa$  is the probability of reaction per encounter and is near unity for  $e_s^- + \text{H}_s^+$  in alcohols (12) and  $R_f$  is the center-to-center encounter radius of  $e_s^- + \text{H}_s^+$  and is taken as 1.6 nm in *t*-butanol (10). The Debye factor is given by

$$[2] \quad f = \frac{x}{e^x - 1} \quad ,$$

$$[3] \quad x = -\xi^2/4\pi\epsilon_0\epsilon R_T k_B T \quad ,$$

where  $\xi$  is the proton charge,  $\epsilon$  is the relative permittivity of the medium between the proton and electron at  $R_T$ , and  $k_B$  is Boltzmann's constant.

An Arrhenius plot of  $k_2(e_s^- + H_s^+)$  is shown in Figure 1, for temperatures 299.5 K to 330.0 K;  $E_2 = 50$  kJ/mol. The value of  $\kappa R_T$  was taken as constant at 1.6 nm (10). The values of the Debye factor  $f$  calculated from known values of  $\epsilon$  (Table 1) are included in Figure 1;  $E_f = 10$  kJ/mol.

From the measured molar conductances of dilute solutions of  $HClO_4$  and  $NH_4ClO_4$  (Table 2), we estimated the ratio  $\mu_{H^+} / \mu_{ClO_4^-}$  and hence  $\mu_{H^+} ; \mu = \lambda/F$ . In ethanol at 298 K the mobility of  $ClO_4^-$  is near the geometric mean of those of  $NH_4^+$  and  $H^+$  (Table 3). For lack of better information we assumed the same to apply in *t*-butanol solvent, and subdivided the conductances of  $NH_4^+ClO_4^-$  and  $H^+ClO_4^-$  in this way. The geometric factor is given by  $\Lambda_0(HClO_4) / \Lambda_0(NH_4ClO_4)$ . The values of  $\mu_{H^+}$  are included in Figure 1;  $E_{\mu_{H^+}} = 28$  kJ/mol.

The derived values of  $\mu_e$  are listed in Table 1 and plotted in Figure 1;  $E_{\mu_e} = 41$  kJ/mol.

### 3. Discussion

Protons diffuse by a Grotthus ( $H^+$  exchange) mechanism in alcohols, which allows  $H^+$  to migrate 4.8 times faster than  $NH_4^+$  and 2.2 times faster than  $ClO_4^-$  in *t*-butanol at about 300 K (Table 2). The  $5 \times 10^{-4}$  mol fraction of water in the alcohol evidently did not quench the Grotthus mechanism. The activation energy of the  $H^+$  exchange mechanism (28 kJ/mol) is 1.6 times larger than that of normal ion transport (17 kJ/mol for  $NH_4^+$  and  $ClO_4^-$  (10)).

Electrons migrate even faster than protons in *t*-butanol, and the activation energy is larger (41 kJ/mol, Table 3). The mobility ratio  $e_s^-/H_s^+$  is 5 at 300 K and 8 at 330 K (Fig. 1). The high mobility and high activation energy indicate that electrons in *t*-butanol migrate by a hopping mechanism.

The value of  $E_{\mu_e} = 41$  kJ/mol is only slightly larger than  $E_\tau = 39$  kJ/mol for molecular electric dipole rotation (Table 3). We suggest that thermally agitated dipole rotation of the solvating molecules is the process that activates the electron hopping.

By comparing  $\mu_e$  with the fluidity  $\eta^{-1}$  of the various solvents (Table 3), and the conductance ratio  $e_s^-/HClO_4$ , one might suggest that electron hopping also occurs in 2-propanol and in all the butanols.

**Table 3-1. Estimation of mobility of  $e_s^-$  in *t*-butanol.<sup>a</sup>**

T(K)	295.5	308.7	318.9	330.0
$\epsilon$	12.1	10.2	8.6	7.4
f	3.05	3.44	3.89	4.33
$\kappa_2(10^6\text{m}^3/\text{mol}\cdot\text{s})^b$	47	82	168	295
$\lambda_{\text{H}^+}/\lambda_{\text{ClO}_4^-}$	2.2	2.5	2.6	3.1
$\mu_{\text{H}^+}(10^{-8}\text{m}^2/\text{V}\cdot\text{s})$	0.8	1.15	1.6	~2.3
$\mu_e + \mu_{\text{H}^+}$	4.9	7.4	13.0	19.8
$\mu_e(10^{-8}\text{m}^2/\text{V}\cdot\text{s})$	4.1	6.3	11.4	17.5

<sup>a</sup>: Using eq. [1],  $\kappa R_T = 1.6 \times 10^{-9} \text{ m}$ ,  $F = 96,500 \text{ C/mol}$ .

<sup>b</sup>:  $\text{HClO}_4$  concentrations 1-6 mmol/m<sup>3</sup>.

**Table 3-2. Measured conductivities of HClO<sub>4</sub> and NH<sub>4</sub>ClO<sub>4</sub>; estimated ionic conductivity of H<sub>g</sub><sup>+</sup> in *t*-butanol.**

T(K)	$\Lambda_0(\text{HClO}_4)^a$ (10 <sup>-4</sup> S•m <sup>2</sup> /mol)	T(K)	$\Lambda_0(\text{NH}_4\text{ClO}_4)^b$ (10 <sup>-4</sup> S•m <sup>2</sup> /mol)	
300.1	11.4	300.9	5.25	
308.5	15.5	308.3	6.18	
318.3	19.4	318.3	7.42	
$T_{\text{ave}}(\text{K})$		300.5	308.4	318.3
$\frac{\lambda_{\text{ClO}_4^-}}{\lambda_{\text{NH}_4^+}} \approx \frac{\lambda_{\text{H}^+}}{\lambda_{\text{ClO}_4^-}}$		2.2	2.5	2.6
$\lambda_{\text{NH}_4^+}$ (10 <sup>-4</sup> S•m <sup>2</sup> /mol)		1.7	1.8	2.0
$\lambda_{\text{ClO}_4^-}$ (10 <sup>-4</sup> S•m <sup>2</sup> /mol)		3.6	4.4	5.4
$\lambda_{\text{H}^+}$ (10 <sup>-4</sup> S•m <sup>2</sup> /mol)		7.8	11.1	14.0
$\mu_{\text{H}^+}$ (10 <sup>-8</sup> m <sup>2</sup> /V•s)		0.81	1.15	1.45

*a*: concentrations: 2–10 mmol/m<sup>3</sup>.

*b*: concentrations: 6–30 mmol/m<sup>3</sup>.



**Table 3-3: Comparison of mobilities of ions and solvated electrons with parameters in alcohols and water at 298 K.**

	$\eta^{-1}{}^a$ (mPa·s) <sup>-1</sup>	$\mu(10^{-8}\text{m}^2/\text{V}\cdot\text{s})$ <i>b,c</i>			
		$\text{NH}_4^+$	$\text{ClO}_4^-$	$\text{H}_s^+$	$e_s^-$
Water	1.12 <sup>13</sup>	7.6	7.0	36.2	19 <sup>5</sup>
MeOH	1.8 <sup>13</sup>	6.0	7.3	14.7	61,6 <sup>b</sup>
EtOH	0.9 <sup>13</sup>	3.0	3.5	6.0	31,6 <sup>b</sup>
2-PrOH	0.5 <sup>14</sup>		0.86	1.7	5 <sup>3</sup>
1-BuOH	0.4 <sup>13</sup>		0.50	1.0	8 <sup>3</sup>
<i>i</i> -BuOH	0.29 <sup>15</sup>		0.49	0.97	7 <sup>3</sup>
<i>t</i> -BuOH <sup><i>i</i></sup>	0.22 <sup>15</sup>	0.16	0.35	0.76	4

	$\Lambda_0(\text{HClO}_4)$ <sup><i>d</i></sup> (10 <sup>-4</sup> S·m <sup>2</sup> /mol)	$\Lambda_0$ Ratio ( $e_s^-/\text{HClO}_4$ )	Activation E (kJ/mol)			
			$\tau_1$	$\tau^e$	$\mu_c^f$	$\Lambda_0(\text{HClO}_4)$
Water	417 <sup>16</sup>	0.44	17	19	20	12 <sup><i>g</i></sup>
MeOH	214 <sup>16</sup>	0.27	11	16		9,4 <sup><i>h</i></sup>
EtOH	93 <sup>16</sup>	0.31	14	18		13 <sup><i>h</i></sup>
2-PrOH	25 <sup>17</sup>		22	27		21 <sup><i>d</i></sup>
1-BuOH	14.6	5.3	19	26		21 <sup><i>d</i></sup>
<i>i</i> -BuOH	14.1 <sup>12</sup>	4.8	24	28		24 <sup><i>d</i></sup>
<i>t</i> -BuOH <sup><i>i</i></sup>	10.6	4	31	39	41	27 <sup><i>d</i></sup>

*a* Fluidity of solvent; ref. nos. are superscripts.

*b* Mobility of ions in water, MeOH and EtOH, ref. 16; in EtOH the conductivity ratios of  $\text{NH}_4^+ : \text{ClO}_4^-$  and  $\text{ClO}_4^- : \text{H}_s^+$  are approximately 1:2 and 1:2, respectively. The same ratios are assumed for the other alcohols (except *t*-BuOH) to estimate the ionic conductivities of  $\text{NH}_4^+$ ,  $\text{ClO}_4^-$  and  $\text{H}_s^+$  from

the measured electrolyte molar conductivities; for *t*-BuOH, ionic conductivities estimated from corresponding electrolyte conductivities and self-consistence gives ratios  $\text{NH}_4^+ : \text{ClO}_4^-$  and  $\text{ClO}_4^- : \text{H}_3^+$  equal to 1 : 2.2 and 1 : 2.2, respectively.

- c* Mobility of electrons; *t*-BuOH, present work.
- d* Molar conductivity of  $\text{HClO}_4$ ; 1-BuOH, R. Chen's unpublished data; *t*-BuOH, present work.
- e* Dielectric relaxation time: ref. 18, except *t*-BuOH, ref. 19.
- f* Electron mobility in water, ref. 5; *t*-BuOH, present work.
- g* Present work.
- h* Calculated from data in ref. 20.
- i* All values extrapolated from measurements at 300 K and higher temperatures; freezing point is 298.7 K.

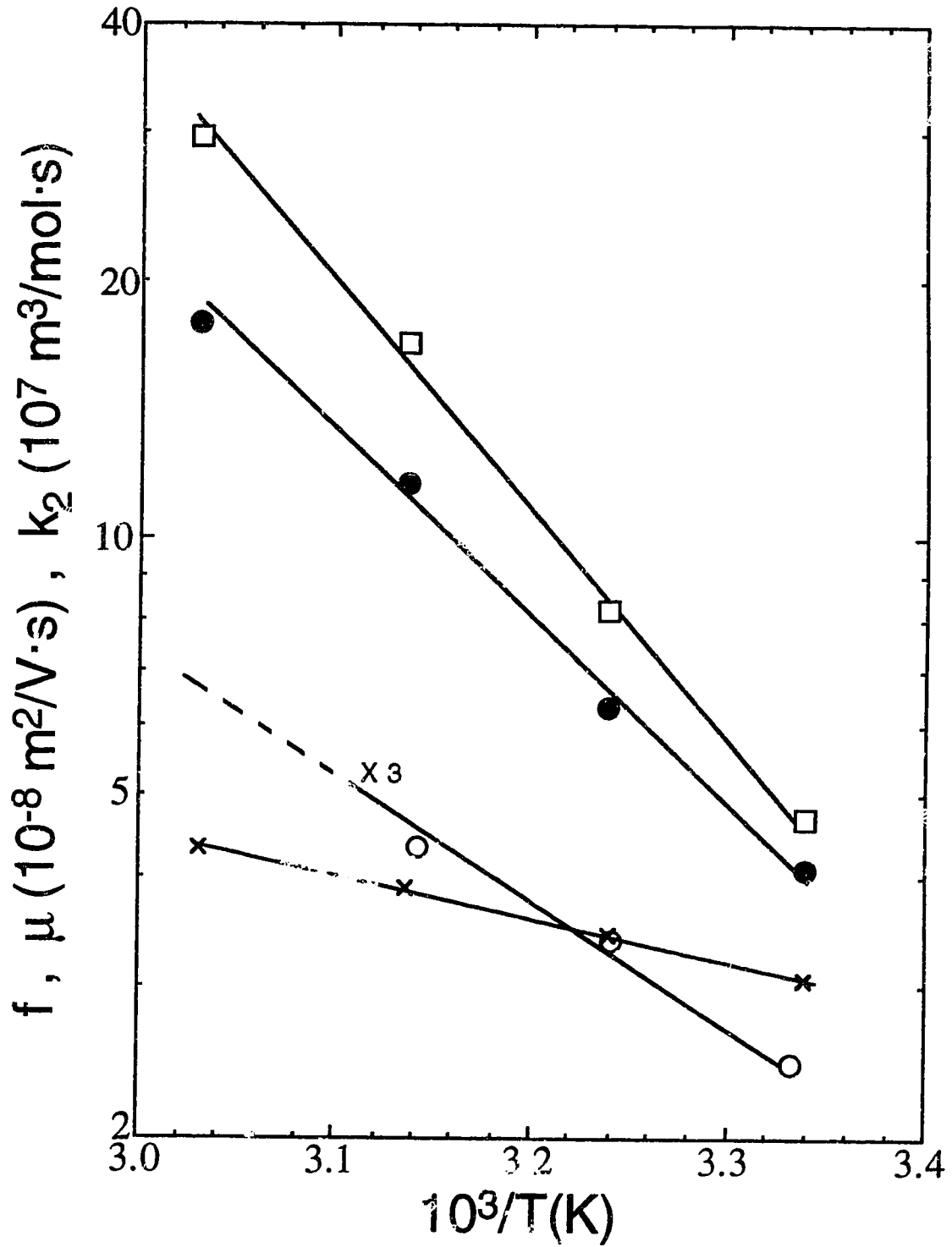


Figure 3-1. Arrhenius plots. □,  $k_2(e_s^- + H_s^+)$ ; ×, Debye  $f$ ; ○,  $\mu_{H^+}$ ; ●,  $\mu_e$ ; in pure *t*-butanol solvent.

**References:**

1. P. Fowles, *Trans. Faraday Soc.* **67**, 428 (1971).
2. A.V. Vannikov, E.I. Mal'tzev, V.I. Zolotarevsky, and A.V. Rudnev, *Int. J. Radiat. Phys. Chem.* **4**, 135 (1972).
3. A.V. Rudnev, A.V. Vannikov, and N.A. Bakh, *High Energ. Chem.* **6**, 416 (1972).
4. K.H. Schmidt, *Int. J. Radiat. Phys. Chem.* **4**, 439 (1972).
5. K.H. Schmidt, P. Han, and D.M. Bartels, *J. Phys. Chem.* **96**, 199 (1992).
6. J.-P. Dodelet and G.R. Freeman, *Can. J. Chem.* **50** (1972), (a) p. 2667, (b) 2729.
7. F. Barat, L. Gilles, B. Hickel, and B. Lesigne, *J. Phys. Chem.* **77**, 1711 (1973).
8. O.I. Micic and B. Cercek, *J. Phys. Chem.* **81**, 833 (1977).
9. Y. Maham and G.R. Freeman, *J. Phys. Chem.* **92**, 1506 (1988).
10. Y. Zhao and G.R. Freeman, *Can. J. Chem.* **73**, 392(1995).
11. R. Chen and G.R. Freeman, *Can. J. Chem.* **71**, 1303 (1993).
12. R. Chen, Y. Avotins, and G.R. Freeman, *Can. J. Chem.* **72**, 1083 (1994).
13. R.C. Weast (ed.), *Handbook of Chemistry and Physics*, 59th edn., CRC Press, Boca Raton, FL. 1979, p. F-52.
14. W. Weber, *Rheol. Acta.* **14**, 1012 (1975).
15. P.C. Senanayake, N. Gee, and G.R. Freeman, *Can. J. Chem.* **65**, 2441 (1987).
16. D. Dobos, *Electrochemical Data*, Elsevier Scientific Publishing, New York, 1975, p. 88-89.
17. S.A. Peiris and G.R. Freeman, *Can. J. Chem.* **69**, 884 (1991).
18. F. Buckley and A.A. Maryott, *Table of Dielectric Dispersion Data for Pure Liquids and Dilute Solutions*, National Bureau of Standards Circular 589.1958.
19. M. Tabellout, P. Lanceleur, J.R. Emery, D. Hayward, and R.A. Pethrick, *J. Chem. Soc. Faraday Trans.* **86**, 1493 (1990).
20. G.J. Janz and R.P.T. Tomkins, *Nonaqueous Electrolytes Handbook*, Vol. 1, Academic Press, New York, 1972, p. 299-301.

## Chapter Four <sup>a</sup>

### Solvent Effects on the Reactivity of Solvated Electrons with $\text{NO}_{3,s}^-$ in C<sub>1</sub> to C<sub>4</sub> Alcohols

#### 1. Introduction

Elucidation of the reactivity of  $e_s^-$  with  $\text{NO}_{3,s}^-$  in water and in alcohol solvents is a long-standing problem (1-11). The reaction rate constant  $k_2$  of  $e_s^-$  with many solutes in a series of alcohols follows the Smoluchowski-Debye model, and increases with increasing fluidity ( $1/\eta$ ) of the solvent (11,12). By contrast, the rate constant  $k_2(e_s^- + \text{NO}_{3,s}^-)$  increases approximately linearly with *decreasing* fluidity in a series of alcohol solvents at 298 K (11). This increase of reaction rate with decrease of diffusion rate points to behavior of the reactant encounter pair. The value  $k_2(e_s^- + \text{NO}_{3,s}^-)$  also increases with decreasing trap depth of  $e_s^-$ , as represented by the optical absorption energy  $E_r$  (13,14). However, there is lack of overall correlation in all C<sub>1</sub> to C<sub>4</sub> alcohols, including secondary and tertiary alcohols (9,10). Therefore, we here bring together data to advance the understanding of the reaction in all C<sub>1</sub> to C<sub>4</sub> alcohols.

---

<sup>a</sup> A version of this chapter has been published. Y. Zhao and G. R. Freeman. Canadian Journal of Chemistry. **73**, 284 (1995)

## 2. Data

Values of  $k_2$  in the different solvents were taken from refs. 3, 4, 6, 7, 9-11 and are listed for 298 K in Table 1.

Kinetic properties of the solvents are viscosity  $\eta$  (15-17) and dielectric relaxation (electric dipole rotation) time (18-22). Values are collected in Table 1.

The tenacity with which an electron is held in a solvation site is assumed to be related to the  $e_s^-$  optical absorption energy (23). Electrons with lower optical absorption energies tend to be more reactive (13,14,24), so the energy  $E_T$  half way up the low energy side of the absorption band is chosen for correlations with reaction rate constants (Table 1).

## 3. Discussion

### *Transport properties*

Fig. 1A shows correlations of  $k_2$  ( $e_s^- + NO_{3,s}^-$ ) with solvent viscosity  $\eta$ . The rate constants in the primary alcohols *increase* with  $\eta$ ; those in the secondary alcohols are higher but have a similar tendency;  $k_2$  is higher in the tertiary alcohol, and the highest in water. This indicates chemical participation of solvent molecules in the reaction (9). The higher the  $\eta$  value, the more difficult it is for the reactants in an encounter pair to diffuse apart, giving more time for reaction to occur. The probability of reaction during an encounter must increase as  $\eta^m$  with  $m \approx 2$ , because the encounter frequency decreases approximately as  $\eta^{-1}$ .

### *Trap-depth model and modification*

The Smoluchowski model is used to investigate the transport properties in diffusion-controlled reactions. However, reactivity is also often dependent on the solvation energy of the reactants, especially of  $e_s^-$  (13,14,24). The mean free energy of solvation of electrons in water, -162 kJ/mol at 298 K (25), is similar to the optical absorption energy  $E_{Amax} = 166$  kJ mol (26). This supports the search for correlations of  $k_2$  with optical absorption energy  $E_T$ .

Fig. 1B shows correlations of  $k_2$  ( $e_s^- + NO_{3,s}^-$ ) with  $E_T$  at 298 K. Among the butanols  $k_2$  decreases with increase of  $E_T$ . The values of  $k_2$  also decrease with decreasing number of carbons, from 4 to 1. However,  $k_2$  is largest in water.

The dielectric relaxation times  $\tau$  of the series of alcohols (excluding *t*-butanol) at different temperatures vary approximately linearly with  $\eta$  (Fig. 2). The equation of the line in Fig. 2 is:

$$[1] \quad \tau(\text{ps}) = 195 [\eta(\text{mPa}\cdot\text{s}) - 0.30]$$

The reported values of  $\tau$  for *t*-butanol at 298 K (20-22) are much smaller than eq [1] indicates for  $\eta = 4.45$  mPa\*s, and those at 323 K and 343 K were obtained by extrapolation from lower temperatures (21,22). The smaller ratio of  $\tau/\eta$  for *t*-butanol probably has to do with the sphere like structure of the molecules, which can rotate and reorient faster than the chain like butanols.

Correlations of electron solvation times with the intermediate dielectric relaxation time  $\tau_2$  (27), and of electron transfer reaction rate constants with the longitudinal relaxation  $\tau_L$  (28) have been made. However, we use the longest relaxation time  $\tau_1 = \tau$  for our general correlation with  $k_2(e_s^- + NO_{3,s}^-)$ , because  $\tau_1$  data are more complete.

The layered structures of Figs. 1A and B suggest that a more basic correlation might be found. From the Smoluchowski-Debye model (6,9,10) one can get:

$$[2] \quad k_2 = 4\pi N_A (D_e + D_s) \kappa R_T f$$

where  $N_A$  is Avogadro's constant,  $D_i$  is the diffusion coefficient of  $i$ ,  $R_T$  is the center-to-center reactant separation when reaction occurs, and  $\kappa$  is the probability that reaction occurs during one encounter and equals unity for diffusion-controlled reactions. The quantity  $\kappa R_T$  is called an effective reaction radius; values have been estimated from the values of  $k_2$  by factoring out the Debye coulombic factor  $f$  and approximate values of the diffusion coefficients (conductances, of the ionic reactants:

$$[3] \quad \kappa R_T(m) \approx 1 \times 10^{-16} k_2 / f T \Lambda_0$$

where  $\Lambda_0$  ( $S \cdot m^2/mol$ ) is the molar conductance of the reactant electrolyte solutions. To obtain accurate values of  $\kappa R_T$  we would require accurate values of conductance of solvated electrons in the alcohols, but they are not available. At this stage we are looking for trends. A log-log plot of apparent  $\kappa R_T$  values against  $E_T/\tau$  at 298 K provides a better over-all correlation of the reactivities in the  $C_1$  to  $C_4$  alcohols (black circles and full line in Fig. 3) than did the plots in Figure 1. The value of  $\kappa R_T$  at 298 K decreases with increasing trap depth of  $e_s^-$  and with decreasing relaxation time in the series of solvents. The value of  $\kappa R_T$  in water is  $\sim 10^2$  times higher than that extrapolated for an alcohol at the same value of  $E_T/\tau$  (Fig. 3), which implies that the reaction is different in water.

A plot of  $\kappa R_T$  against  $E_T/\eta$  shows a correlation similar to that in Fig. 3, as expected because of the linear relationship between  $\tau$  and  $\eta$ .



In the C<sub>1</sub> to C<sub>4</sub> alcohol series at 298 K, if 1) the alcohol has a longer carbon chain, 2) the chain is more branched, or 3) the branch point is closer to the hydroxyl group, then  $E_T/\tau$  is lower and  $\kappa R_T$  is higher. This correlation might indicate that a longer and more branched chain alcohol has more difficulty to orient its -O-H dipole in the field of the electron or ion to solvate them, and that slower or less exoergic solvation results in a higher reaction rate constant with  $\text{NO}_3^-$ . The quantity  $E_T/\tau$  can be understood as an effective trap-depth, since  $E_T$  is approximately equal to the binding energy of the  $e_s^-$  to its solvent site, and  $\tau$  is related to the time during which the electron remains in a higher-than-equilibrium energy state after jumping to a new site. Similar correlations might be obtained with  $E_T/\tau_2$  or  $E_T/\tau_L$ , but sufficient data are not available.

The values of  $\kappa R_T$  and  $E_T/\tau$  in a given alcohol usually increase with temperature (Fig. 3), and can be expressed by the empirical equation

$$[4] \quad \kappa R_T = C_\tau (E_T/\tau)^{p_\tau} .$$

The slope of the line for a given alcohol in Fig. 3 equals  $p_\tau$ , and the value of  $\kappa R_T$  at  $E_T/\tau = 1 \text{ zJ/ps}$  gives  $C_\tau$ . There are four groups of values of  $p_\tau$ :  $\sim 0.0$  for water and methanol, 0.6 for secondary alcohols,  $\sim 1.3$  for primary alcohols, and 1.8 for *t*-butanol. We do not understand the step size of 0.6.

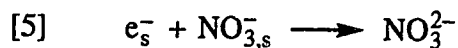
Correlations of  $C_\tau$  with  $\tau$  are shown in Fig. 4. The four groups of  $p_\tau$  probably indicate four different types of solvation structure in alcohols: *tertiary* alcohols, *secondary* alcohols, *primary* alcohols, and methanol. Water remains exceptional.

It has been suggested that solvent molecules participate chemically in the reaction  $e_s^- + \text{NO}_{3,s}^-$  in water and alcohols (4,9). Reactivity in *t*-butanol is highest; it has a relatively long dielectric relaxation time, and it has the maximum number of -CH<sub>x</sub> groups attached to the  $\alpha$ -carbon atom of the alcohol. On the other hand, methanol has the lowest

reactivity, the shortest dielectric relaxation time and no  $-\text{CH}_x$  groups attached to the  $\alpha$ -carbon atom.

The correlations in Fig. 4 suggest two aspects of the solvent effect on the reaction: 1) solvation structure (packing form), and 2) solvent reorientation time. The reactivity in *t*-butanol is higher than in the secondary alcohols. For one thing, the solvation structure in *t*-butanol results in a relatively high mobility of electrons in that alcohol (29); the mobility might be higher than it is in secondary alcohols. For another thing, as  $e_s^-$  approaches  $\text{NO}_{3,s}^-$  the C-H's of the three  $\text{CH}_3$  groups on the  $\text{HOC}(\text{CH}_3)_3$  molecules that solvate the electron are accessible to the  $\text{NO}_3^-$  and product  $\text{NO}_3^{2-}$ , so there are more chances for reaction to occur than in secondary alcohols, and more chances in secondary than in primary alcohols. Methanol has no far reaching  $\beta$ -C-H's, so it has the lowest reactivity in this series.

In a given group of alcohols in Fig. 4 (for example, in primary or secondary alcohols), reactivity increases with solvent molecular reorientation time  $\tau$ . This is because after the reaction



the O-H dipole of the in-between molecule that solvated the electron tends to rotate in the field of the new  $\text{NO}_3^{2-}$  ion. The longer the relaxation time ( $\tau$ ,  $\tau_2$ , or  $\tau_L$ ), the higher is the chance for the  $\text{NO}_3^{2-}$  ion to react with a C-H of the alcohol that was associated with  $e_s^-$ .



Therefore, from 2-propanol to 2-butanol and from ethanol to *i*-butanol, the reactivity increases with the increase of  $\tau$  (Fig. 4). It is not clear why methanol falls into a group with water ( $p_\tau \approx 0$ ).

Fig. 5 shows plots of  $p_\tau$  and  $E_2 - E_{\Lambda 0}$  against  $k_2$ , where  $E_2$  is the Arrhenius activation energy of the reaction ( $e_s^- + NO_{3,s}^-$ ) in a pure alcohol, and  $E_{\Lambda 0}$  is the Arrhenius activation energy of molar conductivity of lithium nitrate in the same alcohol. Both  $p_\tau$  and  $E_2 - E_{\Lambda 0}$  are temperature coefficients;  $p_\tau$  is from apparent values of  $\kappa R_f$  (Fig. 3) whereas  $E_2 - E_{\Lambda 0}$  contains the Debye  $f$  factor. Both contain any non-ion-like mobility of  $e_s^-$ . Methanol and water are at opposite ends of the curve, which indicates that the reaction  $e_s^- + NO_{3,s}^-$  in methanol has a different mechanism from that in water. The latter is nearly a diffusion controlled reaction and the former is entropy controlled (30). Throughout the series the variations of  $p_\tau$  and  $E_2 - E_{\Lambda 0}$  are similar. The peak at *t*-butanol seems to be associated with a high mobility of  $e_s^-$  in that solvent (29)(refer to chapter 3).

**Table 4-1. Reaction Rates and Parameters for  $e_s^- + \text{NO}_3^-$  in  $\text{C}_1$  to  $\text{C}_4$  Alcohols at 298 K.**

Alcohol	$k_2 (10^6 \text{ m}^3/\text{mol}\cdot\text{s})$	$E_r (\text{zJ})^h$	$\eta (\text{mPa}\cdot\text{s})$	$\epsilon^i$	$\tau (\text{ps})^j$	$E_r/\tau (\text{zJ/ps})$
Water <sup>a</sup>	9.47, 9.8 <sup>10</sup>	219	0.89	78.5	8.3	26.4
MeOH <sup>b</sup>	0.026	237	0.557	32.6	46	5.2
EtOH <sup>b</sup>	0.068	210	1.10	24.3	125	1.68
1-PrOH <sup>c</sup>	0.09	229	1.96	20.1	372	0.616
2-PrOH <sup>c</sup>	0.65	173	2.08	18.4	370*	0.468
1-BuOH <sup>d</sup>	0.19	232	2.60	17.4	479	0.484
<i>i</i> -BuOH <sup>e</sup>	0.25	224	3.40	17.6	480*	0.467
2-BuOH <sup>f</sup>	0.75	179	3.05	16.7	610*	0.293
<i>t</i> -BuOH <sup>g</sup>	3.2	104 <sup>k</sup>	4.45	12.4	420	0.247

*a*: Refs. 7, 10.

*b*: Ref. 3.

*c*: Ref. 4.

*d*: Ref. 9.

*e*: Ref. 11.

*f*: Ref. 6.

*g*: Ref. 10.

*h*: Energy at  $A/A_{\text{max}} = 0.5$  on the low energy side of the optical absorption band of  $e_s^-$ ; ref. 23.

*i*: Static permittivity.

*j*: Dielectric relaxation time  $\tau_1$ , for water to 2-butanol from ref. 15 (\*extrapolated value), and *t*-butanol from ref. 21.

*k*: Authors' unpublished work.

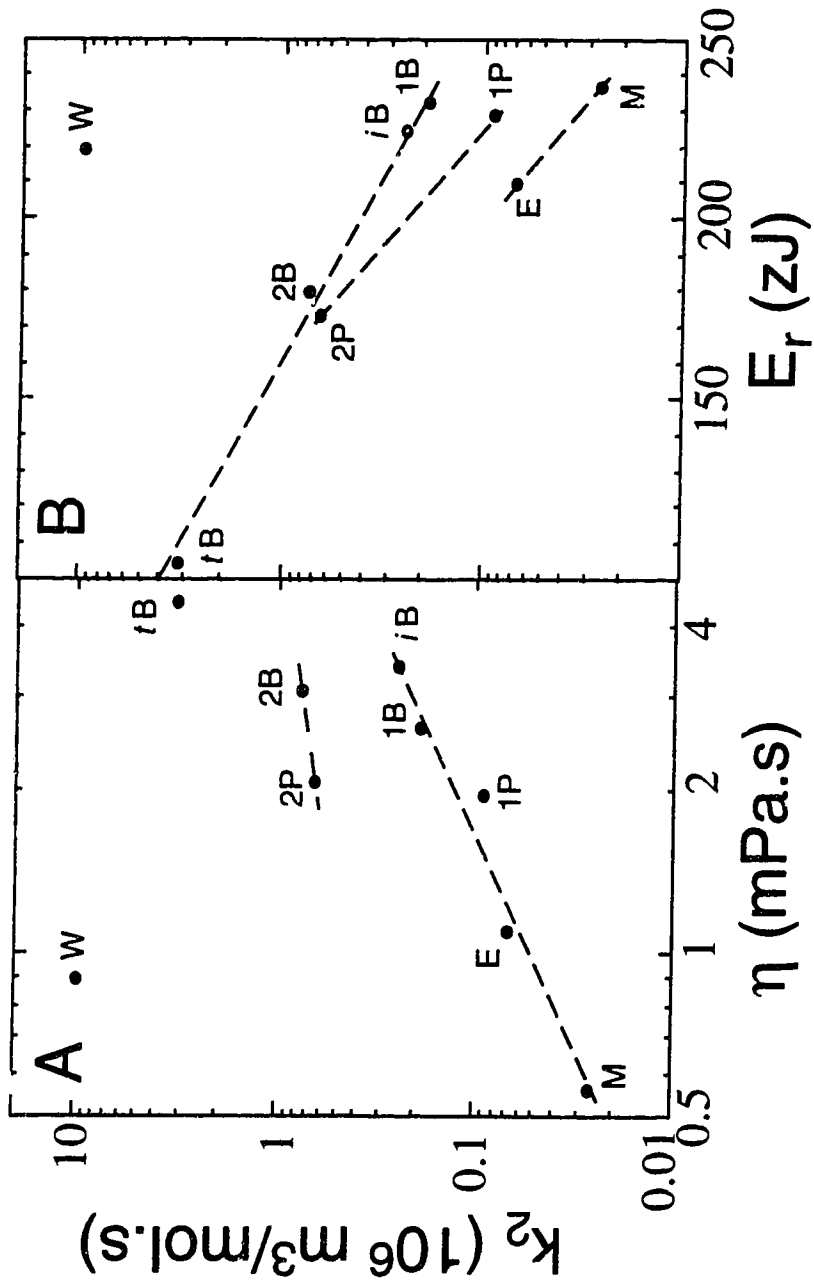


Fig. 4-1. Correlations of  $k_2$  with  $\eta$ (A) and  $E_r$ (B) in C<sub>1</sub> to C<sub>4</sub> alcohols and water at 298 K (Table I).

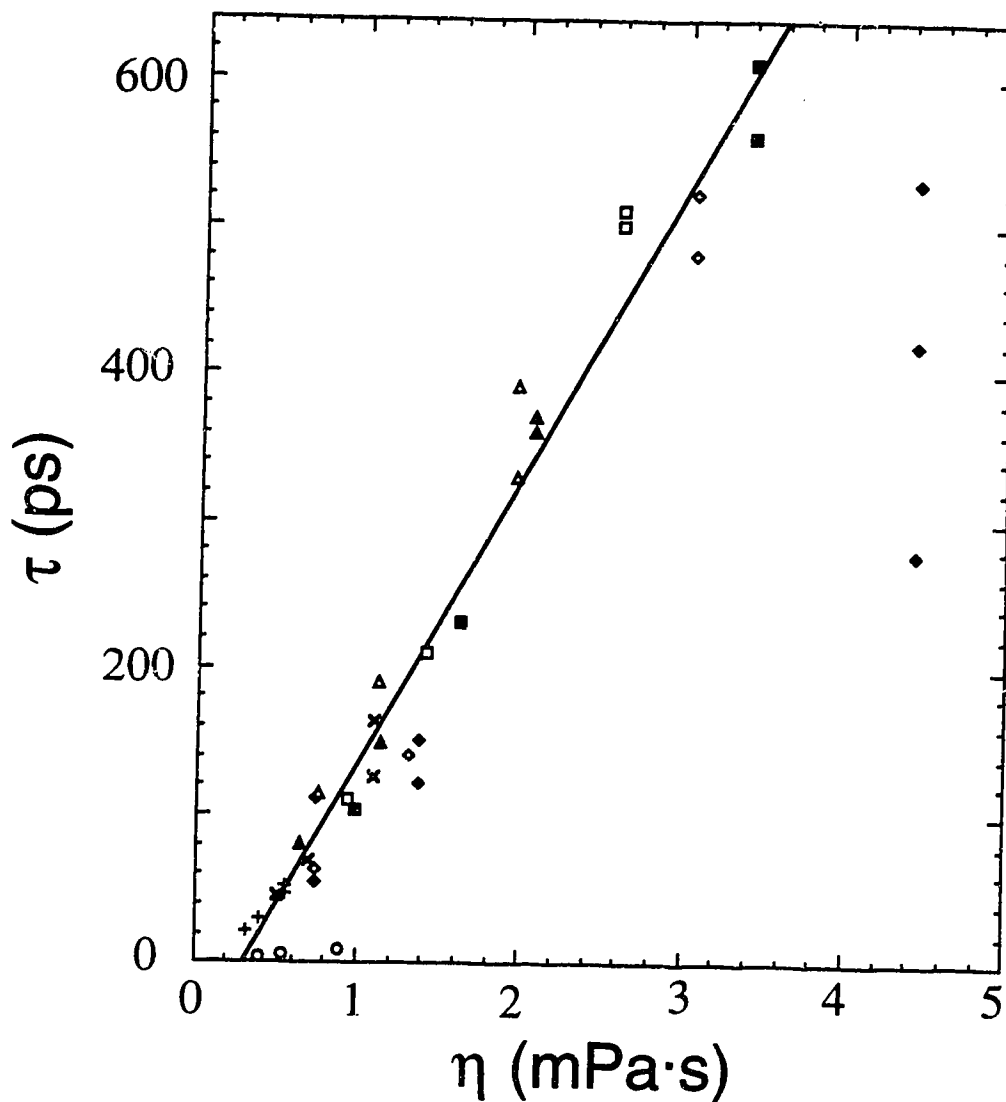


Fig. 4-2. Correlation of viscosity  $\eta$  and dielectric relaxation time  $\tau$  of  $C_1$  to  $C_4$  alcohols and water at 298 K, 323 K and 343 K. Some of the values of  $\tau$  are extrapolated from those at lower temperatures. The symbol for each solvent is followed by the references for  $\eta$ ;  $\tau$ . Water,  $\circ$ , 12; 15. Methanol,  $+$ , 12; 15,16. Ethanol,  $\times$ , 12; 15,16. 1-Propanol,  $\Delta$ , 12; 15,16. 2-Propanol,  $\blacktriangle$ , 13; 15,16. 1-Butanol,  $\square$ , 12; 15,17. *i*-Butanol,  $\blacksquare$ , 14; 15,17. 2-Butanol,  $\diamond$ , 14; 15,17. *t*-Butanol,  $\blacklozenge$ , 14; 17-19. The line through all data (except those for water and *t*-butanol) represents eqn [1].

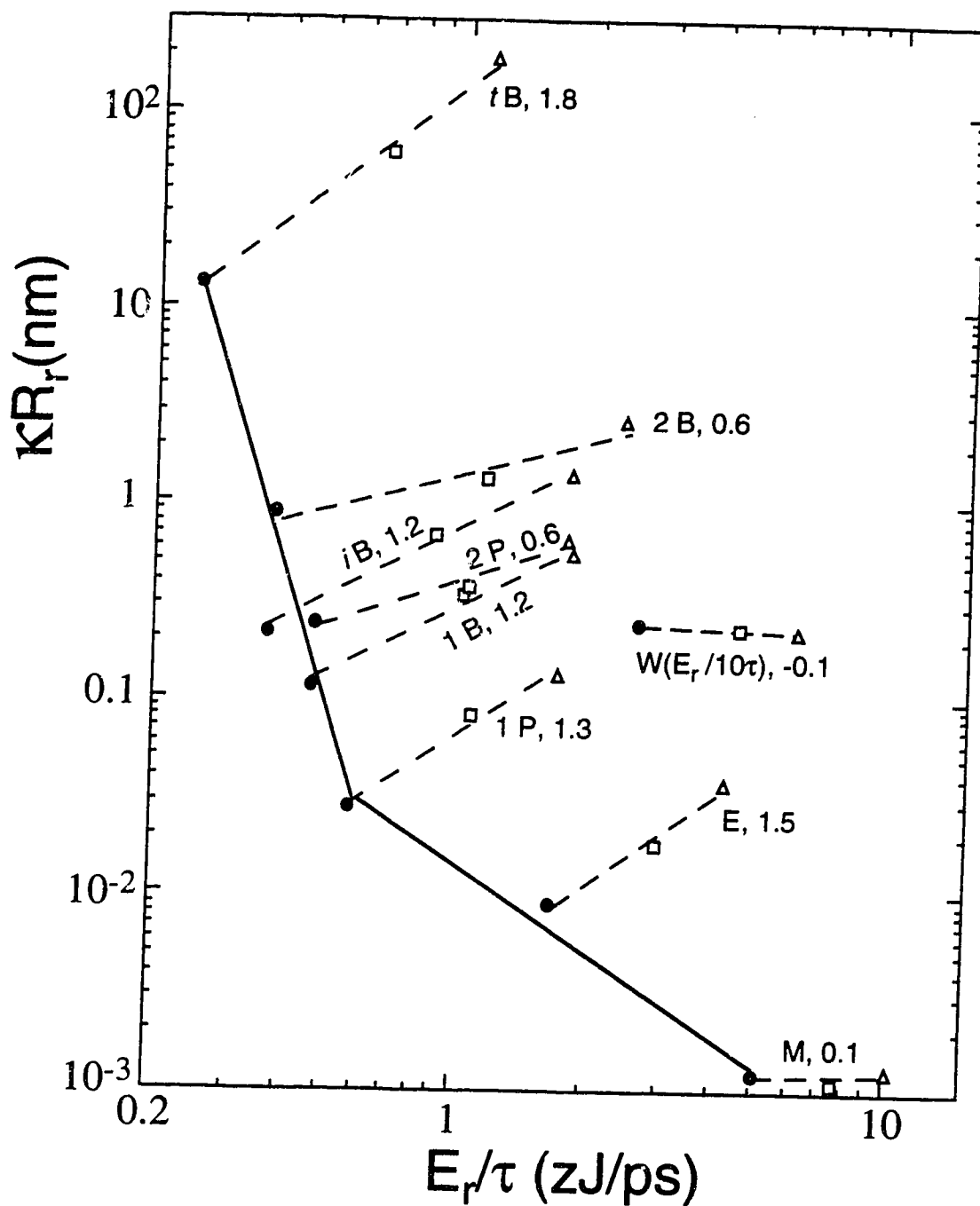


Fig. 4-3. Correlation of apparent  $\kappa R_r$  values and  $E_r/\tau$  in  $C_1$  to  $C_4$  alcohols and water at 298 K (●), 323 K (□) and 343 K (△). The label of each dashed line identifies the solvent and the slope.

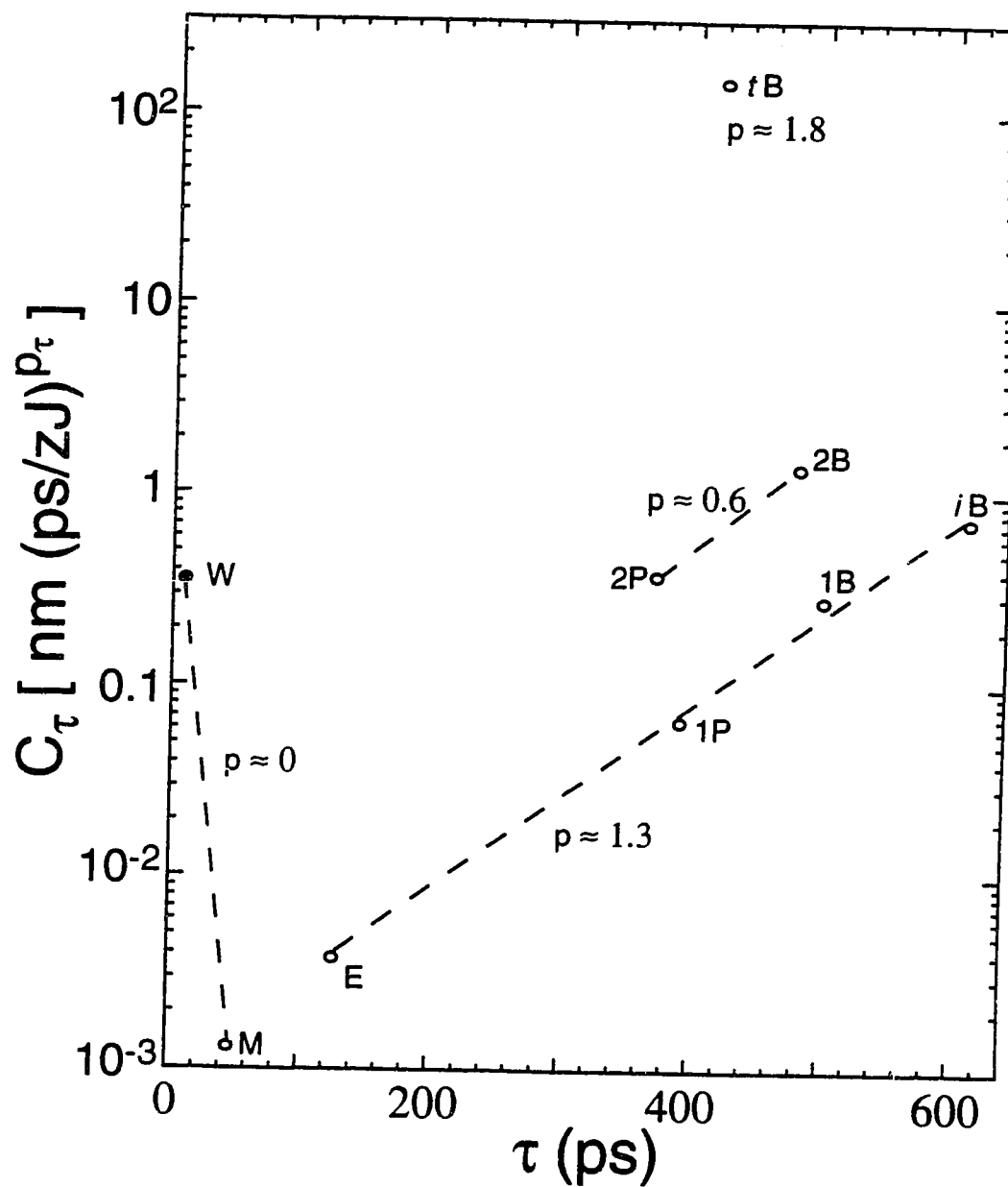


Fig. 4-4. Correlation of  $C_\tau$  (eqn 4) with  $\tau$  (298 K) of C<sub>1</sub> to C<sub>4</sub> alcohols and water. The dashed lines connect species having same  $p_\tau$  values.



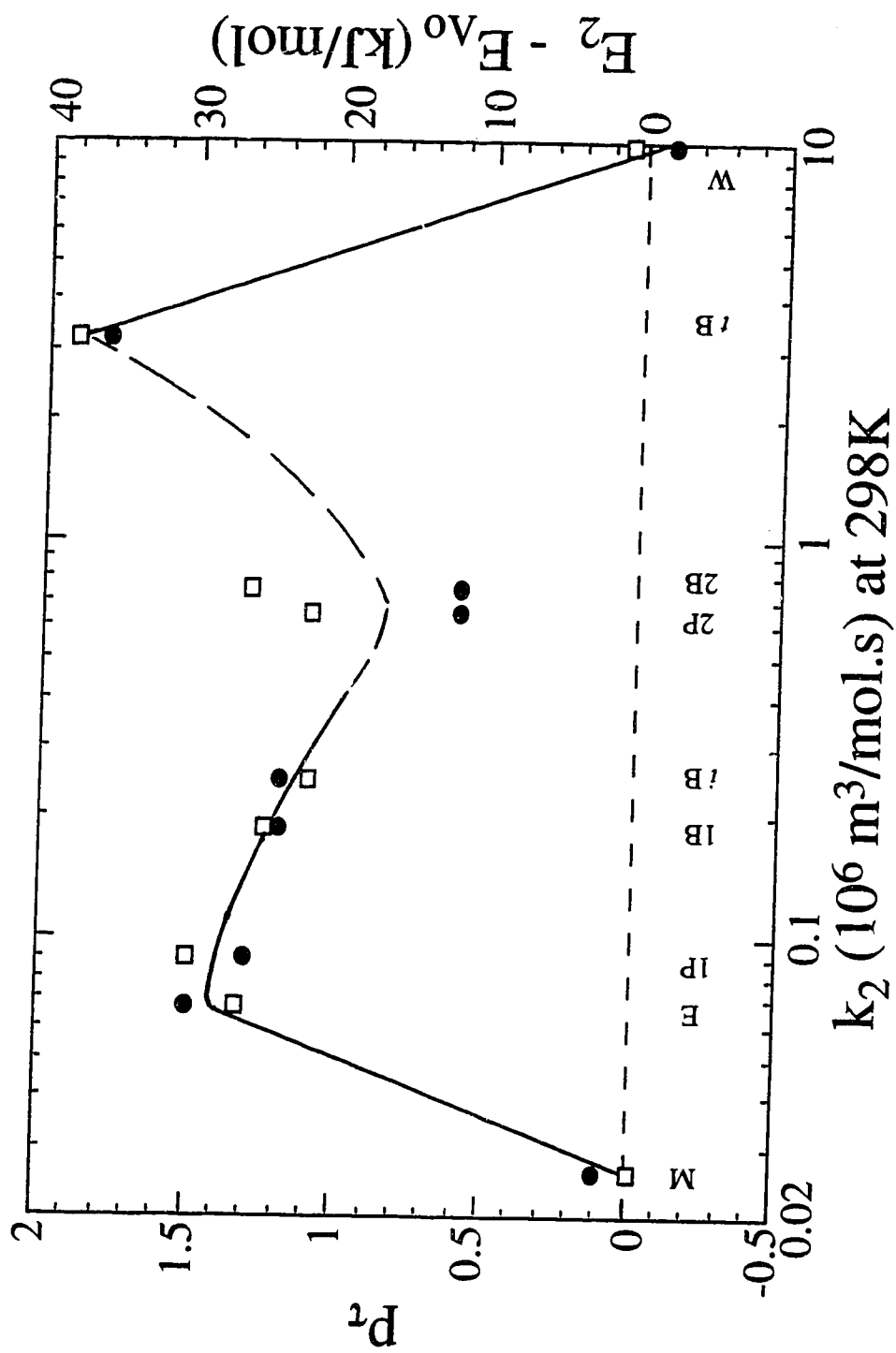


Fig. 4-5. Correlation of  $p_\tau$  (●) and  $E_2 - E_{A_0}$  (□) with  $k_2(e_5^- + \text{NO}_3^-)$  in C1 to C4 alcohols and water at 298 K.

## References

1. B. Hickel. *J. Phys. Chem.* **82**, 1005 (1978).
2. A.J. Elliot, D.R. McCracken, G.V. Buxton and N.D. Wood. *J. Chem. Soc. Faraday Trans.* **86**, 1539 (1990).
3. C.C. Lai and G.R. Freeman. *J. Phys. Chem.* **94**, 4891 (1990).
4. S.A. Peiris and G.R. Freeman. *Can. J. Phys.* **68**, 940 (1990).
5. G. Duplâtre and C.D. Jonah. *J. Phys. Chem.* **95**, 897 (1991).
6. S.A. Peiris and G.R. Freeman. *Can. J. Chem.* **69**, 884 (1991).
7. G.V. Buxton and S.R. Mackenzie. *J. Chem. Soc. Faraday Trans.* **88**, 2833 (1992).
8. T.B. Kang and G.R. Freeman. *Can. J. Chem.* **71**, 1297 (1993).
9. R. Chen and G.R. Freeman. *Can. J. Chem.* **71**, 1303 (1993).
10. Y. Zhao and G.R. Freeman. *Can. J. Chem.* **73**, 392 (1995).
11. R. Chen, Y. Avotinsht and G.R. Freeman. *Can. J. Chem.* **72**, 1083 (1994).
12. M.S. Tunuli and Farhataziz. *J. Phys. Chem.* **90**, 6587 (1986).
13. A.M. Afanassiev, K. Okazaki and G.R. Freeman. *J. Phys. Chem.* **83**, 1244 (1979).
14. P.C. Senanayake and G.R. Freeman. *J. Chem. Phys.* **87**, 7007 (1987).
15. R.C. Weast (ed). *Handbook of Chemistry and Physics*. 70th edn. CRC Press, Boca Raton, FL. 1989. pp. F41-44.
16. W. Weber. *Rheol. Acta* **14**, 1012 (1975).
17. P.C. Senanayake, N. Gee and G.R. Freeman. *Can. J. Chem.* **65**, 2441 (1987).
18. F. Buckley and A.A. Maryott. *Table of Dielectric Dispersion Data for Pure Liquids and Dilute Solutions*. National Bureau of Standards Circular 589. Washington, D.C. 1958.

19. J. Barthel, K. Bachhuber, R. Buchner and H. Hetzenauer. *Chem. Phys. Lett.* **165**, 369 (1990).
20. H. Sato, H. Nakamura, K. Itoh and K. Higasi. *Chem. Lett., Chem. Soc. Japan.* 1167 (1985).
21. M. Tabellout, P. Lancelour, J.R. Emery, D. Hayward and R.A. Pethrick. *J. Chem. Soc. Faraday Trans.* **86**, 1493 (1990).
22. S.M. Puranik, A.C. Kumbharkhane and S.C. Mehrotra. *Indian J. Pure Appl. Phys.* **29**, 47 (1991).
23. A.D. Leu, K.N. Jha and G.R. Freeman. *Can. J. Chem.* **60**, 2342 (1982).
24. K. Okazaki and G.R. Freeman. *Can. J. Chem.* **56**, 2313 (1978).
25. H.A. Schwarz. *J. Phys. Chem.* **95**, 6697 (1991).
26. K.H. Schmidt, P. Han and D.M. Bartels. *J. Phys. Chem.* **96**, 199 (1992).
27. W.J. Chase and J.W. Hunt, *J. Phys. Chem.* **79**, 2835 (1975).
28. M.J. Weaver, *Chem. Rev.* **92**, 463 (1992).
29. Y. Zhao and G.R. Freeman. *Can. J. Chem.* **73**, 389 (1995).
30. A.M. Afanassiev, K. Okazaki and G.R. Freeman. *Can. J. Chem.* **57**, 839 (1979).

## Chapter Five *a*

### Unusual Behavior of the Conductivity of LiNO<sub>3</sub> in *t*-Butanol: Ion Clustering or Ion-Pair Aggregation

#### 1. Introduction

The molar electric conductivity of an electrolyte solution decreases as the concentration of electrolyte is increased. The decrease in dilute solutions in hydroxylic solvents is attributed to the ionic atmosphere effect (1,2) or the formation of ion pairs (3,4). The formation of ion pairs  $\text{Li}_s^+$ ,  $\text{NO}_{3,s}^-$ , where the subscript *s* represents "solvated", in different alcohols has been reported for pure propanols (5), 2-butanol (4), 1-hexanol, 1-octanol, and 1-decanol (6). However, there has been no report about the molar conductivity of lithium nitrate in *t*-butanol. In connection with the study of the reactivity of solvated electrons  $e_s^-$  with nitrate ions (7), the electric conductances of lithium nitrate, ammonium nitrate, lithium perchlorate and ammonium perchlorate were measured in the whole range of *t*-butanol/water mixtures. Unusual behavior was found for lithium nitrate in pure *t*-butanol. It appears to be related to the aggregation of ion pairs found for lithium salts in aprotic solvents (8,9). The conductance data are presented in this paper.

---

*a* A version of this chapter has been submitted for publication to Canadian Journal of Chemistry. Y. Zhao and G. R. Freeman.

## 2. Experimental

The conductance measurement technique was the same as that reported in ref. 10, except that for the measurements of the four salts in 10 mol % water and in pure *t*-butanol, a freshly made solution was used for each temperature to minimize the formation of impurities during heating.

## 3. Results and Discussion

### *Conductance of LiNO<sub>3</sub>: "Normal" in Water, "Abnormal" in t-Butanol*

The dependences of specific conductance on the concentration of LiNO<sub>3</sub> in water/*t*-butanol mixed solvents at different temperatures are plotted in Figs. 1 and 2. In 100 to 70 mol % water solvents the conductance increases linearly with the increase of LiNO<sub>3</sub> concentration over the range used (Fig. 1). However, as the water content of the solvent is further decreased, the conductance becomes concave toward the concentration axis (Fig. 2). In 100 to 30 mol % water the conductance increases monotonically with temperature. However, in 10 mol % water the conductance *decreases* at  $T > 320$  K (Fig. 2, note factors of 0.5 for curves at 308K and 343K). In pure *t*-butanol, as the temperature is increased the conductance decreases monotonically (Fig. 2).

Figs. 1 and 2 show the gradual transition of conductance behavior of LiNO<sub>3</sub> as the *t*-butanol content of the solvent is increased. When the lines are gently concave, we used initial slopes of the curves to estimate the limiting molar conductivity  $\Lambda_0$ . For severely bent curves the values estimated in this way are too small to be  $\Lambda_0$ .

*Comparison of Molar Conductivities of Salts in *t*-Butanol*

The measured specific conductances of four salts in *t*-butanol are shown in Fig. 3. We see again the change from "normal" to "abnormal" behavior. For  $\text{NH}_4\text{ClO}_4$  and  $\text{LiClO}_4$ , the specific conductance increases linearly with increase of concentration at temperatures around 300 K. However, as the temperature is increased the lines become sublinear, and the specific conductance *decreases* at higher temperatures. This behavior is more marked for the  $\text{NH}_4\text{NO}_3$  solution. The concentration and temperature at which the line becomes sublinear decrease from  $\text{NH}_4\text{ClO}_4$  to  $\text{LiClO}_4$  to  $\text{NH}_4\text{NO}_3$  (Fig. 3). The conductance of  $\text{LiNO}_3$  in *t*-butanol is so low that we could not measure it at the low concentrations used for the other salts. At the higher concentrations used (Fig. 3), the conductance at a given concentration decreases monotonically with increasing temperature.

Fig. 4 shows the Arrhenius plots of  $\Lambda_0$  (for straight lines) and initial slopes (for curves, marked \*) in *t*-butanol. A linear Arrhenius plot is obtained for  $\text{NH}_4\text{ClO}_4$  in the temperature range measured. However, it would likely be bent at higher temperatures. The ionic atmosphere effect calculated from the Debye-Hückel equation (1) is negligible at these concentrations (3% at the highest concentration used). For  $\text{LiClO}_4$  the line bends at 328 K, and for  $\text{NH}_4\text{NO}_3$  it seems to have bent at about 300 K. The Arrhenius activation energies obtained at lower temperatures for  $\text{NH}_4\text{ClO}_4$  and  $\text{LiClO}_4$  (Fig. 4) are 17 kJ/mol. The mean Arrhenius activation energy of fluidity ( $1/\eta$ ) of *t*-butanol (11) below 318 K (Fig. 4) is 38 kJ/mol. This indicates that the correlation between molar conductivities of the two salts and the viscosity  $\eta$  of pure *t*-butanol is  $\Lambda_0 \propto \eta^{-n}$ , with  $n = 0.4$ , which is unusual and does not follow Walden's rule,  $n = 1$  (1). The conductances of many salts (Table 1) in water (12) and pure 1- and 2-propanol solvents (13), and in 1- (10), *iso*- (12), and 2-butanol (4) approximately follow Walden's rule. However,  $\text{LiNO}_3$  in *iso*-

(12), and 2-butanol (4) deviate significantly from Walden's rule, with  $n = 0.7\text{--}0.8$ . More study is needed to understand the behavior of salt conduction in these solvents.

For  $\text{NH}_4\text{NO}_3$ , the apparent activation energy calculated from 300 K to 308 K is 14 kJ/mol, and is nearly zero between 308 K and 328 K (Fig. 4). This seems to indicate that clusters of nitrate and ammonium ions form in *t*-butanol solvent at higher temperatures.

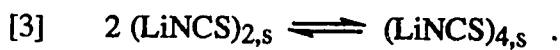
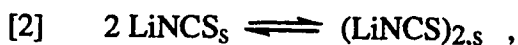
For  $\text{LiNO}_3$ , the Arrhenius plot has a negative slope at  $T > 308$  K (Fig. 4). The value of the initial conductance slope at 299 K (Fig. 3) is  $0.5 \times 10^{-4} \text{ S}\cdot\text{m}^2/\text{mol}$ , which is much lower than the molar conductivities of the other three salts at the same temperature (Table 2). The estimated value of the initial slope of the conductance curve for  $\text{LiNO}_3$  in pure *t*-butanol has an uncertainty of about 20%, but this is an order of magnitude too small to be a possible interpretation of the result. We conclude that  $\text{Li}^+$  and  $\text{NO}_3^-$  ions have a strong tendency to form multi-ion clusters in *t*-butanol.

Comparing the molar conductivities with physical parameters (14) of the four salts (Table 2), the conductivities correlate inversely with the molar density and lattice energy of the crystalline salts. The molar density and lattice energy reflect the ability of the ions to pack together.  $\text{NH}_4\text{ClO}_4$  has the lowest molar density and lattice energy, and the highest molar conductivity (Table 2). The values for  $\text{LiClO}_4$  and  $\text{NH}_4\text{NO}_3$  are in the middle (but their relative order is reversed).  $\text{LiNO}_3$  has the highest molar density and lattice energy, and the lowest molar conductivity.  $\text{LiNO}_3$  is the smallest molecule, with ionic radii (15)  $R_{\text{Li}^+} = 74$  pm and  $R_{\text{NO}_3^-} = 189$  pm;  $\text{NH}_4\text{ClO}_4$  is the largest molecule, with ionic radii (15)  $R_{\text{NH}_4^+} = 146$  pm and  $R_{\text{ClO}_4^-} = 200$  pm.

The approximate inverse relationships between the molar conductivity and the molar density and lattice energy of the salts indicate the extent of formation of ion clusters in *t*-butanol. The *t*-butanol molecules are globular; the planar  $\text{NO}_3^-$  ions would fit less well than the globular  $\text{ClO}_4^-$  ions into the liquid structure, so  $\text{NO}_3^-$  might be less tightly solvated than is  $\text{ClO}_4^-$  in *t*-butanol. The solvent has a low relative permittivity ( $\epsilon = 12.4$

at 298 K) (16), so the coulombic attraction between oppositely charged ions is greater than in solvents with higher permittivities. These factors might explain the reversal of the electrolyte conductivity/crystal lattice energy orders of LiClO<sub>4</sub> and NH<sub>4</sub>NO<sub>3</sub>. We attribute the low observed conductivity of LiNO<sub>3</sub> solutions to the formation of ion clusters, mainly larger than pairs.

In aprotic solvents such as tetrahydrofuran, diethyl ether, pyridine, and diethyl carbonate, the salts LiNCS and LiBr form ion pairs which can agglomerate (8,9). For example, the following species have been detected by various spectroscopic methods (8,9):



The trimer (LiNCS)<sub>3,s</sub> was not detected. The tetramer has a cubane-like structure. The species LiNCS is strongly polar, but the dimer and tetramer are nonpolar. The pairing and agglomeration reactions are entropy driven; each step involves partial desolvation of the species (9).

We suggest that, while *t*-butanol is a protic solvent, the globular alkyl group hinders it from efficiently solvating Li<sup>+</sup> and NO<sub>3</sub><sup>-</sup> ions.

The reason for the unusual temperature dependence of salt conductance in *t*-butanol is that the product of the relative permittivity and temperature  $\epsilon T$  *decreases* rapidly as the temperature is increased. Ion association constants vary inversely as the product  $\epsilon T$  (18).

The value of  $\epsilon T$  for hydroxylic solvents decreases with increasing T, but the relative decrease is much faster for *t*-butanol than for water and other simple alcohols (Fig. 5). Values (16) of  $\epsilon T$  normalized to that at 298 K are plotted in Fig. 5 for water,



ethanol, 1-propanol, and *t*-butanol, as well as for 10% and 30% water in *t*-butanol. The behavior of  $\epsilon T$  for the 30 mol% water solvent is close to that of 1-propanol, and the conductance behavior of  $\text{LiNO}_3$  in this mixed solvent is not excessively abnormal (Fig. 2).

*Estimate of  $\Lambda_0$  for  $(\text{NH}_4^+ + \text{NO}_3^-)$  and  $(\text{Li}^+ + \text{NO}_3^-)$  in *t*-Butanol*

The initial slope method and attempts to fit the data to the Debye-Onsager (1,2) and ion association (3,4) models gave unreasonably low values of  $\Lambda_0$  for the two nitrate salts. More complex models (17) have too many adjustable parameters for our purpose.

We suspect that the planar  $\text{NO}_3^-$  ions are not well solvated by the globular *t*-butanol molecules, and that this makes the nitrate salts susceptible to ion clustering, or aggregation of ion pairs as in aprotic solvents (9). However, for the analysis of reaction rate constants (7) we need values of  $\Lambda_0$ . An indirect method of estimation has therefore been used.

The ratio of  $\Lambda_0$  values for  $\text{NH}_4\text{ClO}_4/\text{LiClO}_4$  equals 1.3 in both water and *t*-butanol (Table 1). In water the values of  $\Lambda_0$  for the two ammonium salts are equal, and those of the two lithium salts are equal (Table 1), so the same is assumed to be true in *t*-butanol. We thereby arrive at the  $\Lambda_0$  values listed in Table 3.

**Table 5-1. Arrhenius activation energies of viscosities and conductances of salts in some solvents at 298 K.**

Solvent	Salt	$\Lambda_0$ ( $10^{-4} \text{ S}\cdot\text{m}^2/\text{mol}$ )	$E_{\Lambda_0}$ (kJ/mol)	$\eta$ (mPa·s)	$E_\eta$ (kJ/mol)	$E_{\Lambda_0}/E_\eta = n$
Water <sup>a</sup>	NH <sub>4</sub> ClO <sub>4</sub>	140, 141 <sup>e</sup>	16	0.89	16	1.0
	NH <sub>4</sub> NO <sub>3</sub>	145 <sup>e</sup>				
	LiClO <sub>4</sub>	106 <sup>e</sup>				
	LiNO <sub>3</sub>	108, 110 <sup>e</sup>	15			0.9
1-PrOH <sup>b</sup>	LiNO <sub>3</sub>	20	16	2.0	18	0.9
2-PrOH <sup>b</sup>	LiNO <sub>3</sub>	20	22	2.0	22	1.0
1-BuOH <sup>c</sup>	NH <sub>4</sub> NO <sub>3</sub>	14	20	2.60	19	1.1
	LiNO <sub>3</sub>	13	18			0.9
2-BuOH <sup>d</sup>	Cu(ClO <sub>4</sub> ) <sub>2</sub>	19	23	3.05	26	0.9
	LiNO <sub>3</sub>	(7) <sup>f</sup>	18			(0.7) <sup>f</sup>
<i>i</i> -BuOH <sup>a</sup>	Cu(ClO <sub>4</sub> ) <sub>2</sub>	19	25	3.40	24	1.0
	LiNO <sub>3</sub>	9	19			0.8
<i>t</i> -BuOH <sup>g</sup>	NH <sub>4</sub> ClO <sub>4</sub>	5.0	17	4.5 <sup>h</sup>	31 <sup>h</sup>	0.55
	LiClO <sub>4</sub>	4.0	17			0.55

<sup>a</sup> Ref. 12.

<sup>e</sup> Ref. 1.

<sup>b</sup> Ref. 13.

<sup>f</sup> Probably low.

<sup>c</sup> Ref. 10.

<sup>g</sup> Present work.

<sup>d</sup> Ref. 4.

<sup>h</sup> Ref. 11.

**Table 5-2. Physical properties of salts at 298 K.**

Crystal Form <sup>a</sup>	Density (kg/m <sup>3</sup> ) <sup>a</sup>	Molar Mass (kg/mol) <sup>a</sup>	Molar Density (mol/m <sup>3</sup> )	Molar Density Ratio <sup>c</sup>	Lattice Energy (kJ/mol) <sup>d</sup>	$\Lambda$ (300 K) <sup>e</sup> (10 <sup>-4</sup> S·m <sup>2</sup> /mol)
NH <sub>4</sub> ClO <sub>4</sub> rhomb <sup>b</sup>	1950	0.117	16,700	0.48	580	5.0
LiClO <sub>4</sub> ?	2428	0.106	22,900	0.66	723	4.0
NH <sub>4</sub> NO <sub>3</sub> rhomb <sup>b</sup>	1725	0.080	21,600	0.63	676	2.4
LiNO <sub>3</sub> trigonal	2380	0.069	34,500	1.00	848	0.5

<sup>a</sup> Ref. 14a.

<sup>b</sup> Orthorhombic or rhombic; NH<sub>4</sub>NO<sub>3</sub> is monoclinic at T > 305.3 K.

<sup>c</sup> Based on LiNO<sub>3</sub>.

<sup>d</sup> Ref. 14b.

<sup>e</sup> From "initial slopes" of the plots in Fig. 4. The values for the nitrates are not  $\Lambda_0$ .

**Table 5-3.**  $\Lambda_0^a$  of salts in *t*-butanol at different temperatures.

	$\Lambda_0$ (300 K)	$\Lambda_0$ (308 K)	$E_{\Lambda_0}$ (kJ/mol)
$\text{NH}_4\text{ClO}_4^b$	5.0	6.0	17
$\text{LiClO}_4^b$	4.0	4.6	17
$\text{NH}_4\text{NO}_3^c$	~5		
$\text{LiNO}_3^c$	~4		

*a*  $10^{-4} \text{ S}\cdot\text{m}^2/\text{mol}$ .

*b* Measured values.

*c* Estimated values, see text.

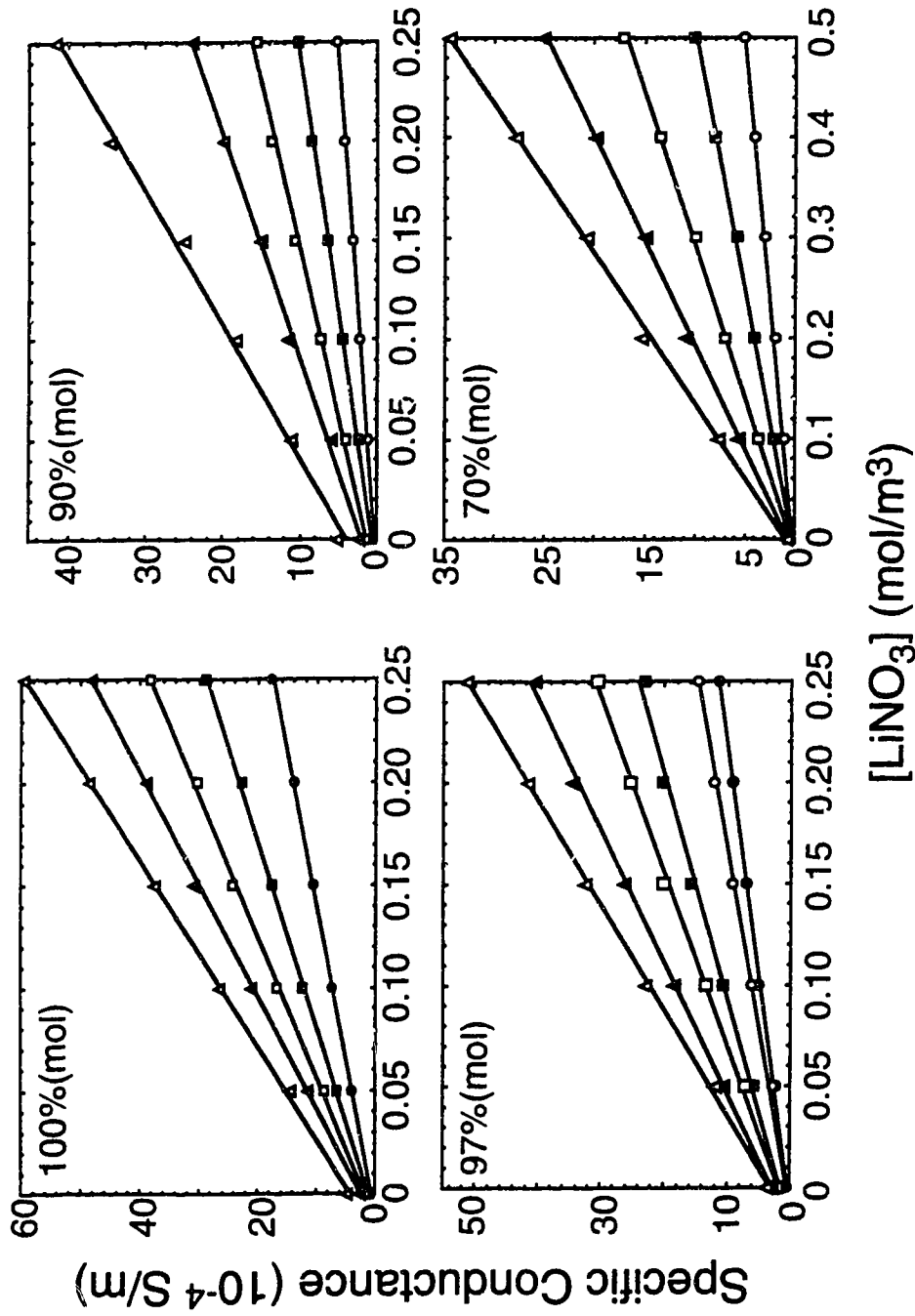


Fig. 5-1: Dependence of specific conductance of  $\text{LiNO}_3$  on concentration in water/*t*-butanol mixtures (100 to 70 mol % water) at different temperatures. ● 278 K, ○ 283 K, ■ 298 K, □ 313 K, ▲ 328 K, △ 343 K.

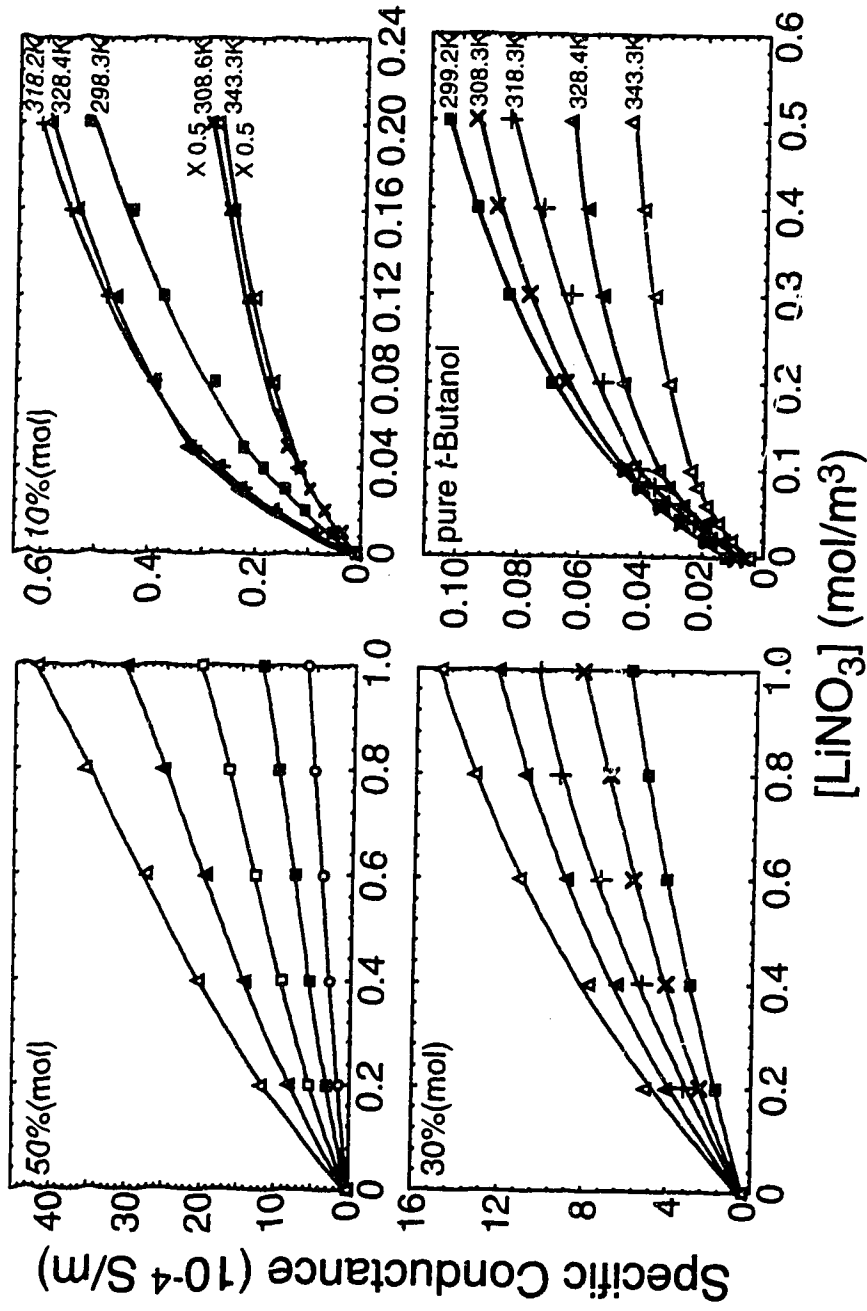


Fig. 5-2: Dependence of specific conductance of  $\text{LiNO}_3$  on concentration in water/*t*-butanol mixtures (50 to 0 mol % water) at different temperatures. Symbols as in Fig. 1, and  $\times$  308 K,  $+$  318 K.

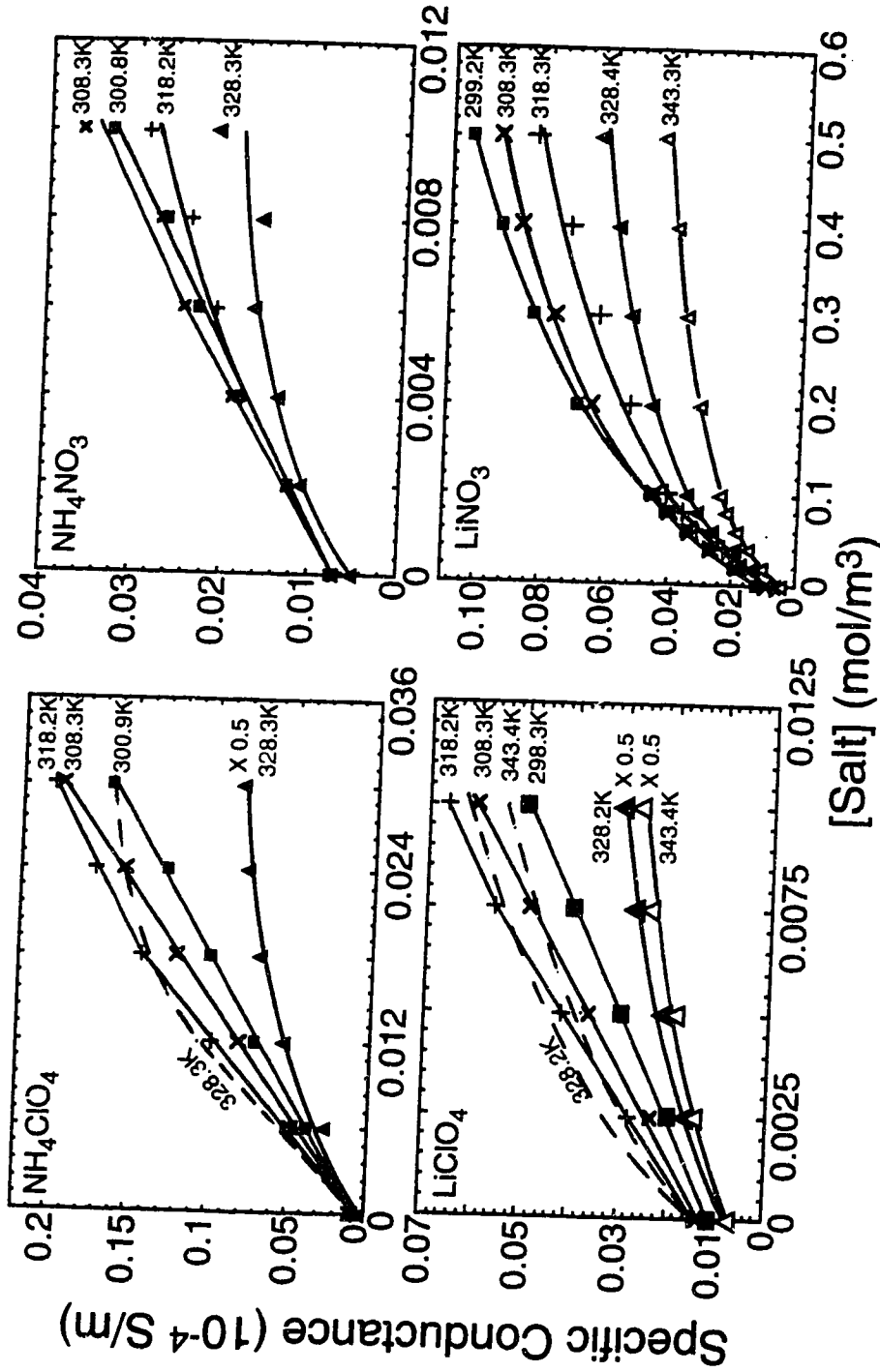


Fig. 5-3: Dependence of specific conductance of NH<sub>4</sub>ClO<sub>4</sub>, LiClO<sub>4</sub>, NH<sub>4</sub>NO<sub>3</sub> and LiNO<sub>3</sub> on concentration in pure *t*-butanol at different temperatures. Symbols as in Figs. 1 and 2. Some conductances are multiplied by 0.5 to separate the curves

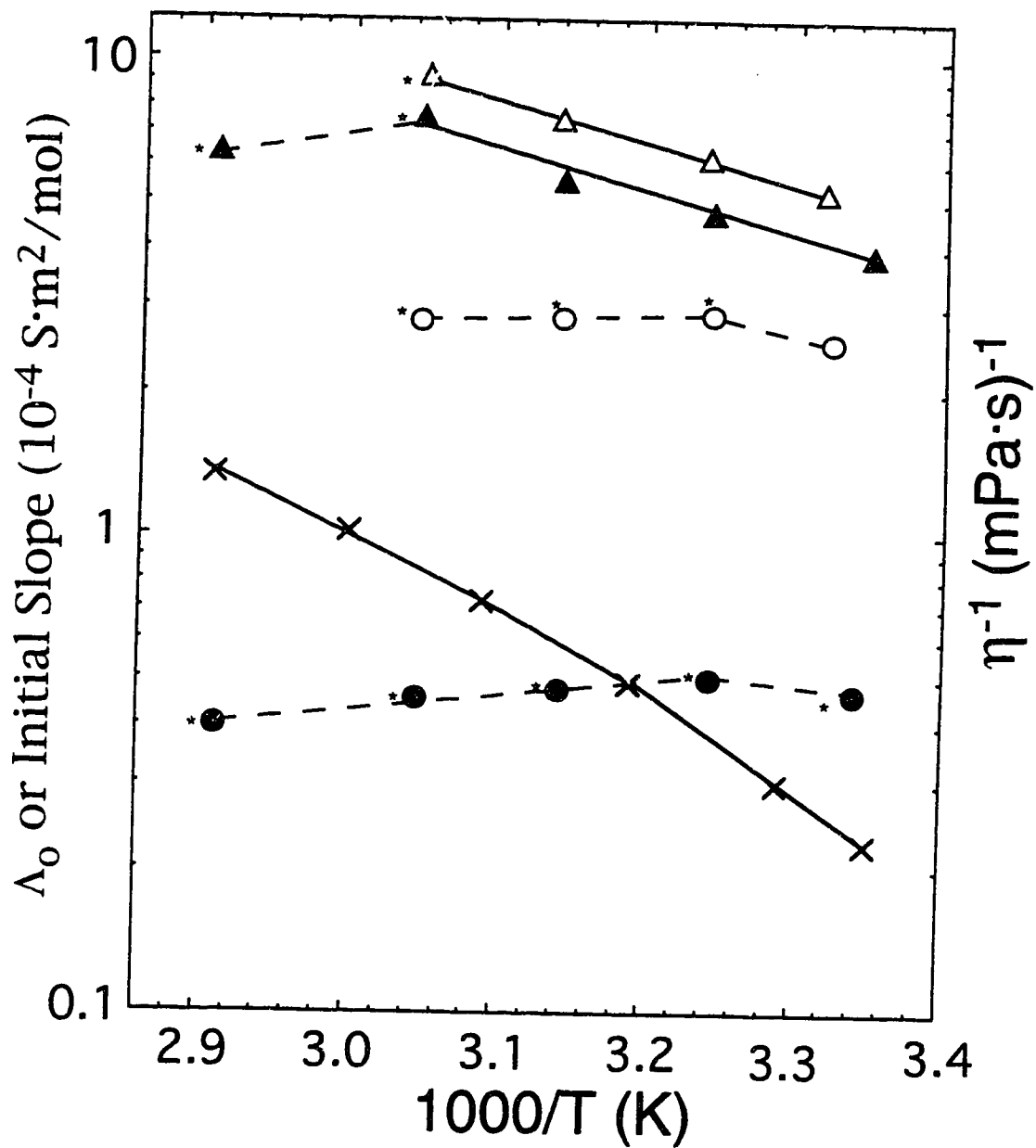


Fig. 5-4: Arrhenius plots of  $\Lambda_0$  or initial slopes of salts in *t*-butanol, and of fluidity ( $1/\eta$ ) of *t*-butanol.  $\Delta$   $\text{NH}_4\text{ClO}_4$ ,  $\blacktriangle$   $\text{LiClO}_4$ ,  $\circ$   $\text{NH}_4\text{NO}_3$ ,  $\bullet$   $\text{LiNO}_3$ ,  $\times$   $1/\eta$ , ref. 11.



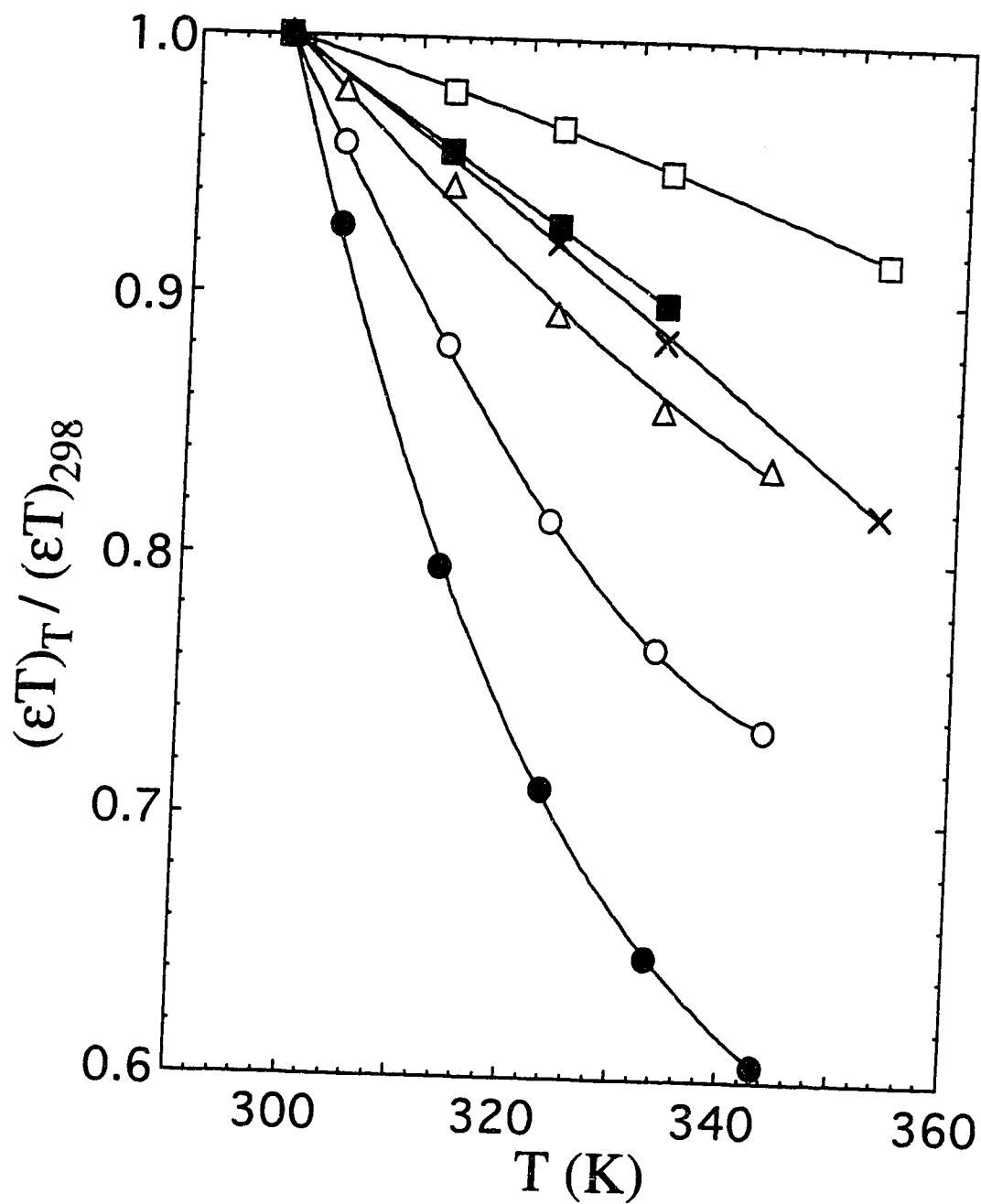


Fig. 5-5: Temperature dependence of  $\epsilon T$  of some solvents, normalized to the values at 298 K (ref. 14): □ water, ■ ethanol, × 1-propanol, ● *t*-butanol, ○ 10 mol% water in *t*-butanol, △ 30 mol% water in *t*-butanol.

## References

1. P. W. Atkins. *Physical Chemistry*, 4th ed. Freeman: New York, 1990. Chap. 25 and p. 963.
2. R. Chen and G. R. Freeman. *J. Phys. Chem.* **96**, 7107 (1992).
3. J. E. Gordon. *The Organic Chemistry of Electrolyte Solutions*. Wiley, New York, 1975. p. 385.
4. S. A. Peiris and G. R. Freeman. *Can. J. Chem.* **69**, 884 (1991).
5. S. A. Peiris and G. R. Freeman. *Can. J. Chem.* **68**, 940 (1990).
6. R. Chen and G. R. Freeman. *J. Phys. Chem.* **99**, 4970 (1995).
7. Y. Zhao and G. R. Freeman. *Can. J. Chem.* **73**, 392 (1995).
8. M. Chabanel and Z. Wang. *Can. J. Chem.* **62**, 2320 (1984).
9. M. Chabanel. *Pure Appl. Chem.* **62**, 35 (1990).
10. R. Chen and G. R. Freeman. *Can. J. Chem.* **71**, 1303 (1993).
11. P. C. Senanayake, N. Gee and G. R. Freeman. *Can. J. Chem.* **65**, 2441 (1987).
12. R. Chen, Y. Avotinskii, and G. R. Freeman. *Can. J. Chem.* **72**, 1083 (1994).
13. T. B. Kang and G. R. Freeman. *Can. J. Chem.* **71**, 1297 (1993).
14. R. C. Weast. *Handbook of Chemistry and Physics*. 70th ed. CRC Press, Boca Raton, FL, 1974. (a) pp. B-93–132. (b) pp. D-89–103.
15. D. A. Johnson. *Some Thermodynamic Aspects of Inorganic Chemistry*. 2nd ed. Cambridge University Press, Cambridge, 1982. pp. 46-49.
16. Y. Y. Akhadvov. *Dielectric Properties of Binary Solutions*. Pergamon Press, New York, 1980. pp. 277, 282, 456.

17. J.-C. Justice. *In* Comprehensive Treatise of Electrochemistry, vol. 5. B. E. Conway, J. O'M. Bockris and E. Yeager, eds. Plenum, New York, 1983. pp. 311-314.
18. H. S. Harned and B. B. Owen. *The Physical Chemistry of Electrolytic Solutions*. 3rd ed. Reinhold, New York, 1958. p. 291.

## Chapter Six <sup>a</sup>

### Optical Absorption Spectra of Solvated Electrons in 1-Butylamine/Water Mixed Solvents

#### 1. Introduction

An excess electron in a polar liquid can occupy a localized state as a result of its interaction with a certain number of neighboring molecules of the solvent. When this interaction leads to a thermally relaxed state of the electron with respect to the medium, the electron is called a solvated electron,  $e_s^-$  (1,2).

The energy levels of  $e_s^-$ , as reflected by the energy of the optical absorption maximum  $E_{Amax}$ , are determined as much by details of the liquid structure as by the dielectric constant or the molecular dipole moment (3-5). The solvated electron in water has an intense optical absorption band in the visible region, with a peak at 715 nm, which corresponds to  $E_{Amax} = 277$  zJ (6), and  $G\epsilon_{max} = 8.3 \times 10^{-21}$  m<sup>2</sup>/16 aJ [ $5.0 \times 10^4$  e<sub>s</sub><sup>-</sup> •L/100 eV•mol•cm] (7,8) at 298 K.

The values of  $E_{Amax}$  are similar in pure *n*-alcohols and water (9-11). However, there is a marked dependence of  $E_{Amax}$  on composition of alcohol/water mixed solvents (10). The values of  $E_{Amax}$  in amines are much smaller than that in water (4,12). It is therefore interesting to discover the composition dependence of  $e_s^-$  spectra in 1-

---

<sup>a</sup> A version of this chapter has been submitted for publication to Canadian Journal of Chemistry. Y. Zhao and G. R. Freeman.

butylamine/water mixed solvents. Data are reported in this paper.

## 2. Experimental

### *Materials*

1-Butylamine (Fluka, >98%) was treated for 24 hours with potassium and sodium alloy under UHP argon (99.999%, Liquid Carbonic Canada Ltd.) at 330 K. Fractional distillation was as reported in ref. 13. The water content, measured by Karl-Fisher titration, was 0.09 mol %. The solvated electron half-life in pure 1-butylamine after a 100 ns pulse of 340 fJ (2.1 MeV) electrons (4 J/kg) at 298 K was about 4  $\mu$ s. The purification of water and the half-life of solvated electrons in water were as in ref. 14.

### *Techniques*

The optical system, irradiation facilities, the silicon detector for wavelengths <1050 nm (14), the dosimetry (10), and the calculation of  $G_{\epsilon_{\max}}$  (15) were described in the references cited. Bauch and Lomb monochromator gratings 1350 (No. 33-86-02) for 400-800 nm, 1350 (No. 33-86-03) for 700-1200 nm, and high-intensity monochromator (no. 33-86-78) for 1100-2600 nm were used in the measurements. Corning filters were placed in front of the monochromator to eliminate higher order light interference: CS 4-97 for 400-500 nm, CS 3-72 for 500-650 nm, CS 2-58 for 650-1050 nm, LL-1000 for 1050-1800 nm, and RL-1500 for 1800-2600 nm. For the measurement of absorbance at wavelengths >1050 nm, the InSb infrared detector (Model I935-IS) was used and is sensitive from 1050 nm to 2600 nm. The 3 to 97% response time of the detector, amplifier and transient digitizer (Tekronix R7912) was 35 ns. The signal to noise ratio of the differential amplifier (Tektronix 7A13) was increased by using the 5 MHz filter, which gave a system response time of 96 ns.

The sample preparation was similar to that reported in ref. 14. Spectrosil optical

cells were used: 10 mm path length for pure water to 70 mol % water, and 5 mm path for 50 mol % water to pure 1-butylamine.

### *Physical properties*

The normal freezing point of 1-butylamine is 224 K, and the normal boiling point is 351 K. The liquid is completely miscible with water.

The optical absorption spectra were measured at the following compositions in mol % water: 0.0, 10.0, 30.0, 50.0, 70.0, 90.0, 95.0, 99.0 and 100.0. The densities and viscosities of the mixed solvents (16), except for 95.0 and 99.0 mol % water, are listed in Table 1. The relative permittivity of water at 298 K is 78.4 (17), and that of 1-butylamine is 4.78 (18).

## **3. Results and discussion**

### *Absorbance and shape of $\epsilon_s^-$ optical spectra at 298 K: solvent dependence.*

The optical spectra of  $\epsilon_s^-$  in 1-butylamine/water mixed solvents at 298 K are shown in Fig 1. The spectra have no fine structure.

As the amount of water is increased in 1-butylamine the optical absorption band changes (Figs. 1-3, Table 1): (i)  $E_{Amax}$  increases; (ii)  $G\epsilon_{max}$  increases; (iii) the band becomes narrower ( $W_{1/2}$  decreases), except at >90 mol % water where the band broadens slightly.

The shift of  $E_{Amax}$  with water content in 1-butylamine (Fig. 2) is much closer to linear than is that in 1- or *t*-butyl alcohol/water mixed solvents (Fig. 2 and ref. 10). This indicates that the amine/water solvents are less structured than are alcohol/water solvents. The spectra in 1-butanol/water and *t*-butanol/water shift greatly with the addition of 10 mol % of water to the alcohol, which indicates that 10 mol % of water in

the alcohols produces a particular structure (molecular packing) that affects the electron trap. This type of structure evidently does not occur in 1-butylamine/water mixed solvents. Hydrogen bonds in  $\text{RNH}_2$  are weaker than those in  $\text{ROH}$ , because the dipole moment of N-H is smaller than that of O-H (19), so the former liquids are less ordered (20).

The change of viscosity with water content in *t*-BuOH (ref. 21 and dashed curve in Fig. 2) also indicates that a particular liquid structure exists at 10 mol % water, whereas there is no evidence for such a structure near 10 mol % water in 1-butylamine (+ curve in Fig. 2).

In view of the greater polarity of water than of 1-butylamine, one might have expected electrons to be more selectively solvated by water than is indicated by the gradual increases of  $E_{\text{Amax}}$  and  $G_{\text{Emax}}$  with water content (Figs. 2 and 3). Many years ago this group began the study of electron spectra and reactivities in alcohol/water mixed solvents expecting to find subtle changes, and found large, structured changes. We have now begun the study of electron behavior in amine/water solvents, and expected much larger solvent-composition effects than we have observed. It seems that water and 1-butylamine form relatively ideal solutions; this might be related to the fact that 1-butylamine and water are completely miscible, whereas 1-butyl alcohol and water are not.

However the effect of solvent composition on  $e_s^-$  may not be as ideal as it appears in the change of  $E_{\text{Amax}}$ . The half life of  $e_s^-$  changes markedly with the composition of 1-butylamine/water mixtures (Table 2). As water is added into 1-butylamine  $t_{1/2}$  changes from 3  $\mu\text{s}$  in pure butylamine to the minimum value of 0.5  $\mu\text{s}$  in 50 mol % butylamine, then when the 1-butylamine is decreased to 1 mol %  $t_{1/2}$  reaches the maximum value of 16  $\mu\text{s}$ , higher than that in pure water. This indicates that the solvent structure in the region of 50 mol % 1-butylamine is different from those of the two extremities.

The value of  $G\epsilon_{\max}$  increases at 298 K from  $1.43 \times 10^{-21} \text{ m}^2/16 \text{ aJ}$  ( $8.6 \times 10^3 \text{ e}_s^- \cdot \text{L}/100 \text{ eV} \cdot \text{mol} \cdot \text{cm}$ ) in pure 1-butylamine to  $8.4 \times 10^{-21} \text{ m}^2/16 \text{ aJ}$  ( $50.4 \times 10^3 \text{ e}_s^- \cdot \text{L}/100 \text{ eV} \cdot \text{mol} \cdot \text{cm}$ ) in pure water (Table 1). The value in water agrees with that previously reported (6,8).

The yield  $G(\text{e}_s^-)$  in water at 298 K is 2.7 ent/16 aJ (6), and  $\epsilon_{\max} = 3.1 \times 10^{-21} \text{ m}^2/\text{e}_s^-$  (1860  $\text{m}^2/\text{mol}$ ). In 1-butylamine at room temperature  $G(\text{e}_s^-) = 0.27$  (22), which indicates  $\epsilon_{\max} = 5.3 \times 10^{-21} \text{ m}^2/\text{e}_s^-$  (3200  $\text{m}^2/\text{mol}$ ).

The observed  $\text{e}_s^-$  are free ions. The low yield of  $\text{e}_s^-$  in 1-butylamine compared to that in water correlates (23,24) with the lower value of the dielectric permittivity, 4.78 (18), in the former than in the latter, 78.4 (17).

*Composition dependence of  $E_r$ ,  $E_b$ ,  $W_{1/2}$ , and asymmetry  $W_b/W_r$  at 298 K.*

Several parameters are used to describe the characteristics of the optical spectrum of  $\text{e}_s^-$ .  $E_r$  and  $E_b$  are the energies on the low energy (red) and high energy (blue) sides of the band at half the maximum absorbance. The width of the band at half height  $W_{1/2}$  is divided at  $E_{A_{\max}}$  into  $W_b$  (high energy side) and  $W_r$  (low energy side). The asymmetry of the band is represented by  $W_b/W_r$ . In Fig. 3 the values of  $E_r$ ,  $E_b$ ,  $W_{1/2}$ , and  $W_b/W_r$  are plotted against composition of 1-butylamine/water mixtures at 298 K. The values of  $E_r$  could only be obtained in pure butylamine and 10 mol % water near their freezing points, around 225 K.

The value of  $E_r$  (Fig. 3) increases smoothly from 1-butylamine to water, similar to the change of  $E_{A_{\max}}$  (Fig. 2). However, there is a big jump in  $E_b$  from pure butylamine to 10 mol % water, and then  $E_b$  increases gently as more water is added.

The optical absorption at  $\lambda < 1000 \text{ nm}$  ( $E > 200 \text{ zJ}$ ) had a long-lived tail that extended more than 100  $\mu\text{s}$  (Fig. 4 and Table 2). The long-lived entity has not been identified. The absorbance due to  $\text{e}_s^-$  is taken as the portion above the long-lived tail. The tail decreases with increase of water content and increase of temperature (Fig. 4).



The unidentified entity is only stable at low temperature and in an adequate amine environment.

The band asymmetry  $W_b/W_r$  increases from 2.3 in pure 1-butylamine to 2.8 in 10 mol % water, then decreases as more water is added, reaching a minimum of 1.26 at 70 mol %, then increasing slightly to 1.53 in pure water (Table 1 and Fig. 3). Thus the solvent composition has a more complex influence on the band asymmetry than on  $E_{Amax}$ .

*Temperature effect on the optical spectra of  $e_s^-$ .*

Fig. 4 shows the optical spectra of  $e_s^-$  in pure 1-butylamine to 50 mol % water at different temperatures. As the temperature is decreased the values of  $G\epsilon_{max}$  and  $E_{Amax}$  increase.

The temperature coefficient of  $E_{Amax}$  has a minimum in 50 mol % water (Figs. 5 and 6). The  $e_s^-$  half-life also has a minimum at 50 mol % water (Table 2). These facts are probably related to the solvent structure, but we have no specific suggestion to offer.

**Table 6-1:** Parameters of solvated electron spectra in 1-butylamine/water at 298 K.

water mol %	$d^a$ (kg/l. )	$\eta^a$ (mPa·s)	$G\epsilon_{\max} 10^{-21}$ (m <sup>2</sup> /16 aJ) <sup>b</sup>	$E_{A\max}$ (zJ)	$W_{1/2}$ (zJ)
0	737	0.50	1.42	115	149 <sup>c</sup>
10	748	0.59	1.58	143	219 <sup>d</sup>
30	770	0.88	2.26	189	178
50	801	1.45	3.72	214	164
70	844	2.21	5.01	248	147
90	925	2.14	7.03	273	134
95			8.60	275	133
99			8.65	277	135
100	997	0.89	8.30	278	139

water mol %	$E_r$ (zJ)	$E_b$ (zJ)	$W_b/W_r$	$-dE_{A\max}/dT$ (zJ/K)
0	102 <sup>c</sup>	215	2.31 <sup>c</sup>	0.43
10	108 <sup>d</sup>	303	2.81 <sup>d</sup>	0.36
30	137	314	2.36	0.30
50	155	319	1.77	0.27
70	183	330	1.26	0.30
90	215	349	1.31	0.41
95	219	352	1.38	0.44
99	221	356	1.41	0.46
100	223	362	1.53	0.47

a. Reference 16.

b.  $1(e_s^- \cdot L/100 \text{ eV} \cdot \text{mol} \cdot \text{cm}) = 1.66 \times 10^{-25} \text{ (m}^2/16 \text{ aJ)}$  in SI.

c. at 225 K, near the fp 224 K.

d. at 226 K.

**Table 6-2.** Half life of solvated electron in 1-butylamine/water mixtures at 298 K.

water (mol %)	0		10		30		50
$\lambda$ (nm)	$t_{1/2}(\mu\text{s})$	tail ( $\mu\text{s}$ ) <sup>a</sup>	$t_{1/2}(\mu\text{s})$	tail ( $\mu\text{s}$ ) <sup>a</sup>	$t_{1/2}(\mu\text{s})$	tail ( $\mu\text{s}$ ) <sup>a</sup>	$t_{1/2}(\mu\text{s})$ <sup>a</sup>
700	4	>100	4	>100	1	>100	0.5
800	3	>100	3	>100	1	>100	0.4
1000	3	none	3	none	1	none	0.4
1200	3	none	3	none	1	none	0.5
1400	3	none	3	none	1	none	

water (mol %)	70	90	95	99	100
$\lambda$ (nm)	$t_{1/2}(\mu\text{s})$	$t_{1/2}(\mu\text{s})$	$t_{1/2}(\mu\text{s})$	$t_{1/2}(\mu\text{s})$	$t_{1/2}(\mu\text{s})$ <sup>b</sup>
700	2	5	8	15	4
800	2	5	8	17	3
1000	2	4	8	16	4

- a.* This long-lived absorption is negligible at  $\lambda > 1000$  nm, and at any  $\lambda$  in solvents containing  $\geq 50\%$  water (Fig. 4).
- b.*  $t_{1/2}$  in pure water is  $> 10 \mu\text{s}$ , but decreases with increasing pulse dose.

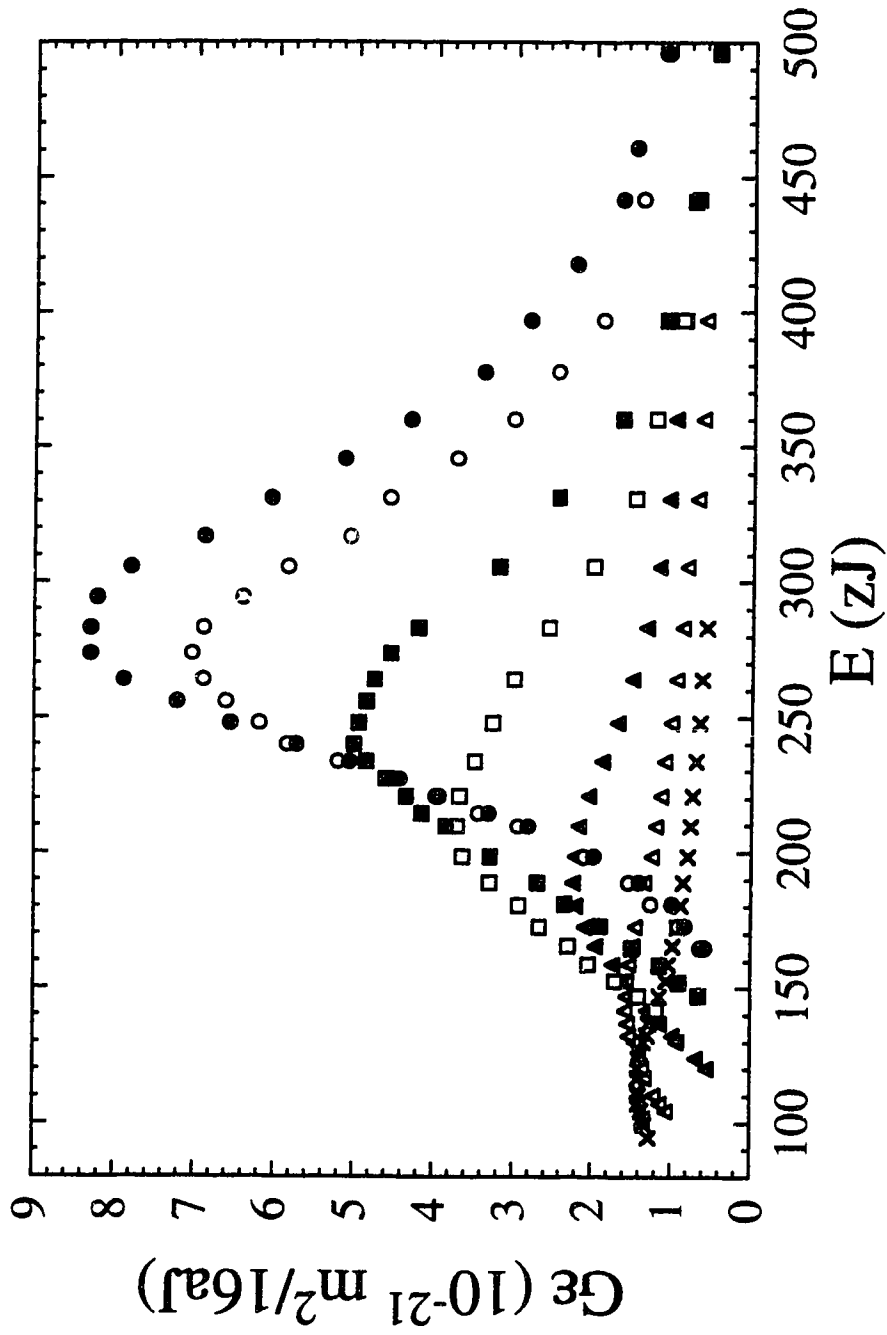


Fig. 6-1. Optical spectra of solvated electrons in 1-butylamine/water mixed solvents at 298 K. Mol % water: ●, 100; ○, 90; ■, 70; □, 50; ▲, 30; △, 10; ×, 0.

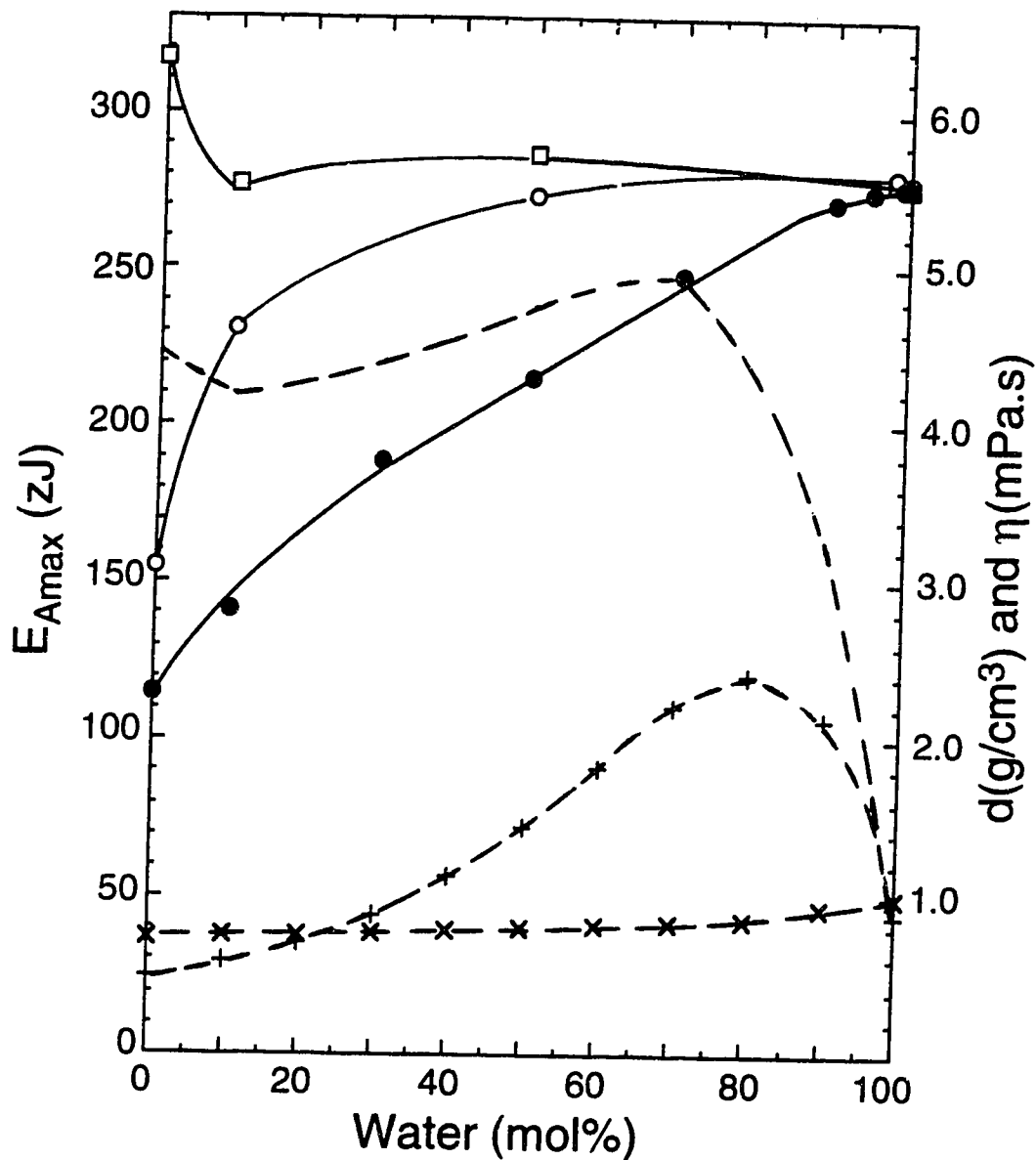


Fig. 6-2. Composition dependence of  $E_{Amax}$  and other parameters for mixed solvents at 298 K. ●,  $E_{Amax}$  in 1-butylamine/water mixtures; ○,  $E_{Amax}$  in *t*-butanol/water mixtures (10); □,  $E_{Amax}$  in 1-butanol/water mixtures (10); ×, densities of 1-butylamine/water mixtures (16); +, viscosities of 1-butylamine/water mixtures (16); ---, viscosities of *t*-butanol/water mixtures (21).

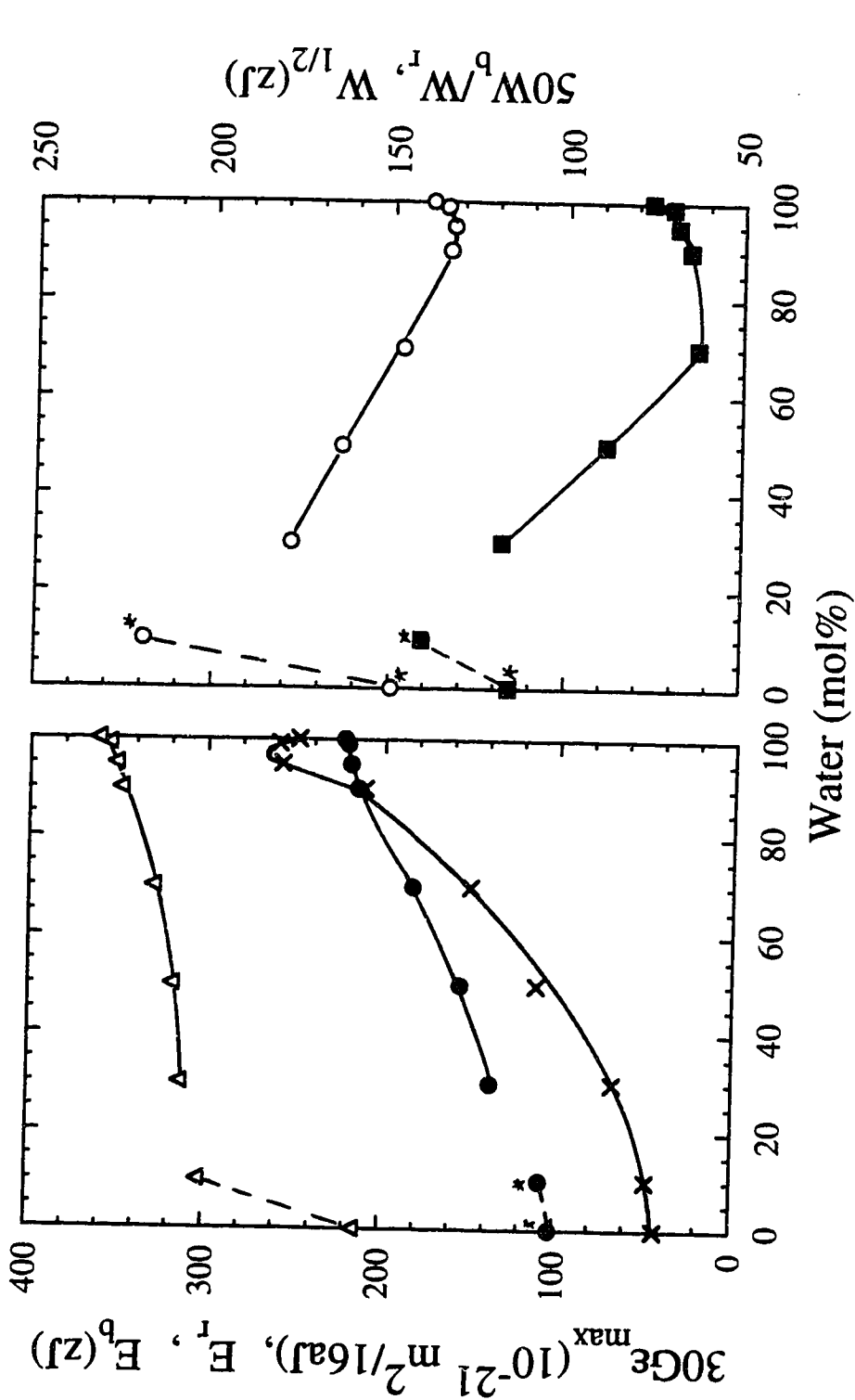


Fig. 6-3. Composition dependence of  $E_b$  ( $\Delta$ ),  $E_r$  ( $\bullet$ ),  $G\epsilon_{\max} \times 30$  ( $\times$ ),  $W_{1/2}$  ( $\circ$ ), and  $W_b/W_r \times 50$  ( $\blacksquare$ ) in 1-butylamine/water mixtures at 298 K. \* indicates the value at 225 K for pure 1-butylamine and 226 K for 90 mol % 1-butylamine.

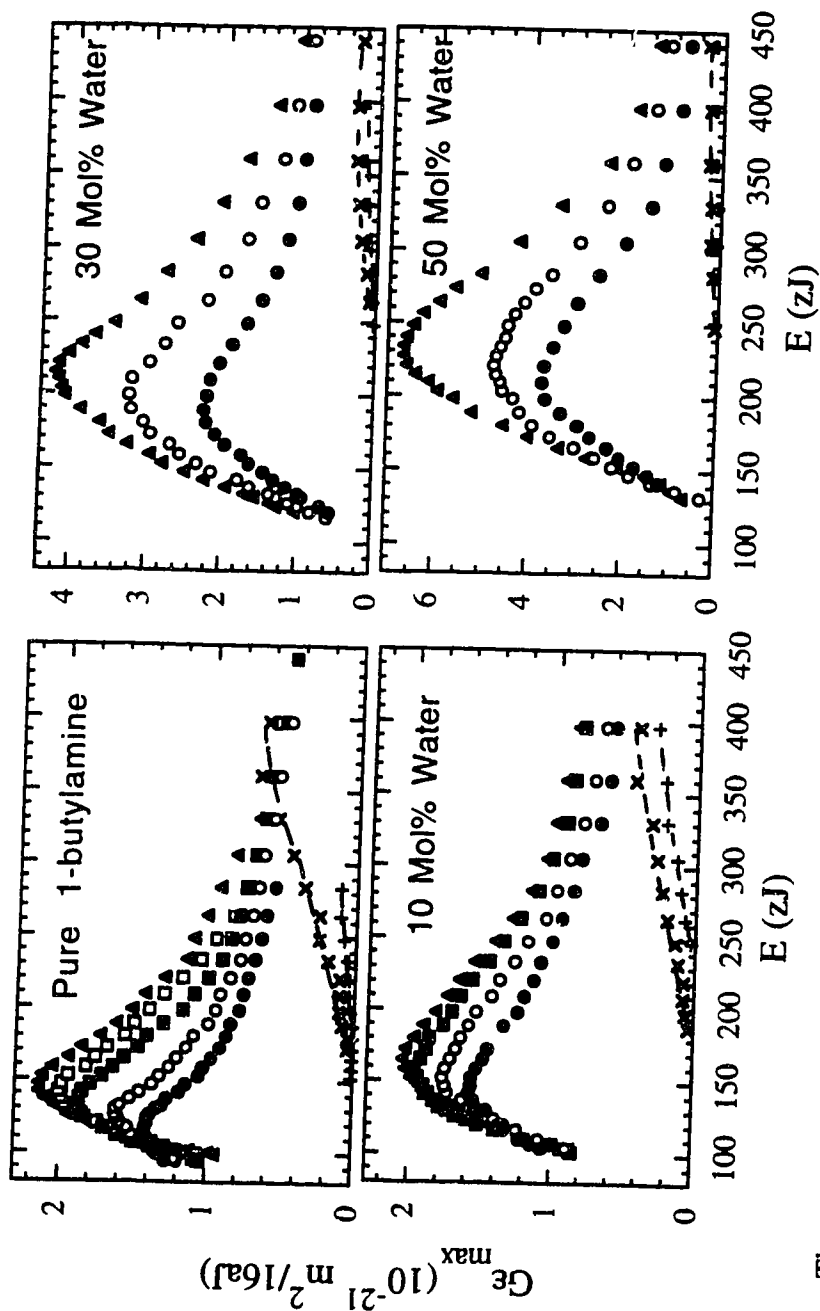


Fig. 6-4. The temperature effect on  $e_s^-$  optical spectra in pure 1-butylamine and the amine-rich mixtures with water. Pure 1-butylamine:  $\blacktriangle$ , 225.3 K;  $\square$ , 236.3 K;  $\blacksquare$ , 247.7 K;  $\circ$ , 271.0 K;  $\bullet$ , 298.7 K. 10 mol % water:  $\blacktriangle$ , 226.7 K;  $\blacksquare$ , 248.2 K;  $\circ$ , 270.7 K;  $\bullet$ , 298.6 K. 30 mol % water:  $\blacktriangle$ , 228.5 K;  $\circ$ , 262.0 K;  $\bullet$ , 298.6 K. 50 mol % water:  $\blacktriangle$ , 230.0 K;  $\circ$ , 262.8 K;  $\bullet$ , 298.8 K. Unidentified absorption tail with half-life longer than 100  $\mu s$ : only the highest ( $+$ ) and lowest ( $\times$ ) temperatures are shown for clarity.

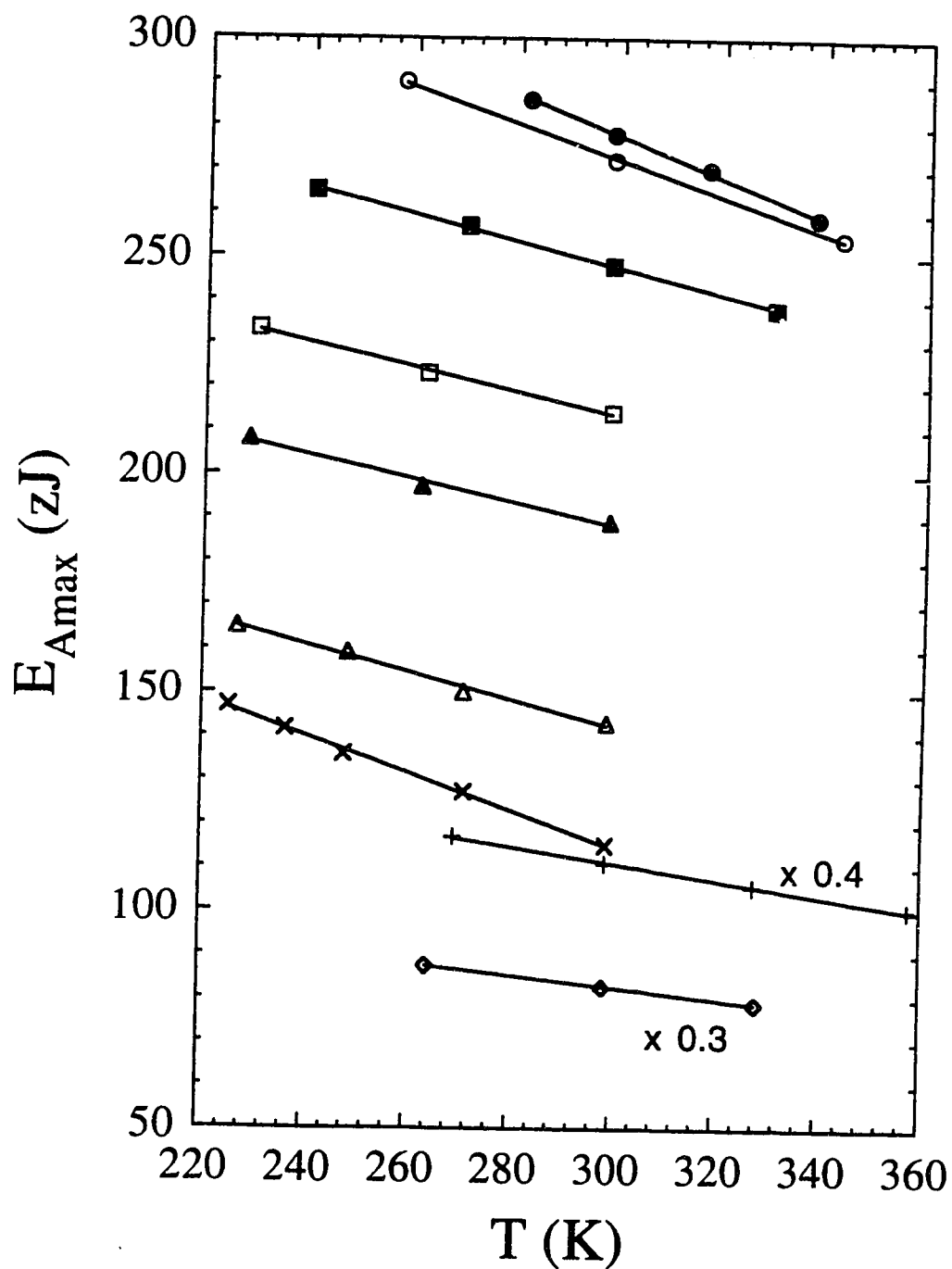


Fig. 6-5. Temperature dependence of  $E_{Amax}$  in 1-butylamine/water mixtures. The symbols are the same as those in Fig. 1, and  $+$ , 99 mol % water;  $\diamond$ , 95 mol % water.



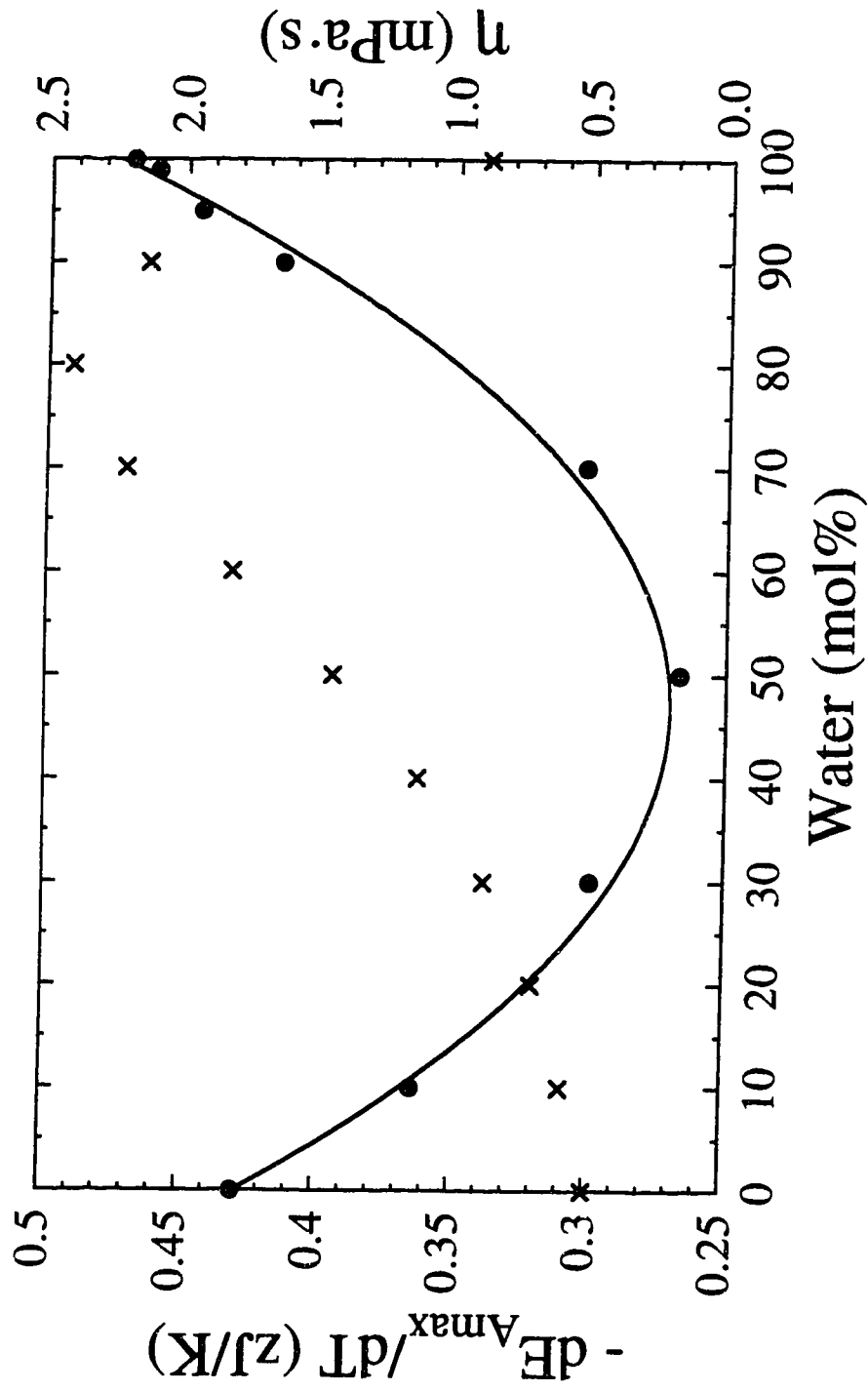


Fig. 6-6. Temperature coefficient ( $-dE_{Amax}/dT$ ) (●) and viscosity (x) (16) in 1-butylamine/water mixtures.

## References

1. R.F. Gould (ed.). *Solvated Electron.*, Adv. Chem. Ser. **50**. Am. Chem. Soc., Washington D.C. 1965.
2. G.R. Freeman. *In Kinetics of Nonhomogeneous Processes*. Edited by G.R. Freeman. Wiley, New York, 1987. Chap. 2.
3. G.R. Freeman. *J. Phys. Chem.* **77**, 7 (1973).
4. F.Y. Jou and G.R. Freeman. *Can. J. Chem.* **60**, 1809 (1982).
5. J. Jay-Gerin and C. Ferradini. *In Excess Electrons in Dielectric Media*. Edited by C. Ferradini and J. Jay-Gerin. CRC Press, London, 1991. Chap. 8.
6. E.J. Hart and M. Anbar. *The Hydrated Electron*. Wiley-Interscience, New York, 1970.
7. B.D. Michael, E.J. Hart, and K.H. Schmidt. *J. Phys. Chem.* **75**, 2798 (1971).
8. F.Y. Jou and G.R. Freeman. *J. Phys. Chem.* **83**, 2383 (1979).
9. F.Y. Jou and G.R. Freeman. *Can. J. Chem.* **57**, 591 (1979).
10. A.D. Leu, K.N. Jha, and G.R. Freeman. *Can. J. Chem.* **60**, 2342 (1982).
11. F.Y. Jou and G.R. Freeman. *J. Phys. Chem.* **88**, 3900 (1984).
12. J.F. Gavlas, F.Y. Jou, and L.M. Dorfman. *J. Phys. Chem.* **78**, 2631 (1974).
13. Y. Zhao and G.R. Freeman. *Can. J. Chem.* **73**, March (1995).
14. R. Chen, Y. Avotinsh, and G.R. Freeman. *Can. J. Chem.* **72**, 1083 (1994).
15. F.Y. Jou and G.R. Freeman. *J. Phys. Chem.* **85**, 629 (1981).
16. M.-J. Lee, S.-M. Hwang, and Y.-C. Kuo. *J. Chem. & Eng. Data.* **38**, 577 (1993).
17. R.C. Weast (ed.). *Handbook of Chemistry and Physics*, 70th edn. CRC Press, Boca Raton, 1979. p. E-61.
18. Y.Y. Akhadov. *Dielectric Properties of Binary Solutions*. Pergamon, Oxford, 1980. p. 144.

19. C.D. Gutsche and D.J. Pasto. *Fundamental of Organic Chemistry*. Prentice-Hall, Englewood Cliffs, 1975. p. 132.
20. R.J. Fessenden and J.S. Fessenden. *Organic Chemistry*. Willard Grant Press, Boston, 1979. p. 24.
21. P.C. Senanyake and G.R. Freeman. *Can. J. Chem.* **65**, 2441 (1987).
22. A.V. Vannikov, E.I. Mal'tzev, V.I. Zolotarevsky, and A.V. Rudnev. *Int. J. Radiat. Phys. Chem.* **4**, 135 (1972).
23. G.R. Freeman and J.M. Fayadh. *J. Chem. Phys.* **43**, 86 (1965).
24. W.A. Seddon, J.W. Fletcher, F.C. Sopchyshyn and J. Jevcak. *Can. J. Chem.* **52**, 3269 (1974).

## Chapter Seven <sup>a</sup>

### Solvent Effects on the Reactivity of Solvated Electrons with Organic Solutes in 1-Butylamine/Water Mixtures

#### 1. Introduction

The study of solvated electron ( $e_s^-$ ) reactivity in mixed alcohol/water solvents has been fruitful in elucidating electron behavior in nonhomogeneous fluids (1-10). The reactivity of  $e_s^-$  depends on the nature of the coreactant and the structure of the solvent. Some reactions of  $e_s^-$  with solutes such as nitrobenzene (1,4),  $Ag_s^+$  (7) and  $H_s^+$  (7) are diffusion-controlled, and some are much slower, as in the case of toluene and phenol (3,5). Solvent structure implies two aspects. One is the molecular structure, which affects, in some cases, the chemical participation of solvent molecules in a reaction (11,12). The other is the solvent molecular packing, such as two and three dimensional structures in alcohol/water mixtures (8,13).

Alcohol, water and their mixtures are all strongly hydrogen-bonded liquids. It is now of interest to study  $e_s^-$  reactivity in mixtures containing a less strongly hydrogen-bonded component. We have chosen 1-butyl amine/water, for practical reasons (ease of handling). The optical absorption spectra of  $e_s^-$  in these mixed solvents have recently been reported (14). There appears to be less selective solvation of electrons by water in

---

<sup>a</sup> A version of this chapter has been submitted for publication to Canadian Journal of Chemistry. Y. Zhao and G. R. Freeman.

these mixtures than was expected.

## 2. Experimental

The method of purification of 1-butylamine was reported in ref. 14. Nitrobenzene (A.C.S. reagent, >99%) and phenol (redistilled, >99%, mp 40–42°C) were obtained from Aldrich. Acetone (HPLC grade, >99.9%) and toluene (HPLC grade, >99.8%) were obtained from Sigma-Aldrich. Nitrobenzene, acetone and phenol were used without further purification. Toluene was fractionally distilled from sodium under UHP argon (99.999%, Liquid Carbonic Canada) and the middle part was collected and stored in a flask under argon positive pressure.

For the measurement of the rate constant of phenol in pure water, phenol was melted in the bottle by placing the bottle in warm water, then phenol was pipetted into a volumetric flask and nanopure water was added. For the rest of the measurements of phenol reaction rate, phenol crystals were taken out of the bottle and placed in a watch glass, and then crystals of phenol without any color were scooped into a beaker to weigh. Then solvent was added, and the solution was transferred to a volumetric flask for final dilution.

Techniques of sample solution preparation, irradiation and optical measurements were the same as described in ref. 9.

## 3. Results and Discussion

### *Rate constants*

Since the reaction of  $e_s^-$  with the solvent amine and water is negligible under our conditions (15), we only consider the following reactions:

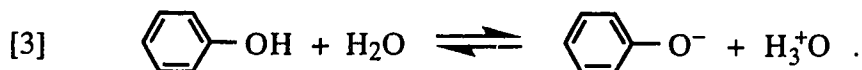


where  $I_s$  represents residual impurities in the solvent and those produced by the radiation pulse, and  $S_s$  is an added solute. The observed first-order decay rate constant  $k_{\text{obs}} = k_1[I] + k_2[S]$  was measured for the pure solvent and six concentrations of solute S. The value of the second-order rate constant  $k_2$  was obtained from the slope of a plot of  $k_{\text{obs}}$  against solute concentration.

1-Butylamine is completely miscible with water. The rate constants of  $e_s^-$  for all solutes were measured in the following compositions in mol % water: 0.0, 10.0, 30.0, 50.0, 70.0, 90.0, 95.0, 97.0 and 100.0. In addition, the rate constants of  $e_s^-$  with phenol in 99.0, 99.5 and 99.8 mol % water were measured. The normal freezing point of 1-butylamine is 224 K, and the normal boiling point is 351 K. The values of  $k_2$  for each solvent were measured from about 230 K to 344 K, depending on the freezing and boiling points of each composition.

Arrhenius plots of  $k_2$  for the four organic solutes nitrobenzene, acetone, phenol and toluene are given in Figs. 1-4; Table 1 contains the symbols for these Figs. The rate constants  $k_2$  ( $10^6 \text{ m}^3/\text{mol}\cdot\text{s}$ ) of nitrobenzene, acetone, phenol and toluene in water at 298 K are: 37, 7.2, 0.024, 0.011, which are consistent within experimental uncertainty with values reported by Maham (16) 38, 7.7, 0.027, 0.013, and Lai (3) 38, 7.7, 0.030, 0.011. Other results reported (15) are: 30, 5.9, 0.018, 0.012.

In water, the rate constant  $k_2(e_s^- + \text{phenol})$  at 298 K was  $2.4 \times 10^4 \text{ m}^3/\text{mol}\cdot\text{s}$ . However, phenol dissociates somewhat in water:



Since the rate constant  $k(e_s^- + H_3^+O) \equiv k_{H^+}$  at 298 K is  $2.9 \times 10^7 \text{ m}^3/\text{mol}\cdot\text{s}$  in water at very low ionic strengths (10), it contributes to  $k_{\text{obs}}$  in the measurement of  $k_2(e_s^- + \text{phenol})$ . We used the method in ref. 8 to correct  $k_2$  for phenol alone. That is,  $[H_3^+O] = \sqrt{K_a[\text{phenol}]}$  is calculated over the range of  $[\text{phenol}] = 5\text{--}30 \text{ mol}/\text{m}^3$ , where  $K_a$  is the dissociation constant and at 298 K it is  $1.3 \times 10^{-7} \text{ mol}/\text{m}^3$  (17). Then the actual value of  $k_2(e_s^- + \text{phenol})$  was calculated from the slope of  $(k_{\text{obs}} - k_{H^+}[H_3^+O])$  against  $[\text{phenol}]$ , and is  $2.1 \times 10^4 \text{ m}^3/\text{mol}\cdot\text{s}$ , which is 13% less than the uncorrected value. Since the values of  $K_a$  at other temperatures in water, and in all the other solvents, are not known we could not make this correction for the other values. For this reason the values in Fig. 3 and Table 2 are uncorrected. Modern studies of the chemical-physical properties of the amine/water mixed solvents and of the phenol solutions would be valuable.

#### *Composition dependence of $k_2$ at 298 K.*

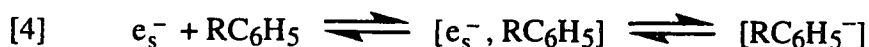
Fig. 5 shows the solvent composition dependences of  $k_2(e_s^- + \text{organic solute})$  in 1-butylamine/water mixed solvents at 298 K. Reaction parameters are listed in Table 2. From Fig. 5 we see that the reactions are divided into two groups: (i) nitrobenzene and acetone, which have  $k_2 > 10^6 \text{ m}^3/\text{mol}\cdot\text{s}$ , and (ii) phenol and toluene, which have  $k_2 < 10^5 \text{ m}^3/\text{mol}\cdot\text{s}$  at most compositions. Both the order of magnitude and the patterns of change of  $k_2$  in the mixtures indicate that these two groups of reactions follow different reaction mechanisms.

Nitrobenzene and acetone are efficient electron scavengers. The magnitudes of  $k_2(e_s^- + \text{nitrobenzene})$  and  $k_2(e_s^- + \text{acetone})$  in 1-butylamine/water mixtures are similar to those in methanol/water and ethanol/water mixtures (3), 1-propanol/water mixtures (4), and all isomeric butanol/water mixtures (18). However, the values of  $k_2(e_s^- + \text{nitrobenzene})$  and  $k_2(e_s^- + \text{acetone})$  in the alcohol-rich region of all alcohol/water mixtures are nearly independent of water content, whereas the  $k_2(e_s^- + \text{nitrobenzene})$  and  $k_2(e_s^-$

+ acetone) in the amine-rich region of 1-butylamine/water mixtures decrease as the water content is increased to 70 mol %. These rate constants in 1-butylamine/water mixtures decrease as the viscosity increases (19,20). This implies that the reactions are close to diffusion-controlled.

Phenol and toluene are less efficient scavengers. Although the orders of magnitude of  $k_2(e_s^- + \text{phenol})$  and  $k_2(e_s^- + \text{toluene})$  in 1-butylamine/water mixtures at 298 K are in the same range as in alcohol/water mixtures (3,4,17,21), the pattern of the change in the mixed solvents is quite different from that in alcohol/water mixtures. Instead of having a minimum at 60–70 mol % water as in alcohol/water mixtures,  $k_2(e_s^- + \text{phenol})$  and  $k_2(e_s^- + \text{toluene})$  have a maximum at 50 mol % water in 1-butylamine, and a sharp minimum at ~99 mol % water (Fig. 5). The values of  $k_2(e_s^- + \text{toluene})$  could not be measured in 99.0 to 99.8 mol % water due to very low rate constants and low solubility of toluene in the solvents. The values of  $k_2$  increase as the values of viscosity and  $E_{A_{\text{max}}}$  increase in the amine-rich region.

The increase of  $k_2(e_s^- + \text{RC}_6\text{H}_5)$ ,  $R = \text{CH}_3$  or  $\text{OH}$ , with increasing viscosity  $\eta$  (Fig. 5) is reminiscent of the behavior of  $k(e_s^- + \text{NO}_{3,s}^-)$  in pure alcohols on increasing the length of the alkyl chain (12,22). In both cases a transient intermediate reacts with the solvent (3,12,16,21,22), and the probability of this reaction increases rapidly with increasing duration  $\tau$  of the  $[e_s^-, S_s]$  encounter pair. For toluene and phenol:



In the  $(e_s^- + \text{NO}_{3,s}^-)$  reaction  $k_2$  increased approximately linearly with  $\eta$ , which means  $k_2 \propto \tau^2$ , whereas in the  $\text{RC}_6\text{H}_5$  reaction between zero and 30 mol % water in 1-butylamine  $k_2$  increases approximately as  $\eta^3$ , which means  $k_2 \propto \tau^4$ . There seems to be



an additional effect in the latter reaction, and we suggest it is that water, being a stronger acid than is the amine (17), is a better protonating agent for the toluene and phenol anions in reaction [5].

At water contents >30 mol % the values of  $k_2(e_s^- + RC_6H_5)$  increase less rapidly, and from 50 to 99 mol % water they decrease (Fig. 5). The decrease is attributed to nonhomogeneous solvation of the reacting entities: in the water-rich solvents  $e_s^-$  is preferentially solvated by the water, while phenol and toluene are selectively solvated by the butyl amine. It becomes progressively more difficult for the  $e_s^-$  and  $RC_6H_5$  to come within the reaction radius of each other.

The increase of  $k_2(e_s^- + RC_6H_5)$  on going from 99.0 to 99.5, 99.8 and 100 mol % water is attributed to the  $RC_6H_5$  being progressively less "coated" by amine molecules, thereby facilitating reactions [4] and [5]. The compressibility of solutions of butyl amine in water has a minimum at 98.3 mol % water, which implies optimal packing of the molecules (23). This might be related to the minimum reaction rate, which we observed at our composition closest to 98.3 % namely 99.0%. The partial molar volume of 1-butylamine has a minimum at 99.1 mol % water (23).

The first order decay rates in the solvents without added solute showed a solvent composition dependence similar to those of the reactions with phenol and toluene (see  $k_1[I_s]$  in Table 2). It therefore appears that the impurities react inefficiently with  $e_s^-$ , and are probably olefinic.

#### *Smoluchowski-Stokes-Debye model*

In the study of the reactions of  $e_s^-$  with organic solutes, the Smoluchowski-Stokes-Debye model has been used (3,18,24). The diffusion-controlled rate constant  $k_2(e_s^- + S)$  for reaction of  $e_s^-$  with a polar solute S is approximately related to the solvent viscosity  $\eta$  by the Smoluchowski-Stokes-Debye equation (3,8,10,25)

$$[6] \quad k_2 = \frac{N_A k_B T}{1.5\eta} \left( \frac{1}{r_e} + \frac{1}{r_s} \right) (R_e + R_s) \kappa f = \frac{N_A k_B T}{1.5\eta} \cdot \frac{1}{r_d} \cdot f \kappa R_r \quad ,$$

where  $N_A$  is Avogadro's constant,  $k_B$  is Boltzmann's constant,  $T$  is temperature,  $r_e$ ,  $r_s$  and  $R_e$ ,  $R_s$  are the effective radii for diffusion and reaction, respectively,  $\kappa$  is the probability that reaction occurs during one encounter,  $r_d$  is the effective radius for mutual diffusion of  $e_s^-$  and solute,  $R_r$  is the average center-to-center reactant separation when reaction occurs,  $\kappa R_r$  is considered as an effective reaction radius, and the Debye factor  $f$  is given by:

$$[7] \quad f = \frac{x}{(e^x - 1)} \quad ,$$

$$[8] \quad x = - \frac{\mu \xi^2}{4\pi \epsilon_0 \epsilon R_r k_B T} \quad ,$$

where  $x$  is the ratio of the coulombic interaction energy of the reactants at  $R_r$  to thermal agitation energy  $k_B T$ , and  $\epsilon$  is the relative permittivity (26) of the medium between the reactants at separation  $R_r$ , and  $\mu$  is the dipole moment of the solute reactant.

Eqn [6] suggests that for diffusion controlled reactions,

$$[9] \quad \eta k_2 \approx \text{constant} \quad .$$

The solvent composition dependences of  $\eta k_2$  are shown in Fig. 6. The efficient reactants nitrobenzene and acetone approximately follow relation [9]. However, the inefficient reactants phenol and toluene do not, as might be expected from the preceding discussion.

#### *Correlation of small values of $k_2$ with $-dE_{Amax}/dT$*

The temperature coefficient of the optical absorption energy of  $e_s^-$  in these

solvents  $-dE_{Amax}/dT$ , has a minimum at 50 mol % water (14), where  $k_2(e_s^- + \text{phenol or toluene})$  has a maximum (Fig. 5). A plot of  $\log k_2$  against  $-dE_{Amax}/dT$  is roughly linear, with the exception of the 99-100% water zone (Fig. 7). We attributed the two sides of the hump in Fig. 5 to different effects, and we cannot interpret the approximate correlation shown in Fig. 7. We display it as a clue to future interpretation.

### *Activation Energies*

The solvent dependences of the activation energies of reaction,  $E_2$ , are compared with those of viscosity,  $E_\eta$ , and the temperature coefficient  $-dE_{Amax}/dT$  (Fig. 8). As might be expected,  $E_2$  for the efficient reactions of  $e_s^-$  with nitrobenzene and acetone vary in a manner similar to  $E_\eta$ . The larger values of  $E_2$  compared to  $E_\eta$  in the amine-rich solutions might be attributed to a larger mobility  $\mu$  and activation energy of mobility  $E_\mu$  of electrons than of molecules in the amine. A similar situation was noted in *t*-butanol solvent (10).

The variations of  $E_2$  for the inefficient reactions of  $e_s^-$  with phenol and toluene are in the opposite direction of those for the efficient reactions, and are in the same direction as those in  $-dE_{Amax}/dT$  (Fig. 8). The zone 99-100% water remains an exception. The decrease of  $E_2$  upon adding water to 1-butylamine is attributed to the increased ease of reaction [5]. The increase of  $E_2$  at water contents  $>50$  mol % is attributed to the increased segregation of the reactants by selective solvation in the different components of the solvent, which makes it more difficult for the reactants to encounter each other. The decrease of  $E_2(e_s^- + \text{phenol})$  on going from 99.8 to 100.0 mol % water is attributed to the decrease of that segregation.

The values of both  $k_2$  and  $E_2$  for  $(e_s^- + \text{toluene})$  are much smaller than those for  $(e_s^- + \text{phenol})$  in all the solvents that contain 1-butylamine (Figs. 5 and 8). Thus the overall entropy of activation of the multi-step reactions is much more negative for the

toluene than for the phenol reaction. Phenol is hydrogen-bonded to the solvent, whereas toluene is not. In the amine-containing solvents, the ratio of concentrations of amine/toluene was always  $\geq 10$ , and of amine/phenol was  $\geq 2$ . We think the toluene and phenol were always clustered by 1-butylamine. It is possible that the lack of hydrogen-bonding of toluene to the solvent, and the presence of it for phenol, affects the relative orientations of the  $e_s^-$  and toluene or phenol as they diffuse together in reaction [4], and affects rotatability of the solvent molecules as the protonation reaction [5] occurs.

The reason for the minimum in  $-dE_{Amax}/dT$  remains a challenge for future work.

**Table 7-1: Symbols for Figures 7-1 to 7-4**

<u>mol % water</u>		<u>mol % water</u>	
◆	0	■	95
▲	10	▶	97
‡	30	▷	99
△	50	▼	99.5
●	70	▽	99.8
○	90	□	100

**Table 7-2: Reaction Rate Parameters in 1-Butylamine/Water Mixed Solvents at 298 K.**

H <sub>2</sub> O mol %	$k_2(10^4$ $m^3/mol\cdot s)$	$E_2$ (kJ/mol)	$\eta^a$ (mPa·s)	$E_\eta^b$ (kJ/mol)	$E_{Amax}$ (zJ) <sup>c</sup>	$k_1[I_s]^d$ ( $10^4 s^{-1}$ )	$-dE_{Amax}/dT^c$ (zJ/K)
<b>Phenol (1 – 60 mol/m<sup>3</sup> for <math>k_2</math>)</b>							
0	1.0	19	0.47	9	115	17	0.43
10	2.0	17	0.59	12	143	17	0.36
30	9.6	15	0.88	15	189	70	0.30
50	15.	16	1.45	19	214	140	0.27
70	3.4	22	2.21	21	248	35	0.30
90	0.74	27	2.14	21	273	14	0.41
95	0.31	31	~1.8		275	9	0.44
97	0.21	33	~1.5			5	
99	0.17	35	~1.3		277	4	0.46
99.5	0.20	38	~1.1			2	
99.8	0.33	36	~1.0			3	
100.0	2.4	20	0.89	17	278	7	0.47

**Toluene (0.7 – 150 mol/m<sup>3</sup> for  $k_2$ )**

H <sub>2</sub> O mol %	$k_2$ ( $10^4 m^3/mol\cdot s$ )	$E_2$ (kJ/mol)
0	0.28	10
10	0.54	8
30	2.2	7
50	3.4	6
70	1.3	8
90	0.29	16
95	0.19	18
97	0.086	21
100	1.1	19

**Table 7-2: Continued**

H <sub>2</sub> O	k <sub>2</sub>	E <sub>2</sub>
mol %	(10 <sup>4</sup> m <sup>3</sup> /mol·s)	(kJ/mol)

**Nitrobenzene (0.1 – 4.5 × 10<sup>-2</sup> mol/m<sup>3</sup> for k<sub>2</sub>)**

0	8400	17
10	7100	20
30	5100	21
50	3000	22
70	2100	22
90	2400	21
95	2800	20
100	3700	17

**Acetone (1.7 – 50 × 10<sup>-2</sup> mol/m<sup>3</sup> for k<sub>2</sub>)**

0	730	24
10	600	25
30	420	26
50	300	27
70	200	27
90	250	27
95	320	25
100	720	14

- a* Reference 18, except for the pure 1-butylamine from ref. 19.
- b* Calculated from the data in reference 18.
- c* Reference 14.
- d* In solvent without added solute.

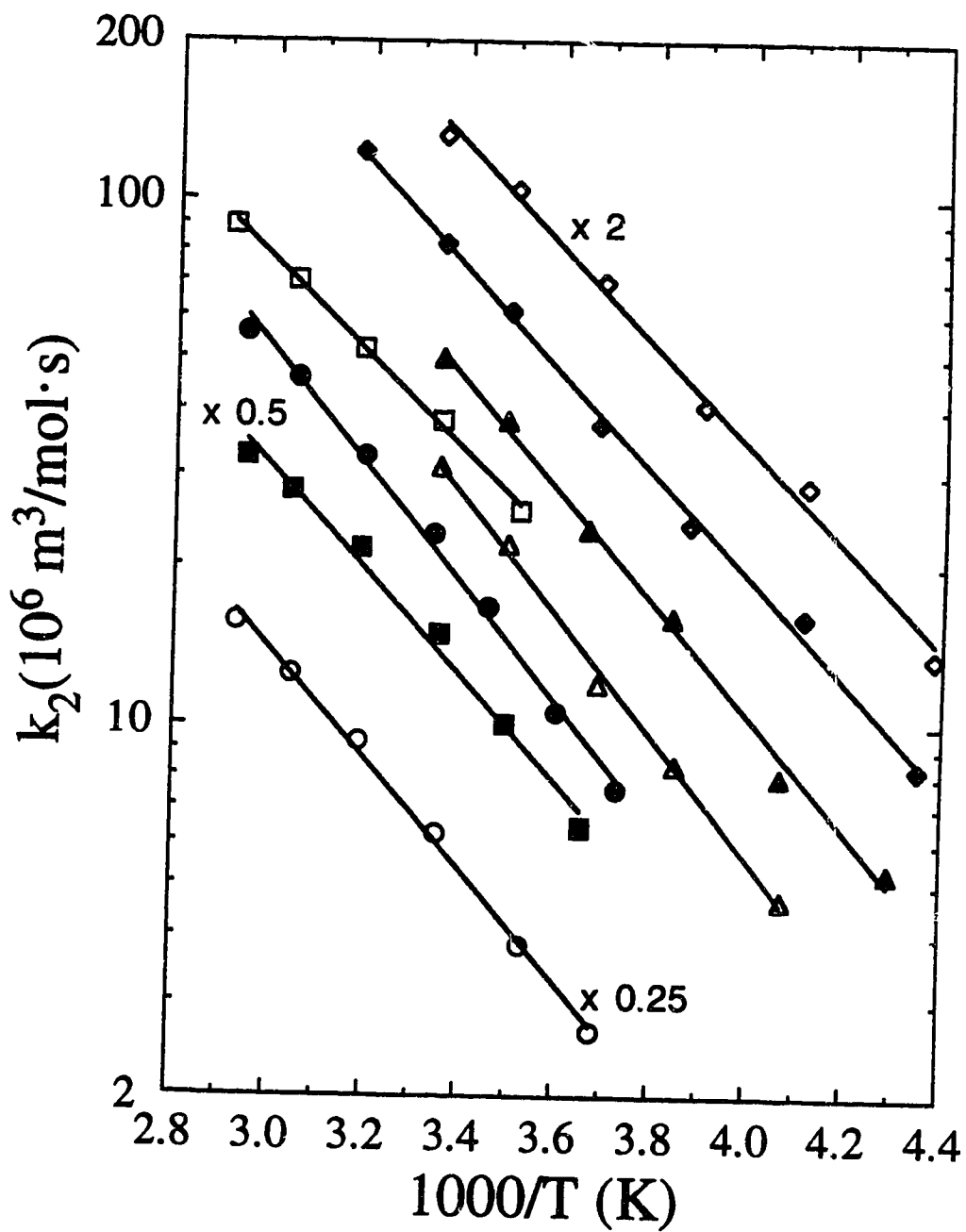


Fig. 7-1. Arrhenius plots of  $k_2(e_s^- + \text{nitrobenzene})$  in 1-butylamine/water mixed solvents. Refer to Table 1 for symbols.



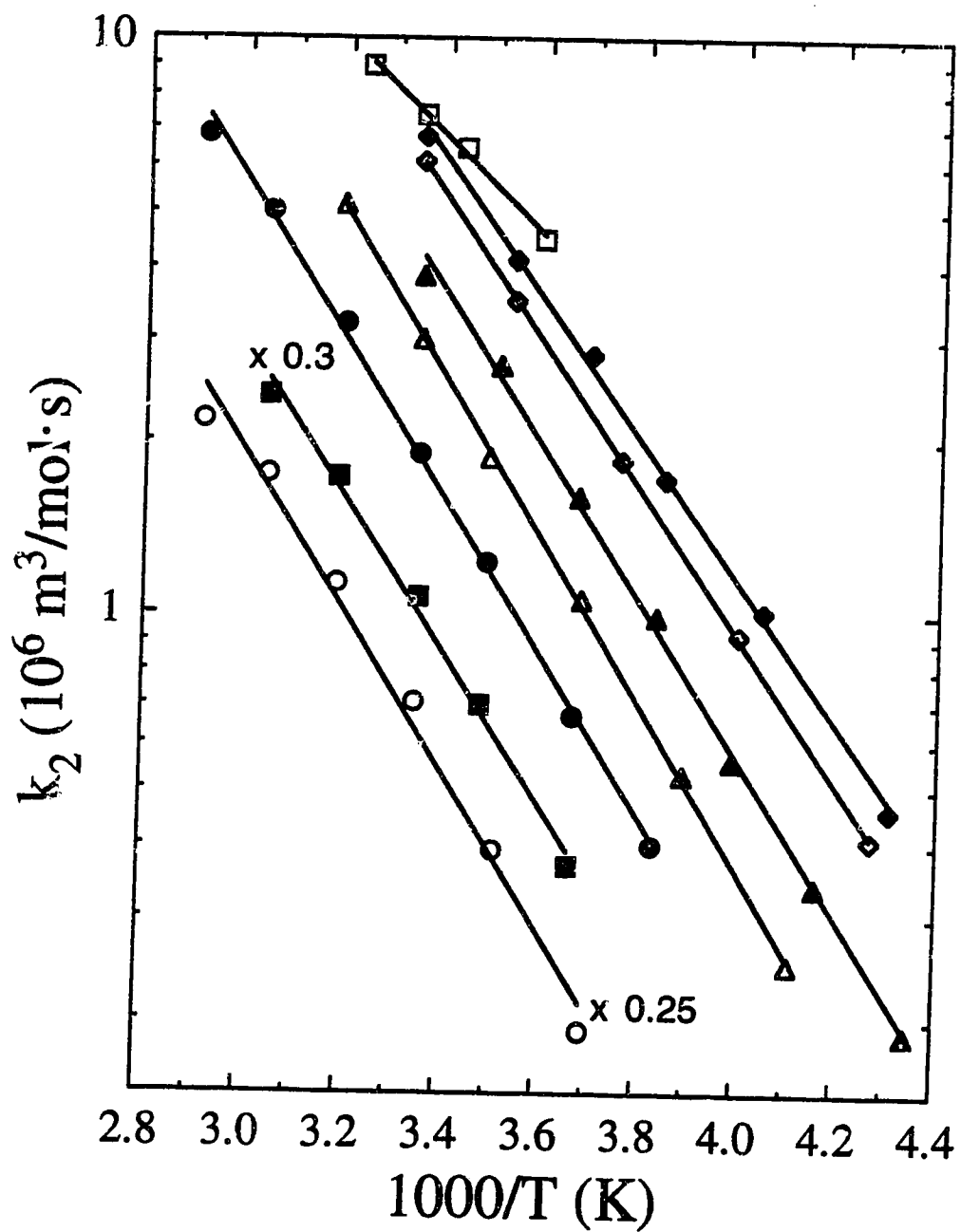


Fig. 7-2. Arrhenius plots of  $k_2(e_s^- + \text{acetone})$  in 1-butylamine/water mixed solvents. Refer to Table 1 for symbols.

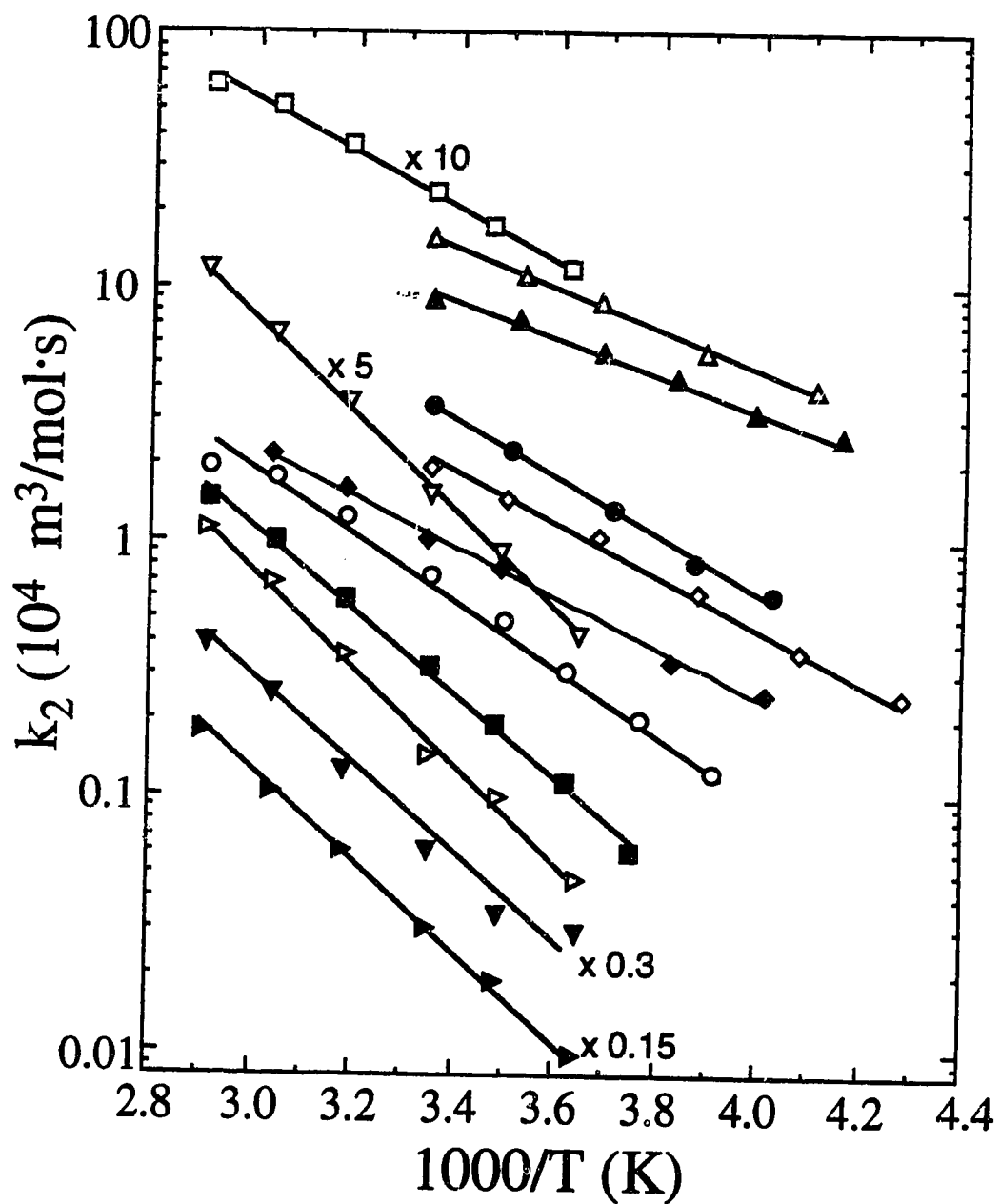


Fig. 1-3. Arrhenius plots of  $k_2(e_s^- + \text{phenol})$  in 1-butylamine/water mixed solvents. Refer to Table 1 for symbols.

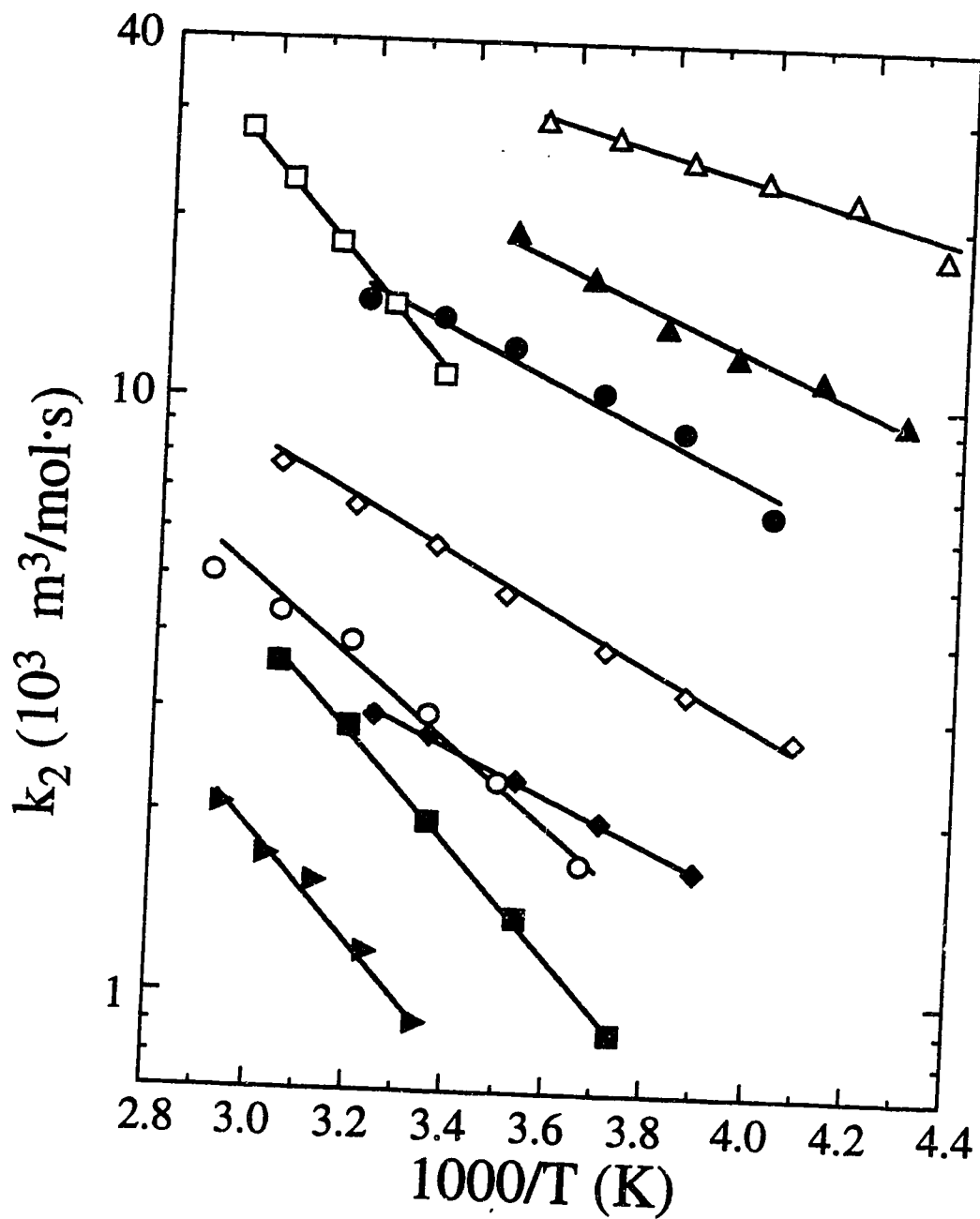


Fig. 7-4. Arrhenius plots of  $k_2(e_5^- + \text{toluene})$  in 1-butylamine/water mixed solvents. Refer to Table 1 for symbols.

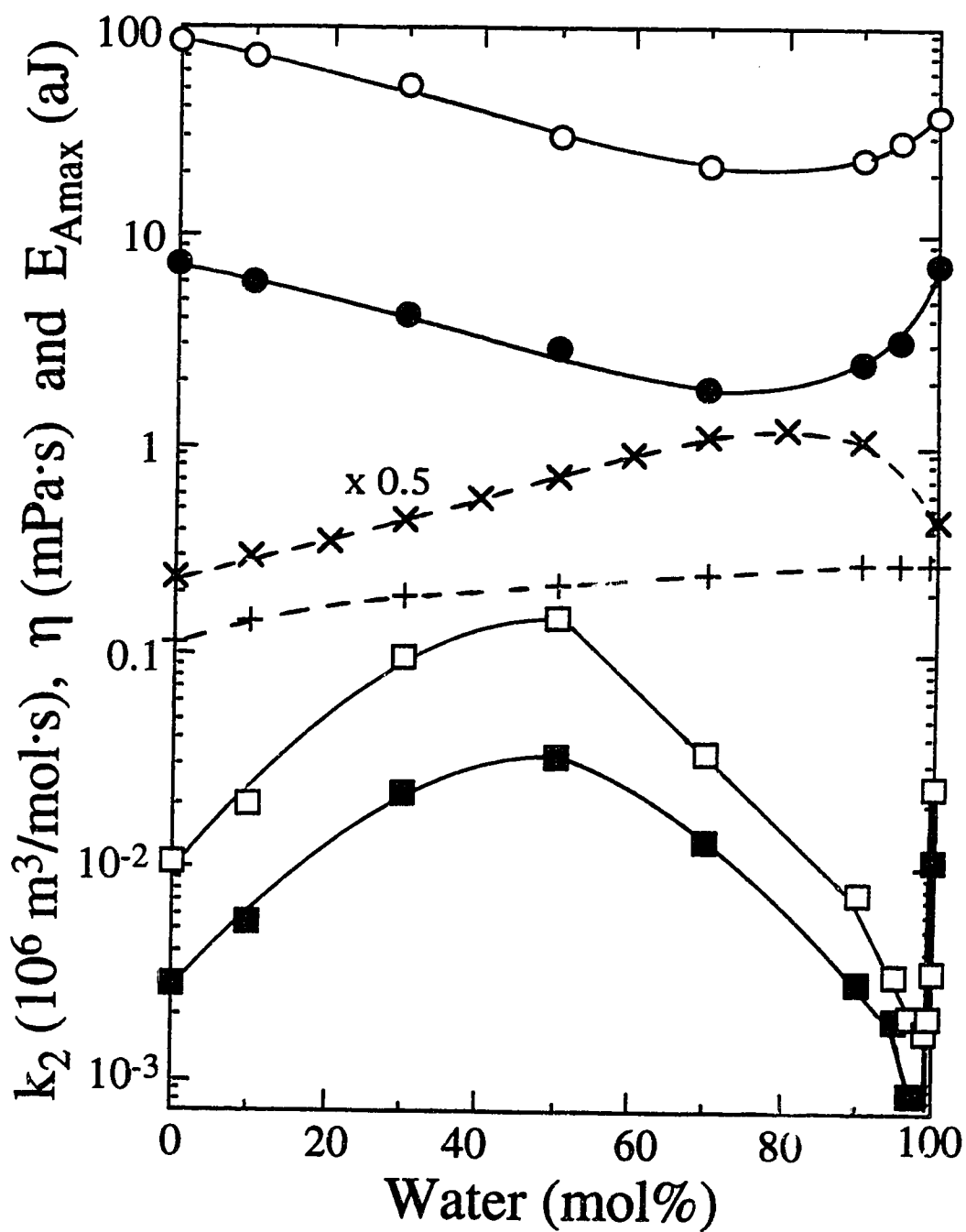


Fig. 7-5. Solvent composition dependence of  $k_2$  in 1-butylamine/water mixed solvents at 298 K.  $\circ$ , nitrobenzene;  $\bullet$ , acetone;  $\square$ , phenol;  $\blacksquare$ , toluene. Physical parameter reference lines are:  $\times$ , viscosity (18,19);  $+$ ,  $E_{Amax}$  (14).

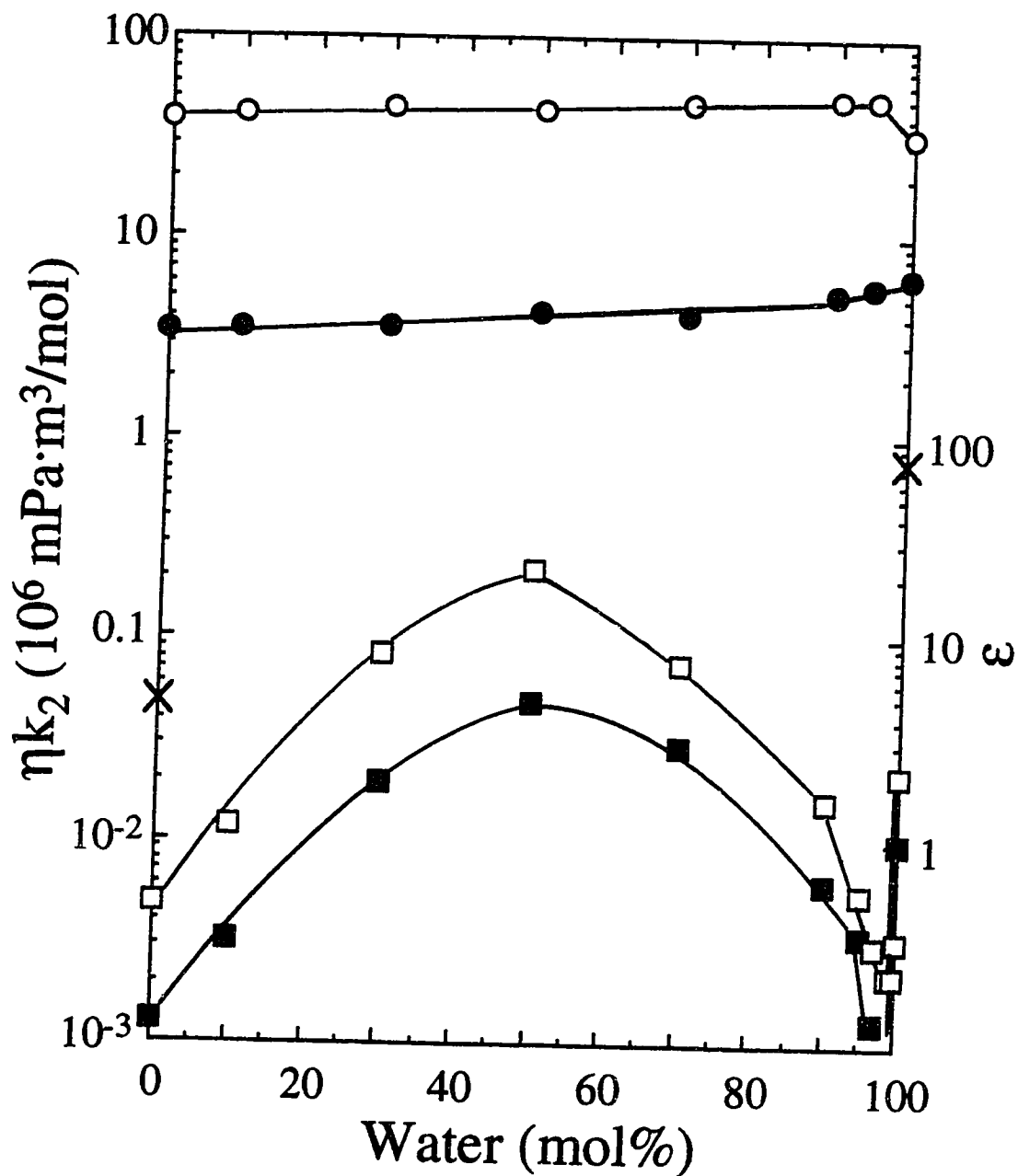


Fig. 7-6. Solvent composition dependence of  $\eta k_2$  in 1-butylamine/water mixtures at 298 K. The symbols are as in Fig. 5.  $\times$ , relative permittivity  $\epsilon$  (26).

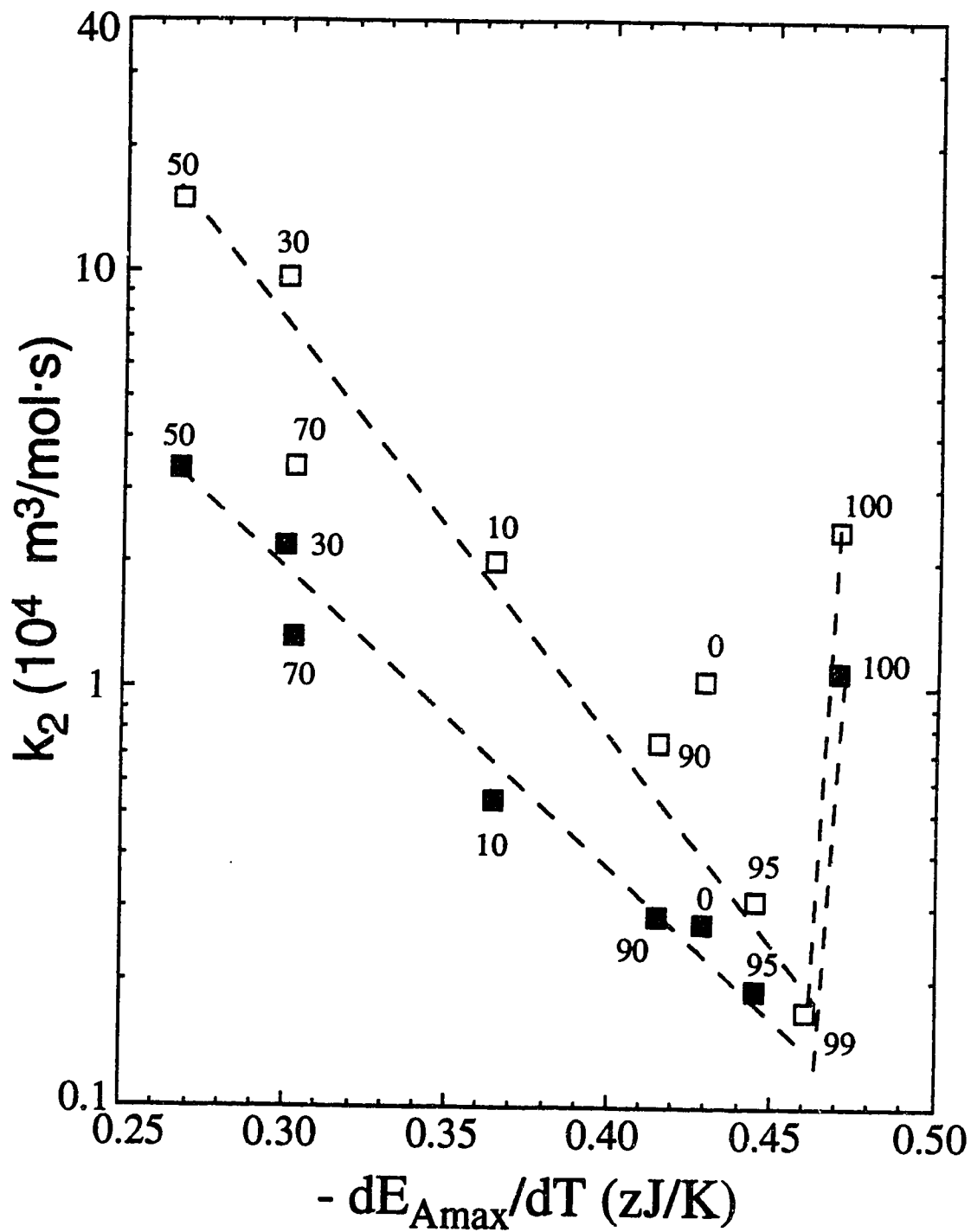


Fig. 7-7. Correlations of  $k_2$  (phenol and toluene) with  $-dE_{Amax}/dT$  (14) in 1-butylamine/water mixtures at 298 K.  $\square$ , phenol;  $\blacksquare$ , toluene.

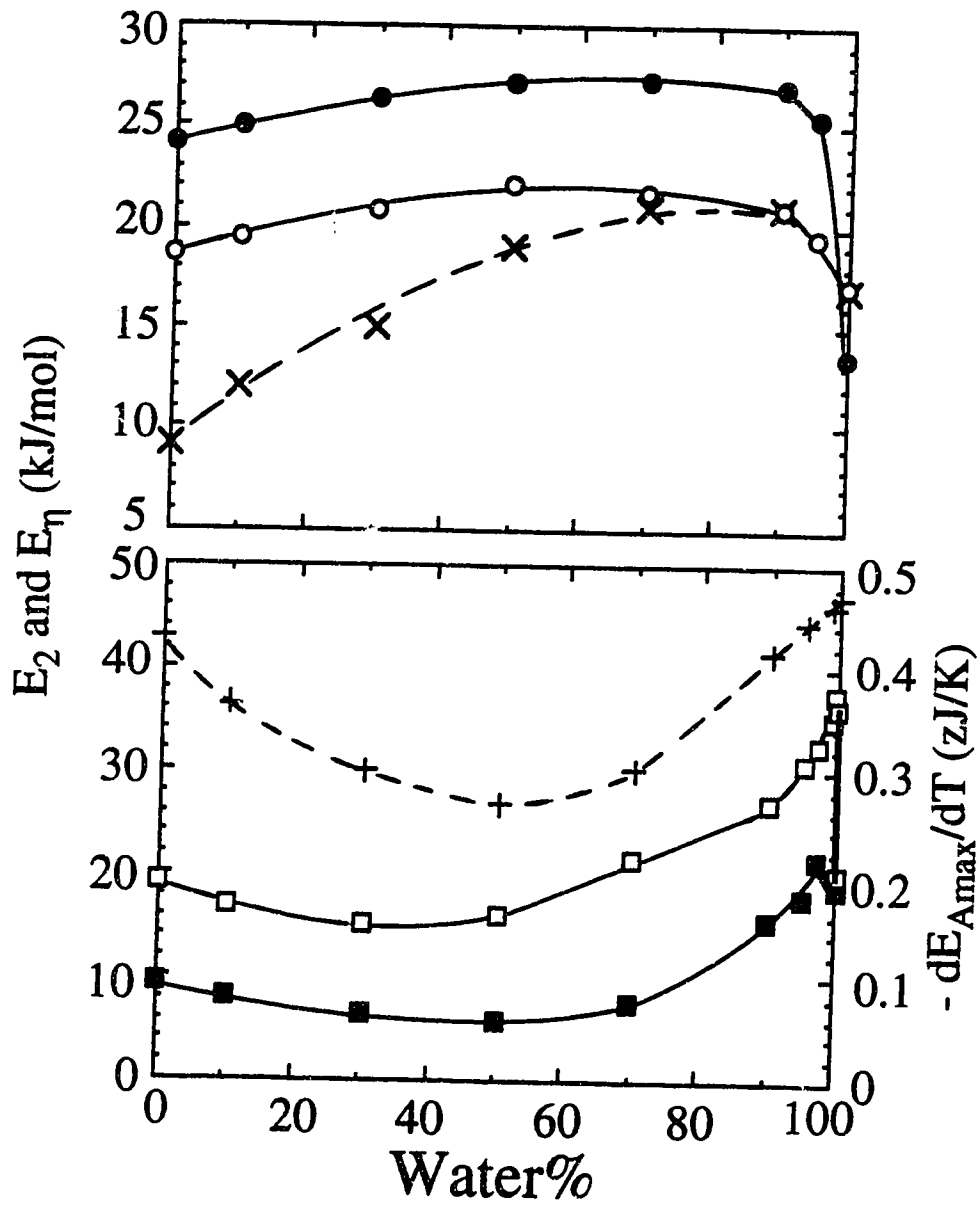


Fig. 7-8. Solvent composition dependence of  $E_2$ . Symbols are as in Fig. 5, And  $E_\eta$  (×) and  $-dE_{Amax}/dT$  (+) in 1-butylamine/water mixtures.

**References**

1. O.I. Mičić and B.Čerček. *J. Phys. Chem.* **81**, 833 (1977).
2. B.H. Milosavljević and O.I. Mičić. *J. Phys. Chem.* **82**, 1359 (1978).
3. C.C. Lai and G.R. Freeman. *J. Phys. Chem.* **94**, 302 (1990).
4. Y. Maham and G.R. Freeman. *J. Phys. Chem.* **89**, 4347 (1985).
5. Y. Maham and G.R. Freeman. *Can. J. Chem.* **66**, 1706 (1988).
6. S.A. Peiris and G.R. Freeman. *Can. J. Phys.* **68**, 940 (1990).
7. S.A. Peiris and G.R. Freeman. *Can. J. Chem.* **69**, 157 (1991).
8. R. Chen and G.R. Freeman. *Can. J. Chem.* **71**, 1303 (1993).
9. R. Chen, Y. Avotinsh, and G.R. Freeman. *Can. J. Chem.* **72**, 1083 (1994).
10. Y. Zhao and G.R. Freeman. *Can. J. Chem.* **73**, 392 and 389 (1995).
11. T.B. Kang and G.R. Freeman. *Can. J. Chem.* **71**, 1297 (1993).
12. Y. Zhao and G.R. Freeman. *Can. J. Chem.* **73**, 284 (1995).
13. A.D. Leu, K.N. Jha, and G.R. Freeman. *Can. J. Chem.* **60**, 2342 (1982).
14. Y. Zhao and G.R. Freeman. *Can. J. Chem.* submitted (1995).
15. M. Anbar, M. Bambenek, and A.B. Ross. *Selected Specific Rates of Reactions of Transients from Water in Aqueous Solution. I. Hydrated Electron.* NSRDS-NBS **43**, U.S. Dept. of Commerce, Washington, D.C., 1973.
16. Y. Maham and G.R. Freeman. *J. Phys. Chem.* **91**, 1561 (1987).
17. P.W. Atkins. *Physical Chemistry*. 4 ed. Freeman, New York. 1990. pp. 765, 951.
18. P.C. Senanayake. *J. Chem. Phys.* **87**, 7007 (1987).
19. M.-J. Lee, S.-M. Hwang, and Y.-C. Kuo. *J. Chem. & Eng. Data.* **38**, 577 (1993).



20. K.Y. Liew, C.E. Seng, and C.G. Lee. *J. Sol. Chem.* **23**, 1293 (1994).
21. P.C. Senanayake and G.R. Freeman. *J. Phys. Chem.* **91**, 2123 (1987).
22. R. Chen and G.R. Freeman. *J. Phys. Chem.* **99**, 4970 (1995).
23. T. Moriyoshi, T. Tsubota, and K. Hamaguchi. *J. Chem. Thermodynamics* **23**, 155 (1991).
24. Y. Maham and G.R. Freeman. *J. Phys. Chem.* **92**, 1506 (1988).
25. P. Debye. *Trans. Electrochem. Soc.* **82**, 265 (1942).
26. Y.Y. Akhadov. *Dielectric Properties of Binary Solutions*. Pergamon Press, Oxford. 1980. p. 144.

## Chapter Eight

### Conclusions and Future Work

#### 1. Conclusions

The reactivity of solvated electrons ( $e_s^-$ ) strongly depends on the composition and structure of the solvent. The reactions of  $e_s^-$  show different kinetic behavior in *t*-butanol/water than in 1-butylamine/water mixed solvents. The former solvents are more strongly hydrogen-bonded than are the latter.

The reactions of  $e_s^-$  with  $\text{NH}_4\text{NO}_3$  in *t*-butanol/water mixed solvents have high rate constants. In the water-rich region the reaction is mainly due to the  $\text{NO}_3^-$  ion, and in the alcohol-rich region the reaction is mainly due to the  $\text{NH}_4^+$  ion.

The rate constants of  $e_s^-$  with  $\text{H}_s^+$  are the highest of those of the ions studied, in the whole region of *t*-butanol/water mixtures, because  $\text{H}_s^+$  has the highest diffusion coefficient.

The calculated effective reaction radius ( $\kappa R_r$ ) of each ionic solute decreases from pure *t*-butanol to pure water. The large effective reaction radius and high activation energy ( $E_2$ ) in pure *t*-butanol are attributed to a high mobility and activation energy of diffusion of  $e_s^-$  in the alcohol.

In the measured optical absorption spectra of  $e_s^-$  in 1-butylamine/water mixtures, the absorbance  $G\epsilon_{\text{max}}$  decreases on going from pure water to pure 1-butylamine except for 100 to about 97 mol% water where there is a small increase in the intensity. The value of  $E_{\text{Amax}}$  decreases smoothly from water to 1-butylamine; this indicates that electrons are less selectively solvated by water molecules than anticipated, and the amine/water mixtures are more randomly structured than are alcohol/water mixed

solvents. However, the temperature coefficient ( $-dE_{Amax}/dT$ ) has a minimum at 50 mol% water, which indicates that the solvent structure in the amine-rich region may be different from that in the water-rich region.

The rate constants of the efficient reaction of  $e_s^-$  with nitrobenzene ( $k_2 = 10^7 - 10^8$  m<sup>3</sup>/mol·s) are higher than that of acetone ( $k_2$  is between  $10^6$  and  $10^7$  m<sup>3</sup>/mol·s), but both sets of  $k_2$  are inversely proportional to the viscosity of the 1-butylamine/water mixed solvents.

The rate constants of the efficient reactions of  $e_s^-$  with toluene and phenol ( $k_2 < 10^5$  m<sup>3</sup>/mol·s) have a maximum at 10 mol% water and a minimum at 99 mol% water; there is no correlation with viscosity. The solvent molecules protonate the transient anions of toluene and phenol to secure the electron capture. In the amine-rich region, from pure 1-butylamine to 50 mol% water, the rate constant increases with the addition of water because water is a stronger acid than is the amine. In the water-rich solvents,  $e_s^-$  is preferentially solvated by water and toluene or phenol is preferentially solvated by amine; this tends to keep the reactants apart, and decreases the value of  $k_2$ .

The variation of the activation energies ( $E_2$ ) for the efficient reactions in 1-butylamine/water mixed solvents is similar to the change of the activation energy ( $E_\eta$ ) for diffusion. The activation energies for the inefficient reactions have a rough correlation with the temperature coefficient of the optical absorption energy ( $-dE_{Amax}/dT$ ).

## II. Suggestions for Future Work

- i. Measurement of mobility of  $e_s^-$  in butanols and amines:

An approximation of  $e_s^-$  diffusion rates in alcohols has been used in explaining the kinetic behavior of  $e_s^-$ , since reliable values of  $e_s^-$  diffusion coefficients are not

available. In the study of the reactivity of  $e_s^-$  in *t*-butanol/water mixtures (chapter 2) we have estimated a high mobility of  $e_s^-$  in *t*-butanol (Chapter 3). Direct measurements of the  $e_s^-$  mobilities are needed.

The new research on amine/water mixed solvents requires that  $e_s^-$  mobilities be measured in these solvents also.

ii. Optical absorption spectra of  $e_s^-$  in other amine/water mixtures:

The measured optical absorption spectra in 1-butylamine/water mixed solvent (Chapter 6) show that the structure of the amine/water mixtures is quite different from that of alcohol/water mixed solvent. Different amines have different molecular structure, and would pack together differently in the liquid state. This would affect the properties of  $e_s^-$ . Optical absorption spectra should be measured in other amine/water mixtures to get more information about  $e_s^-$  and solvent structure.

iii. Reactivity of  $e_s^-$  with inorganic ions in 1-butylamine/water mixtures:

We have started the study of  $e_s^-$  reaction with organic solutes in 1-butylamine/water mixtures (Chapter 7). The study of  $e_s^-$  reactions with ionic solutes could show quite different composition dependences. This research also requires measurement of the dielectric permittivities of the 1-butylamine/water mixed solvents.

iv. Reactivity of  $e_s^-$  in other amine/water mixtures:

The reasons are the same as those in item ii.

## Appendix One

### Experimental Methodology

#### I. Apparatus for Optical Measurement

##### A. *Sample Cells*

Cells of Spectrosil Quartz from VWR Scientific, and Cells of Suprasil Quartz from Terochem Laboratories were used at atmospheric pressure for temperatures varying from ~275K to ~453K. The inside dimensions of the width and height of the cell are 10 x 45 mm. For the measurements of the rate constants of  $e_s^-$  in *t*-butanol/water mixed solvents, the optical path length of the cells is 10 mm. For the measurements of the optical absorption spectra of  $e_s^-$  in 1-butylamine/water mixed solvents, two kind of Spectrosil optical cells were used: 10 mm optical path length for pure water to 70 mol % water, and 5 mm path for 50 mol % water to pure 1-butylamine. The cell was topped by a graded seal so that it can be attached to a Pyrex glass tube.

## ***B. Irradiation, Optical, and Control Systems***

### ***1. Van de Graaff Accelerator***

A Van de Graaff accelerator (type AK-60 2 MeV) manufactured by High Voltage Engineering Corporation was used as the source of high energy electrons. The maximum peak current delivered during a pulsed operation was 150 mA. Pulse widths of 3, 10, 30, and 100 nanoseconds (ns), and 1 microsecond ( $\mu$ s) were available. Of these only 100ns pulse width was used to obtain an appropriate pulse of 340 fJ (2.1 MeV) electron beam, delivering a dose of  $\sim$ 4 Gy (J/kg).

A concrete maze shielded the entrance from the control room to the irradiation room and accelerator. Closing and locking the iron gate at the control room end of the maze sounded a warning buzzer for 15 seconds. It was not possible to operate the accelerator until the cessation of the buzzer. Unlocking the iron gate resulted in immediate shut down of the accelerator.

Steering and focusing of the electron beam was normally done by fixing a piece of phosphorescent paper to the end of the accelerator beam pipe. The paper could be viewed by closed circuit television. Each pulse of electrons caused a visible glow where it struck the phosphor. Accurate steering and focusing were done by adjusting the current in electromagnets. When equipment blocked visual observation of the end of the beam pipe, steering of the beam was done by maximizing the optical absorption of solvated electrons in a water sample.

### ***2. Secondary Emission Monitor (SEM)***

A secondary emission monitor indicated the relative dose for each electron pulse. It consisted of three thin metal foils placed inside the accelerator beam pipe perpendicular to the path of high energy electron beam (Figure A-1-1). These foils were positioned near the exit window and they were made of cobalt-based, high strength alloy

(Havar, obtained from the Hamilton Watch Company, Precision Metal Division). This material (average atomic number 27) was better than gold (atomic number 79) because of less beam attenuation by electron scattering.

The diameter of these foils was 5 cm and they were 0.5 cm apart from each other. The outer two were charged to +50 V relative to the central foil at ground. Passage of an electron pulse generated secondary electrons in the foils. The electrons ejected from the center foil were collected by the outer foils, the net result being a current flow from the center foil. Current flow occurred only during a high energy electron pulse and was measured by a gated integrator, digitized and displayed on a digital readout.

### 3. *Optical System*

(a) The light source was a high pressure Xenon arc lamp (Optical Radiation Co., model XLN1000) contained in a lamp housing (Photochemical Research Assoc., model PRA ALH220). A rhodium-coated, off axis parabolic mirror (Melles Griot-02 POH 015) placed in the beam path absorbed the UV light with wavelength shorter than 320 nm. Formation of excess ozone was prevented by this. The lamp was run at 1000 W.

A schematic diagram of the path of the analyzing light is shown in Figure A-1-2. The light shutter was used to protect the sample from unnecessary exposure. It was opened for only 55 ms. The light beam was focused to near the edge of the side of the irradiation cell facing the electron beam by using the above mentioned mirror. The light beam was reflected from front surface aluminized mirrors coated with silicon monoxide, through a 10 cm diameter hole in the 1.2 m thick concrete wall, to the control room. Finally, the light was focused into the monochromator housing by a concave mirror.

(b) Monochromator grating and filters:

i) The measurements of rate constant  $k_{\text{obs}}$ :

A Bausch and Lomb monochromator grating, type 33-86-25, was used with the grating type 33-86-03 (700–1000 nm), and a Corning filter type CS-2-64 (700–1000 nm). The light intensity reaching the detector was controlled by adjusting the slits on the monochromator. The wavelength of the analyzing light was 850 nm with bandwidth 9 nm, to obtain an optimal absorption signal.

ii) The measurement of the optical absorption spectrum measurements:

Bausch and Lomb monochromator gratings 1350 (No. 33-86-02) for 400-800 nm, 1350 (No. 33-86-03) for 700-1200 nm, and high-intensity monochromator (no. 33-86-78) for 1100-2600 nm were used in the measurements. Corning filters were placed in front of the monochromator to eliminate higher order light interference: CS 4-97 for 400-500 nm, CS 3-72 for 500-650 nm, CS 2-58 for 650-1050 nm, LL-1000 for 1050-1800 nm, and RL-1500 for 1800-2600 nm.

(c) Data acquisition and plotting: The light detector (pin silicon photodiode SD 040) was sensitive over the wavelength range 400–1100 nm. The 3 to 97% response time of the detector, amplifier and transient digitizer (Tektronix R7912) was 6 ns. The signal to noise ratio of the differential amplifier (Tektronix 7A13) was increased by using the 5 MHz filter, which gave a system response time of 96 ns. For the measurement of absorbance at wavelengths >1050 nm, the InSb infrared detector (Model 1935-IS) was used and is sensitive from 1050 nm to 2600 nm. The 3 to 97% response time of the detector, amplifier and transient digitizer (Tektronix R7912) was 35 ns. The signal to noise ratio of the differential amplifier (Tektronix 7A13) was increased by using the 5 MHz filter, which gave a system response time of 96 ns.

The incident light intensity at the detector, recorded as a voltage on a digital multimeter (Fluke 8810A), was displayed on an oscilloscope (Tektronix R7623). The signals were displayed as plots of voltage against time on a digital plotter (Zeta1200).



All information related to the particular signal, such as total light intensity ( $I_0$ ), dose, temperature, sensitivity, time scale, half-life trace, and cell holder number were also printed on the chart.

#### 4. *Temperature Control System*

(a) Cooling and heating: Temperatures from 277K to 298K were achieved by boiling liquid nitrogen and regulating the temperature of the nitrogen gas by a heat exchanger. Liquid nitrogen was boiled at a controlled rate from a 50 L, narrow-necked aluminum Dewar vessel (Lakeshore Cryotronics Inc.). A stainless steel pipe (5 cm diameter) which was fixed to a lid, fitted snugly into the neck of the Dewar. This pipe extended to the bottom of the Dewar. A nichrome heating coil (600W) was attached to the inside of the steel pipe to about 7 cm from the bottom.

A Rubatex foam-rubber pipe (1 meter long) was used to transport the cold nitrogen gas to the sample box. Both ends of the pipe had glass inserts to which a leather seal was connected. Before entering the cell box, the cold gas that came through this pipe flowed through another stainless steel pipe (2.5 cm diameter) that had another nichrome heating wire (0.24 mm diameter, 4 m long) inserted inside it. The temperature of the nitrogen gas was regulated by this heating wire.

A laboratory heat gun (Master Appliance Corporation, Model AH0751) was used to achieve temperatures from 296K to 372K. The nichrome wire heated the air to the required temperature.

(b) Cell holder box: A box insulated with foam glass (Pittsburgh Corning Corporation) contained eight holders which were mounted on a circular (7 cm diameter) aluminum base. The base was connected to a motor so that the cells holder could make clockwise and counterclockwise full cycle rotations when the cells were not being irradiated. Just before irradiation the pre-selected cell stopped in the front of the electron

exit window. The gas that flowed through the holes in the aluminum base was stirred by the rotating cell holder before leaving via a hole (2.5 cm diameter ) in the lid.

A thermocouple mounted in a cell (Thermocouple cell) filled with solvent monitored the temperature of the system. The temperature controller (Taylor Microscan 1300) utilized a temperature sensor which was fixed to one of the cell holders. A Fluke Digital thermometer (Model 2100A) displayed the temperature of the thermocouple. The temperature of the thermocouple cell and the difference between the temperature setting and the cell holder were plotted on a chart recorder (Clevite Corporation, Model Brush Mark 220). When the chart recorder displayed a steady temperature for a period of 30 minutes the thermal equilibrium in the system was deemed to be established. At this time, the variation of the temperature of the thermocouple cell was only  $\pm 0.1$  K.

## II. Apparatus for Electrical Conductivity Measurement

### A. Impedance Bridge

Conductivity measurements were done with an impedance bridge (type 1608-A, General Radio Co.). It was a self-contained system which included six bridges for the measurements of conductance, capacitance, resistance, and inductance, as well as the internal generator and detectors for AC and DC measurements. To obtain the conductance reading the variable resistor and capacitor were adjusted until the null balance was achieved. Most of the time the conductance mode ( $G_p$  Mode) was used. For the values of conductances less than about 0.6 microSiemen, the bridge was set to one of the capacitance modes ( $C_p$  or  $C_s$  Modes). Then values of conductance were calculated from the capacitance data. The oscillator frequency was 1 kHz for AC measurement.

### ***B. Conductance Cells***

Pyrex conductivity cells (YSI3403) were obtained from Yellow Springs Instrument Co., Inc. The temperature range of the measurements was ~277K to ~353K. The cell chamber was 5 cm deep. The overall length was 20 cm and the outer diameter was 1.2 cm.

Graduated cylinders, 25 cm<sup>3</sup> (16 cm long, 1.4 cm inner diameter), were used to contain the electrolyte solutions. In order to have a tight seal between the container and the cell, a rubber adapter made from No. 2 stopper was fixed to the cell. Two layers of Parafilm (American Can Co.) were wrapped around the adapter-container junction to provide a tight seal, especially at high temperatures.

A secondary standard solution (YSI3161, specific conductance of 1000±5 mS/cm) available from Yellow Springs Instrument Co., Inc. was used to calibrate the cells. This solution contained water, 0.002% iodine (an anti-microbial), and potassium chloride (ACS Reagent Grade).

The electrodes of the cells were coated with platinum black which was very important for cell operation. When the electrodes looked gray the cells were replatinized using a replatinizing solution (YSI3140) on a platinizing instrument (YSI3139). The current was kept at about 50 milliamp during the platinization. When a strong clearing of the cells was required they were treated with a solution of equal parts of isopropyl alcohol and 10 M HCl before the replatinization.

### ***C. Constant Temperature Bath***

A 10 L glass Dewar filled with water was used to measure conductances at various temperatures (Figure A-1-3). Inserted in this water were a motor controlled

stirrer, a refrigeration unit (Tecumseh Model AE1343 AA), a heating coil, and a knife-heater (Cenco, 53 ohm, 350W). The heating coil was controlled by a variable transformer (Ohmite, Model VT). It was mainly used for the faster change of temperature from one setting to the another. The knife-heater was controlled by a temperature regulating system (Figure A-1-4). The temperature was measured with a platinum resistance digital thermometer (Fluke, Model 2189A) to  $\pm 0.01$  K. A chart recorder (Hewlett Packard, Model 7100B) was used to record the temperature variation in the bath. When the chart recorder displayed a steady temperature for a period of 30 minutes the thermal equilibrium in the system was deemed to be established. At this time, the variation of the temperature in the bath was only  $\pm 0.01$ K.

### III. Experimental Techniques

#### A. Purification Methods

##### i) Water

Single distilled water was further purified in a Barnstead Nanopure II ion exchange device. The half-life of the solvated electrons after a 100 ns pulse of 340 fJ electrons (4 J/kg) at 298 K was  $> 10$   $\mu$ s.

##### ii) *t*-Butanol

The *t*-butanol was obtained from BDH (Assured grade, 98%), and later from Fluka ( $>99.7\%$ ). The purification method was similar to that in ref. 11a. *t*-Butanol was dried at 304 K for at least one week on Davison 3Å Molecular Sieves, then bubbled with UHP argon (99.999%, Liquid Carbonic Canada) and treated with sodium borohydride (2 g/L) under argon at 323 K for 24 hrs. Then the alcohol was fractionally distilled under argon through an 80 x 2.3 cm column packed with glass beads (6 mm). The first 20-

25% of the distillate was discarded; distillate was collected after there was no further reduction in optical absorption between 260 and 280 nm, which is due to carbonyl compounds (12). The middle 50% portion was collected and stored in a flask under argon positive pressure. The water content, measured by Karl-Fisher titration, was 0.05 mol %. The solvated electron half-life after a 100 ns pulse of 340 fJ (2.1 MeV) electrons (4J/kg) at 300 K was over 10  $\mu$ s.

iii) 1-Butyl amine

1-Butylamine (Fluka, >98%) was treated for 24 hours with potassium and sodium alloy under UHP argon (99.999%, Liquid Carbonic Canada Ltd.) at 330 K. Fractional distillation was the same as described above in the purification of *t*-butanol. The water content, measured by Karl-Fisher titration, was 0.09 mol %. The solvated electron half-life of pure 1-butylamine after a 100 ns pulse of 340 fJ (2.1 MeV) electrons (4 J/kg) at 298 K was about 4  $\mu$ s.

iv) Toluene

Toluene (HPLC grade, >99.8%) from Sigma-Aldrich was purified in the same way as described in the purification of 1-butyl amine above.

v) Other solutes were used as received.

## ***B. Sample Preparation***

New glassware, including the Spectrosil cells, were cleaned according to the following procedure. First they were rinsed with ethanol, and then some concentrated nitric acid was added and allowed to react with residual ethanol to generate heat. The acid was discarded and the cells were washed many times with distilled water. In early experiments they were then washed with dilute potassium hydroxide solution, but this step was found to be unnecessary, and was deleted. Finally the cells were rinsed many times with Nanopure water and dried at ~383 K in an oven.

*t*-Butanol/water and 1-butyl amine/water mixed solvents were prepared in a one L volumetric flask, by volume measurements at 298 K. Solid solutes were weighed into proper volumetric flasks on an analytical balance (the precision was 1 mg) and liquid solutes were measured by the volumetric pipettes. The solutes were then dissolved in the mixed solvent to get the stock solution. Sample solutions were made by diluting aliquots of stock solution, using volumetric pipettes. For the measurement of the rate constant of phenol in pure water, phenol was melted in the bottle by placing the bottle in warm water, then phenol was pipetted into a volumetric flask and Nanopure water was added. For the rest of the measurements of phenol reaction rate, phenol crystals were taken out of the bottle and placed in a watch glass, and then crystals of phenol without any color were scooped into a beaker to weigh. Then solvent was added, and the solution was transferred to a volumetric flask for final dilution. Four to six sample solutions with different concentrations were prepared for each solute.

### *C. Removal of Oxygen from Samples*

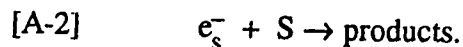
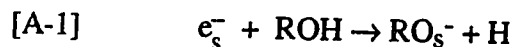
The sample solutions were poured into quartz optical cells, deaerated by bubbling with ultra high pure argon, and sealed before the measurements. The bubbling system (Figure A-1-5) was made by connecting 1 mL syringes to long Pyrex tubes. Pyrex/Teflon stopcocks (No. 72 Canadian Laboratory Supplies Ltd.) at the top of the syringes controlled the gas flow. Bubbling was done through long stainless steel needles (30 cm long, and 0.625 mm inner diameter) attached to the syringes. The rate of bubbling was  $\sim 17 \text{ cm}^3/\text{min}$ . The bubbling for *t*-butanol/water mixed solvent sample solutions was about 25 minutes, and for 1-butyl amine/water mixed solvent sample solutions was about 15 minutes. The sealing procedure is illustrated in Figure A-1-6. Step one took place at room temperature. The syringe needle was then withdrawn to just

above the liquid as shown in step two and the argon flow rate was increased. The area around the sealing position was heated by a low flame to flush the volatile substances from the glass wall. The syringe needle was then further withdrawn as illustrated in step three and the seal was made as rapidly as possible.

#### D. *Rate Constant Measurement*

##### 1. *Half-life and $k_{obs}$ Measurement*

The solvated electrons generated in the electrolyte solutions made from the alcohol/water mixed solvents can react with the solvent molecules (ROH) or the solvated ions (S) according to the following equations:



Both reactions are first-order since the concentration of the solvent and of the reactant ions are much larger than that of  $e_s^-$ . Therefore, the observed first-order rate constant from the  $e_s^-$  optical absorption decay curve is,

$$[A-3] \quad k_{obs} = k_1 + k_2 [S] \quad ,$$

where  $k_1$  is the first order rate constant of the reaction [A-1],  $k_2$  is the second order rate constant of reaction [A-2], and [S] is the concentration of the reactant ion.

Since the reaction of  $e_s^-$  with the solvent amine and water is negligible under our conditions (15), we only consider the following reactions:



where  $I_s$  represents residual impurities in the solvent and those produced by the radiation pulse, and  $S_s$  is an added solute. The observed first-order decay rate constant

$$[A-6] \quad k_{\text{obs}} = k_1[I] + k_2[S]$$

was measured for the pure solvent and six concentrations of solute S.

The optical absorption decay curve of the solvated electrons in each solution was measured at a wavelength which gave the optimal source intensity and  $e_s^-$  absorption signal. Figure A-1-7 shows an example of the decay curve of the solvated electrons in  $0.091 \text{ mol/m}^3$  of ammonium nitrate in 1-butanol/water mixed solvent, of 35 mol% water at 315.0K. The optical absorption decay half-life of the solvated electrons was computed as a function of time in each measurement, and recorded along with the optical absorption trace. The half-life was then obtained by measuring the vertical distance between the reference point ( the lower + mark in Figure A-1-7) and the half-life trace. A time-independent half-life horizontal trace corresponds to first-order decay. The decay curve of solvated electrons at the beginning of the decay was sometimes not first order. This initial fast decay could be due to the reaction of  $e_s^-$  inside the microzones (geminate reaction). Therefore, the beginning of the trace was ignored for the calculation of half-life in this case. From the half-life of the first-order decay  $k_{\text{obs}}$  can be calculated,

$$[A-7] \quad k_{\text{obs}} = \text{Ln } 2 / t_{1/2}$$

where  $t_{1/2}$  is the half-life of the first order decay. The  $k_{\text{obs}}$  value was calculated using an average of two to four half-lives from consecutive measurements for each sample.

## 2. $k_2$ and $E_2$ Measurements

The second order rate constant  $k_2$  obtained from the slope of the plot of the first order decay constants  $k_{\text{obs}}$  against solute concentration  $[S]$  (equation [A-3] and [A-6]).



The number of pulses per sample was 2 or 3 at each temperature, and the number of temperatures per sample was 4 or 5.

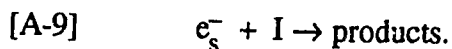
For most reactions, the linear plots of  $k_{\text{obs}}$  against the solute concentrations have positive intercepts at pure solvent. However, in the measurements of rate constants of the reactions of solvated electron with perchloric acid, negative intercepts were obtained in most compositions of *t*-butanol/water mixed solvents. This is because a small amount of acid, equivalent to about  $0.002 \text{ mol/m}^3$ , became absorbed on the wall of the quartz cell. This had been observed earlier (K.N. Jha, G.L. Bolton, and G.R. Freeman. *Can. J. Chem.* **50**, 3073 (1972)). In these cases the linear slopes were taken, ignoring the point for pure solvent.

The values of  $k_2$  obtained at different temperatures allowed the determination of reaction parameter such as activation energy  $E_2$ . It was derived from the plot of  $\text{Ln } k_2$  against the reciprocal of the absolute temperature:

$$[\text{A-8}] \quad \text{Ln } k_2 = \text{Ln } A_2 - E_2 / RT$$

### 3. *Effect of Impurities*

(a) Impurity in the Solvent: When the impurity originates in the solvent, the amount of the impurity at each solute concentration is the same.



where I stands for impurity. In this case, We have:

$$[\text{A-10}] \quad k_{\text{obs}} = k_1 + k_i[I] + k_2[S]$$

where [I] is the concentration of the impurity. The effect of the impurity appears in the intercept of the  $k_{\text{obs}}$  versus [S] plot and has no effect on  $k_2$  which is the slope. If  $k_i[\text{I}] \gg k_2[\text{S}]$  then all half-lives are the same regardless of different solute concentrations. This occurs when the solute is an inefficient electron scavenger and the impurity an efficient electron scavenger. Absence of efficient impurities was conformed by measuring the half-life of the pure solvent.

(b) **Impurity in the Solute:** When the impurity originates in the solute, the amount of impurity is a fraction  $p$  of the solute concentration [S].

$$[\text{A-11}] \quad k_{\text{obs}} = k_1 + (pk_i + k_s) [\text{S}] \quad ,$$

since  $p \leq 10^{-5}$  for lithium nitrate and ammonium nitrate;  $\leq 0.01$  for ammonium perchlorate, silver perchlorate, and lithium perchlorate; and  $\leq 0.02$  for copper(II) perchlorate and aluminum(III) perchlorate, so for a solute of efficient electron scavenger we have,

$$[\text{A-12}] \quad k_2 = pk_i + k_s \approx k_s \quad .$$

If the impurity was an efficient electron scavenger and the solute an inefficient electron scavenger, the value of  $pk_i$  could be similar to that of  $k_s$ , hence  $k_2 = pk_i + k_s$ .

## E. Optical Absorption Spectrum Measurement

### 1. Absorbance Measurement

In the measurements of the optical absorption spectra of  $e_s^-$  in 1-butyl amine/water mixed solvents, the decay traces (Fig.A-1-7) were measured at different

wavelengths ranging from 400 nm to 2300 nm. Absorbance can be calculated from the following formula:

$$[A-13] \quad A = \log\left(\frac{I_0}{I - I_t}\right)$$

where  $A$  is absorbance at time  $t$  after the beginning of the electron pulse,  $I_0$  is the incident analyzing light in volts and  $I_t$  is the absorbed light in volts at time  $t$ .

$$[A-14] \quad A/D = \frac{D_0}{D} \cdot \log\left(\frac{I_0}{I - I_t}\right)$$

where  $A/D$  is absorbance normalized to SEM dose reading,  $D_0/D$  is a dose normalization factor where  $D$  is the SEM dose and  $D_0$  is an average dose, usually chosen to be 1.0 nanocoulomb from the SEM. When the solvated electron lifetime was short, there was significant decay of the electrons during the pulse. This was particularly true in the 1-butyl amine/water mixture compositions from 30 to 50 mol% water at higher temperatures. A correction for the decay  $(A/D)_c$  was applied where necessary using:

$$[A-15] \quad (A/D)_c = (A/D)_{\text{obs}} \cdot \left(\frac{x}{1 - e^{-x}}\right) \quad ,$$

where  $(A/D)_{\text{obs}}$  is the observed normalized absorbance calculated from equation [A-14], and

$$[A-16] \quad x = \frac{\text{Ln}2 \cdot t_p}{t_{1/2}} \quad ,$$

where  $t_p$  is the pulse length in ns and  $t_{1/2}$  is the half-life of the decay in ns. In our experiments, we used 100 ns pulse and the difference before and after the correction is less than 4% when the half-life of the decay is longer than 1  $\mu$ s. Therefore, the correction was made only if the  $t_{1/2} < 1 \mu$ s.

## 2. *Dosimetry and Ge Value Calculation*

The dose received by a sample was calibrated and calculated from in situ actinometry. The routine actinometry used the optical absorption produced in oxygen-saturated 5 mM KSCN aqueous solution. The molar absorption,  $\epsilon$ , (molar extinction coefficient) used was 7500/M/cm for  $(\text{SCN})_2^-$  at 478 nm. The wavelength of maximum absorbance and the absorbance are independent of temperature from 293 to 332. All dosimetry was done at 298 K. It was assumed that  $G(\text{OH}) = 2.8$ , which is the number of OH radicals scavenged by  $\text{SCN}^-$  in the aqueous solution for each 100 eV of dose absorbed. Then the dose in eV/g was calculated from the absorbance measured from the optical decay curves by

$$[\text{A-17}] \quad D = \frac{A \cdot N}{\epsilon \cdot G(\text{OH}) \cdot b \cdot d \cdot 10} \text{ (eV/g)}$$

where A is absorbance from equation [A-13], N is Avogadro's number,  $\epsilon$  is molar absorptivity, b is optical path length, and d is the density of the solvent.

After the calibration of the dose received in a sample solution, the values of Ge can be calculated by substitution of A obtained from the decay curves, known density of the solvent, and fixed value of optical path length into equation [A-17].

## 3. *Optical Absorption Spectra and Parameters*

The values of Ge were plotted against the corresponding energies (zJ) to get the optical absorption spectrum of  $e_s^-$  in a solvent at a certain temperature (see Fig.6-1 and 6-4). Then the parameters  $GE_{A_{\text{max}}}$ ,  $E_{A_{\text{max}}}$ ,  $E_T$ ,  $E_b$ ,  $W_{1/2}$ ,  $W_T$  and  $W_b$  can be obtained from the spectrum. For each solvent composition the measurement of the spectrum was done at least at three different temperatures to get the temperature coefficient  $-\frac{dE_{A_{\text{max}}}}{dT}$ .

### F. *Electrical Conductivity Measurement*

Most of the time the conductance mode ( $G_p$ ) was used. The specific conductance ( $\Lambda_{\text{obs}}$ : S/m) was calculated from the following equation,

$$[\text{A-18}] \quad \Lambda_{\text{obs}} = C L \quad ,$$

where  $L$  is the conductance (in S: Siemen) and  $C$  is the cell constant ( $\text{m}^{-1}$ ). For conductances in the range:  $0.1 < L < 0.6$  mS, the bridge was set to one of the capacitance modes ( $C_p$ ) and the conductance was calculated from the capacitance data using the following equation,

$$[\text{A-19}] \quad L = \omega C_p D \quad ,$$

where  $\omega$  is the phase angular speed (radian/s) of the AC voltage,  $C_p$  is the capacitance (picofarad) and  $D$  is the dissipation factor. For conductances  $L < 0.1$  mS, the bridge was set to the other of the capacitance modes ( $C_s$ ) and the conductance was calculated from the capacitance data using the following equation,

$$[\text{A-20}] \quad L = \omega C_s D / (1 + D^2) \quad .$$

To test the detection limit of the apparatus, the dry cells were connected to the impedance bridge and the specific conductance was measured. The average dry cell's specific conductance was  $1.2 \mu\text{S/m}$ , which indicated a lower limit for the electrical conductivity measurement. The specific conductance of pure water used was controlled to be  $\leq 0.1$  mS/m and those of pure *iso*-butanol or 1-butanol were  $\leq 3.0 \mu\text{S/m}$  at 298K. The specific conductance of the mixed solvent varied as a function of composition (see Figure 5-1 to 5-3). The molar conductance ( $\Lambda$ ) was obtained from the plot of specific conductance against solute concentration. The activation energies of the conductivities ( $E_\Lambda$ ) were obtained from the plots of the  $\text{Ln } \Lambda$  against the reciprocal of the absolute temperature.

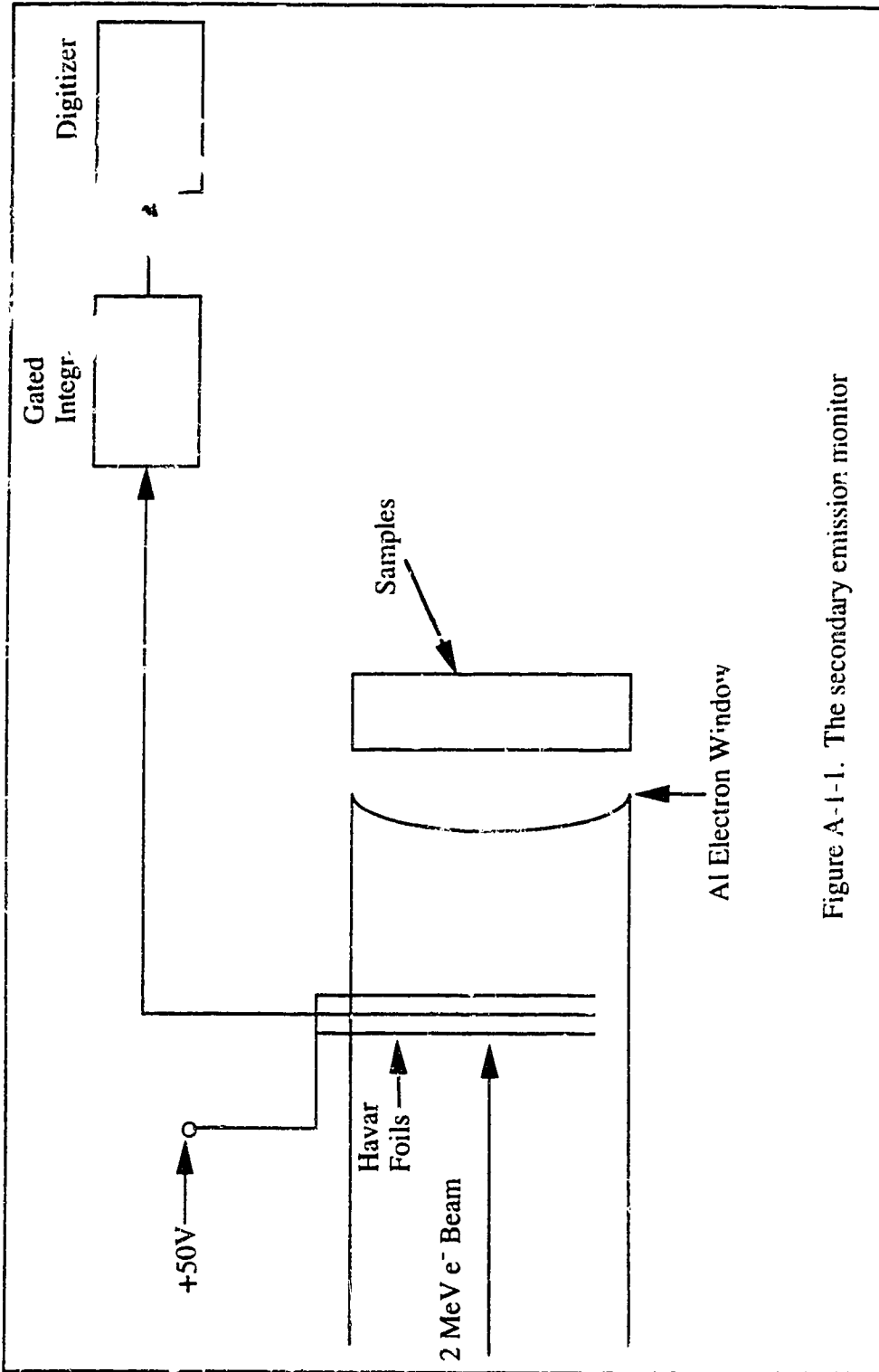


Figure A-1-1. The secondary emission monitor

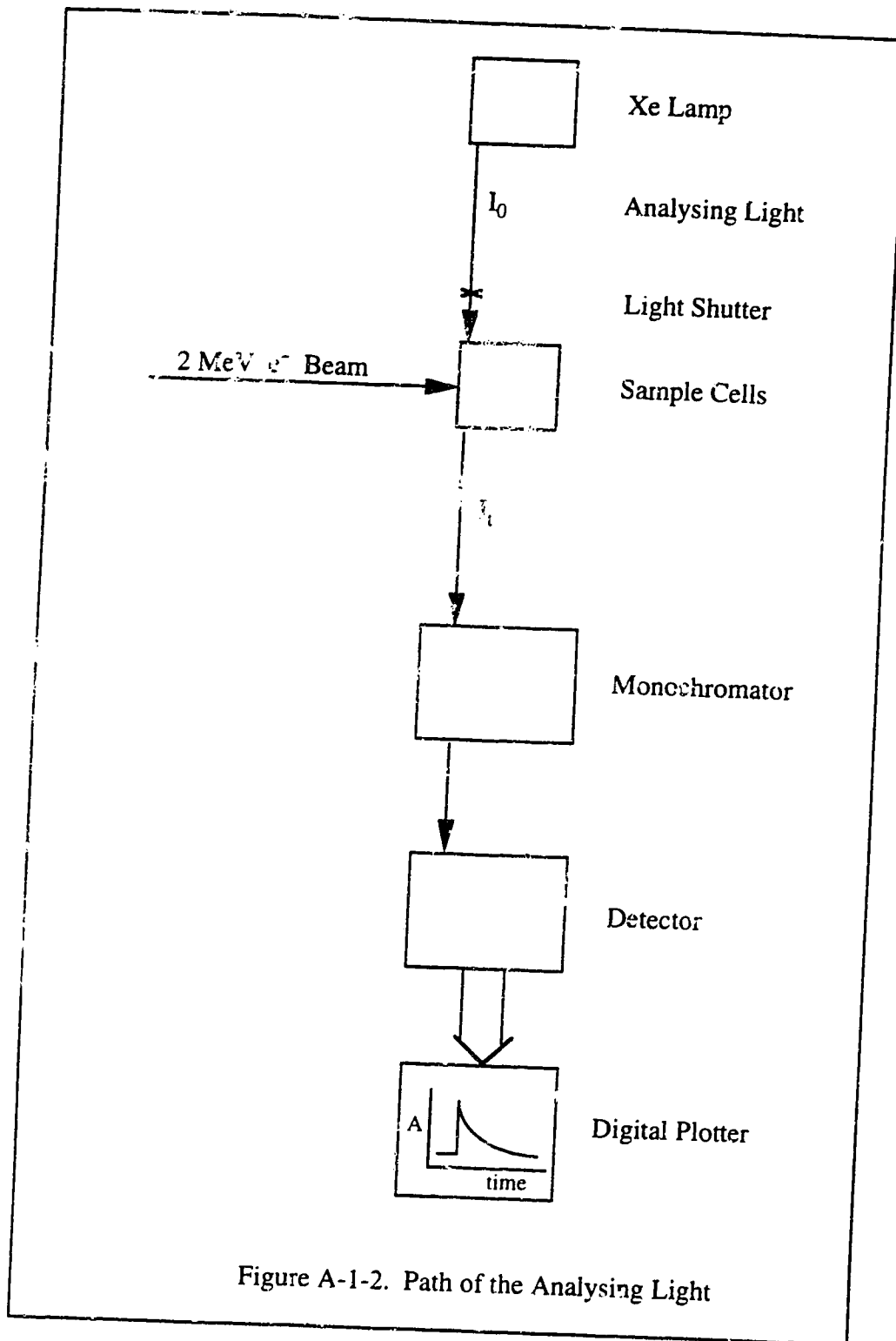


Figure A-1-2. Path of the Analysing Light

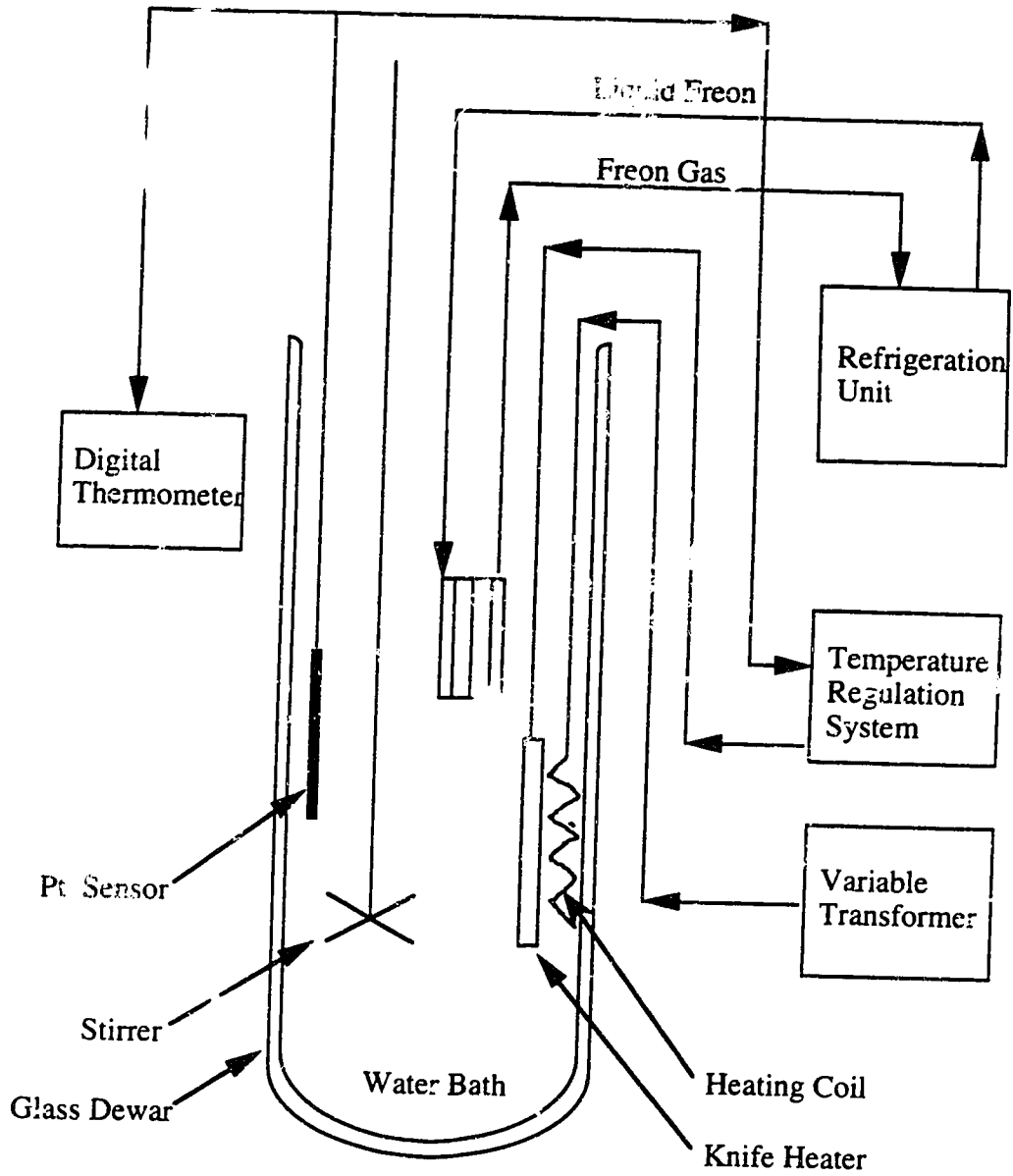


Figure A-1-3. Temperature Control of the Water Bath



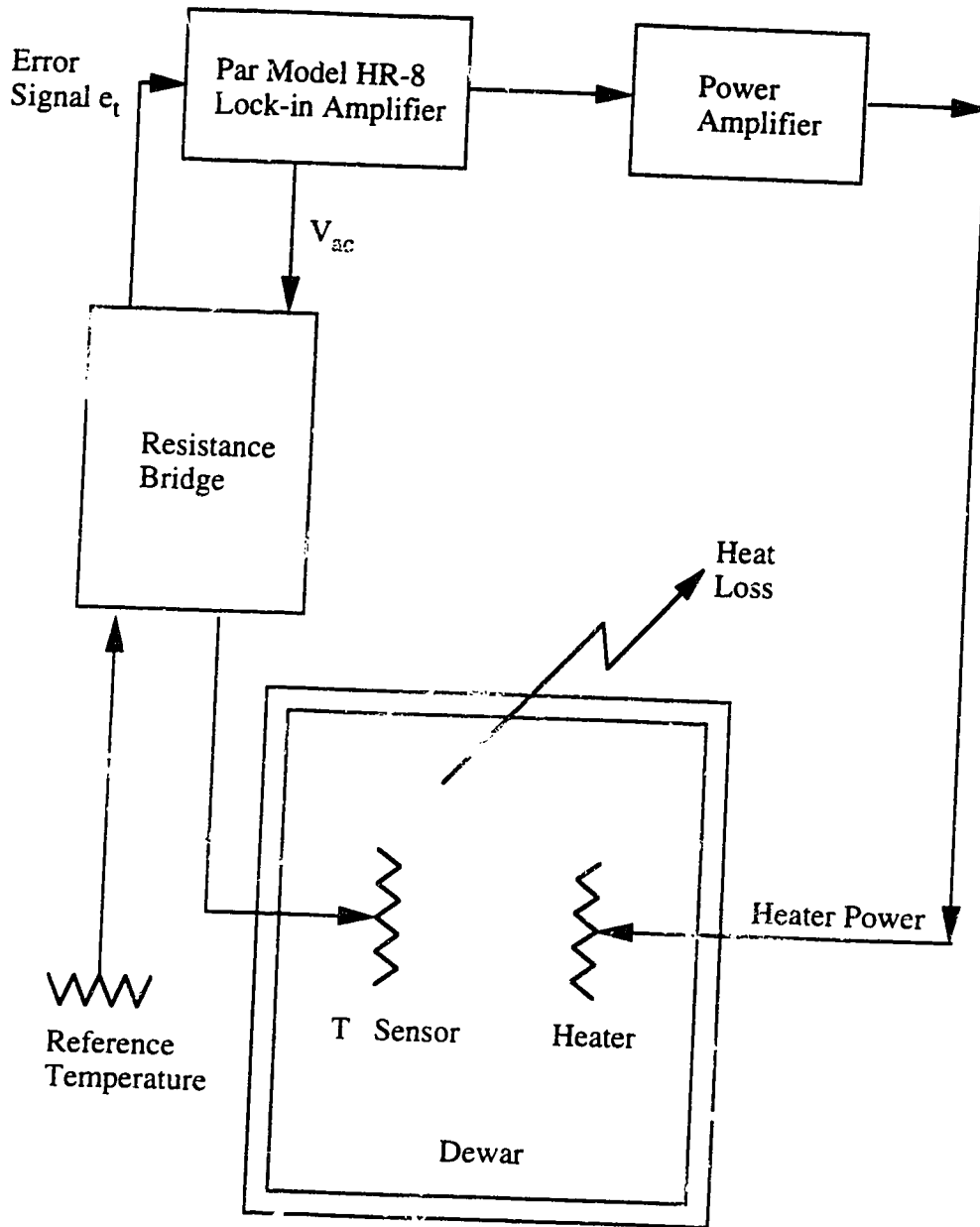


Figure A-1-4. The Temperature Regulation System

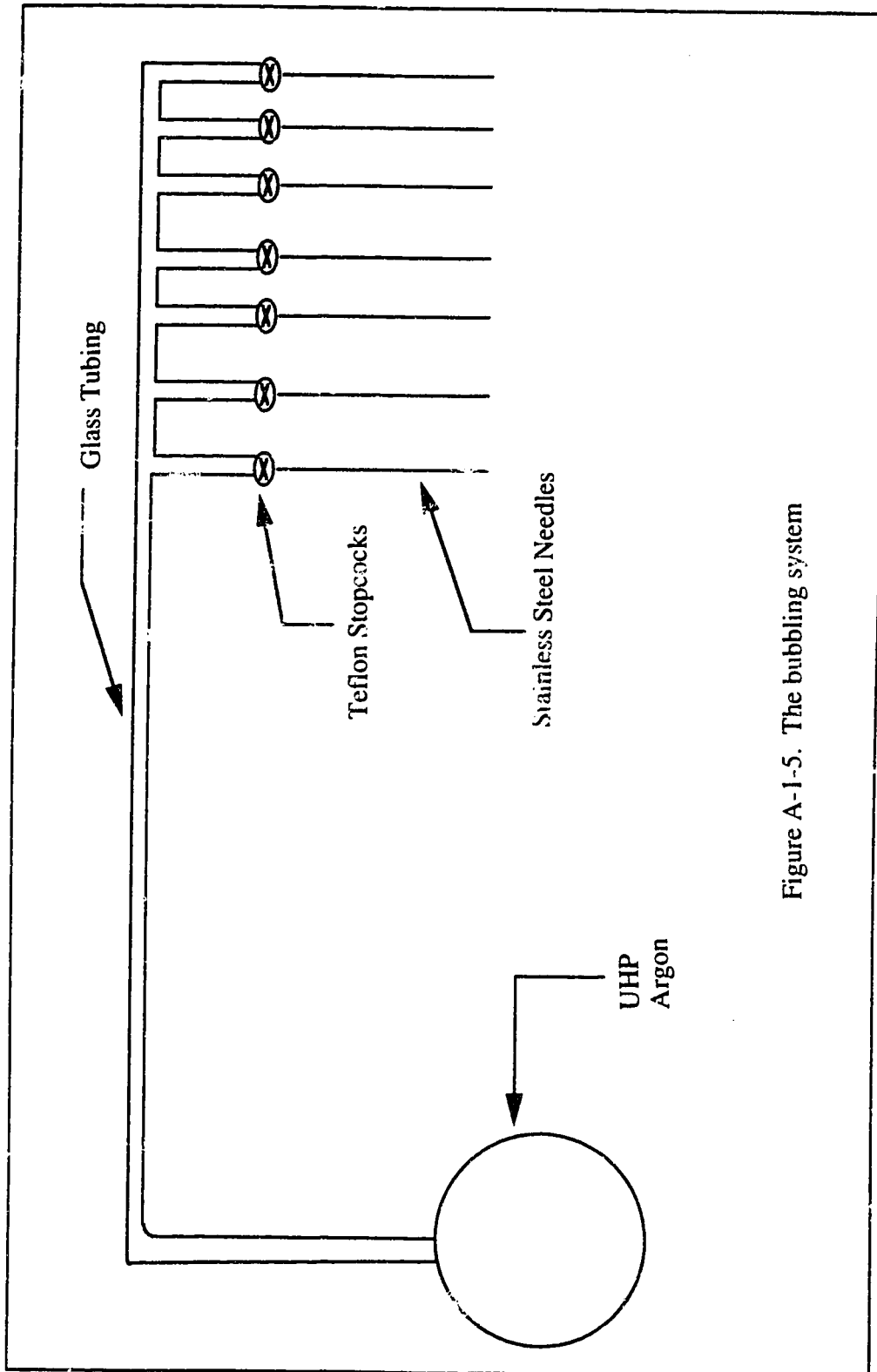


Figure A-1-5. The bubbling system

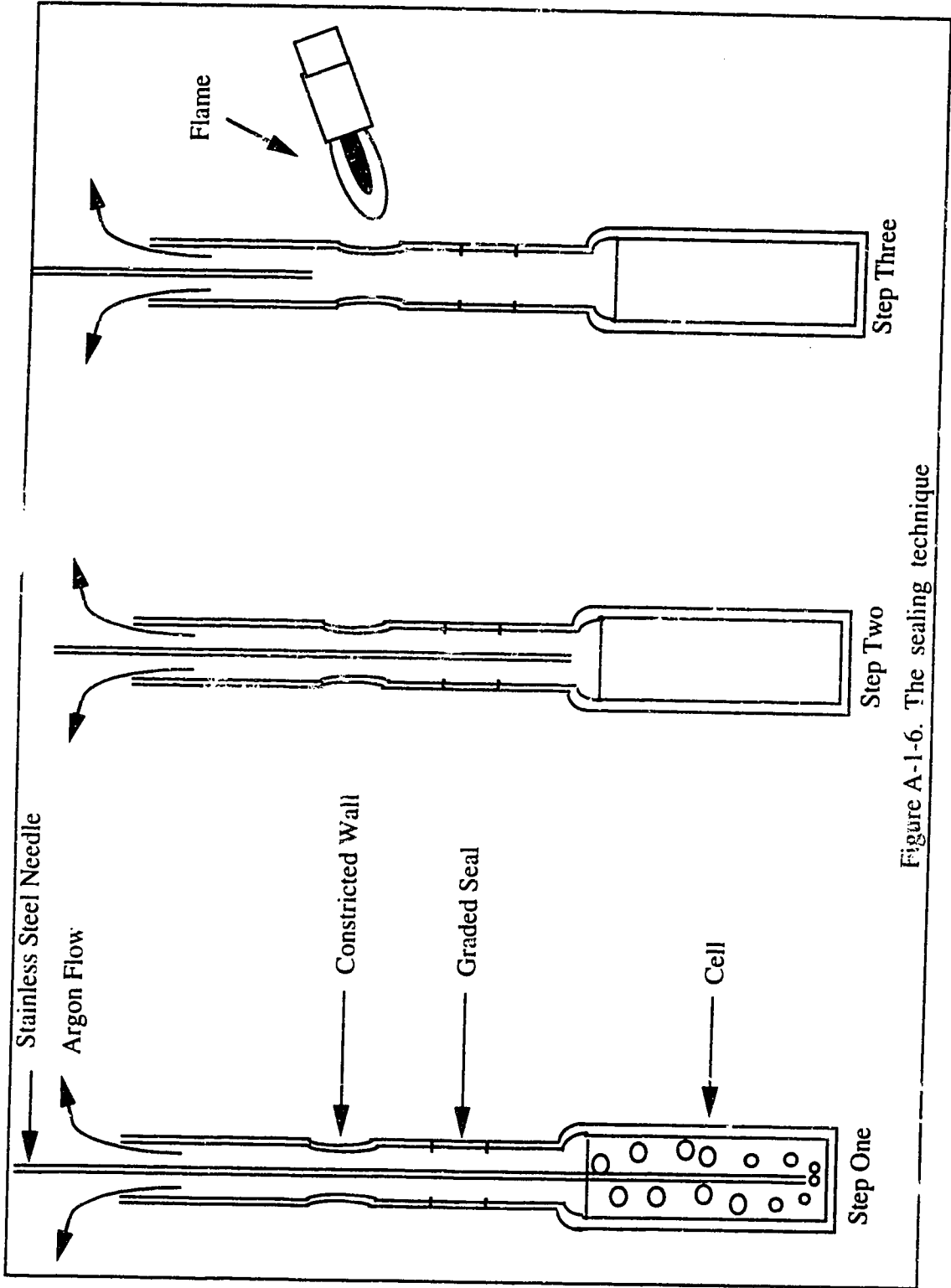


Figure A-1-6. The sealing technique

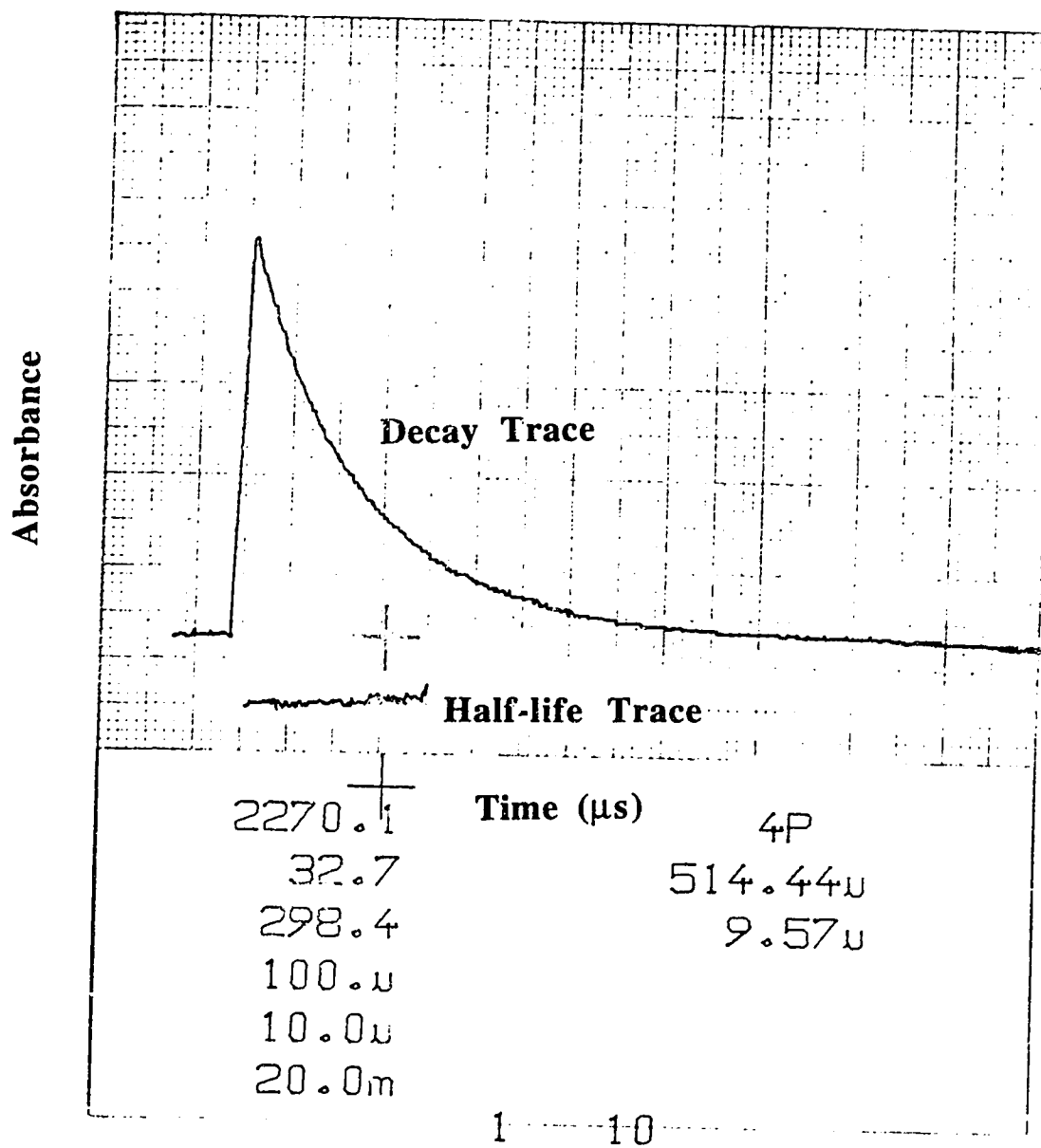


Figure A-1-7. The typical solvated electron optical absorption decay trace

## Appendix Two

### Experimental Results

In this part, we report the experimental results of:

- i) the reactions of solvated electrons with lithium nitrate, ammonium nitrate, ammonium perchlorate and perchloric acid in *t*-butanol/water mixtures;
- ii) the reactions of solvated electrons with nitrobenzene, acetone, phenol and toluene in 1-butylamine/water mixtures;
- iii) the electrical conductivity measurements of lithium nitrate, ammonium nitrate, ammonium perchlorate, perchloric acid and lithium perchlorate in *t*-butanol/water mixtures;
- iv) the optical absorption spectra of solvated electrons in 1-butylamine/water mixtures.

#### 1. Results of The Rate Constant Measurements in *t*-Butanol/water mixtures

The rate constant measurements for the reactions of solvated electrons with lithium nitrate, ammonium nitrate, ammonium perchlorate and perchloric acid in *t*-butanol/water mixtures were carried out in the following compositions in mol% water: 0.0, 5.0, 10.0, 30.0, 50.0, 70.0, 90.0, 97.0, and 100.0. The units of the concentration of salts, the first order rate constant ( $k_{\text{obs}}$ ) and the second order rate constant ( $k_2$ ) are indicated in the tables.

Table A-2-1. The values of  $k_{\text{obs}}$  of the reactions of solvated electrons with ammonium nitrate in *t*-butanol/water mixed solvent.

Composition: Water

C (Salt) ( $10^{-2}$ mol/m <sup>3</sup> )	$k_{\text{obs}}$ ( $10^6$ s <sup>-1</sup> )				
	284.5 K	299.4 K	313.9 K	327.2 K	343.8 K
0.00	0.05	0.06	0.08	0.11	0.13
2.00	0.20	0.28	0.38	0.47	0.63
4.00	0.34	0.53	0.65	0.81	1.08
6.00	0.44	0.67	0.88	1.14	1.44
8.00	0.61	0.89	1.14	1.52	1.86
10.0	0.72	1.08	1.44	1.78	2.35
12.0	0.84	1.28	1.65	2.23	2.77

Composition: 97 mol% Water

C (Salt) ( $10^{-2}$ mol/m <sup>3</sup> )	$k_{\text{obs}}$ ( $10^6$ s <sup>-1</sup> )				
	285.0 K	298.3 K	312.6 K	328.2 K	342.9 K
0.00	0.03	0.05	0.04	0.07	0.08
2.00	0.12	0.17	0.24	0.34	0.42
4.00	0.19	0.30	0.40	0.52	0.71
6.00	0.26	0.40	0.54	0.79	1.01
8.00	0.35	0.55	0.75	1.04	1.26
10.0	0.42	0.65	0.89	1.22	1.57
12.0	0.50	0.79	1.08	1.43	1.88

Composition: 90 mol% Water

C (Salt) ( $10^{-2}$ mol/m <sup>3</sup> )	$k_{\text{obs}}$ ( $10^6$ s <sup>-1</sup> )				
	283.4 K	298.8 K	313.8 K	328.4 K	342.0 K
0.00	0.02	0.03	0.04	0.07	0.08
2.00	0.06	0.11	0.18	0.24	0.32
4.00	0.09	0.18	0.28	0.36	0.50
6.00	0.13	0.25	0.38	0.53	0.70
8.00		0.32	0.51	0.70	0.90
10.0	0.21	0.40	0.58	0.85	1.07
12.0	0.26	0.49	0.69	1.05	1.35

Table A-2-1 continued

Composition: 70 mol% Water

C (Salt) ( $10^{-2}$ mol/m <sup>3</sup> )	$k_{\text{obs}}$ ( $10^6$ s <sup>-1</sup> )				
	283.2 K	298.4 K	313.9 K	328.5 K	343.0 K
0.00	0.03	0.03	0.06	0.07	0.10
4.00	0.05	0.08	0.15	0.22	0.30
8.00	0.09	0.15	0.28	0.36	0.56
12.0	0.11	0.19	0.33	0.52	0.75
16.0		0.27	0.49	0.75	0.97
20.0	0.17	0.35	0.56	0.89	1.26
24.0	0.24	0.46	0.73	1.13	1.50

Composition: 50 mol% Water

C (Salt) ( $10^{-2}$ mol/m <sup>3</sup> )	$k_{\text{obs}}$ ( $10^6$ s <sup>-1</sup> )				
	288.5 K	298.4 K	313.8 K	328.3 K	342.9 K
0.00	0.017	0.02	0.05	0.08	0.08
2.00		0.17	0.30	0.49	0.80
4.00	0.18	0.33	0.59	1.04	1.66
6.00	0.27	0.44	0.82	1.35	2.15
8.00	0.35	0.58	1.01	1.82	2.77
10.0	0.48	0.78	1.39	2.34	3.69
12.0	0.56	0.95	1.60	2.83	4.39

Composition: 30 mol% Water

C (Salt) ( $10^{-2}$ mol/m <sup>3</sup> )	$k_{\text{obs}}$ ( $10^6$ s <sup>-1</sup> )				
	289.6 K	298.8 K	313.9 K	328.4 K	342.9 K
0.00		0.04	0.06	0.12	0.18
1.00	0.12	0.18	0.33	0.51	0.74
2.00	0.18	0.28	0.52	0.81	1.12
3.00	0.23	0.35	0.69	1.08	1.61
4.00		0.52	0.94	1.48	2.17
5.00	0.44	0.66	1.10	1.93	2.67
6.00	0.54	0.77	1.36	2.35	3.38

Table A-2-1 continued

Composition: 10 mol% Water

C (Salt) ( $10^{-2}$ mol/m <sup>3</sup> )	$k_{\text{obs}}$ ( $10^6$ s <sup>-1</sup> )				
	288.5 K	298.4 K	313.8 K	328.3 K	342.9 K
0.00	0.04	0.06	0.11	0.15	0.24
1.00	0.07	0.11	0.18	0.27	0.37
2.00	0.12	0.18	0.29	0.45	0.57
3.00	0.16	0.23	0.40	0.64	0.81
4.00	0.19	0.30	0.48	0.72	0.98
5.00	0.24	0.36	0.61	0.94	1.24
6.00	0.27	0.40	0.70	1.08	1.43

Composition: 5 mol% Water

C (Salt) ( $10^{-2}$ mol/m <sup>3</sup> )	$k_{\text{obs}}$ ( $10^6$ s <sup>-1</sup> )				
	298.6 K	309.2 K	321.0 K	331.1 K	342.8 K
0.00	0.09	0.07	0.14	0.17	0.28
0.75	0.10	0.14	0.21	0.28	0.42
1.50	0.15	0.20	0.31	0.43	0.61
2.25	0.19	0.28	0.41	0.53	0.79
3.00	0.22	0.35	0.47	0.65	0.90
3.75	0.28	0.40	0.58	0.81	1.10
4.50	0.33	0.49	0.66	0.92	1.29

Composition: *t*-Butanol

C (Salt) ( $10^{-2}$ mol/m <sup>3</sup> )	$k_{\text{obs}}$ ( $10^6$ s <sup>-1</sup> )				
	298.7 K	308.5 K	318.8 K	328.4 K	342.0 K
0.00	0.05	0.09	0.15	0.30	0.49
1.00	0.07	0.13	0.19	0.38	0.84
2.00	0.10	0.17	0.31	0.51	1.01
3.00	0.13	0.20	0.36	0.60	1.28
4.00	0.14	0.22	0.44	0.72	1.51
5.00	0.16	0.29	0.51	0.87	1.82
6.00	0.20	0.35	0.61	1.08	2.17



Table A-2-2. Temperature and composition dependences of  $k_2$  for the reaction of  $e_s^-$  with ammonium nitrate in *t*-butanol/water mixed solvents.

Water mol%	T (K)	$k_2$ ( $10^6 \text{ m}^3/\text{mol}\cdot\text{s}$ )	Water mol%	T (K)	$k_2$ ( $10^6 \text{ m}^3/\text{mol}\cdot\text{s}$ )
100	284.5	6.9	30	289.6	8.0
	299.4	10.		298.8	12.
	313.9	14.		313.9	21.
	327.8	17.		328.4	35.
	343.8	21.		342.9	51.
97	283.0	4.0	10	288.5	4.2
	298.3	6.2		298.4	6.4
	312.6	8.6		313.8	11.
	328.2	12.		328.3	17.
	343.9	15		342.9	22.
90	283.4	2.0	5	298.6	6.4
	298.8	3.6		309.2	9.2
	313.8	5.5		321.0	13.
	328.4	8.2		331.1	17.
	342.0	11.		342.8	24.
70	283.1	0.83	0	298.7	12.
	298.4	1.6		308.5	19.
	313.9	2.8		318.8	32.
	328.3	4.4		328.4	54.
	343.0	6.1		342.0	101.
50	288.5	4.8			
	298.4	7.5			
	313.8	13.			
	328.3	24.			
	342.9	36.			

Table A-2-3. The values of  $k_{\text{obs}}$  of the reactions of solvated electrons with lithium nitrate in *t*-butanol/water mixed solvent.

Composition: Water

C (Salt) ( $10^{-2}$ mol/m <sup>3</sup> )	$k_{\text{obs}}$ ( $10^6$ s <sup>-1</sup> )				
	283.1 K	298.7 K	313.8 K	328.4 K	344.0 K
0.00	0.18	0.23	0.31	0.41	0.49
2.00	0.27	0.36	0.44	0.61	0.74
4.00	0.33	0.47	0.59	0.81	0.98
6.00	0.49	0.67	0.86	1.13	1.48
8.00	0.53	0.92	1.20	1.50	1.81
10.0	0.75	1.20	1.51	1.87	2.25
12.0	0.87	1.35	1.72	2.21	2.74

Composition: 90 mol% Water

C (Salt) ( $10^{-2}$ mol/m <sup>3</sup> )	$k_{\text{obs}}$ ( $10^6$ s <sup>-1</sup> )				
	283.2 K	298.1 K	313.3 K	327.8 K	343.3 K
0.00	0.04	0.05	0.07	0.11	0.14
2.00	0.11	0.18	0.25	0.33	0.44
4.00	0.19	0.30	0.40	0.55	0.76
6.00	0.27	0.40	0.54	0.74	0.97
8.00	0.34	0.54	0.74	0.97	1.29
10.0	0.45	0.73	1.06	1.31	1.73
12.0	0.50	0.82	1.14	1.46	2.05

Composition: 90 mol% Water

C (Salt) ( $10^{-2}$ mol/m <sup>3</sup> )	$k_{\text{obs}}$ ( $10^6$ s <sup>-1</sup> )					
	282.8 K	290.7 K	298.0 K	313.4 K	328.0 K	343.5 K
0.00	0.03	0.05	0.05	0.07	0.10	0.14
2.00	0.06	0.09	0.10	0.16	0.21	0.29
4.00	0.10	0.13	0.17	0.28	0.37	0.49
6.00	0.12	0.17	0.21	0.34	0.48	0.62
8.00	0.15	0.22	0.27	0.46	0.64	0.81
10.0	0.20	0.27	0.34	0.56	0.78	0.99
12.0	0.25	0.33	0.41	0.65	0.93	1.22

Table A-2-3 continued

Composition: 70 mol% Water

C (Salt) ( $10^{-2}$ mol/m <sup>3</sup> )	$k_{\text{obs}}$ ( $10^6$ s <sup>-1</sup> )					
	282.8 K	290.7 K	298.1 K	313.5 K	333.9 K	348.4 K
0.00	0.03	0.04	0.04	0.07	0.10	0.14
4.00	0.05	0.07	0.10	0.14	0.21	0.28
8.00	0.07	0.10	0.12	0.22	0.34	0.43
12.0	0.10	0.14	0.20	0.33	0.50	0.63
16.0	0.09	0.16	0.24	0.37	0.60	0.79
20.0	0.15	0.22	0.30	0.46	0.75	0.95
24.0	0.19	0.24	0.36	0.58	0.88	1.16

Composition: 50 mol% Water

C (Salt) ( $10^{-2}$ mol/m <sup>3</sup> )	$k_{\text{obs}}$ ( $10^6$ s <sup>-1</sup> )				
	282.8 K	298.3 K	313.6 K	328.3 K	344.1 K
0.00	0.03	0.06	0.09	0.12	0.20
7.00	0.03	0.07	0.10	0.14	0.22
14.0	0.05	0.09	0.17	0.23	0.36
21.0	0.08	0.17	0.27	0.41	0.56
28.0	0.13	0.21	0.42	0.63	0.91
35.0	0.15	0.27	0.50	0.80	1.12
42.0	0.17	0.33	0.59	0.96	1.37

Composition: 30 mol% Water

C (Salt) ( $10^{-2}$ mol/m <sup>3</sup> )	$k_{\text{obs}}$ ( $10^6$ s <sup>-1</sup> )				
	285.2 K	298.3 K	312.6 K	328.2 K	343.8 K
0.00	0.01	0.03	0.04	0.08	0.10
7.00	0.06	0.07	0.13	0.25	0.38
14.0	0.06	0.12	0.24	0.40	0.66
21.0	0.11	0.21	0.40	0.70	1.08
28.0	0.29	0.29	0.53	0.84	1.41
35.0	0.27	0.40	0.69	1.13	1.79
42.0	0.22	0.46	0.79	1.40	2.18

Table A-2-3 continued

Composition: 10 mol% Water

C (Salt) (10 <sup>-2</sup> mol/m <sup>3</sup> )	k <sub>obs</sub> (10 <sup>6</sup> s <sup>-1</sup> )				
	289.6 K	298.7 K	313.7 K	328.1 K	342.6 K
0.00	0.03	0.04	0.07	0.11	0.14
7.00	0.07	0.11	0.22	0.35	0.58
14.0	0.12	0.20	0.38	0.62	0.84
21.0	0.16	0.28	0.51	0.80	1.24
28.0		0.37	0.70	1.08	1.61
35.0		0.43	0.80	1.37	2.17
42.0	0.32	0.52	0.95	1.55	2.54

Composition: 5 mol% Water

C (Salt) (10 <sup>-2</sup> mol/m <sup>3</sup> )	k <sub>obs</sub> (10 <sup>6</sup> s <sup>-1</sup> )				
	298.6 K	308.5 K	319.3 K	330.2 K	342.8 K
0.00	0.03	0.04	0.07	0.10	0.21
7.00	0.12	0.21	0.35	0.54	0.92
10.5	0.19	0.30	0.50	0.70	1.25
14.0	0.29	0.44	0.68	1.10	1.48
17.5	0.29	0.50	0.71	1.13	2.04
21.0	0.33	0.54	0.87	1.35	2.22

Composition: *t*-Butanol

C (Salt) (10 <sup>-2</sup> mol/m <sup>3</sup> )	k <sub>obs</sub> (10 <sup>6</sup> s <sup>-1</sup> )				
	298.3 K	308.3 K	318.3 K	328.2 K	338.4 K
0.00	0.06	0.12	0.25	0.42	0.63
1.50	0.11	0.20	0.39	0.63	1.16
3.00	0.16	0.29	0.61	0.92	1.94
4.50	0.22	0.39	0.75	1.32	2.15
6.00	0.25	0.49	0.87	1.63	2.80
7.50	0.39	0.65	1.23	1.98	3.56
9.00	0.36	0.69	1.34	2.37	4.36

Table A-2-4. Temperature and composition dependences of  $k_2$  for the reaction of  $e_s^-$  with lithium nitrate in *t*-butanol/water mixed solvents.

Water mol%	T (K)	$k_2$ ( $10^6$ m <sup>3</sup> /mol·s)	Water mol%	T (K)	$k_2$ ( $10^6$ m <sup>3</sup> /mol·s)
100	283.5	6.2	30	285.2	0.50
	298.9	9.7		298.3	1.1
	314.2	13.		312.6	1.8
	328.9	16.		328.2	3.1
	343.4	19.		343.8	5.1
97	283.2	3.7	10	289.6	0.69
	298.1	6.4		298.7	1.1
	313.3	8.8		313.7	2.2
	327.8	11.		328.1	3.6
	343.3	15.		342.6	5.8
90	282.8	1.9	5	298.6	1.6
	290.7	2.5		308.5	2.8
	298.0	3.2		319.3	4.0
	313.4	5.0		330.2	6.1
	328.0	7.4		342.8	9.9
	343.5	11.			
70	282.8	0.73	0	298.3	3.1
	290.7	0.96		308.3	6.5
	298.1	1.3		318.3	13.
	313.5	2.1		328.3	22.
	333.9	3.5		338.4	41.
	348.4	4.3			
50	282.8	0.38			
	298.3	0.79			
	313.6	1.4			
	328.3	2.3			
	344.1	3.2			

Table A-2-5. The values of  $k_{\text{obs}}$  of the reactions of solvated electrons with perchloric acid in *t*-butanol/water mixed solvent.

Composition: Water

C (Acid) ( $10^{-2}$ mol/m <sup>3</sup> )	$k_{\text{obs}}$ ( $10^6$ s <sup>-1</sup> )				
	285.3 K	298.4 K	313.2 K	328.2 K	342.2 K
0.00	0.02	0.03	0.04	0.06	0.09
0.50	0.08	0.10	0.12	0.16	0.20
1.00	0.17	0.24	0.32	0.37	0.48
1.50	0.31	0.37	0.48	0.57	0.69
2.00	0.38	0.49	0.63	0.77	0.89
2.50	0.56	0.68	0.81	1.04	1.18
3.00	0.67	0.80	1.00	1.28	1.44

Composition: 97 mol% Water

C (Acid) ( $10^{-2}$ mol/m <sup>3</sup> )	$k_{\text{obs}}$ ( $10^6$ s <sup>-1</sup> )				
	284.0 K	299.1 K	313.6 K	328.1 K	342.6 K
0.00	0.01	0.02	0.03	0.04	0.05
0.20	0.05	0.08	0.10	0.12	0.14
0.40	0.09	0.13	0.19	0.23	0.27
0.60	0.21	0.29	0.36	0.45	0.55
0.80	0.24	0.30	0.39	0.49	0.60
1.00	0.31	0.40	0.51	0.65	0.76
1.20	0.37	0.47	0.61	0.74	0.91

Composition: 90 mol% Water

C (Acid) ( $10^{-2}$ mol/m <sup>3</sup> )	$k_{\text{obs}}$ ( $10^6$ s <sup>-1</sup> )				
	288.7 K	298.8 K	313.3 K	327.9 K	342.9 K
0.00	0.02	0.02	0.05	0.06	0.07
0.30		0.08	0.11	0.16	0.19
0.60	0.17	0.17	0.26	0.33	0.41
0.90	0.22	0.31	0.42	0.54	0.69
1.20	0.30	0.39	0.55	0.70	0.94
1.50	0.39	0.50	0.72	0.92	1.20
1.80	0.47	0.63	0.87	1.13	1.42

Table A-2-5 continued

Composition: 70 mol% Water

C (Acid) ( $10^{-2}$ mol/m <sup>3</sup> )	$k_{\text{obs}}$ ( $10^6$ s <sup>-1</sup> )				
	289.8 K	298.8 K	313.3 K	327.9 K	342.6 K
0.00	0.02	0.03	0.04	0.06	0.07
0.15		0.08	0.12	0.16	0.21
0.30	0.08	0.13	0.19	0.28	0.38
0.45	0.14	0.21	0.34	0.48	0.66
0.60	0.18	0.28	0.44	0.64	0.87
0.75	0.31	0.37	0.56	0.80	1.07
0.90	0.29	0.42	0.67	0.95	1.31

Composition: 50 mol% Water

C (Acid) ( $10^{-2}$ mol/m <sup>3</sup> )	$k_{\text{obs}}$ ( $10^6$ s <sup>-1</sup> )				
	287.5 K	299.2 K	313.9 K	328.4 K	343.0 K
0.00	0.02	0.03	0.05	0.05	0.08
0.20	0.02	0.04	0.08	0.11	0.14
0.40	0.05	0.08	0.14	0.24	0.37
0.60	0.10	0.16	0.30	0.46	0.67
0.80	0.17	0.28	0.44	0.69	1.01
1.00	0.21	0.36	0.61	0.94	1.36
1.20	0.35	0.64	1.02	1.61	2.52

Composition: 30 mol% Water

C (Acid) ( $10^{-2}$ mol/m <sup>3</sup> )	$k_{\text{obs}}$ ( $10^6$ s <sup>-1</sup> )				
	289.0 K	298.8 K	313.3 K	327.9 K	342.4 K
0.00	0.01	0.03	0.04	0.06	0.09
0.10	0.04	0.06	0.13	0.17	0.30
0.20		0.10	0.19	0.29	0.43
0.30	0.07	0.12	0.23	0.35	0.49
0.40	0.08	0.15	0.29	0.46	0.67
0.60	0.12	0.21	0.36	0.56	0.90

Table A-2-5 continued

Composition: 10 mol% Water

C (Acid) ( $10^{-2}$ mol/m <sup>3</sup> )	$k_{\text{obs}}$ ( $10^6$ s <sup>-1</sup> )				
	289.9 K	308.6 K	318.9 K	329.0 K	342.8 K
0.00	0.09	0.15	0.22	0.32	0.44
0.20	0.12	0.18	0.30	0.43	0.56
0.40	0.17	0.26	0.41	0.56	0.81
0.60	0.21	0.32	0.49	0.70	0.00
0.80	0.27	0.40	0.63	0.83	1.22
1.00	0.32	0.49	0.72	0.99	1.39
1.20	0.35	0.56	0.86	1.17	1.58

Composition: 5 mol% Water

C (Acid) ( $10^{-2}$ mol/m <sup>3</sup> )	$k_{\text{obs}}$ ( $10^6$ s <sup>-1</sup> )				
	299.0 K	308.5 K	319.2 K	328.6 K	342.4 K
0.00	0.05	0.06	0.10	0.13	0.21
0.20	0.07	0.10	0.16	0.24	0.45
0.40	0.09	0.13	0.21	0.32	0.54
0.60	0.12	0.17	0.32	0.50	0.80
0.80	0.16	0.27	0.43	0.68	1.08
1.00	0.21	0.36	0.55	0.81	1.36
1.20	0.25	0.41	0.66	0.98	1.58

Composition: *t*-Butanol

C (Acid) ( $10^{-2}$ mol/m <sup>3</sup> )	$k_{\text{obs}}$ ( $10^6$ s <sup>-1</sup> )			
	299.5 K	308.7 K	318.9 K	330.0 K
0.00	0.06	0.09	0.16	0.39
0.10	0.12	0.13	0.30	0.46
0.20	0.13	0.20	0.35	0.67
0.30	0.16	0.27	0.46	0.83
0.40	0.19	0.35	0.67	1.14
0.50	0.24	0.43	0.85	1.48
0.60	0.31	0.50	1.01	1.74



Table A-2-6. Temperature and composition dependences of  $k_2$  for the reaction of  $e_s^-$  with perchloric acid in *t*-butanol/water mixed solvents.

Water mol%	T (K)	$k_2$ ( $10^7$ m <sup>3</sup> /mol·s)	Water mol%	T (K)	$k_2$ ( $10^7$ m <sup>3</sup> /mol·s)
100	285.3	2.4	30	289.0	1.7
	298.4	2.8		298.8	2.9
	313.2	3.5		313.3	5.1
	328.2	4.3		327.9	8.4
	342.2	5.0		342.4	13.
97	284.0	2.2	10	298.9	2.2
	299.1	3.7		308.6	3.4
	313.6	4.7		318.9	5.2
	328.1	6.3		329.0	7.5
	342.6	7.7		342.8	11.
90	288.7	2.8	5	299.0	2.2
	298.8	3.8		308.5	3.7
	313.3	5.3		319.2	5.9
	327.9	6.9		328.6	8.7
	342.9	8.8		342.4	14.
70	289.8	3.0	0	299.5	4.7
	298.8	4.4		308.7	8.2
	313.3	7.3		318.9	17.
	327.9	11.		330.0	30.
	342.6	15.			
50	287.5	2.5			
	299.3	4.1			
	313.9	6.8			
	328.4	11.			
	343.0	15.			

Table A-2-7. The values of  $k_{\text{obs}}$  of the reactions of solvated electrons with ammonium perchlorate in *t*-butanol/water mixed solvent.

Composition: Water

C (Salt) ( $10^{-2}$ mol/m <sup>3</sup> )	$k_{\text{obs}}$ ( $10^5$ s <sup>-1</sup> )				
	286.4 K	298.6 K	313.3 K	327.9 K	342.6 K
0.00	0.50	0.70	0.98	1.28	1.49
500	0.75	1.10	1.51	2.18	3.57
1000	0.99	1.42	2.04	3.15	5.06
1500	1.06	1.59	2.37	3.83	6.30
2000	1.22	1.88	2.89	4.47	7.45
2500	1.28	2.03	3.27	5.25	8.15
3000	1.37	2.21	3.59	5.82	8.80

Composition: 97 mol% Water

C (Salt) ( $10^{-2}$ mol/m <sup>3</sup> )	$k_{\text{obs}}$ ( $10^5$ s <sup>-1</sup> )				
	285.4 K	298.6 K	313.3 K	328.0 K	342.2 K
0.00	0.32	0.48	0.67	0.94	1.22
150	0.42	0.71	1.21	1.90	3.18
300	0.50	0.87	1.40	2.37	3.94
450	0.60	1.03	1.69	3.07	4.95
600	0.73	1.22	2.07	3.36	5.68
750	0.68	1.32	2.27	3.77	6.48
900	0.82	1.46	2.64	4.33	7.45

Composition: 90 mol% Water

C (Salt) ( $10^{-2}$ mol/m <sup>3</sup> )	$k_{\text{obs}}$ ( $10^5$ s <sup>-1</sup> )				
	288.2 K	298.6 K	313.1 K	328.4 K	342.9 K
0.00	0.19	0.21	0.28	0.43	0.55
150	0.48	0.82	1.35	2.24	2.72
300	0.64	1.00	1.67	3.10	4.80
450		1.54	2.48	4.13	6.67
600	1.41	1.87	3.12	5.21	8.35
750	1.59	2.30	3.96	6.54	10.8
900	1.95	2.85	4.85	7.70	12.2

Table A-2-7. continued\*

Composition: Water

C (Salt) ( $10^{-2}$ mol/m <sup>3</sup> )	$k_{\text{obs}}$ ( $10^5$ s <sup>-1</sup> )				
	286.4 K	298.6 K	313.3 K	327.9 K	342.6 K
0.00	0.49	0.53	0.70	0.96	0.95
500	0.51	0.66	0.64	0.55	0.38
1000	0.65	0.80	0.82	0.83	0.76
1500	0.66	0.85	0.88	0.97	1.0
2000	0.75	1.0	1.2	1.2	1.3
2500	0.75	1.1	1.3	1.6	1.3
3000	0.79	1.2	1.5	1.8	1.2

Composition: 97 mol% Water

C (Salt) ( $10^{-2}$ mol/m <sup>3</sup> )	$k_{\text{obs}}$ ( $10^5$ s <sup>-1</sup> )				
	285.4 K	298.6 K	313.3 K	328.0 K	342.2 K
0.00	0.31	0.45	0.62	0.83	1.0
150	0.30	0.47	0.74	0.99	1.5
300	0.33	0.53	0.73	1.1	1.6
450	0.39	0.62	0.87	1.5	2.1
600	0.48	0.74	1.1	1.6	2.4
750	0.41	0.79	1.2	1.7	2.8
900	0.52	0.88	1.5	2.1	3.4

Composition: 90 mol% Water

C (Salt) ( $10^{-2}$ mol/m <sup>3</sup> )	$k_{\text{obs}}$ ( $10^5$ s <sup>-1</sup> )				
	288.2 K	298.6 K	313.1 K	328.4 K	342.9 K
0.00	0.17	0.18	0.23	0.31	0.33
150	0.34	0.58	0.87	1.3	1.1
300	0.44	0.66	1.0	2.0	2.5
450		1.1	1.7	2.6	3.8
600	1.1	1.4	2.2	3.4	5.0
750	1.3	1.8	2.9	4.5	7.0
900	1.6	2.2	3.7	4.5	8.1

\* Corrected values for water, 97 and 90 mol% water. Refer to chapter two for the correction method.

Table A-2-7 continued

Composition: 70 mol% Water

C (Salt) ( $10^{-2}$ mol/m <sup>3</sup> )	$k_{\text{obs}}$ ( $10^6$ s <sup>-1</sup> )				
	284.8 K	298.6 K	313.1 K	328.0 K	342.7 K
0.00	0.04	0.08	0.10	0.13	0.18
50.0	0.18	0.32	0.54	0.85	1.48
100	0.27	0.44	0.72	1.19	1.80
150	0.35	0.62	1.11	1.70	2.67
200	0.44	0.79	1.26	2.04	3.30
250	0.53	0.91	1.54	2.48	3.90
300	0.58	0.99	1.62	2.33	3.71

Composition: 50 mol% Water

C (Salt) ( $10^{-2}$ mol/m <sup>3</sup> )	$k_{\text{obs}}$ ( $10^6$ s <sup>-1</sup> )				
	283.5 K	298.6 K	313.0 K	328.0 K	342.6 K
0.00	0.09	0.14	0.21	0.32	0.41
4.00	0.23	0.48	0.77	1.28	1.89
8.00	0.40	0.72	1.36	2.17	3.10
12.0	0.54	1.01	1.73	3.02	4.30
16.0	0.68	1.33	2.31	3.65	6.42
20.0	0.81	1.57	2.88	4.28	5.87
24.0	0.92	1.73	3.24	4.82	6.67

Composition: 30 mol% Water

C (Salt) ( $10^{-2}$ mol/m <sup>3</sup> )	$k_{\text{obs}}$ ( $10^6$ s <sup>-1</sup> )				
	287.2 K	298.6 K	313.5 K	328.4 K	343.1 K
0.00	0.46	1.57	3.15	4.88	4.50
2.00	0.20	0.34	0.59	0.96	1.25
4.00	0.35	0.60	1.12	1.93	2.95
6.00	0.51	0.90	1.61	2.57	3.59
8.00	0.67	1.17	2.20	3.27	4.75
10.0	0.84	1.52	2.65	4.18	6.30
12.0	0.99	1.80	3.18	4.53	7.15

Table A-2-7 continued

Composition: 10 mol% Water

C (Salt) ( $10^{-2}$ mol/m <sup>3</sup> )	$k_{\text{obs}}$ ( $10^6$ s <sup>-1</sup> )				
	298.7 K	308.9 K	321.0 K	330.8 K	342.7 K
0.00	0.03	0.04	0.07	0.12	0.17
1.00	0.15	0.25	0.35	0.46	0.61
2.00	0.27	0.38	0.59	0.72	0.92
3.00	0.38	0.56	0.79	1.08	1.39
4.00	0.44	0.68	0.92	1.22	1.78
5.00	0.57	0.80	1.21	1.49	2.07
6.00	0.67	1.01	1.33	1.71	2.24

Composition: 5 mol% Water

C (Salt) ( $10^{-2}$ mol/m <sup>3</sup> )	$k_{\text{obs}}$ ( $10^6$ s <sup>-1</sup> )				
	298.9 K	308.7 K	319.6 K	329.4 K	342.6 K
0.00	0.05	0.05	0.10	0.14	0.20
0.30	0.14	0.18	0.26	0.39	0.54
0.60	0.19	0.30	0.40	0.54	0.83
0.90	0.27	0.39	0.54	0.75	1.07
1.20	0.34	0.49	0.69	0.95	1.29
1.50	0.41	0.59	0.85	1.17	1.58
1.80	0.49	0.71	0.99	1.33	1.84

Composition: *t*-Butanol

C (Salt) ( $10^{-2}$ mol/m <sup>3</sup> )	$k_{\text{obs}}$ ( $10^6$ s <sup>-1</sup> )				
	298.6 K	309.0 K	321.7 K	332.0 K	342.9 K
0.00	0.10	0.18	0.30	0.51	1.04
0.50	0.14	0.28	0.54	0.77	1.48
1.00	0.20	0.41	0.75	1.01	1.87
1.50	0.29	0.53	0.83	1.45	2.49
2.00	0.34	0.69	1.25	1.95	3.24
2.50	0.42	0.78	1.44	2.28	3.85
3.00	0.51	0.89	1.61	2.69	4.20

Table A-2-8. Temperature and composition dependences of  $k_2$  for the reaction of  $e_s^-$  with ammonium perchlorate in *t*-butanol/water mixed solvents\*.

Water mol%	T (K)	$k_2$ ( $10^6 \text{ m}^3/\text{mol}\cdot\text{s}$ )	Water mol%	T (K)	$k_2$ ( $10^6 \text{ m}^3/\text{mol}\cdot\text{s}$ )
100	286.4	0.0011	30	287.2	7.7
	298.6	0.0020		298.6	14.
	313.3	0.0036		313.5	26.
	327.9	0.0051		328.4	40.
		343.1		61.	
97	285.4	0.0026	10	298.7	9.6
	298.6	0.0048		308.9	14.
	313.3	0.0080		321.9	21.
	328.0	0.013		330.8	29.
	342.2	0.025		342.7	38.
90	288.7	0.0014	5	298.9	9.7
	298.6	0.019		308.7	14.
	313.1	0.036		319.6	21.
	328.4	0.057		329.4	36.
	342.9	0.085		342.6	51.
70	284.8	0.15	0	298.6	11.
	298.6	0.34		309.0	26.
	313.1	0.57		321.7	45.
	328.0	0.98		332.0	78.
	342.7	1.4		342.9	116.
50	283.5	3.1			
	298.6	6.3			
	313.0	12.			
	328.0	19.			
	342.6	27.			

\* Corrected values for water, 97 and 90 mol% water. Refer to chapter two for the correction method.

Table A-2-9. The values of  $k_{\text{obs}}$  of the reactions of solvated electrons with lithium perchlorate in *t*-butanol/water mixed solvent.

Composition: Water

C (Salt) ( $10^{-2}$ mol/m <sup>3</sup> )	$k_{\text{obs}}$ ( $10^5$ s <sup>-1</sup> )				
	282.4 K	298.6 K	313.3 K	327.8 K	342.7 K
0.00	0.42	0.65	0.88	0.92	1.36
10000	0.46	0.67	1.03	1.12	1.58
20000	0.54	0.79	1.17	1.52	2.27
30000	0.62	0.90	1.31	1.78	2.71
40000	0.62	1.09	1.54	2.21	3.04
50000	0.60	1.10	1.65	2.34	3.27
60000	1.16	1.73	2.17	2.90	3.89

Composition: *t*-Butanol

C (Salt) ( $10^{-2}$ mol/m <sup>3</sup> )	$k_{\text{obs}}$ ( $10^6$ s <sup>-1</sup> )			
	299.1 K	309.1 K	319.0 K	327.8 K
0.00	0.10	0.14	0.21	0.39
10000	0.22	0.43	0.71	1.14
20000	0.23	0.43	0.72	1.14
30000	0.24	0.44	0.75	1.19
40000	0.25	0.45	0.77	1.21
50000	0.25	0.45	0.79	1.26

Table A-2-10. Temperature and composition dependences of  $k_2$  for the reaction of  $e_s^-$  with lithium perchlorate in *t*-butanol/water mixed solvents.

Water mol%	T (K)	$k_2$ ( $10^2$ m <sup>3</sup> /mol·s)	Water mol%	T (K)	$k_2$ ( $10^2$ m <sup>3</sup> /mol·s)
100	282.4	0.58	0	299.1	7.0
	298.6	1.1		309.1	11.
	313.3	2.0		319.0	22.
	327.8	3.3		327.8	33.
	342.7	4.8			

## 2. Results of The Rate Constant Measurements in 1-Butylamine/water mixtures

The rate constant measurements for the reactions of solvated electrons with nitrobenzene, acetone, phenol and toluene in 1-butylamine/water mixtures were carried out in the following compositions in mol% water: 0.0, 10.0, 30.0, 50.0, 70.0, 90.0, 95.0, and 100.0. In addition, the rate constants of  $e_s^-$  with phenol in 97.0, 99.0, 99.5 and 99.8 mol % water were measured, and the rate constants of  $e_s^-$  with toluene in 97.0 mol % water was measured. The units of the concentration of salts, the first order rate constant ( $k_{obs}$ ) and the second order rate constant ( $k_2$ ) are indicated in the tables.

Table A-2-11. The values of  $k_{obs}$  of the reactions of solvated electrons with nitrobenzene in 1-butylamine/water mixed solvent.

C (Solute) ( $10^{-2}$ mol/m <sup>3</sup> )	Composition: Water				
	$k_{obs}$ ( $10^6$ s <sup>-1</sup> )				
	284.4 K	298.4 K	313.9 K	328.4 K	343.2 K
0.00	0.035	0.050	0.075	0.080	0.11
0.50	0.14	0.23	0.30	0.41	0.53
1.00	0.25	0.37	0.53	0.69	0.89
1.50	0.40	0.62	0.83	1.1	1.4
2.00	0.50	0.74	1.1	1.5	1.9
2.50	0.87	1.0	1.4	1.9	2.4



Table A-2-11, continued

Composition: 95 mol% Water

C (Solute) ( $10^{-2}$ mol/m <sup>3</sup> )	$k_{\text{obs}}$ ( $10^6$ s <sup>-1</sup> )					
	273.8 K	286.5 K	298.4 K	313.9 K	328.5	339.5 K
0.00	0.026	0.044	0.077	0.14	0.21	0.24
0.50	0.065	0.12	0.16	0.26	0.38	0.45
1.00	0.13	0.22	0.30	0.44	0.63	0.78
1.50	0.18	0.32	0.43	0.64	0.92	1.1
2.00	0.25	0.41	0.59	0.87	1.2	1.4
2.50	0.31	0.50	0.75	1.1	1.4	1.7

Composition: 90 mol% Water

C (Solute) ( $10^{-2}$ mol/m <sup>3</sup> )	$k_{\text{obs}}$ ( $10^6$ s <sup>-1</sup> )					
	271.7 K	283.4 K	298.5 K	313.9 K	328.5 K	341.4 K
0.00	0.020	0.035	0.11	0.11	0.16	0.24
0.50	0.069	0.14	0.20	0.30	0.38	0.51
1.00	0.14	0.20	0.34	0.50	0.67	0.84
1.50	0.18	0.32	0.46	0.69	0.90	1.1
2.00	0.24	0.37	0.59	0.85	1.1	1.5
2.50	0.30	0.44	0.73	1.1	1.4	1.8
3.00	0.38	0.56	0.89	1.3	1.7	2.2

Composition: 70 mol% Water

C (Solute) ( $10^{-2}$ mol/m <sup>3</sup> )	$k_{\text{obs}}$ ( $10^6$ s <sup>-1</sup> )						
	268.4 K	278.0 K	289.7 K	299.6 K	313.3 K	327.9 K	339.8 K
0.00	0.11	0.17	0.28	0.37	0.60	0.94	1.2
0.75	0.17	0.24	0.38	0.51	0.75	1.1	1.5
1.50	0.22	0.35	0.50	0.67	0.99	1.4	1.8
2.25	0.28	0.42	0.63	0.86	1.2	1.7	2.3
3.00	0.35	0.49	0.75	1.1	1.5	2.0	2.7
3.75	0.40	0.58	0.89	1.2	1.7	2.5	3.1
4.50	0.46	0.65	1.0	1.4	2.1	2.7	3.6

Table A-2-11 continued

Composition: 50 mol% Water

C (Solute) ( $10^{-2}$ mol/m <sup>3</sup> )	$k_{\text{obs}}$ ( $10^6$ s <sup>-1</sup> )					
	245.6 K	260.0 K	271.5 K	286.4 K	298.6 K	316.7 K
0.00	0.17	0.41	0.69	1.1	1.8	2.3
0.75	0.28	0.56	0.87	1.6	1.7	
1.50	0.24	0.53	0.87	1.5	2.3	3.0
2.25	0.30	0.62	0.96	1.6	2.6	3.4
3.00	0.34	0.65	1.0	1.8	2.8	3.7
3.75	0.37	0.77	1.2	2.0	3.0	4.0
4.50	0.42	0.85	1.3	2.1	3.2	4.4

Composition: 30 mol% Water

C (Solute) ( $10^{-2}$ mol/m <sup>3</sup> )	$k_{\text{obs}}$ ( $10^6$ s <sup>-1</sup> )					
	233.0 K	246.0 K	260.6 K	273.2 K	286.8 K	298.4 K
0.00	0.11	0.20	0.48	0.75	1.2	1.5
0.25	0.15	0.31	0.54	0.80	1.4	1.6
0.50	0.16	0.35	0.61	0.85	1.5	1.8
0.75	0.17	0.35	0.61	0.94	1.5	1.8
1.00	0.18	0.37	0.68	0.92	1.5	2.0
1.25	0.22	0.40	0.76	1.1	1.7	2.2
1.50	0.23	0.44	0.77	1.1	1.9	2.2

Composition: 10 mol% Water

C (Solute) ( $10^{-2}$ mol/m <sup>3</sup> )	$k_{\text{obs}}$ ( $10^6$ s <sup>-1</sup> )					
	228.2 K	243.1 K	256.6 K	271.2 K	285.7 K	298.6 K
0.00	0.021	0.037	0.047	0.054	0.077	0.11
0.10	0.037	0.053	0.075	0.080	0.12	0.16
0.20	0.042	0.063	0.085	0.12	0.16	0.19
0.30	0.040	0.072	0.10	0.15	0.20	0.24
0.40	0.048	0.087	0.12	0.18	0.27	0.31
0.50	0.066	0.10	0.14	0.21	0.33	0.38
0.60	0.066	0.12	0.17	0.26	0.37	0.45

Table A-2-11 continued

Composition: 1-Butylamine

C (Solute) ( $10^{-2}$ mol/m <sup>3</sup> )	$k_{\text{obs}}$ ( $10^6$ s <sup>-1</sup> )						
	229.8 K	243.3 K	258.4 K	271.7 K	286.4 K	298.4 K	314.8 K
0.00	0.040	0.077	0.094	0.14	0.15	0.20	0.27
0.25	0.055	0.12	0.12	0.21	0.30	0.40	0.53
0.50	0.069	0.12	0.17	0.23	0.40	0.63	0.63
0.75	0.10	0.18	0.27	0.37	0.61	0.77	1.2
1.00	0.15	0.24	0.34	0.45	0.75	1.0	1.5
1.25	0.14	0.28	0.41	0.61	0.87	1.2	1.7
1.50	0.19	0.33	0.48	0.69	1.1	1.5	2.1

Table A-2-12. Temperature and composition dependences of  $k_2$  for the reaction of  $e_s^-$  with nitrobenzene in 1-butylamine/water mixed solvents

Water mol%	T (K)	$k_2$ ( $10^7$ m <sup>3</sup> /mol·s)	Water mol%	T (K)	$k_2$ ( $10^7$ m <sup>3</sup> /mol·s)
100	284.4	2.6	50	245.6	0.47
	298.4	3.8		260.0	0.84
	313.9	5.2		271.5	1.2
	328.4	7.0		286.4	2.2
	343.2	8.9		298.6	3.1
95	273.8	1.3	30	233.0	0.53
	286.5	2.0		246.0	0.80
	298.4	3.0		260.6	1.6
	313.9	4.3		273.2	2.4
	328.9	5.6		286.8	3.8
	339.5	6.5		298.4	5.0
90	271.7	1.1	10	228.2	0.68
	283.4	1.5		243.1	1.4
	298.5	2.5		256.6	2.0
	313.9	3.7		271.2	3.5
	328.5	5.0		285.7	5.2
	341.4	6.3		298.6	6.6
70	268.4	7.6	0	229.8	0.83
	278.0	1.1		243.3	1.6
	289.7	1.7		258.4	2.4
	299.6	2.3		271.7	3.7
	313.3	3.3		286.4	6.1
	327.9	4.6		298.4	8.2
	339.8	5.6		314.8	12.

Table A-2-13. The values of  $k_{\text{obs}}$  of the reactions of solvated electrons with acetone in 1-butylamine/water mixed solvent.

Composition: Water

C (Solute) ( $10^{-2}$ mol/m <sup>3</sup> )	$k_{\text{obs}}$ ( $10^6$ s <sup>-1</sup> )			
	278.4 K	291.5 K	298.6 K	308.6 K
0.00	0.05	0.075	0.11	0.12
10.0	0.55	0.77	0.94	1.2
20.0	1.5	2.1	1.9	2.9
30.0	1.5	2.1	2.5	2.9
40.0	1.8	2.8	3.1	3.8
50.0	2.4		3.9	4.7

Composition: 95 mol% Water

C (Solute) ( $10^{-2}$ mol/m <sup>3</sup> )	$k_{\text{obs}}$ ( $10^6$ s <sup>-1</sup> )				
	273.1 K	287.4 K	298.4 K	313.9 K	328.4 K
0.00	0.062	0.11	0.18	0.29	0.39
5.00	0.099	0.19	0.30	0.44	0.64
10.0	0.15	0.32	0.46	0.75	0.99
15.0	0.21	0.42	0.64	0.96	1.4
20.0	0.28	0.54	0.80	1.2	1.7
25.0	0.37	0.67	1.0	1.6	2.1
30.0	0.41	0.78	1.2	1.9	2.7

Composition: 90 mol% Water

C (Solute) ( $10^{-2}$ mol/m <sup>3</sup> )	$k_{\text{obs}}$ ( $10^6$ s <sup>-1</sup> )					
	270.7 K	284.8 K	298.9 K	313.9 K	328.4 K	343.0 K
0.00	0.046	0.084	0.15	0.23	0.33	0.51
5.00	0.083	0.16	0.27	0.43	0.66	0.92
10.0	0.12	0.22	0.42	0.69	1.0	1.3
15.0	0.15	0.31	0.57	0.87	1.3	1.8
20.0	0.19	0.38	0.69	1.1	1.7	2.1
25.0	0.22	0.46	0.83	1.3	2.0	2.7
30.0	0.28	0.54	0.99	1.6	2.5	3.1

Table A-2-13, continued

Composition: 70 mol% Water

C (Solute) ( $10^{-2}$ mol/m <sup>3</sup> )	$k_{\text{obs}}$ ( $10^6$ s <sup>-1</sup> )						
	261.1 K	272.8 K	286.7 K	298.6 K	313.0 K	328.4 K	343.0 K
0.00	0.085	0.13	0.21	0.34	0.53	0.86	1.4
5.00	0.10	0.15	0.27	0.42	0.72	1.2	1.7
10.0	0.11	0.19	0.33	0.48	0.87	1.3	2.2
15.0	0.13	0.22	0.38	0.59	0.99	1.6	2.5
20.0	0.14	0.24	0.41	0.65	1.1	1.8	2.7
25.0	0.15	0.27	0.46	0.74	1.3	2.1	2.9
30.0	0.17	0.29	0.53	0.87	1.4	2.3	3.4

Composition: 50 mol% Water

C (Solute) ( $10^{-2}$ mol/m <sup>3</sup> )	$k_{\text{obs}}$ ( $10^6$ s <sup>-1</sup> )					
	243.1 K	257.2 K	271.7 K	286.4 K	298.5 K	313.9 K
0.00	0.14	0.37	0.74	1.3	2.2	3.5
2.50	0.15	0.39	0.77	1.3	2.2	3.6
5.00	0.15	0.40	0.79	1.4	2.3	3.8
7.50	0.16	0.41	0.81	1.4	2.4	3.9
10.0	0.17	0.41	0.83	1.4	2.5	4.0
12.5	0.18	0.46	0.89	1.5	2.5	4.1
15.0	0.18	0.47	0.93	1.6	2.6	4.2

Composition: 30 mol% Water

C (Solute) ( $10^{-2}$ mol/m <sup>3</sup> )	$k_{\text{obs}}$ ( $10^6$ s <sup>-1</sup> )						
	230.1 K	240.3 K	250.7 K	260.9 K	272.3 K	285.0 K	298.5 K
0.00	0.13	0.23	0.43	0.65	0.99	1.5	2.0
5.00	0.17	0.30	0.53	0.75	1.2	1.7	2.3
10.0	0.19	0.33	0.55	0.79	1.3	1.8	2.5
15.0	0.20	0.37	0.58	0.94	1.4	2.0	2.7
20.0	0.20	0.38	0.63	0.94	1.4	2.0	2.9
25.0	0.20	0.39	0.65	0.96	1.5	2.2	3.0
30.0	0.22	0.41	0.69	1.0	1.6	2.4	3.3

Table A-2-13, continued

Composition: 10 mol% Water

C (Solute) ( $10^{-2}$ mol/m <sup>3</sup> )	$k_{\text{obs}}$ ( $10^6$ s <sup>-1</sup> )					
	234.2 K	249.9 K	266.2 K	282.8 K	298.6 K	313.9 K
0.00	0.099	0.14	0.20	0.27	0.28	0.43
1.67	0.11	0.15	0.23	0.30	0.31	0.51
3.33	0.12	0.17	0.25	0.35	0.43	0.55
5.00	0.13	0.19	0.30	0.39	0.51	0.58
6.67	0.17	0.25	0.34	0.49	0.63	0.72
8.33	0.16	0.22	0.37	0.53	0.74	0.77
10.0	0.17	0.26	0.40	0.59	0.81	0.99

Composition: 1-Butyl Amine

C (Solute) ( $10^{-2}$ mol/m <sup>3</sup> )	$k_{\text{obs}}$ ( $10^6$ s <sup>-1</sup> )					
	232.2 K	247.0 K	260.0 K	270.7 K	282.8 K	298.6 K
0.00	0.055	0.077	0.12	0.16	0.18	0.21
2.60	0.060	0.090	0.15	0.20	0.27	0.37
5.20	0.073	0.12	0.21	0.27	0.39	0.53
7.80	0.082	0.14	0.26	0.34	0.50	0.69
10.4	0.089	0.16	0.29	0.41	0.61	0.84
13.0	0.10	0.19	0.32	0.50	0.69	1.1
15.6	0.11	0.22	0.37	0.57	0.77	1.3

Table A-2-14. Temperature and composition dependences of  $k_2$  for the reaction of  $e_s^-$  with acetone in 1-butylamine/water mixed solvents

Water mol%	T (K)	$k_2$ ( $10^6 \text{ m}^3/\text{mol}\cdot\text{s}$ )	Water mol%	T (K)	$k_2$ ( $10^6 \text{ m}^3/\text{mol}\cdot\text{s}$ )
100	278.4	4.5	50	243.1	0.25
	291.5	6.4		257.2	0.53
	298.6	7.4		271.7	1.1
	308.6	9.0		286.4	1.9
		298.5		3.0	
		313.9		5.1	
95	273.1	1.2		30	230.1
	287.4	2.3	240.3		0.34
	298.4	3.6	250.7		0.56
	313.9	5.8	260.9		0.99
	328.4	8.0	272.3		1.6
		285.0	2.7		
		298.5	3.9		
90	270.7	0.77	10	234.2	0.41
	284.8	1.6		249.9	0.92
	298.9	2.8		266.2	1.9
	313.9	4.5		282.8	3.5
	328.4	7.0		298.8	6.1
	343.0	8.7			
70	261.1	0.40	0	232.2	0.46
	272.8	0.67		247.0	1.0
	286.7	1.2		260.0	1.7
	298.6	1.9		270.7	2.8
	313.0	3.2		282.8	4.1
	328.4	5.0		298.6	6.7
	343.0	6.8			



Table A-2-15. The values of  $k_{\text{obs}}$  of the reactions of solvated electrons with phenol in 1-butylamine/water mixed solvent.

Composition: Water

C (Solute) ( $10^{-2}$ mol/m <sup>3</sup> )	$k_{\text{obs}}$ ( $10^6$ s <sup>-1</sup> )					
	276.4 K	288.6 K	298.6 K	313.9 K	328.4 K	343.2 K
0.00	0.018	0.027	0.033	0.043	0.052	0.079
500	0.064	0.10	0.14	0.22	0.31	0.37
1000	0.11	0.17	0.24	0.39	0.51	0.65
1500	0.15	0.26	0.35	0.55	0.77	0.99
2000	0.22	0.35	0.48	0.77	1.1	1.3
2500	0.26	0.43	0.60	0.92	1.3	1.7
3000	0.32	0.51	0.71	1.1	1.6	1.9

Composition: 99.8 mol% Water

C (Solute) ( $10^{-2}$ mol/m <sup>3</sup> )	$k_{\text{obs}}$ ( $10^6$ s <sup>-1</sup> )					
	274.1 K	286.4 K	298.5 K	313.8 K	328.4 K	344.1 K
0.00	0.011	0.015	0.023	0.032	0.050	0.077
500	0.014	0.021	0.034	0.056	0.092	0.13
1000	0.018	0.033	0.047	0.090	0.16	0.28
1500	0.020	0.038	0.060	0.12	0.24	0.39
2000	0.027	0.050	0.080	0.16	0.31	0.52
2500	0.029	0.053	0.094	0.21	0.37	0.65
3000	0.033	0.059	0.12	0.25	0.44	0.79

Composition: 99.5 mol% Water

C (Solute) ( $10^{-2}$ mol/m <sup>3</sup> )	$k_{\text{obs}}$ ( $10^6$ s <sup>-1</sup> )					
	274.2 K	286.4 K	298.5 K	313.9 K	328.4 K	343.1 K
0.00	0.0092	0.015	0.023	0.037	0.059	0.094
500	0.015	0.020	0.035	0.061	0.090	0.15
1000	0.017	0.026	0.042	0.077	0.13	0.20
1500	0.020	0.032	0.051	0.099	0.18	0.28
2000	0.023	0.037	0.063	0.11	0.22	0.35
2500	0.026	0.041	0.070	0.14	0.26	0.41
3000	0.029	0.045	0.085	0.16	0.30	0.49

Table A-2-15, continued

Composition: 99.0 mol% Water

C (Solute) ( $10^{-2}$ mol/m <sup>3</sup> )	$k_{\text{obs}}$ ( $10^6$ s <sup>-1</sup> )					
	274.2 K	286.4 K	298.4 K	313.6 K	328.4 K	343.2 K
0.00	0.014	0.019	0.029	0.044	0.076	0.11
1000	0.016	0.028	0.043	0.077	0.12	0.20
2000	0.023	0.040	0.063	0.11	0.19	0.32
3000	0.027	0.048	0.076	0.14	0.25	0.39
4000	0.035	0.055	0.091	0.17	0.32	0.53
5000	0.038	0.064	0.096	0.21	0.39	0.66
6000	0.041	0.075	0.12	0.27	0.50	0.85

Composition: 97 mol% Water

C (Solute) ( $10^{-2}$ mol/m <sup>3</sup> )	$k_{\text{obs}}$ ( $10^6$ s <sup>-1</sup> )					
	274.5 K	286.8 K	298.5 K	314.0 K	328.4 K	344.0 K
0.00	0.018	0.032	0.055	0.089	0.13	0.20
1000	0.027	0.045	0.076	0.13	0.19	0.32
2000	0.031	0.056	0.091	0.17	0.27	0.41
3000	0.035	0.066	0.11	0.20	0.34	0.53
4000	0.041	0.080	0.13	0.26	0.40	0.68
5000	0.048	0.095	0.15	0.29	0.49	0.80
6000	0.056	0.11	0.17	0.34	0.54	0.93

Composition: 95 mol% Water

C (Solute) ( $10^{-2}$ mol/m <sup>3</sup> )	$k_{\text{obs}}$ ( $10^6$ s <sup>-1</sup> )						
	266.9 K	276.5 K	287.5 K	298.5 K	313.9 K	328.4 K	343.1 K
0.00	0.019	0.031	0.051	0.073	0.14	0.19	0.27
1000	0.026	0.042	0.068	0.11	0.19	0.29	0.41
2000	0.033	0.054	0.089	0.13	0.26	0.40	0.57
3000	0.037	0.064	0.11	0.16	0.31	0.47	0.74
4000	0.043	0.075	0.13	0.19	0.38	0.57	0.87
5000	0.049	0.087	0.15	0.23	0.41	0.68	0.99
6000	0.056	0.097	0.17	0.27	0.48	0.78	1.1

Table A-2-15, continued

Composition: 90 mol% Water

C (Solute) ( $10^{-2}$ mol/m <sup>3</sup> )	$k_{\text{obs}}$ ( $10^6$ s <sup>-1</sup> )					
	274.3 K	286.7 K	298.5 K	313.8 K	328.3 K	342.5 K
0.00	0.062	0.10	0.16	0.25	0.37	0.55
1000	0.094	0.14	0.25	0.38	0.57	0.79
2000	0.12	0.20	0.31	0.51	0.77	1.0
3000	0.14	0.23	0.38	0.62	0.90	1.2
4000	0.17	0.30	0.46	0.74	1.1	1.5
5000	0.20	0.35	0.52	0.86	1.2	1.8
6000	0.23	0.39	0.57	0.95	1.4	2.0

Composition: 70 mol% Water

C (Solute) ( $10^{-2}$ mol/m <sup>3</sup> )	$k_{\text{obs}}$ ( $10^6$ s <sup>-1</sup> )				
	248.4 K	258.5 K	269.6 K	285.3 K	298.5 K
0.00	0.045	0.071	0.13	0.24	0.40
1000	0.22	0.37	0.54	0.91	1.3
2000	0.32	0.51	0.72	1.2	1.7
3000	0.40	0.59	0.87	1.4	2.0
4000	0.45	0.68	0.99	1.6	2.3
5000	0.48	0.74	1.1	1.8	2.6
6000	0.54	0.82	1.2	2.1	3.0

Composition: 50 mol% Water

C (Solute) ( $10^{-2}$ mol/m <sup>3</sup> )	$k_{\text{obs}}$ ( $10^6$ s <sup>-1</sup> )				
	243.3 K	257.2 K	271.6 K	286.3 K	298.5 K
0.00	0.072	0.16	0.29	0.55	0.88
100	0.19	0.40	0.71	1.2	1.9
200	0.23	0.43	0.78	1.3	2.1
300	0.27	0.50	0.89	1.4	2.2
400	0.30	0.57	0.95	1.6	2.4
500	0.35	0.61	1.0	1.7	2.5
600	0.38	0.68	1.2	1.8	2.7

Table A-2-15, continued

Composition: 30 mol% Water

C (Solute) ( $10^{-2}$ mol/m <sup>3</sup> )	$k_{\text{obs}}$ ( $10^6$ s <sup>-1</sup> )						
	230.1 K	240.2 K	250.7 K	260.8 K	271.1 K	283.8 K	298.5 K
0.00	0.12	0.22	0.41	0.58	0.87	1.3	1.7
100	0.19	0.35	0.55	0.81	1.2	1.7	2.2
200	0.20	0.36	0.57	0.88	1.2	1.8	2.4
300	0.21	0.38	0.59	0.92	1.3	1.8	2.4
400	0.27	0.42	0.63	0.99	1.4	1.9	2.5
500	0.28	0.43	0.65	1.0	1.4	2.0	2.6
600	0.32	0.48	0.72	1.1	1.4	2.0	2.7

Composition: 10 mol% Water

C (Solute) ( $10^{-2}$ mol/m <sup>3</sup> )	$k_{\text{obs}}$ ( $10^6$ s <sup>-1</sup> )				
	233.2 K	244.9 K	271.5 K	285.6 K	298.6 K
0.00	0.033	0.046	0.077	0.12	0.12
250	0.040	0.053	0.097	0.15	0.17
500	0.044	0.063	0.12	0.19	0.21
750	0.052	0.073	0.15	0.22	0.27
1000	0.059	0.080	0.17	0.26	0.31
1250	0.066	0.094	0.20	0.28	0.32

Composition: 1-Butyl Amine

C (Solute) ( $10^{-2}$ mol/m <sup>3</sup> )	$k_{\text{obs}}$ ( $10^6$ s <sup>-1</sup> )					
	249.2 K	261.2 K	286.4 K	298.8 K	314.2 K	328.9 K
0.00	0.070	0.099	0.15	0.20	0.28	0.40
250	0.085	0.12	0.19	0.24	0.31	0.46
500	0.087	0.12	0.21	0.26	0.37	0.51
1000	0.098	0.14	0.25	0.31	0.43	0.62
1250	0.11	0.14	0.26	0.33	0.47	0.67
1500	0.12	0.16	0.28	0.36	0.52	0.73

Table A-2-16. Temperature and composition dependences of  $k_2$  for the reaction of  $e_s^-$  with phenol in 1-butylamine/water mixed solvents

Water mol%	T (K)	$k_2$ ( $10^4$ m <sup>3</sup> /mol·s)	Water mol%	T (K)	$k_2$ ( $10^4$ m <sup>3</sup> /mol·s)
100	276.4	1.2	97	274.5	0.064
	288.6	1.7		286.8	0.13
	298.6	2.3		298.5	0.20
	313.9	3.6		314.0	0.41
	328.4	5.2		328.4	0.68
	343.2	6.3		344.0	1.2
99.8	274.1	0.080	95	266.9	0.06
	286.4	0.18		276.5	0.11
	298.5	0.30		287.5	0.19
	313.8	0.70		298.5	0.32
	328.4	1.3		313.9	0.58
	344.1	2.3		328.4	1.0
99.5	274.2	0.096	90	274.3	0.27
	286.4	0.11		286.7	0.48
	298.5	0.20		298.5	0.70
	313.9	0.41		313.8	1.2
	328.4	0.82		328.3	1.8
	343.1	1.3		342.5	2.5
99	274.2	0.046	70	248.4	0.62
	286.4	0.098		258.5	0.82
	298.4	0.14		269.6	1.3
	313.6	0.35		285.3	2.3
	328.4	0.67		298.5	3.4
	343.2	1.1			

Table A-2-16 continued

Water mol%	T (K)	$k_2$ ( $10^4 \text{ m}^3/\text{mol}\cdot\text{s}$ )	Water mol%	T (K)	$k_2$ ( $10^4 \text{ m}^3/\text{mol}\cdot\text{s}$ )
50	243.3	3.9	10	233.2	0.24
	257.2	5.4		244.9	0.37
	271.6	8.5		257.7	0.62
	286.3	1.1		271.5	1.0
	298.5	1.5		285.6	1.4
				298.6	1.9
30	240.2	2.5	0	249.2	0.25
	250.7	3.2		261.2	0.33
	260.8	4.3		286.4	0.77
	271.1	5.5		298.8	0.99
	283.8	7.3		314.2	1.6
	298.5	8.7		328.9	2.1

Table A-2-17. The values of  $k_{\text{obs}}$  of the reactions of solvated electrons with toluene in 1-butylamine/water mixed solvent.

Composition: Water

C (Solute) ( $10^{-2}$ mol/m <sup>3</sup> )	$k_{\text{obs}}$ ( $10^6$ s <sup>-1</sup> )					
	298.6 K	308.3 K	319.1 K	329.3 K	339.0 K	349.6 K
0.00	0.039	0.039	0.049	0.063	0.077	0.11
67	0.044	0.050	0.066	0.082	0.094	0.12
133	0.053	0.058	0.073	0.099	0.11	0.13
200	0.058	0.066	0.084	0.090	0.13	0.15
267	0.066	0.079	0.095	0.12	0.15	0.15
334	0.075	0.087	0.12	0.14	0.17	0.20
400	0.064	0.098	0.12	0.15	0.14	0.15

Composition: 97 mol% Water

C (Solute) ( $10^{-2}$ mol/m <sup>3</sup> )	$k_{\text{obs}}$ ( $10^6$ s <sup>-1</sup> )					
	298.8 K	308.6 K	319.0 K	329.3 K	339.6 K	350.8 K
0.00	0.047	0.070	0.099	0.13	0.17	0.23
2000	0.066	0.094	0.13	0.17	0.21	0.27
4000	0.085	0.12	0.16	0.20	0.26	0.32
6000	0.095	0.13	0.18	0.22	0.28	0.35
8000	0.13	0.17	0.22	0.27	0.32	0.37
10000	0.14	0.18	0.23	0.29	0.33	0.40

Composition: 95 mol% Water

C (Solute) ( $10^{-2}$ mol/m <sup>3</sup> )	$k_{\text{obs}}$ ( $10^6$ s <sup>-1</sup> )					
	268.0 K	283.0 K	298.6 K	313.9 K	328.4 K	344.2 K
0.00	0.019	0.039	0.077	0.13	0.20	0.28
2500	0.037	0.066	0.12	0.19	0.26	0.37
5000	0.059	0.11	0.17	0.27	0.32	0.39
7500	0.083	0.15	0.26	0.36	0.43	0.57
10000	0.099	0.18	0.29	0.41	0.51	0.68
12500	0.13	0.21	0.32	0.50	0.63	0.78
15000	0.14	0.25	0.39	0.55	0.68	0.77

Table A-2-17 continued

Composition: 90 mol% Water

C (Solute) ( $10^{-2}$ mol/m <sup>3</sup> )	$k_{\text{obs}}$ ( $10^6$ s <sup>-1</sup> )					
	273.2 K	286.7 K	298.7 K	314.0 K	328.7 K	344.4 K
0.00	0.048	0.087	0.14	0.22	0.35	0.50
1000	0.064	0.12	0.18	0.27	0.40	0.58
2000	0.084	0.14	0.20	0.30	0.42	0.62
3000	0.10	0.16	0.23	0.35	0.48	0.64
4000	0.12	0.18	0.26	0.38	0.50	0.69
5000	0.13	0.21	0.30	0.42	0.58	0.75

Composition: 70 mol% Water

C (Solute) ( $10^{-2}$ mol/m <sup>3</sup> )	$k_{\text{obs}}$ ( $10^6$ s <sup>-1</sup> )						
	248.4 K	260.4 K	272.3 K	286.8 K	299.2 K	313.4 K	328.8 K
0.00	0.050	0.087	0.15	0.25	0.41	0.66	1.0
500	0.082	0.13	0.22	0.35	0.50	0.76	1.3
1000	0.11	0.17	0.27	0.41	0.54	0.83	1.3
1500	0.13	0.20	0.30	0.44	0.59	0.88	1.4
2000	0.17	0.26	0.35	0.51	0.69	0.96	1.4
2500	0.21	0.30	0.41	0.58	0.73	1.0	1.5
3000	0.24	0.35	0.45	0.63	0.83	1.1	1.5

Composition: 50 mol% Water

C (Solute) ( $10^{-2}$ mol/m <sup>3</sup> )	$k_{\text{obs}}$ ( $10^6$ s <sup>-1</sup> )					
	229.9 K	240.0 K	250.5 K	260.5 K	270.7 K	282.2 K
0.00	0.070	0.12	0.22	0.39	0.56	0.90
250	0.12	0.20	0.33	0.53	0.77	1.3
500	0.17	0.26	0.39	0.61	0.86	1.4
750	0.21	0.32	0.43	0.65	0.91	1.4
1000	0.27	0.38	0.51	0.72	1.0	1.5
1250	0.31	0.42	0.54	0.77	1.0	1.6
1500	0.35	0.45	0.59	0.81	1.1	1.7



Table A-2-17 continued

Composition: 30 mol% Water

C (Solute) ( $10^{-2}$ mol/m <sup>3</sup> )	$k_{\text{obs}}$ ( $10^6$ s <sup>-1</sup> )					
	233.3 K	243.0 K	253.5 K	263.4 K	273.9 K	286.5
0.00	0.15	0.27	0.46	0.69	0.99	1.3
672	0.23	0.35	0.58	0.80	1.1	1.5
1344	0.29	0.42	0.62	0.88	1.2	1.5
2016	0.38	0.47	0.69	0.99	1.3	1.7
2688	0.42	0.58	0.81	1.1	1.4	1.8
3360	0.48	0.65	0.87	1.2	1.5	1.9

Composition: 10 mol% Water

C (Solute) ( $10^{-2}$ mol/m <sup>3</sup> )	$k_{\text{obs}}$ ( $10^6$ s <sup>-1</sup> )					
	244.8 K	258.8 K	270.3 K	286.1 K	298.5 K	313.9 K
0.00	0.039	0.055	0.072	0.092	0.13	0.17
667	0.063	0.074	0.099	0.13	0.17	0.22
1333	0.086	0.10	0.12	0.17	0.20	0.26
2000	0.096	0.12	0.15	0.19	0.24	0.29
2667	0.12	0.14	0.16	0.22	0.28	0.33

Composition: 1-Butyl Amine

C (Solute) ( $10^{-2}$ mol/m <sup>3</sup> )	$k_{\text{obs}}$ ( $10^6$ s <sup>-1</sup> )				
	257.2 K	270.1 K	283.0 K	298.8 K	308.4 K
0.00	0.11	0.14	0.18	0.28	0.32
2000	0.19	0.22	0.29	0.34	0.40
4000	0.22	0.26	0.32	0.40	0.48
6000	0.29	0.33	0.38	0.44	0.53
10000	0.35	0.38	0.46	0.55	0.60
12000	0.38	0.40	0.49	0.58	0.70

Table A-2-18. Temperature and composition dependences of  $k_2$  for the reaction of  $e_s^-$  with toluene in 1-butylamine/water mixed solvents

Water mol%	T (K)	$k_2$ ( $10^4$ m <sup>3</sup> /mol·s)	Water mol%	T (K)	$k_2$ ( $10^4$ m <sup>3</sup> /mol·s)
100	298.6	1.1	90	273.2	0.17
	308.3	1.4		286.7	0.23
	319.1	1.8		298.7	0.30
	329.2	2.3		314.0	0.40
	339.0	2.8		328.7	0.43
			344.4	0.50	
97	298.8	0.09	70	248.4	0.64
	308.6	0.12		260.4	0.90
	319.0	0.15		272.3	1.0
	329.3	0.17		286.8	1.2
	339.6	0.21		299.2	1.4
			313.4	1.4	
95	268.0	0.09	50	229.9	1.8
	283.0	0.14		240.0	2.2
	298.6	0.20		250.5	2.4
	313.9	0.28		260.5	2.5
	328.4	0.36		270.7	2.8
			282.2	2.9	

Table A-2-18 continued

Water mol%	T (K)	$k_2$ ( $10^4 \text{ m}^3/\text{mol}\cdot\text{s}$ )	Water mol%	T (K)	$k_2$ ( $10^4 \text{ m}^3/\text{mol}\cdot\text{s}$ )
30	233.3	0.94	0	257.2	0.16
	243.0	1.1		270.1	0.20
	253.5	1.2		283.0	0.23
	263.4	1.3		298.8	0.27
	273.9	1.6		308.4	0.29
	286.5	1.9			
10	244.8	0.27			
	258.8	0.32			
	270.3	0.38			
	286.1	0.47			
	298.5	0.56			
	313.9	0.65			
	329.5	0.76			

### 3. Results of The Electrical Conductance Measurements in *t*-Butanol/water mixtures

The electrical conductance measurements of lithium nitrate, ammonium nitrate, ammonium perchlorate, lithium perchlorate and perchloric acid in *t*-butanol/water mixtures were carried out in the following compositions in mol% water: 0.0, 10.0, 30.0, 50.0, 70.0, 90.0, 97.0, and 100.0. The units of the concentration of salts, the specific conductance ( $\kappa$ ) and the molar conductivity ( $\Lambda_0$ ) are indicated in the tables.

Table A-2-19. The values of specific conductance ( $\kappa$ ) of perchloric acid in *t*-butanol/water mixed solvent.

Composition: Water

C (Acid) ( $10^{-1}$ mol/m <sup>3</sup> )	$\Lambda_0$ ( $10^{-4}$ S/m)				
	298.3 K	308.3 K	318.3 K	328.4 K	343.5 K
0.00	0.64	0.79	0.92	1.1	1.9
0.50	20.	23.	26.	29.	34.
1.0	38.	46.	50.	58.	66.
1.5	62.	74.	81.	91.	102.
2.0	78.	94.	104.	117.	131.
2.5	102.	121.	133.	149.	169.

Composition: 97 mol% Water

C (Acid) ( $10^{-1}$ mol/m <sup>3</sup> )	$\Lambda_0$ ( $10^{-4}$ S/m)				
	283.4 K	298.3 K	313.6 K	328.3 K	343.5 K
0.00	0.67	0.79	1.3	2.0	2.9
0.50	12.	17.	21.	26.	31.
1.0	22.	32.	42.	51.	60.
1.5	36.	49.	72.	85.	97.
2.0	53.	75.	92.	111.	141.
2.5	63.	92.	114.	138.	161.

Table A-2-19 continued

Composition: 90 mol% Water

C (Acid) ( $10^{-1}$ mol/m <sup>3</sup> )	$\Lambda_o$ ( $10^{-4}$ S/m)				
	278.2 K	283.2 K	298.3 K	313.6 K	328.3 K
0.00	0.30	0.36	0.64	1.2	1.7
0.50	3.5	4.4	7.8	11.	15.
1.0	8.1	10.	18.	28.	36.
1.5	12.	15.	27.	42.	50.
2.0	16.	21.	36.	55.	66.
2.5	20.	26.	46.	66.	83.

Composition: 70 mol% Water

C (Acid) ( $10^{-1}$ mol/m <sup>3</sup> )	$\Lambda_o$ ( $10^{-4}$ S/m)				
	283.2 K	298.3 K	313.5 K	328.3 K	343.2 K
0.00	0.050	0.090	0.19	0.45	0.97
0.50	2.1	3.8	5.8	8.0	10.
1.0	3.5	5.9	11.	14.	19.
1.5	5.4	10.	17.	21.	27.
2.0	7.8	14.	22.	30.	37.
2.5	9.5	18.	29.	39.	49.

Composition: 50 mol% Water

C (Acid) ( $10^{-1}$ mol/m <sup>3</sup> )	$\Lambda_o$ ( $10^{-4}$ S/m)			
	298.2 K	313.2 K	328.3 K	343.5 K
0.00	0.030	0.044	0.088	0.10
0.25	0.75	1.2	1.8	2.2
0.5	1.5	2.3	3.4	4.7
0.75	2.2	3.6	5.5	7.3
1.00	2.9	4.7	6.8	9.4
1.25	3.6	6.0	8.7	12.

Table A-2-19 continued

Composition: 30 mol% Water

C (Acid) ( $10^{-1}$ mol/m <sup>3</sup> )	$\Lambda_0$ ( $10^{-4}$ S/m)			
	298.4 K	313.3 K	328.5 K	343.6 K
0.00	0.016	0.038	0.054	0.060
1.00	1.8	2.8	4.5	6.0
2.00	3.2	5.3	8.1	11.
3.00	5.0	8.2	12.	16.
4.00	6.3	10.	15.	19.
5.00	7.8	13.	18.	23.

Composition: 10 mol% Water

C (Acid) ( $10^{-1}$ mol/m <sup>3</sup> )	$\Lambda_0$ ( $10^{-4}$ S/m)				
	283.3 K	298.4 K	313.4 K	328.3 K	343.4 K
0.00	0.019	0.024	0.020	0.030	0.030
2.0	1.5	2.8	3.7	4.8	5.0
4.0	2.3	4.3	5.4	6.5	7.4
6.0	3.4	6.2	8.2	9.4	9.6
8.0	4.1	7.4	10.	11.	12.
10.0	5.2	8.9	11.	13.	14.

Composition: *t*-Butanol

C (Acid) ( $10^{-1}$ mol/m <sup>3</sup> )	$\Lambda_0$ ( $10^{-4}$ S/m)				
	300.1 K	308.5 K	318.3 K	328.4 K	343.5 K
0.00	0.0090	0.010	0.012	0.087	0.006
0.02	0.031	0.04	0.046	0.026	0.019
0.04	0.047	0.06	0.081	0.063	0.055
0.06	0.082	0.10	0.13	0.11	0.095
0.08	0.095	0.13	0.16	0.15	0.14
0.10	0.12	0.17	0.21	0.22	0.20

Table A-2-20. Temperature and composition dependences of molar conductivity ( $\Lambda_0$ ) of perchloric acid in *t*-butanol/water mixed solvents.

Water mol%	T (K)	$\Lambda_0$ ( $10^{-3} \text{ S}\cdot\text{m}^2/\text{mol}$ )	Water mol%	T (K)	$\Lambda_0$ ( $10^{-3} \text{ S}\cdot\text{m}^2/\text{mol}$ )
100	298.3	41.	50	298.2	3.0
	308.3	48.		313.2	4.9
	318.3	52.		328.3	7.1
	328.3	60.		343.5	9.5
	343.5	67.			
97	283.4	25.	30	298.4	1.6
	298.3	37.		313.3	2.7
	313.5	46.		328.3	3.9
	328.3	54.		343.6	5.1
	343.5	69.			
90	278.2	7.9	10	283.3	0.76*
	283.2	10.		298.4	1.4*
	298.3	19.		313.4	2.0*
	313.6	27.		328.2	3.1*
	328.3	33.		343.2	4.1*
70	283.2	3.8	0	300.1	1.1
	298.3	6.9		308.5	1.6
	313.5	11.		318.3	1.9
	328.3	16.		328.4	2.4
	343.2	24.		343.5	2.2

\* Initial slope.

Table A-2-21. The values of specific conductance ( $\kappa$ ) of lithium nitrate in *t*-butanol/water mixed solvent.

Composition: Water

C (Salt) ( $10^{-1}$ mol/m <sup>3</sup> )	$\Lambda_0$ ( $10^{-4}$ S/m)				
	278.1 K	298.2 K	313.4 K	328.4 K	343.6 K
0.00	0.57	1.0	1.6	2.5	4.7
0.50	4.1	6.6	8.8	11.	14.
1.00	7.5	12.	17.	21.	26.
1.50	1.1	18.	24.	31.	37.
2.00	14.	23.	30.	39.	48.
2.50	18.	29.	38.	48.	60.

Composition: 97 mol% Water

C (Salt) ( $10^{-1}$ mol/m <sup>3</sup> )	$\Lambda_0$ ( $10^{-4}$ S/m)				
	278.3 K	283.3 K	298.4 K	313.6 K	328.2 K
0.00	0.59	0.93	1.4	2.1	2.7
0.50	2.3	2.8	5.8	7.1	11.
1.00	5.0	6.2	11.	13.	18.
1.50	7.0	9.2	16.	20.	26.
2.00	9.3	12.	20.	25.	34.
2.50	11.	15.	23.	31.	40.

Composition: 90 mol% Water

C (Salt) ( $10^{-1}$ mol/m <sup>3</sup> )	$\Lambda_0$ ( $10^{-4}$ S/m)				
	283.0 K	298.2 K	313.2 K	328.2 K	343.6 K
0.00	0.57	0.71	1.5	2.1	5.0
0.50	1.2	2.5	4.0	5.8	11.
1.00	2.3	4.5	7.4	12.	18.
1.50	3.3	6.5	11.	15.	25.
2.00	4.3	8.5	14.	20.	34.
2.50	5.2	10.	16.	24.	42.



Table A-2-21 continued

Composition: 70 mol% Water

C (Salt) ( $10^{-1}$ mol/m <sup>3</sup> )	$\Lambda_0$ ( $10^{-4}$ S/m)				
	283.1 K	298.1 K	313.1 K	328.3 K	343.6 K
0.00	0.42	0.49	0.60	0.64	0.70
1.00	1.0	2.13	3.6	5.6	7.6
2.00	2.0	4.1	7.0	11.	15.
3.00	3.0	5.8	9.9	15.	21.
4.00	4.1	8.0	13.	20.	28.
5.00	5.1	10.	17.	25.	34.

Composition: 50 mol% Water

C (Salt) ( $10^{-1}$ mol/m <sup>3</sup> )	$\Lambda_0$ ( $10^{-4}$ S/m)				
	283.2 K	298.3 K	313.4 K	328.4 K	343.7
0.00	0.040	0.060	0.10	0.19	0.26
2.00	1.6	3.1	5.5	8.2	12.
4.00	2.8	5.5	9.3	14.	20.
6.00	3.9	7.6	13.	20.	27.
8.00	5.2	9.9	17.	25.	36.
10.0	6.2	12.	20.	30.	42.

Composition: 30 mol% Water

C (Salt) ( $10^{-1}$ mol/m <sup>3</sup> )	$\Lambda_0$ ( $10^{-4}$ S/m)				
	298.3 K	308.4 K	318.2 K	328.3 K	343.4
0.00	0.39	0.38	0.38	0.43	0.43
2.00	1.7	2.5	3.2	4.1	5.0
4.00	3.0	4.1	5.2	6.4	7.7
6.00	4.1	5.7	7.3	8.9	11.
8.00	5.1	6.9	9.4	11.	13.
10.0	6.0	8.2	10.	12.	15.

Table A-2-21 continued

Composition: 10 mol% Water

C (Salt) ( $10^{-1}$ mol/m <sup>3</sup> )	$\Lambda_0$ ( $10^{-4}$ S/m)				
	298.2 K	308.3 K	318.2 K	328.4 K	343.3 K
0.00	0.013	0.017	0.018	0.020	0.02
0.40	0.18	0.22	0.25	0.26	0.24
0.80	0.28	0.34	0.39	0.39	0.34
1.20	0.35	0.44	0.48	0.47	0.41
1.60	0.43	0.52	0.55	0.54	0.50
2.00	0.53	0.59	0.61	0.59	0.56

Composition: 10 mol% Water

C (Salt) ( $10^{-1}$ mol/m <sup>3</sup> )	$\Lambda_0$ ( $10^{-4}$ S/m)			
	298.4 K	308.3 K	318.2 K	328.4 K
0.00	0.0086	0.0091	0.0084	0.0072
0.10	0.054	0.068	0.085	0.091
0.20	0.11	0.14	0.16	0.17
0.30	0.14	0.19	0.22	0.23
0.40	0.19	0.24	0.27	0.28
0.50	0.22	0.28	0.32	0.33

Composition: *t*-Butanol

C (Salt) ( $10^{-1}$ mol/m <sup>3</sup> )	$\Lambda_0$ ( $10^{-4}$ S/m)				
	299.2 K	308.3 K	318.3 K	328.3 K	343.4 K
0.00	0.012	0.0088	0.0074	0.0065	0.005
1.00	0.046	0.045	0.043	0.041	0.028
2.00	0.070	0.065	0.053	0.046	0.031
3.00	0.084	0.077	0.062	0.053	0.036
4.00	0.094	0.088	0.073	0.057	0.040
5.00	0.10	0.095	0.084	0.064	0.045

Table A-2-21 continued

Composition: *t*-Butanol

C (Salt) (10 <sup>-1</sup> mol/m <sup>3</sup> )	$\Lambda_0$ (10 <sup>-4</sup> S/m)				
	299.3 K	308.3 K	318.2 K	328.3 K	343.4 K
0.00	0.011	0.0088	0.0070	0.0052	0.0037
0.20	0.019	0.018	0.015	0.013	0.010
0.40	0.027	0.026	0.022	0.019	0.015
0.60	0.034	0.033	0.031	0.026	0.019
0.80	0.041	0.040	0.035	0.031	0.022
1.00	0.046	0.045	0.041	0.034	0.024

Table A-2-22. Temperature and composition dependences of molar conductivity ( $\Lambda_0$ ) of lithium nitrate in *t*-butanol/water mixed solvents.

Water mol%	T (K)	$\Lambda_0$ ( $10^{-3} \text{ S}\cdot\text{m}^2/\text{mol}$ )	Water mol%	T (K)	$\Lambda_0$ ( $10^{-3} \text{ S}\cdot\text{m}^2/\text{mol}$ )
100	278.2	6.8	50	283.2	0.81*
	298.2	11.		298.3	1.5*
	313.4	15.		313.4	2.5*
	328.4	18.		328.4	3.9*
	343.6	22.		343.7	6.0*
97	278.3	4.4	30	298.3	0.74*
	283.3	5.4		308.4	1.1*
	298.4	9.0		313.2	1.5*
	313.6	12.		328.3	2.1*
	328.2	16.		343.4	2.8*
90	283.0	2.0	10	298.2	0.47*
	298.1	3.9		308.3	0.59*
	313.2	6.0		318.2	0.73*
	328.2	8.9		328.4	0.83*
	343.6	15.		343.3	0.62*
70	283.1	1.0	0	299.2	0.045*
	298.1	2.0		308.3	0.049*
	313.1	3.3		318.3	0.055*
	328.3	4.9		328.4	0.047*
	343.6	6.8		343.4	0.042*

\* Initial slope.

Table A-2-23. The values of specific conductance ( $\kappa$ ) of ammonium nitrate in *t*-butanol/water mixed solvent.

Composition: Water

C (Salt) ( $10^{-1}$ mol/m <sup>3</sup> )	$\Lambda_0$ ( $10^{-4}$ S/m)				
	283.3 K	298.3 K	313.4 K	328.2 K	343.4 K
0.00	0.090	0.12	0.18	0.27	0.41
0.50	0.63	0.86	1.1	1.4	1.7
1.00	1.2	1.7	2.4	3.7	5.4
1.50	1.7	2.3	3.0	4.0	5.6
2.00	2.2	3.0	4.0	5.2	6.9
2.50	2.7	3.9	5.3	7.4	10.

Composition: 97 mol% Water

C (Salt) ( $10^{-1}$ mol/m <sup>3</sup> )	$\Lambda_0$ ( $10^{-4}$ S/m)						
	273.2 K	278.2 K	283.3 K	298.6 K	313.5 K	328.2 K	343.4 K
0.00	0.54	0.58	0.69	0.99	1.6	1.7	2.2
0.50	2.7	3.3	3.9	6.4	9.2	12.	14.
1.00	5.8	7.0	8.1	13.	19.	24.	27.
1.50	8.4	10.	12.	20.	30.	32.	41.
2.00	9.9	13.	15.	24.	36.	48.	50.
2.50	14.	18.	21.	32.	45.	53.	61.

Composition: 90 mol% Water

C (Salt) ( $10^{-1}$ mol/m <sup>3</sup> )	$\Lambda_0$ ( $10^{-4}$ S/m)				
	283.3 K	298.4 K	313.5 K	328.2 K	343.4
0.00	0.45	0.48	0.63	0.94	1.0
0.50	1.5	3.0	4.7	6.4	8.6
1.00	3.5	7.8	12.	16.	21.
1.50	4.3	8.7	13.	19.	27.
2.00	6.4	12.	18.	24.	34.
2.50	7.5	15.	22.	31.	40.

Table A-2-23 continued

Composition: 70 mol% Water

C (Salt) ( $10^{-1}$ mol/m <sup>3</sup> )	$\Lambda_0$ ( $10^{-4}$ S/m)				
	283.4 K	298.4 K	313.4 K	328.3 K	343.5 K
0.00	0.45	0.42	0.52	0.52	0.53
1.00	1.3	2.6	4.3	6.2	8.5
2.00	2.5	5.1	9.0	12.	17.
3.00	4.0	7.7	13.	20.	27.
4.00	5.4	10.	17.	27.	35.
5.00	6.9	14.	24.	31.	39.

Composition: 50 mol% Water

C (Salt) ( $10^{-1}$ mol/m <sup>3</sup> )	$\Lambda_0$ ( $10^{-4}$ S/m)				
	283.2 K	298.2 K	313.5 K	328.2 K	343.4 K
0.00	0.030	0.050	0.070	0.10	0.38
2.00	1.7	3.4	5.7	7.5	12.
4.00	3.1	7.3	11.	16.	20.
6.00	4.6	8.8	14.	21.	30.
8.00	5.9	11.	18.	28.	38.
10.0	7.1	14.	24.	33.	44.

Composition: 30 mol% Water

C (Salt) ( $10^{-1}$ mol/m <sup>3</sup> )	$\Lambda_0$ ( $10^{-4}$ S/m)				
	283.3 K	298.2 K	313.3 K	328.2 K	343.4 K
0.00	0.30	0.41	0.36	0.43	0.45
2.00	1.1	1.8	3.0	4.2	5.1
4.00	1.6	3.2	4.4	6.4	7.8
6.00	2.2	4.0	6.2	8.2	9.9
8.00	2.8	4.9	7.4	10.	12.
10.0	3.2	5.8	8.7	11.	13.

Table A-2-23 continued

Composition: 10 mol% Water

C (Salt) ( $10^{-1}$ mol/m <sup>3</sup> )	$\Lambda_o$ ( $10^{-4}$ S/m)				
	298.3 K	308.2 K	318.2 K	328.3 K	343.3 K
0.00	0.012	0.014	0.017	0.017	0.012
0.40	0.20	0.22	0.25	0.27	0.25
0.80	0.28	0.34	0.37	0.38	0.36
1.20	0.35	0.42	0.45	0.45	0.41
1.60	0.42	0.50	0.54	0.54	0.50
2.00	0.47	0.57	0.61	0.60	0.53

Composition: *t*-Butanol

C (Salt) ( $10^{-1}$ mol/m <sup>3</sup> )	$\Lambda_o$ ( $10^{-4}$ S/m)			
	300.8 K	308.3 K	318.2 K	328.3 K
0.00	0.0074	0.0067	0.0065	0.0051
0.02	0.013	0.013	0.012	0.011
0.04	0.018	0.019	0.018	0.014
0.06	0.023	0.025	0.021	0.017
0.08	0.027	0.029	0.024	0.016
0.10	0.033	0.036	0.029	0.021

Table A-2-24. Temperature and composition dependences of molar conductivity ( $\Lambda_0$ ) of ammonium nitrate in *t*-butanol/water mixed solvents.

Water mol%	T (K)	$\Lambda_0$ ( $10^{-3} \text{ S}\cdot\text{m}^2/\text{mol}$ )	Water mol%	T (K)	$\Lambda_0$ ( $10^{-3} \text{ S}\cdot\text{m}^2/\text{mol}$ )
100	283.3	11.	50	283.2	0.86*
	298.3	14.		298.2	1.8*
	313.4	20.		313.5	2.9*
	328.2	25.		328.2	4.4*
	343.4	35.		343.4	6.5*
97	273.2	5.9	30	283.0	0.45*
	278.2	7.2		298.2	8.5*
	283.3	8.2		313.3	1.4*
	298.6	13.		328.2	2.1*
	313.5	18		343.4	2.8*
	328.2	21.			
	343.4	28.			
90	283.3	3.3	10	298.3	0.46*
	298.4	5.9		308.2	0.60*
	313.5	8.7		318.2	0.77*
	328.2	12.		328.3	0.92*
	343.4	20.		343.3	1.1*
70	283.4	1.3	0	300.8	0.26
	298.4	2.6		308.3	0.29
	313.4	4.3		318.2	0.28*
	328.3	6.6		328.3	0.28*
	343.5	8.9			

\* Initial slope.



Table A-2-25. The values of specific conductance ( $\kappa$ ) of ammonium perchlorate in *t*-butanol/water mixed solvent.

Composition: Water

C (Salt) ( $10^{-1}$ mol/m <sup>3</sup> )	$\Lambda_0$ ( $10^{-4}$ S/m)			
	298.3 K	313.2 K	328.2 K	343.3 K
0.00	0.71	1.3	2.0	3.0
0.50	31.	40.	51.	61.
1.00	56.	73.	95.	126.
1.50	87.	113.	142.	173.
2.00	113.	149.	188.	234.
2.50	142.	187.	239.	304.

Composition: 97 mol% Water

C (Salt) ( $10^{-1}$ mol/m <sup>3</sup> )	$\Lambda_0$ ( $10^{-4}$ S/m)				
	278.5 K	298.3 K	313.3 K	328.3 K	343.5 K
0.00	0.39	0.68	0.92	1.3	1.7
0.50	2.8	5.2	7.4	9.7	12.
1.00	5.2	9.8	14.	19.	24.
1.50	7.6	14.	20.	27.	34.
2.00	10.	19.	27.	36.	45.
2.50	13.	23.	32.	42.	56.

Composition: 90 mol% Water

C (Salt) ( $10^{-1}$ mol/m <sup>3</sup> )	$\Lambda_0$ ( $10^{-4}$ S/m)				
	278.4 K	298.3 K	313.2 K	328.4 K	343.4
0.00	0.38	0.50	0.59	0.70	0.97
1.00	2.0	5.3	8.3	12.	16.
2.00	3.9	9.9	16.	23.	31.
3.00	5.8	15,	23.	33.	44.
4.00	7.9	20.	32.	45.	60.
5.00	9.8	25.	39.	54.	73.

Table A-2-25 continued

Composition: 70 mol% Water

C (Salt) ( $10^{-1}$ mol/m <sup>3</sup> )	$\Lambda_0$ ( $10^{-4}$ S/m)				
	288.2 K	298.3 K	313.2 K	328.3 K	343.4 K
0.00	0.32	0.42	0.49	0.52	0.61
1.00	1.6	2.5	4.3	6.3	7.9
2.00	3.0	4.7	7.8	12.	17.
3.00	4.7	7.2	12.	18.	25.
4.00	6.2	9.6	16.	23.	32.
5.00	7.6	12.	19.	29.	40.

Composition: 50 mol% Water

C (Salt) ( $10^{-1}$ mol/m <sup>3</sup> )	$\Lambda_0$ ( $10^{-4}$ S/m)				
	298.4 K	308.3 K	318.3 K	328.3 K	343.4 K
0.00	0.29	0.32	0.35	0.36	0.37
2.00	3.6	5.2	9.4	9.4	13.
4.00	6.7	9.6	17.	17.	24.
6.00	9.9	14.	25.	25.	35.
8.00	13.	18.	32.	32.	45.
10.0	16.	23.	39.	39.	54.

Composition: 30 mol% Water

C (Salt) ( $10^{-1}$ mol/m <sup>3</sup> )	$\Lambda_0$ ( $10^{-4}$ S/m)				
	298.3 K	308.3 K	318.2 K	328.2 K	343.3 K
0.00	0.35	0.36	0.36	0.36	0.36
1.00	1.3	1.8	2.4	3.1	4.1
2.00	2.2	3.1	4.1	5.3	6.9
3.00	3.2	4.4	5.8	7.3	9.4
4.00	4.0	5.6	7.3	9.1	12.
5.00	4.7	6.5	8.6	10.	13.

Table A-2-25 continued

Composition: 10 mol% Water

C (Salt) ( $10^{-1}$ mol/m <sup>3</sup> )	$\Lambda_0$ ( $10^{-4}$ S/m)				
	298.4 K	308.3 K	318.3 K	328.3 K	343.4 K
0.00	0.01	0.01	0.01	0.01	0.01
1.00	0.37	0.41	0.40	0.36	0.30
2.00	0.55	0.59	0.56	0.51	0.43
3.00	0.73	0.77	0.73	0.65	0.54
4.00	0.87	0.91	0.86	0.78	0.64
5.00	0.97	1.0	0.97	0.87	0.72

Composition: *t*-Butanol

C (Salt) ( $10^{-1}$ mol/m <sup>3</sup> )	$\Lambda_0$ ( $10^{-4}$ S/m)			
	300.9 K	308.3 K	318.2 K	328.3 K
0.00	0.0088	0.0092	0.0078	0.0068
0.06	0.038	0.048	0.049	0.053
0.12	0.072	0.082	0.099	0.11
0.18	0.10	0.12	0.14	0.14
0.24	0.13	0.16	0.17	0.16
0.30	0.17	0.20	0.20	0.17

Table A-2-26. Temperature and composition dependences of molar conductivity ( $\Lambda_0$ ) of ammonium perchlorate in *t*-butanol/water mixed solvents.

Water mol%	T (K)	$\Lambda_0$ ( $10^{-3} \text{ S}\cdot\text{m}^2/\text{mol}$ )	Water mol%	T (K)	$\Lambda_0$ ( $10^{-3} \text{ S}\cdot\text{m}^2/\text{mol}$ )
100	298.3	14.	50	298.4	1.5
	313.2	19.		308.4	2.2
	328.2	23.		318.3	2.9
	343.3	30.		328.3	3.8
		343.4		5.4	
97	278.5	5.0	30	298.3	0.92
	298.3	9.2		308.3	1.3
	313.3	13.		318.3	1.6
	328.3	17.		328.3	2.0
	343.5	22.			
90	278.4	2.0	10	298.4	0.61*
	298.3	5.0		308.3	0.81*
	313.2	7.8		318.3	1.1*
	328.4	11.		328.3	1.3*
	343.5	15.		343.4	1.6*
70	288.2	1.5	0	300.9	0.53
	298.2	2.3		308.3	0.62
	313.2	3.8		318.2	0.74*
	328.2	5.7		328.3	0.91*
	343.4	8.0			

\* Initial slope.

Table A-2-27. The values of specific conductance ( $\kappa$ ) of lithium perchlorate in *t*-butanol/water mixed solvent.

Composition: Water

C (Salt) ( $10^{-1}$ mol/m <sup>3</sup> )	$\Lambda_0$ ( $10^{-4}$ S/m)				
	298.3 K	308.3 K	318.3 K	328.4 K	343,4
0.00	0.73	0.79	1.4	1.7	2.5
0.50	6.2	7.7	9.2	11.	14.
1.00	11.	13.	16.	19.	25.
1.50	17.	21.	24.	29.	35.
2.00	21.	26.	31.	37.	46.
2.50	26.	32.	38.	44.	54.

Composition: 97 mol% Water

C (Salt) ( $10^{-1}$ mol/m <sup>3</sup> )	$\Lambda_0$ ( $10^{-4}$ S/m)				
	298.3 K	308.3 K	318.2 K	328.2 K	343.3 K
0.00	0.66	0.84	0.98	1.2	1.6
0.50	3.8	4.9	6.1	7.3	9.3
1.00	7.1	9.3	12.	14.	19.
1.50	12.	16.	24.	23.	30.
2.00	14.	19.	23.	28.	35.
2.50	20.	25.	30.	36.	48.

Composition: 90 mol% Water

C (Salt) ( $10^{-1}$ mol/m <sup>3</sup> )	$\Lambda_0$ ( $10^{-4}$ S/m)				
	298.2 K	308.3 K	318.4 K	328.2 K	343.3 K
0.00	0.46	0.52	0.55	0.68	0.89
1.00	3.5	5.0	6.7	8.6	12.
2.00	7.7	11.	15.	18.	24.
3.00	11.	15.	20.	24.	33.
4.00	14.	20.	28.	35.	45.
5.00	17.	24.	34.	41.	57.

Table A-2-27 continued

Composition: 70 mol% Water

C (Salt) ( $10^{-1}$ mol/m <sup>3</sup> )	$\Lambda_0$ ( $10^{-4}$ S/m)				
	298.2 K	308.4 K	318.2 K	328.3 K	343.4 K
0.00	0.30	0.46	0.49	0.57	0.61
1.00	1.9	2.9	3.9	5.1	7.2
2.00	3.7	5.4	7.3	9.6	14.
3.00	5.6	8.2	11.	15.	21.
4.00	7.2	11.	14.	18.	27.
5.00	9.0	13.	18.	24.	33.

Composition: 50 mol% Water

C (Salt) ( $10^{-1}$ mol/m <sup>3</sup> )	$\Lambda_0$ ( $10^{-4}$ S/m)				
	298.3 K	308.3 K	318.3 K	328.3 K	343.4 K
0.00	0.33	0.37	0.42	0.46	0.50
2.00	2.6	3.8	5.3	7.0	9.9
4.00	5.0	7.4	10.	13.	19.
6.00	7.3	11.	15.	19.	27.
8.00	9.6	14.	19.	25.	35.
10.0	12.	17.	24.	31.	43.

Composition: 30 mol% Water

C (Salt) ( $10^{-1}$ mol/m <sup>3</sup> )	$\Lambda_0$ ( $10^{-4}$ S/m)				
	298.3 K	308.3 K	318.2 K	328.2 K	343.4 K
0.00	0.33	0.38	0.44	0.46	0.48
1.00	1.2	1.6	2.2	2.9	3.9
2.00	2.0	2.9	3.9	5.0	6.7
3.00	2.9	4.1	5.5	7.0	9.3
4.00	3.7	5.2	6.9	8.8	12.
5.00	4.3	6.2	8.2	10.	14.

Table A-2-27 continued

Composition: 10 mol% Water

C (Salt) ( $10^{-1}$ mol/m <sup>3</sup> )	$\Lambda_0$ ( $10^{-4}$ S/m)				
	298.3 K	308.3 K	318.2 K	328.3 K	343.4 K
0.00	0.013	0.011	0.012	0.012	0.014
1.00	0.096	0.14	0.18	0.20	0.25
2.00	0.17	0.24	0.32	0.37	0.42
3.00	0.24	0.33	0.42	0.50	0.52
4.00	0.30	0.43	0.56	0.63	0.67
5.00	0.35	0.48	0.60	0.70	0.73

Composition: *t*-Butanol

C (Salt) ( $10^{-1}$ mol/m <sup>3</sup> )	$\Lambda_0$ ( $10^{-4}$ S/m)				
	298.3 K	308.3 K	318.2 K	328.2 K	343.4 K
0.00	0.011	0.013	0.015	0.014	0.014
0.025	0.020	0.024	0.028	0.033	0.029
0.050	0.030	0.037	0.042	0.043	0.038
0.075	0.040	0.049	0.056	0.055	0.049
0.010	0.050	0.060	0.066	0.061	0.054

Table A-2-28. Temperature and composition dependences of molar conductivity ( $\Lambda_0$ ) of lithium perchlorate in *t*-butanol/water mixed solvents.

Water mol%	T (K)	$\Lambda_0$ ( $10^{-3} \text{ S}\cdot\text{m}^2/\text{mol}$ )	Water mol%	T (K)	$\Lambda_0$ ( $10^{-3} \text{ S}\cdot\text{m}^2/\text{mol}$ )
100	298.3	9.9	50	298.3	1.2
	308.3	12.		308.3	1.7
	318.3	15.		318.3	2.3
	328.2	17.		328.3	3.0
	343.2	21.		343.4	4.3
97	298.2	7.3	30	298.3	0.85
	308.3	9.4		308.3	1.2
	318.2	12.		318.2	1.7
	328.2	14.		328.3	2.1
	343.3	19.		343.4	2.7
90	298.2	3.5	10	298.3	0.75
	308.3	4.9		308.3	0.99
	318.4	6.6		318.3	1.2
	328.2	8.3		328.3	1.4
	343.3	11.		343.4	1.8*
70	298.3	1.8	0	298.3	0.39
	308.4	2.6		308.3	0.47
	318.2	3.5		318.2	0.55
	328.3	4.7		328.3	0.75*
	343.3	6.6		343.4	0.63*

\* Initial slope.



#### 4. Results of the Optical Absorption Spectra of Solvated Electrons in 1-Butylamine/Water Mixtures.

Table A-2-29 Parameters of Solvated Electron Spectra in 1-Butylamine/Water Mixed Solvents at Different Temperatures.

Composition: Water

T(K)	281.8 K	298.5 K	317.1 K	338.3 K
$GE_{Amax}$ ( $10^{-21}/16$ aJ)	7.3	8.3	6.9	7.1
$E_{Amax}$ (zJ)	286	278	270	259
$E_b$ (zJ)	367	362	348	340
$E_r$ (zJ)	230	222	211	200
$W_b$ (zJ)	81	84	78	81
$W_r$ (zJ)	56	56	59	59
$W_{1/2}$ (zJ)	137	140	137	140
$W_b/W_r$	1.41	1.50	1.32	1.37
$-dE_{Amax}/dT$ (zJ/K)		0.47		

Table A-2-29 continued.

Composition: 99 mol% Water

T(K)	269.1 K	298.7 K	327.7 K	357.7 K
$GE_{Amax}$ ( $10^{-21}/16$ aJ)	8.9	8.7	8.6	8.0
$E_{Amax}$ (zJ)	292	276	263	250
$E_b$ (zJ)	367	355	340	331
$E_r$ (zJ)	236	221	207	188
$W_b$ (zJ)	75	79	77	81
$W_r$ (zJ)	56	55	56	62
$W_{1/2}$ (zJ)	131	134	133	143
$W_b/W_r$	1.34	1.44	1.38	1.31
$-dE_{Amax}/dT$ (zJ/K)		0.46		

Composition: 95 mol% Water

T(K)	264.1 K	298.5 K	328.4 K
$GE_{Amax}$ ( $10^{-21}/16$ aJ)	10.	8.6	8.3
$E_{Amax}$ (zJ)	292	275	262
$E_b$ (zJ)	373	352	343
$E_r$ (zJ)	239	220	204
$W_b$ (zJ)	81	77	81
$W_r$ (zJ)	53	55	58
$W_{1/2}$ (zJ)	134	132	139
$W_b/W_r$	1.53	1.40	1.40
$-dE_{Amax}/dT$ (zJ/K)		0.44	

Table A-2-29 continued.

Composition: 90 mol% Water

T(K)	257.5 K	298.6 K	343.2 K
$GE_{Amax}$ ( $10^{-21}/16$ aJ)	7.8	7.0	6.8
$E_{Amax}$ (zJ)	292	273	254
$E_b$ (zJ)	375	349	332
$E_r$ (zJ)	240	215	195
$W_b$ (zJ)	83	76	78
$W_r$ (zJ)	52	58	59
$W_{1/2}$ (zJ)	135	134	137
$W_b/W_r$	1.60	1.31	1.32
$-dE_{Amax}/dT$ (zJ/K)		0.41	

Composition: 70 mol% Water

T(K)	240.5 K	270.3 K	298.6 K	330.4 K
$GE_{Amax}$ ( $10^{-21}/16$ aJ)	5.5	5.1	5.0	5.0
$E_{Amax}$ (zJ)	265	258	248	236
$E_b$ (zJ)	315	330	338	350
$E_r$ (zJ)	203	191	183	174
$W_b$ (zJ)	85	80	82	79
$W_r$ (zJ)	62	67	65	62
$W_{1/2}$ (zJ)	147	147	147	141
$W_b/W_r$	1.37	1.19	1.27	1.27
$-dE_{Amax}/dT$ (zJ/K)		0.30		

Table A-2-29 continued.

Composition: 50 mol% Water

T(K)	230.0 K	262.8 K	298.8 K
$GE_{Amax}$ ( $10^{-21}/16$ aJ)	6.7	4.8	3.7
$E_{Amax}$ (zJ)	233	223	214
$E_b$ (zJ)	332	327	319
$E_r$ (zJ)	164	156	155
$W_b$ (zJ)	99	104	105
$W_r$ (zJ)	69	67	59
$W_{1/2}$ (zJ)	168	171	164
$W_b/W_r$	1.43	1.55	1.80
$-dE_{Amax}/dT$ (zJ/K)		0.27	

Composition: 30 mol% Water

T(K)	228.5 K	262.0 K	298.6 K
$GE_{Amax}$ ( $10^{-21}/16$ aJ)	4.2	3.2	2.2
$E_{Amax}$ (zJ)	208	197	189
$E_b$ (zJ)	325	320	314
$E_r$ (zJ)	140	137	135
$W_b$ (zJ)	117	123	125
$W_r$ (zJ)	68	60	53
$W_{1/2}$ (zJ)	185	183	178
$W_b/W_r$	1.72	2.05	2.36
$-dE_{Amax}/dT$ (zJ/K)		0.30	

Table A-2-29 continued.

Composition: 10 mol% Water

T(K)	226.7 K	248.2 K	270.7 K	298.4 K
$GE_{Amax}$ ( $10^{-21}/16$ aJ)	2.1	2.0	1.8	1.6
$E_{Amax}$ (zJ)	165	159	150	143
$E_b$ (zJ)	327	319	310	303
$E_r$ (zJ)	108	106	103	
$W_b$ (zJ)	162	160	160	160
$W_r$ (zJ)	57	53	47	
$W_{1/2}$ (zJ)	219	213	207	
$W_b/W_r$	2.84	3.02	3.40	
$-dE_{Amax}/dT$ (zJ/K)		0.36		

Composition: 0 mol% Water

T(K)	225.3 K	236.3 K	247.7 K	271.0 K	298.7 K
$GE_{Amax}$ ( $10^{-21}/16$ aJ)	2.1	2.0	1.9	1.6	1.4
$E_{Amax}$ (zJ)	147	142	135	127	115
$E_b$ (zJ)	251	242	233	231	215
$E_r$ (zJ)	102				
$W_b$ (zJ)	104	100	98	104	100
$W_r$ (zJ)	45				
$W_{1/2}$ (zJ)	149				
$W_b/W_r$	2.31				
$-dE_{Amax}/dT$ (zJ/K)			0.43		